A national laboratory of the U.S. Department of Energy
Office of Energy Efficiency & Renewable Energy

National Renewable Energy Laboratory

Innovation for Our Energy Future

Integrated Wind Energy/ Desalination System

October 11, 2004 — July 29, 2005

GE Global Research
Niskayuna, New York

Subcontract Report
NREL/SR-500-39485
October 2006

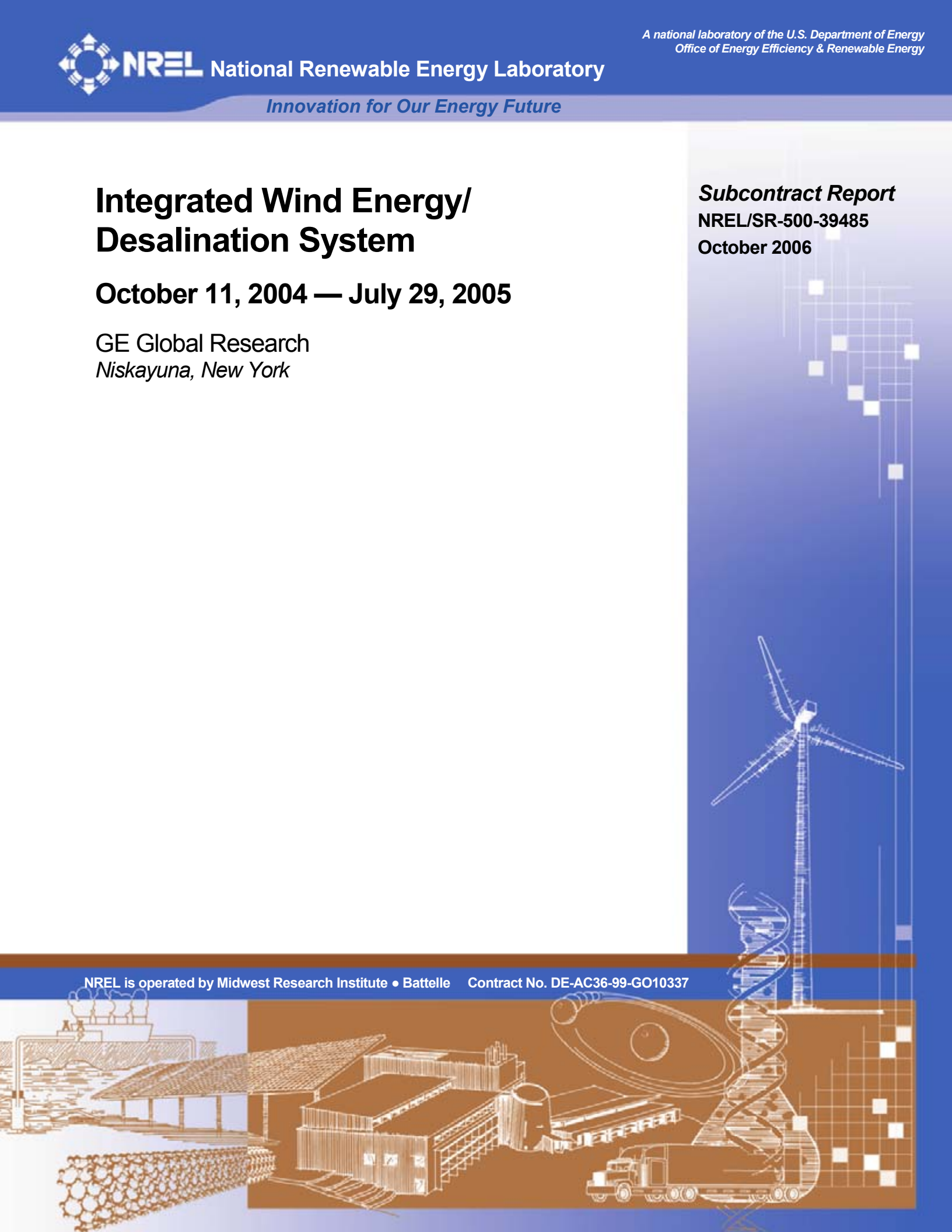

NREL is operated by Midwest Research Institute • Battelle Contract No. DE-AC36-99-GO10337

Integrated Wind Energy/ Desalination System

Subcontract Report
NREL/SR-500-39485
October 2006

October 11, 2004 — July 29, 2005

GE Global Research
Niskayuna, New York

NREL Technical Monitor: Scott Schreck
Prepared under Subcontract No. YAM-4-33200-09

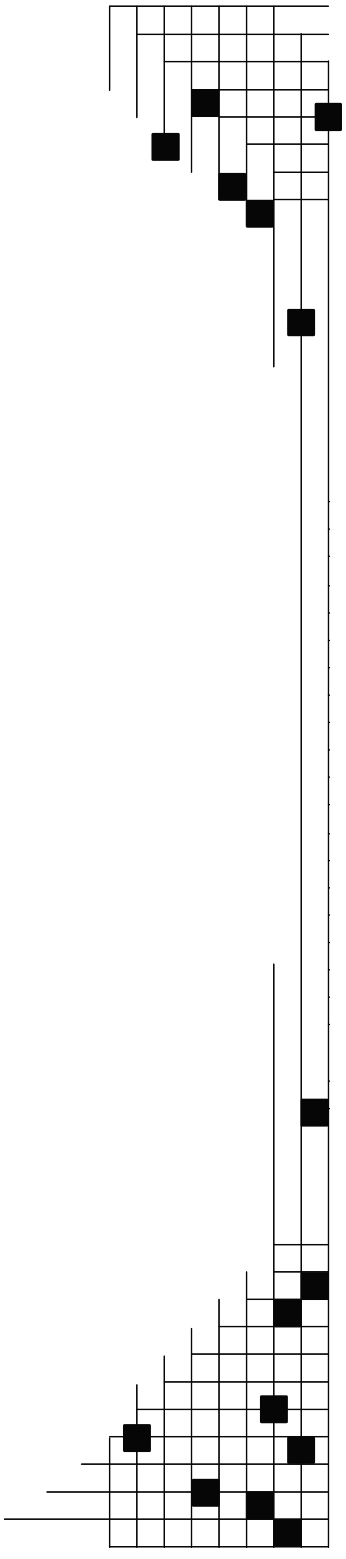

National Renewable Energy Laboratory
1617 Cole Boulevard, Golden, Colorado 80401-3393
303-275-3000 • www.nrel.gov

Operated for the U.S. Department of Energy
Office of Energy Efficiency and Renewable Energy
by Midwest Research Institute • Battelle

Contract No. DE-AC36-99-GO10337

Available electronically at http://www.osti.gov/bridge

Available for a processing fee to U.S. Department of Energy
and its contractors, in paper, from:
U.S. Department of Energy
Office of Scientific and Technical Information
P.O. Box 62
Oak Ridge, TN 37831-0062
phone: 865.576.8401
fax: 865.576.5728
email: mailto:reports@adonis.osti.gov

Available for sale to the public, in paper, from:
U.S. Department of Commerce
National Technical Information Service
5285 Port Royal Road
Springfield, VA 22161
phone: 800.553.6847
fax: 703.605.6900
email: orders@ntis.fedworld.gov
online ordering: http://www.ntis.gov/ordering.htm

This publication received minimal editorial review at NREL

Printed on paper containing at least 50% wastepaper, including 20% postconsumer waste

Contents

Figures

Tables

Acronyms and Abbreviations

cmh.....cubic meters per hour
COE.....cost of energy
COW .....cost of water
DET.....delivered equipment total
DFIG .....doubly fed induction generator
DOE .....U.S. Department of Energy
ED .....electrodialysis
ERD.....energy recovery device
GE .....General Electric Company
GEGR.....GE Global Research
gfd .....gallons per square foot per day
gpm .....gallons per minute
lmh .....liter per square meter per hour
MED.....multi-effect distillation
MSF.....multistage flash
MW .....megawatt
O&M .....operation and maintenance
PM.....permanent magnet
ppm .....parts per million
PSD .....power spectral density
psi.....pounds per square inch
PV .....photovoltaic
REC.....rural energy cooperative
RES .....renewable energy source
RO.....reverse osmosis
SCOW .....specific cost of water
TDS .....total dissolved solids
WHO.....World Health Organization
WTG .....wind turbine generator

1 Executive Summary

Water needs have been increasing rapidly worldwide, even in nations like the United States, where abundant freshwater has been available at a relatively low cost. Population growth, increased industrial use, and pollution may limit the nation's capability to satisfy freshwater demands over the next few decades. Hence, in the United States, developing new water resources by purifying impaired resources is critical for meeting future water needs.

Desalination techniques are characterized by large energy expenditures to generate potable water. The associated cost of energy (COE) is a dominant factor in the water desalination economy. In this scenario, reverse osmosis (RO), a major approach to desalination, is gaining increased acceptance as a viable technique, mainly because of its low energy consumption and design flexibility.

Because of recent and projected technological advances, reverse osmosis will most likely continue to be the lowest cost technology associated with potable water production. However, for many projected water-starved regions of the United States and remote, inland areas where grid connectivity is limited, the energy cost associated with reverse osmosis based desalination may render the desalination solution economically infeasible. Hence, alternative solutions are required to produce potable water.

A likely candidate for replacing traditional RO desalination systems is a hybrid approach in which renewable energy sources (RES) such as wind energy are coupled with an RO desalination system. The broad acceptance of RES-RO systems is limited by:

- Operability over a large power envelope
- Robustness to feedwater variation
- Management of multiple, often conflicting, requirements
- In-situ monitoring of membrane degradation and compensation via operations and chemicals
- Reduction in cost of water (COW) for commercialization.

An approach to interfacing RES and RO systems must address the issues of operability, robustness, and management of membrane constraints with regard to power fluctuations. At the same time, a highly flexible RO system must be developed in conjunction with energy management and operational strategies. An RES-RO system with advanced operations can be developed, but its effectiveness must be measured in terms of its energy consumption and ultimately COW. Hence, the overall goal of this particular study is to investigate multiple concepts for integrating wind turbines and RO desalination systems for feasibility and efficiency. This effort is unique in that it addresses the constraints of variable power input on desalination system operation to arrive at a process that can accommodate a maximum level of wind turbine power variation and remain economically viable. A principal motivation for this project is the simplicity and low cost with which water can be delivered where energy, a major component of RO-based desalination system cost, is reduced.

The program focuses on the following fundamental activities to address its objectives:

- Develop component models, including wind turbine system, RO system, energy recovery devices, and energy storage, for the major components of an RES-RO system and their integration into a system-level concept. Develop an integrated energy and water cost model that can be used to evaluate and trade off various RES-RO configurations.
- Develop and analyze various RES-RO configurations as to their robustness to power fluctuations and ability to meet water quality requirements with the lowest COW.
- Develop a methodology to size, evaluate, and operate an RES-RO system in operational modes such as grid connected, grid connected with direct coupling, and grid isolated with energy storage.

2 Introduction

Water needs have been increasing rapidly worldwide because of population and industrial growth. In the past, water was seen as mainly a Middle Eastern or African issue; however, with the growth in Asia and North America, this viewpoint may no longer hold. In contrast to many areas of the world, the United States has enjoyed an abundant supply of freshwater at relatively low cost. Over the next few decades, however, population growth, increased industrial use, and pollution may strain the nation's ability to supply the necessary quantities of safe freshwater. A case in point is the recent and projected growth in the southeastern and southwestern regions of the country where safe freshwater shortages occur routinely in drought years. The potential inability to meet the growing needs for freshwater can adversely affect public health and various economic sectors such as agriculture. A combination of water conservation, reuse, recycling, and development of new water sources is critical to ensure an adequate supply of safe freshwater at a reasonable cost. Since conventional water resources are limited, the development of new ones will most likely come from impaired resources such as brackish water and seawater in addition to water generated during energy production (oil, natural gas, and coal bed methane production)[1].

Developing new water resources by purifying impaired resources is seen as critical for meeting future water needs. For desalination, impaired resources may be grouped into various categories by their saline content, which is referred to as total dissolved salts (TDS). Typically, freshwater contains less than 1,000 milligrams of salt per liter of water, or 1000 parts per million (ppm). Brackish water, on the other hand, is associated with TDS content of 1,000−10,000 ppm. Finally, seawater typically has at least 10,000 ppm of TDS. The goal of desalination is to purify the water stream of these impaired resources so the TDS content in the resultant stream is 500 ppm or lower.

At present, there are two major approaches to desalination: thermal-based and membrane-based solution. Thermal-based desalination is predicated on the use of phase change or distillation techniques to reduce the TDS content of an impaired water resource. Mature thermal-based technologies such as multistage flash (MSF) or multi-effect distillation (MED) use simple processes. Simply put, thermal-based solutions use energy input in the form of heat to evaporate the impaired water and then condense the resulting vapor stream to produce potable water. Because a large amount of heat input is required, thermal desalination systems are typically colocated with power plants for electrical generation where steam is readily available. Consequently, the economics of thermal desalination require large centralized water and power production and low cost of energy (COE) for steam production. These factors are easily achieved in some regions such as the Middle East, so thermal desalination is a cost-effective technology for producing potable water in these areas[2].

In many regions, thermal-based solutions are not cost effective because of the high COE associated with steam production. Consequently, in these regions, membrane-based desalination is a viable solution. Membrane-based solutions use either electrical potential or pressure as the driving force to separate substances via diffusion across a semipermeable membrane. In the case of electrical potential, the technology is often referred to as electrodialysis (ED). In ED, positive (cation) and negative (anion) ions are transported through a semipermeable membrane by applying a voltage across a pair of electrodes.

Alternate configurations of cation- and anion-permeable membranes are placed between each pair of electrodes. As the ions are driven to the electrode with the opposite charge, dissolved salt is separated and concentrated in a separate channel and results in a potable water stream[3]. ED has favorable economics for brackish water and small-scale systems compared to other desalination methods. However, for TDS concentrations higher than 10,000 ppm, the COE associated with the ED is higher than with other desalination technologies. In addition, for large-scale plants, the economies of scale are more favorable for other membrane technologies such as reverse osmosis (RO)[3].

RO is a pressure-driven membrane separation process in which the water from a pressurized saline solution is separated from the solutes via diffusion across a semipermeable membrane. The pressure required to drive the separation process depends on the resistance of the membrane and on the saline concentration of the water. RO systems consist of additional process steps beyond pressurization and separation for producing potable water. An overview of the RO system and its major components is shown in Figure 2-1.

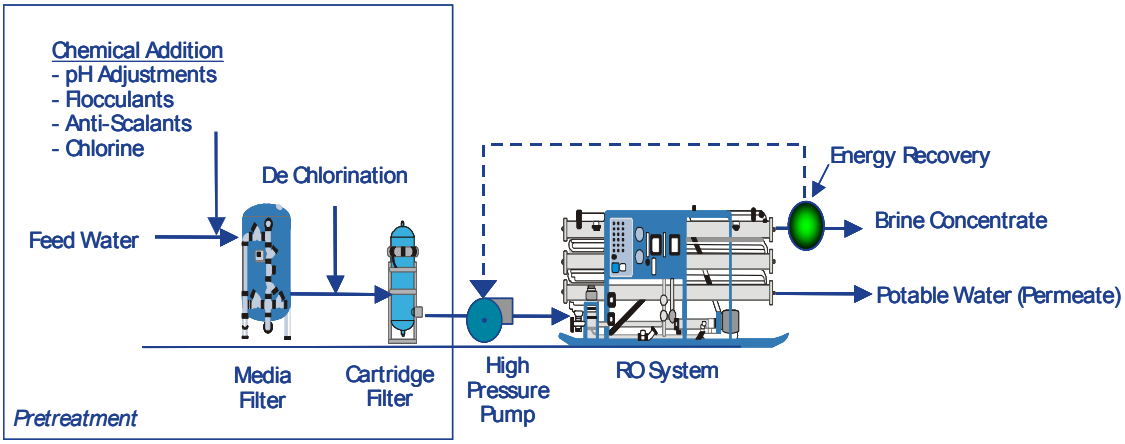

Figure 2-1. Process steps and components of RO desalination systems

The initial process step of an RO system is pretreatment, which is critical to ensure membrane surfaces remain clean to maintain performance and reduce fouling or degradation. Therefore, suspended solids are removed via sand filtration or filtration through other media. Pretreatment consists of fine filtration. and addition of acid or other chemicals to inhibit salt precipitation and microbial growth. Finally, chemicals are added to ensure pH and alkalinity levels are within a specified range that corresponds to the membrane manufacturer's requirements.

The second process step in an RO system consists of increasing the pressure of the feedwater and pumping the feedwater through closed vessels. An RO system consists of multiple closed vessels that are connected in parallel; each closed vessel consists of multiple elements in series. Since the feedwater input at each closed vessel is approximately equivalent with regard to pressure and flowrate, the performance of the overall system can be ascertained by the performance of a single vessel. In a closed vessel, each element separates the dissolved salts from the water, which results in a potable water flux across the membrane. The flux declines axially along the length of the membrane because of the increase in salinity of the water, which is caused by the separation process and the pressure loss along the length of the

membrane. In each closed vessel, the potable water, often termed permeate, is collected as is the concentrate or brine solution. The brine solution is of higher TDS than the inlet stream because of the salt separation.

The third and fourth process steps are applied to the permeate and the brine concentrate, respectively. The permeate is post-treated to stabilize the water for distribution; gases such as hydrogen sulfide may be removed and pH may be adjusted. Since the pressure drop in an RO system is slight, the brine concentrate has significant pressure energy, which if recovered can improve overall system efficiency and cost. Hence, in the fourth process step, pressure energy in the brine is recovered through an energy recovery device (ERD) and then disposed.

The widespread use of desalination techniques, whether thermal or membrane based, is predicated on the economics associated with the process. In both approaches, capital and energy costs dominate. One method to compare the economics associated with thermal processes and membrane processes, specifically RO, is to look at energy used per cubic meter of potable water for seawater desalination. For seawater, thermal systems consume 3.5–4.5 kWh/m^3 versus 3.0–4.5 kWh/m^3 for RO systems. Thermal and RO systems have similar energy use; RO has a slightly lower energy use. In contrast to thermal techniques, which are mature and have little technology development, RO-based systems have continued to improve their energy efficiency through technology development. In fact, with the current focus on improving ERDs, development of low-pressure membranes, and pH-robust membranes, RO is expected to continue to provide the lowest energy use and hence, lowest cost associated with potable water production. Finally, because significant heat must be input in the form of steam for thermal systems, the ability to site a thermal desalination facility in noncentralized distribution systems is limited. RO-based solutions, on the other hand, do not face this issue because the main energy input is electrical, which is readily available from the electrical grid. For grid-isolated cases, RO systems can be integrated with power generation devices such as diesel engines or renewable energy sources such as wind or photovoltaic (PV) power. Thus, RO-based desalination is gaining momentum and increased acceptance as a viable desalination technique.

2.1 Motivation for Wind Desalination

The development of potable water from underused resources such as brackish water and seawater is predicated on the use of desalination techniques. Desalination has the potential to address current and future water needs, but it has been plagued by high cost, which makes it noncompetitive with natural resources used today. Of the available desalination techniques (RO, multistage flash (MSF), multi-effect distillation (MED), electrodialysis (ED), and vapor compression (VC), RO consistently has the highest demonstrated energy efficiency, typically 3–4.5 kWh/m^3. Even with its higher efficiency, energy cost still accounts for roughly 45% of the cost of water (COW) in RO-based systems (Figure 2-2)[1]. For many projected water-starved regions of the United States and remote, inland areas where grid connectivity is limited, the retail COE is \$0.08–\$0.12/kWh. Even though the cost of generating energy has dropped to approximately \$0.04/kWh for remote areas, the costs associated with transmission and distribution make up a large percentage of the retail energy cost. Hence, alternative solutions are required to produce potable water.

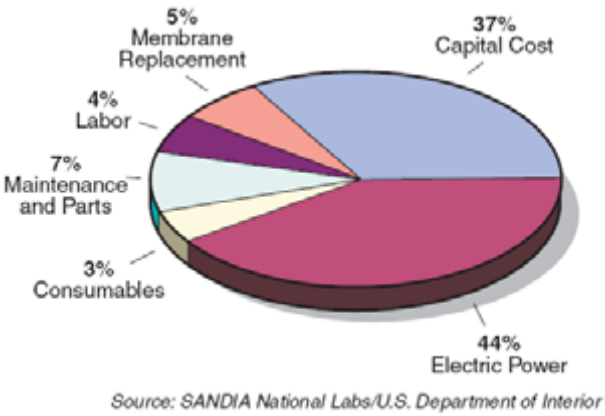

Figure 2-2. Cost categories for an RO-based desalination system

A likely candidate for replacing traditional RO desalination systems is a hybrid approach where renewable energy sources (RES) such as wind energy and photovoltaics (PV) are coupled with an RO desalination system. To understand the advantages of RES-RO systems, we considered the cost structure associated with traditional desalination systems (Figure 2-2). Energy, capital, and operation and maintenance (O&M) costs are major factors. The advantages of RES-RO systems address these factors.

- The COE associated with transmission and distribution is avoided by coupling energy generation directly to RO systems with RES. Hence, the COE of desalination systems can be significantly reduced. Energy generation costs associated with photovoltaic systems (PV) are still high, but wind energy cost is projected to reach $0.04/kWh, which will make wind desalination cost competitive.
- The predominant cost of RES systems is capital expenditures. For wind energy, roughly 89% of the COE is associated with capital expenditures; the remaining 11% is O&M. The shift in RES systems from fuel cost to capital cost significantly alters the cost structure for RES-based desalination systems. The shift from COE to capital expenditures is a favorable proposition, since capital cost can be amortized over a longer horizon. In addition, the shift to capital expenditures reduces the sensitivity to fluctuations in fuel cost. For RES some of the COE shown in Figure 2-2 would also shift to O&M. The resulting cost structure of RES-RO systems, in conjunction with the high energy efficiency of RO, provides a cost-competitive approach for addressing the nation's water needs.
- The availability of RES throughout the nation correlates to potential impaired water resources that can be used to develop new, safe freshwater (Figure 2-3). Specifically, the plains states have significant saline aquifers that can be cultivated to yield freshwater for the agricultural economy. Wind and photovoltaic energy sources are prevalent in these areas and can be used for desalination. In the Southwest, specifically New Mexico, Texas, and Colorado, significant population growth is projected. Additional challenges to meeting the ever-increasing water demand include restrictions of water rights on the use of available freshwater sources. If the saline aquifers can be processed through RES-RO systems, the water shortages might be alleviated in this area.

- A final example is associated with rural energy cooperatives (RECs). Approximately 55% of RECs are located in the same region as the saline aquifers. Renewable sources are available and government grants have been offered for their development, so RECs represent a large customer base for the proposed technology (Figure 2-3).

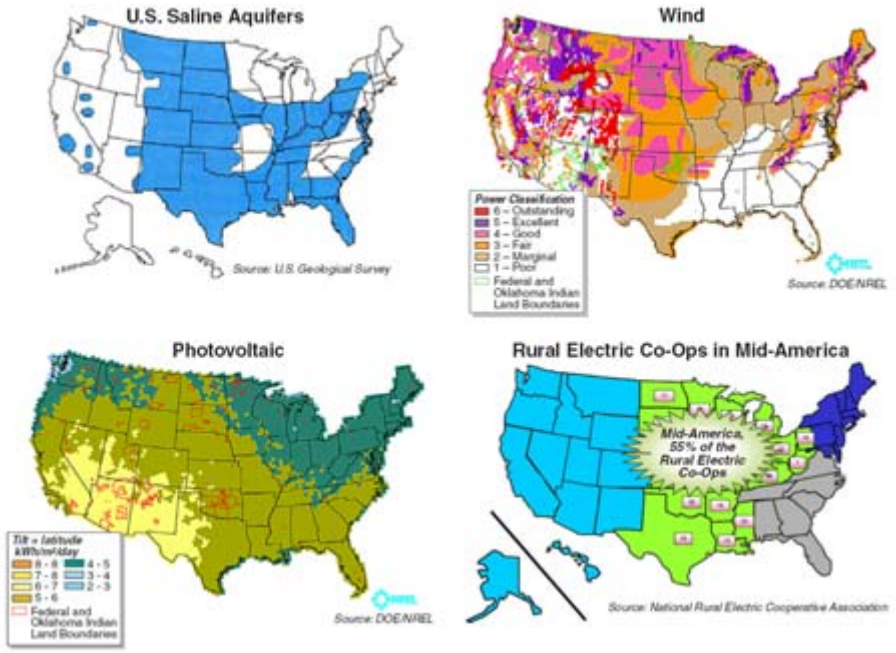

Figure 2-3. RES resource availability correlated to potential impaired water sources and potential beneficiaries

The challenge with RES-RO systems, however, is how to interface these two technologies. RES systems are characterized by transient operation that leads to electrical energy variation. Desalination systems, especially RO systems, are designed for continuous steady-state operation. Conventional approaches for addressing the operability mismatch between RES and RO use electrical energy storage systems such as batteries or alternative energy sources such as diesel engines to yield a stable power source. This approach, however, greatly increases the capital cost of the hybrid system and, in some cases, the system's COE. The end result is an increase in COW.

Novel RES-desalination systems have been proposed in the literature, and some have been demonstrated[4–10]. For example, Thomson et al. consider the use of a Clark pump in conjunction with advanced control strategies to reduce the specific energy consumption in a laboratory-scale demonstration[4]. Carta et al. describe a wind desalination system in the Canarian Archipelago where various desalination approaches have been tested in conjunction with wind[5]. This work highlights that RO is the most appropriate technique for stand-alone power generation situations. The operational strategy brings the flywheel, pumps, and RO segments online as power is available and removes sections of the RO system as power is reduced. Finally, Miranda et al. employ a control strategy that attempts to maximize energy extracted and water throughput despite power fluctuations[6]. These recent results address the fundamental issue of RES-RO systems—the design of a system and the selection of an operational strategy that accommodates the maximum power variation without compromising

water quality or COW. These results show promise, but issues of economic feasibility, performance, and commercialization still remain. The technical limitations that prevent the broad acceptance of RES-RO systems can be broken down into the following areas:

- Operability over a large power envelope
- Robustness to feedwater variation (TDS, temperature, etc.)
- Management of multiple, often conflicting, requirements (load balancing, membrane operability, water quality, permeate flux)
- In-situ monitoring of membrane degradation and compensation via operations and chemicals
- Reduction in cost of water (COW) for commercialization.

2.2 Scope of Program

An approach to interfacing RES and RO systems addresses the issues of operability, robustness, and management of membrane constraints with regard to power fluctuations, and must develop a highly flexible RO system in conjunction with energy management and operational strategies. An RES-RO system with advanced operations can be developed, but its effectiveness must be measured in terms of its energy consumption and ultimately COW. Hence, the overall goal of this study is to investigate multiple concepts for integrating wind turbines and RO desalination systems for feasibility and efficiency. This effort is unique in that it addresses the constraints of variable power input on desalination system operation to arrive at a process that can accommodate a maximum level of wind turbine power variation and remain economically viable. A principal motivation of this project is the simplicity and low cost with which water can be delivered where a major component of RO-based desalination system cost—energy—is reduced.

The program focuses on the following fundamental activities to address its objectives:

- Develop component models for the major components, including wind turbine system, RO system, energy recovery devices (ERDs), and energy storage of the RES-RO system and their integration into a system-level concept.
- The component models include wind turbine system, RO system, energy recovery devices, and energy storage.
- Develop an integrated energy and water cost model that can be used to evaluate and trade off various RES-RO configurations.
- Develop and analyze various RES-RO configurations as to their robustness to power fluctuations and ability to meet water quality requirements with the lowest COW.
- Develop a methodology to size, evaluate, and operate an RES-RO system in operational modes such as grid connected, grid connected with direct coupling, and grid isolated with energy storage.

These activities and the corresponding results are described in the following sections. Section 3 provides a description of the component models that are used to analyze the RES-RO system. Section 4 provides details about the integrated energy and water cost model. Section 4

highlights the assumptions in the cost analysis for the energy and water portions of the RES-RO system. Section 5 describes the RES-RO configurations that have been investigated for this concept study. The nominal operating points associated with each configuration and the operational design space are described. Section 5 considers seawater and brackish water conditions. For developing a methodology to size a RES-RO system and its operating strategy, the most cost-effective seawater RES-RO configuration is chosen. The design optimization associated with the selected configuration is described in Section 6. In Section 6, design optimization and cost analysis for grid-connected, grid-connected with direct coupling, and grid-isolated operational scenarios are described. Section 7 summarizes the conclusions of the concept study and Section 8 highlights potential avenues for future work.

3 Model Description

3.1 Overview of Required Models

In this section, we present a brief description of the models used in later sections to:

1. Develop a methodology to design and analyze hybrid wind-RO systems that handle all the physical constraints and the process economy simultaneously.
2. Define the operating space of a flexible RO system and explore it to achieve maximum performance.
3. Develop a realistic wind-RO COW that accounts for fluctuations in available power and product water flow rate and quality.
4. Develop operating strategies for minimizing COW.

The complexity of the models has been adjusted to give accurate physical representation for these objectives, without incurring unnecessary computational effort. More precisely, the performance of the RO process may be insensitive to fast transients in the power electronics that may achieve their steady-state operation in a few milliseconds. In these cases, standard model reduction techniques were applied to eliminate dynamic behaviors that would render simulations impractical without improving modeling accuracy. The main focus has been to capture cause-and-effect behavior of wind power variations on membrane performance and RO economy. Thus, models of dynamics with time scales of 0.1 s or shorter; for example, fast transients in the electrical systems, have been greatly simplified.

3.2 Component Model Description

3.2.1 Wind Model

Wind speed is highly variable, both geographically and temporally, and varies over a multitude of temporal and spatial time scales. In terms of using a wind turbine to generate power, this variation is amplified by the fact that the available energy in the wind varies as the cube of the wind speed. Consequently, the location of a wind farm or any other plant that relies on the exploitation of the wind resource for power generation must be considered to ensure superior economic performance.

Wind is driven by differences in the temperature of the Earth's surface. Geographic variations in wind speed thus originate in differences in solar exposure between geographic regions. Surface heating by the sun is stronger during the daytime, close to the equator, and on land masses. Warm air rises and circulates in the atmosphere before it sinks back to cooler regions. This results in various wind characteristics such as:

- A daily peak in wind speed caused by the Earth's rotation
- Characteristic wind directions in various that are caused by the air flow between the poles and the equator
- Local wind effects such as characteristic diurnal wind speeds near coasts or in mountains that are caused by the nonuniformity of the Earth's surface

- Surface roughness and the nature of the terrain in specific locations such as mountains or forests also affect the variation of the wind speed.

From a temporal point of view, wind speeds vary over several time scales[7]. Of particular interest are the annual variations in wind speed, which are used in the next sections to estimate the average annual power generation by a wind turbine, and, further, to find an annual average COW produced with a wind-powered water desalination plant. Also of interest are short-term (turbulent) variations in the wind speed, as their models represent the basis for generating time-dependent wind speed profiles that are used to obtain the dynamic simulation results presented in the sections to follow.

- In some locations, a very **slow long-term** (year-to-year) variation of the wind can occur. Such effects are not easy to estimate or predict, given the limited historical data. Long-term changes in wind speed are induced by climate change (global warming) and global climate phenomena like *el nino*. Long-term variations in wind speed are not accounted for in the present calculations.
- **Annual and Seasonal Variations**: Although year-to-year variations in the annual mean wind speeds are hard to predict, wind speed variations during one year can be well characterized statistically. The Weibull distribution gives a good representation of the distribution of mean wind speeds over a year (the mean wind speed is the wind speed averaged over a short period of time, typically 10 min). The Weibull probability density function in Eq. 3-1

$$f(\overline{V}) = k\frac{\overline{V}^{k-1}}{A^k}\exp\left(-\left(\frac{\overline{V}}{A}\right)^k\right) \qquad \text{Eq. 3-1}$$

can be used to determine that the average yearly wind speed for a specific location (site) in Eq. 3-2,

$$\overline{\overline{V}} = \int_0^\infty \overline{V} f(\overline{V}) d\overline{V} \qquad \text{Eq. 3-2}$$

and the probability of the mean wind speed at a site be within a certain wind speed range $[\overline{V}_1, \overline{V}_2]$ in Eq. 3-3.

$$P_{1,2} = \int_{\overline{V}_1}^{\overline{V}_2} f(\overline{V}) d\overline{V} \qquad \text{Eq. 3-3}$$

The scale parameter A and the shape parameter k are determined experimentally from wind speed measurements and are site specific. If k is exactly 2, the distribution is known as a Rayleigh distribution, and is in fact typical to many locations.

- **Synoptic and Diurnal Variations**: Over intervals shorter than one year, wind speed changes are more random and, evidently, less predictable. Considering a spectral approach to the analysis of wind speeds at a certain site, a peak in the frequency spectrum of wind is often seen around four days. This peak corresponds to relatively

short-term variations in the wind speed, called synoptic variations, which are associated with large-scale weather changes such as the appearance or disappearance of areas with high or low atmospheric pressure and weather fronts moving across the Earth's surface. Many locations also show large diurnal peaks that are driven by local thermal effects. Because there is no generally valid model, and because synoptic and diurnal variations in wind speed depend on location, they are not considered in this work.

- Changes over seconds and minutes occur as well. These wind speed fluctuations are called **turbulence**. Over short time intervals (a few seconds to about 10 minutes), wind speed can be described as the sum of the mean wind speed $\overline{V}$ (taken as a 10-min average) and the turbulent variation of the wind speed,

  $$V(t) = \overline{V} + V_0(t).$$

  In this expression, turbulent variations of the wind have a zero mean when averaged over 10 minutes.

The principal causes of turbulence are the friction between moving air masses and the Earth's surface and the thermal effects that cause air masses to move vertically as a result of temperature and density gradients between the atmospheric layers. These effects are often interconnected.

Turbulence is a complex stochastic phenomenon that cannot be characterized in terms of deterministic equations; therefore, statistical methods are used. Turbulence is well described mathematically by its intensity and by power spectral density (PSD).

Turbulence intensity is a measure of the overall level of turbulence. It is defined in Eq. 3-4 as:

$$I = \frac{\sigma}{\overline{V}} \qquad \text{Eq. 3-4}$$

where σ is the standard deviation of wind speed variations about the mean wind speed $\overline{V}$, usually defined as a 10-min average.

Turbulence intensity depends on the roughness of the ground surface, on the height above the surface, and on topographical features such as hills or mountains and local features, including trees and buildings.

The turbulence intensity contains no temporal information; i.e., data regarding the frequency of wind speed change. This information is given by the turbulence power spectral density function (PSD), *S(f)*. A power spectral density model is also needed to generate wind speed time series that depend on different mean wind speeds $\overline{V}$ and turbulence intensities *I*.

One commonly used power spectral density model is the one proposed by Kaimal. The Kaimal PSD is given in Eq. 3-5 by:

$$S(f) = \sigma^2 \frac{4L_1/\overline{V}}{(1 + 6fL_1/\overline{V})^{5/3}} \qquad \text{Eq. 3-5}$$

where

S = the longitudinal velocity spectrum

σ = is the standard deviation of wind speed

$\overline{V}$ = the mean wind speed

f = the frequency (in Hz)

Another commonly accepted PSD model is the one proposed by von Karman, which is given in Eq. 3-6 by:

$$S(f) = \sigma^2 \frac{4L_2/\overline{V}}{(1+70.8(fL_2/\overline{V})^2)^{5/6}} \quad \text{Eq. 3-6}$$

For this study, the values of the length scales in the PSD models above were considered to be $L_1 = 170\,m$ and $L_2 = 72.992m$.

3.2.1.1 WIND PROFILE GENERATION

WindSim, a software package developed at GE Energy, was used to generate wind speed profiles to test the transient operation of the wind-powered desalination plant. The profiles were generated with mean wind speeds of 1−27 m/s, considering a turbulence intensity of 0.1. Figures 3-1 and 3-2 present a 50-min wind profile for a mean speed of 5 m/s, along with the power spectrum of the wind and, for comparison purposes, the Kaimal PSD computed with the same mean wind speed and standard deviation.

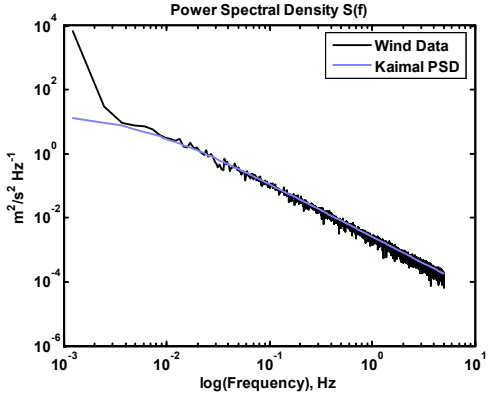

Figure 3-1. Wind PSD

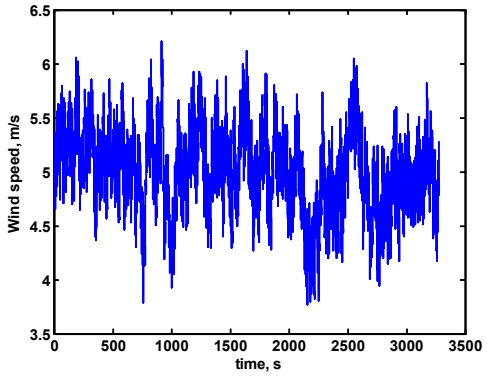

Figure 3-2. Wind speed profile generated with the Kaimal PSD model

The spectrum of the generated wind closely follows the Kaimal model for frequencies greater than 0.004 Hz, that is, for time scales of 5 min or shorter.

3.2.2 Wind Turbine Model (wind input to power output)

The GE 1.5-megawatt (MW) wind turbine has been used as a base to model the wind turbine for this wind desalination study. A doubly fed induction generator (DFIG), like the one used in the GE 1.5-MW wind turbine generator (WTG) is modeled for grid-connected study based on extensive GE knowledge and experience with the machine model. However, technical constraints that are associated with DFIG prevent it from being applied to the grid-isolated

case. To model the grid-isolated wind desalination system, a permanent magnet (PM) synchronous generator is modeled. The PM machine model is simulated based on literature and engineering experiences with similar turbine and generator parameters such as speed, voltage rating, and inertia, used by the GE 1.5-MW DFIG model to be comparable.

DFIG has AC excitation supplied by a back-to-back converter that is directly connected at the rotor winding. The PM synchronous generator has no external electric excitation system, and a back-to-back converter that is connected to its stator is used to interface it with the grid. The models provided have been simplified to reduce the computation time, so only the sections of the model with time constants that are significant to the rest of the system are left. Specifically, the very fast dynamics associated with the control of the generators and converters (current and voltage regulators) have been modeled as algebraic approximations of their response. Representation of the turbine mechanical controls has been simplified as well. The simplified model has a compound time constant of approximately 0.5 s. The models are valid only for balanced three-phase system time domain simulations. Although simplified, these models still allow the accurate representation of the effect of wind speed fluctuation on the electrical output of the WTG.

The WTG model has two major components:

- The wind turbine and turbine control model include simplified mechanical controls, rotor inertia, rotor speed, and wind power as a function of wind speed (power curve).
- The generator and converter model uses an algebraic model to approximate the long time constant dynamics (> 0.5 s) and steady-state performance of the generator, back-to-back converters, their interface with downstream system (desalination system and grid), and several hardware-related constraints. For the PM generator, simple dump load and battery characteristics are also included.

Figure 3-3 shows an overview block diagram of the model structure.

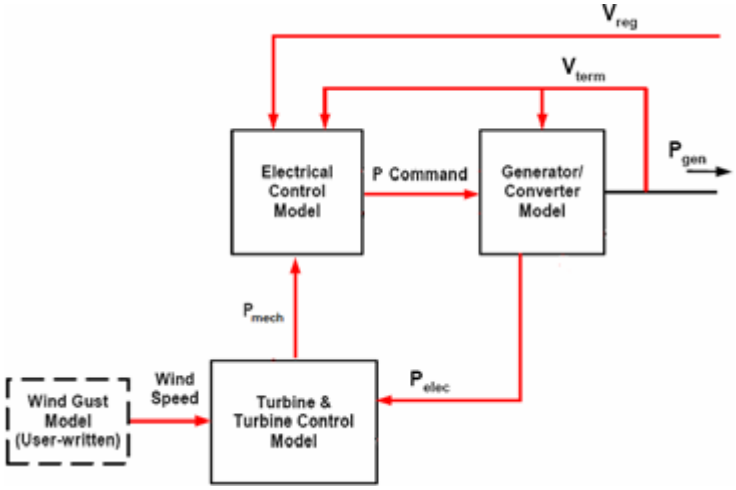

Figure 3-3. WTG model structure

3.2.2.1 WIND TURBINE AND TURBINE CONTROL MODEL

The wind turbine model provides a simplified representation of a complex electromechanical system. The block diagram is shown in Figure 3-4. In simple terms, the function of the wind

turbine is to extract as much power from the available wind as possible within its designed capability (current, voltage, and power). The wind turbine model represents the relevant controls and mechanical dynamics of the wind turbine.

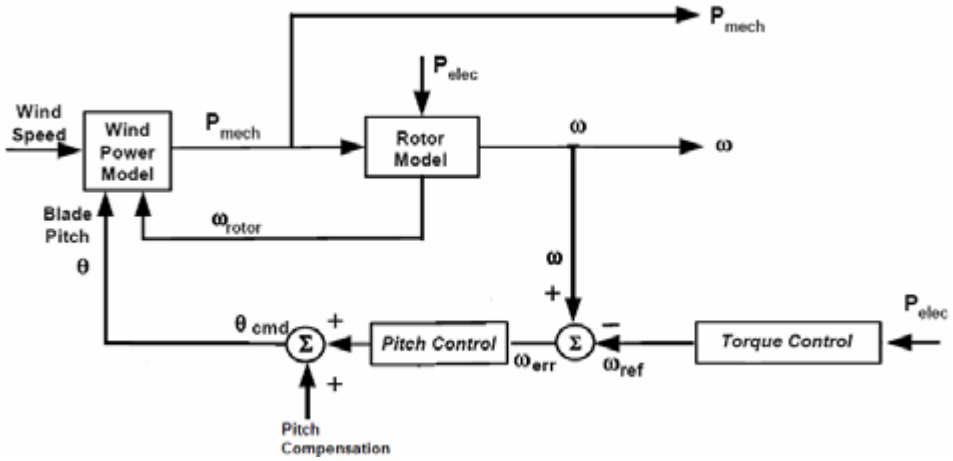

Figure 3-4. Wind turbine model block diagram

Rotor Model

The rotor model includes the rotor inertia for the WTG rotor, which uses the mechanical power and the electrical power to compute the rotor speed. A two-mass rotor model has been used with separate masses for the turbine and generator (Figure 3-5) to allow the possible mechanical oscillations in the WTG shaft to be simulated.

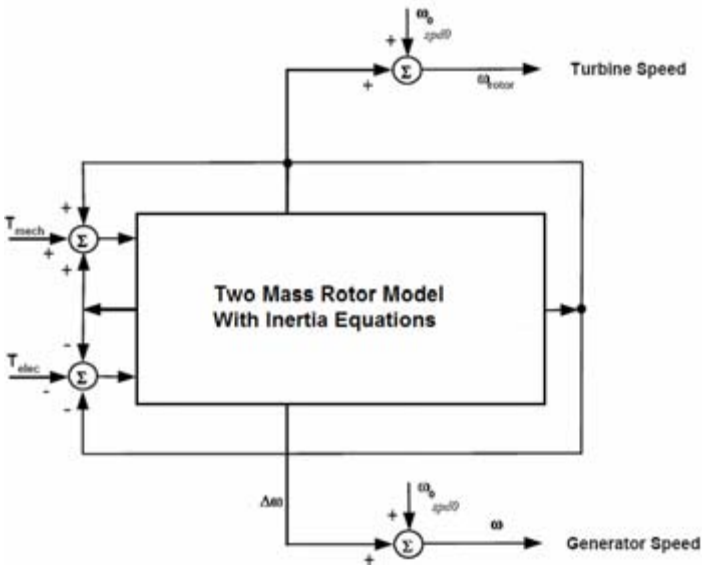

Figure 3-5. Two mass rotor model

Wind Power Module

The wind power module of the model computes the wind turbine mechanical power from the energy contained in the wind with the formula in Eq 3-7:

$$P = \frac{\rho}{2} A_r v_w^3 C_p(\lambda, \theta) \qquad \text{Eq. 3-7}$$

Where

P = the mechanical power extracted from the wind

ρ = the air density in kg/m^3

A_r = the area swept by the rotor blade in m^2

V_W = the wind speed in m/s

Cp = the power coefficient, which is a function of λ and θ

λ = the ratio of the rotor blade tip speed and the wind speed

θ = the blade pitch angle in degree

Cp is a characteristic of the wind turbine and is usually provided as a set of curves that relate Cp to λ with θ as a parameter. An example of a set of Cp curves is shown in Figure 3-6. Curves were fitted on a representative GE wind turbine Cp curve to find the best mathematical representation of the Cp curves used in the model.

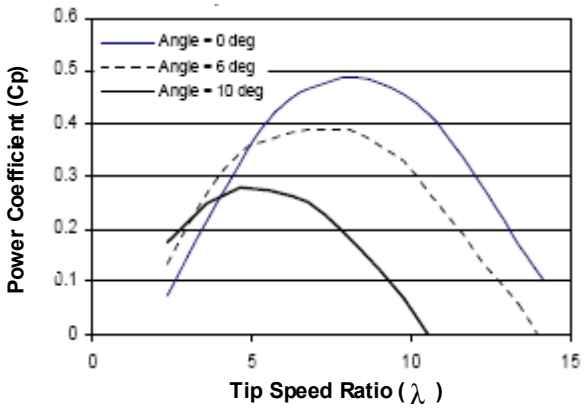

Figure 3-6. Wind power Cp curves

3.2.2.2 GENERATOR AND CONVERTER MODEL

Grid-Connected WTG Model

The generator is model based on GE 1.5-MW WTG, which is a DFIG. Its detailed electrical and control diagram is shown in Figure 3-7.

The generator model combines the behavior of the induction generator and the field converters, and ignores the fast transient such as the pulse width-modulated switching of the converters. This simplified model takes as inputs the mechanical power, electrical speed from the gearbox, and grid references such as voltage and frequency, and output the currents as well as the electrical power. Therefore, no mechanical state variables are modeled in this generator model. They are included in the turbine model as addressed in previous section.

As with conventional generator models, a set of equivalent circuits in d-q frame is used to represent the DFIG (Figure 3-8).

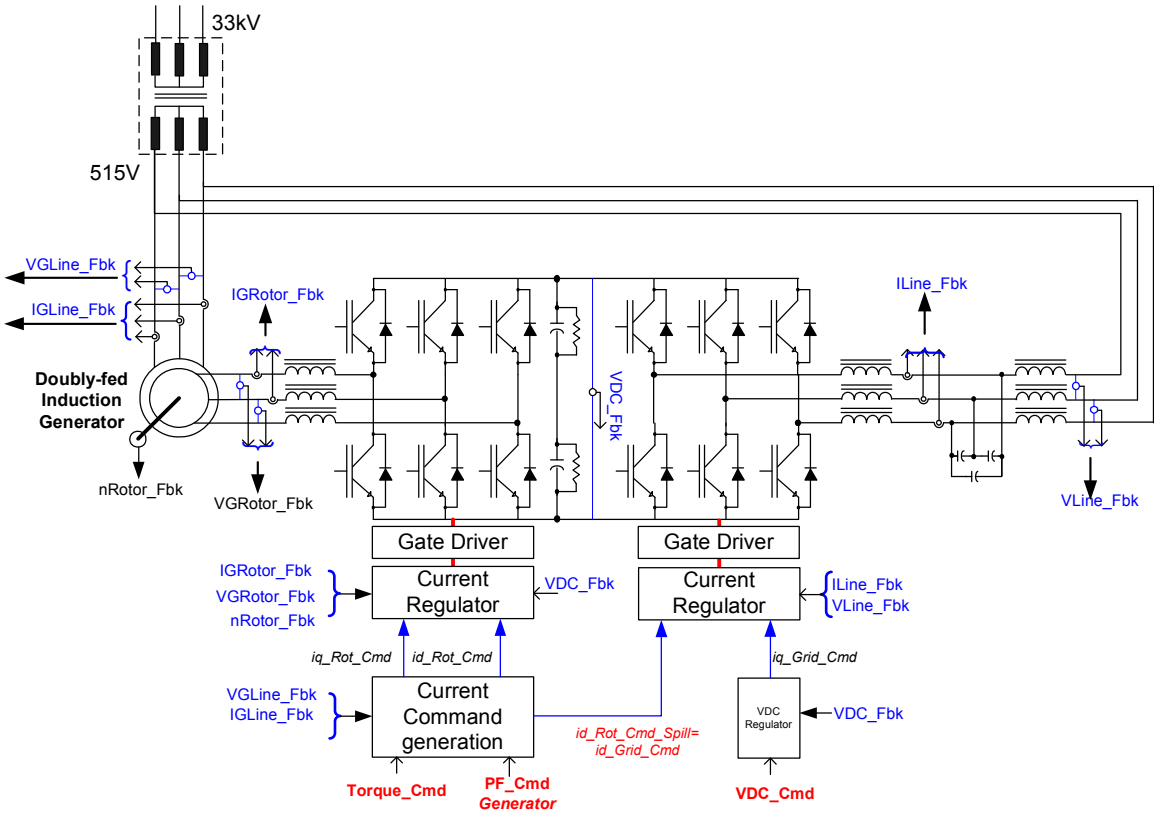

Figure 3-7. Diagram of DFIG and converters

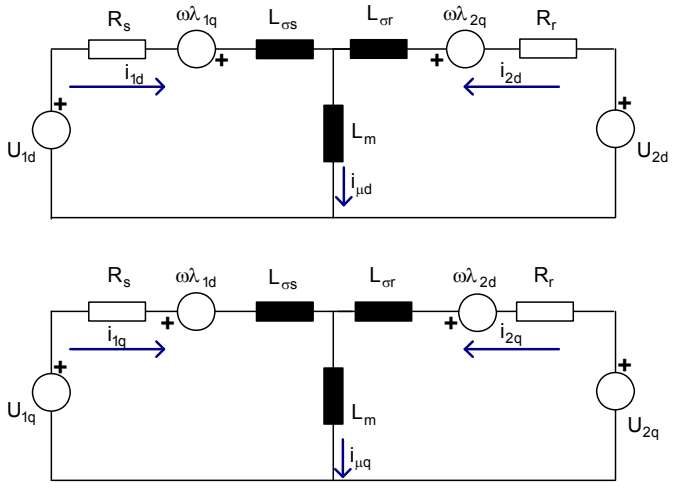

Figure 3-8. DFIG equivalent circuit

In the figure, λ is the flux linkage, U and i are the voltage and current, R and L represent the resistance and inductance. The related state equations for current, voltage, and flux linkage are derived from these equivalent circuits.

Several assumptions were made based on the characteristics of the DFIG and the needs of wind desalination studies:

- The system is grid connected, which is required by current DFIG technology.
- Fast transient of converters are ignored. The system represents the WTG response to wind speed variation at long time constant dynamics (> 0.5 s) and steady state.
- The system is represented in d-q frame and is referenced to the stator side.

Grid-Isolated WTG Model

The DFIG WTG, as presently implemented, cannot be operated as grid isolated. A PM generator and converter system was modeled to study a stand-alone wind desalination system. The detailed electrical and control diagram of the system is shown in Figure 3-9.

Because specific PM WTG design and manufacturing experience is limited, a simplified model was developed based on textbook theory[8] and engineering experience on related systems. The model applies Kirchoff's law and DC link voltage stability control theory to represent a typical PM generator and its converter interface with loads. DC link current and voltage between the back-to-back grid converters were used as the main system stability and control measures. The modeled system control block diagram is shown in Figure 3-10.

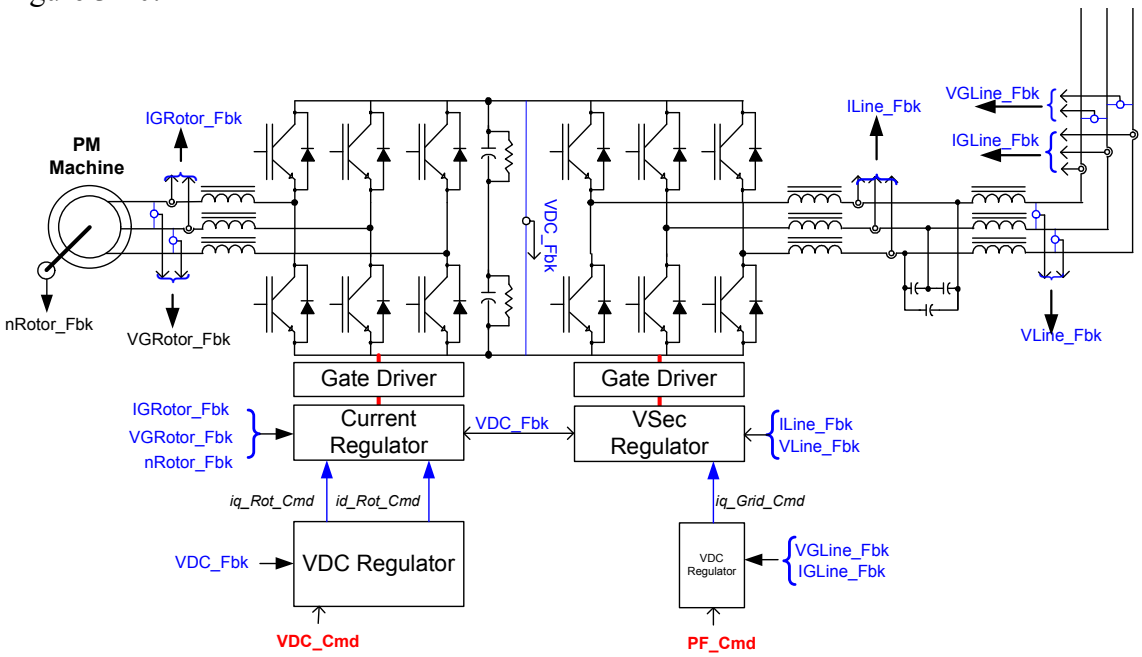

Figure 3-9. Diagram of PM synchronous generator

Due to limited design and manufacturing experience specifically on PM wind turbine generator, a simplified model was developed based on textbook theory [9] and engineering experience on related systems. The model applies Kirchoff's law and DC link voltage stability control theory to provide a representation of a typical PM generator and its converter interface with loads. DC link current and voltage between the back-to-back grid converters were used as main system stability and control measures. The modeled system control block diagram is shown in Figure 3-10.

The required sampling time of the simulated system forced a reduction in the order of the machine and inverter simulation. The only state variables considered are the DC link capacitor and the machine shaft mechanical inertia. The machine side inverter current control is represented only through its active current regulator (q-axis) that generates the current charging or discharging the DC link capacitor as well as the torque generated by the machine. The typical bandwidth for the actual current regulator is on the order of a thousand radian/s and can be replaced by a unity gain. The command for this current comes from a DC link voltage controller of much lower bandwidth that was included in the model.

The block diagram shows the computation of the DC link voltage. The integrator representing the mechanical shaft receives as inputs the torque from wind power, and the generator loading. The mechanical speed together with the inverter current is used to calculate the power fed from the machine into the DC bus circuit. The active power requested by the load through the grid side inverter is subtracted from this generator power and then divided by the DC link voltage. The result represents the actual current flowing from the machine and grid side inverter. The other contributors to charge or discharge of the capacitor are the current coming in and out of the battery, and the current to a dump whenever a predetermine over-voltage is reached. This can be reduced to Eq. 3-8. A simplified supervisory control was represented by a power flow limiter that controls the amount of active power sent to the desalination plant.

$$I_{DCLink} = I_{generator} - I_{load} + I_{battery} - I_{dumpload} \qquad \text{Eq. 3-8}$$

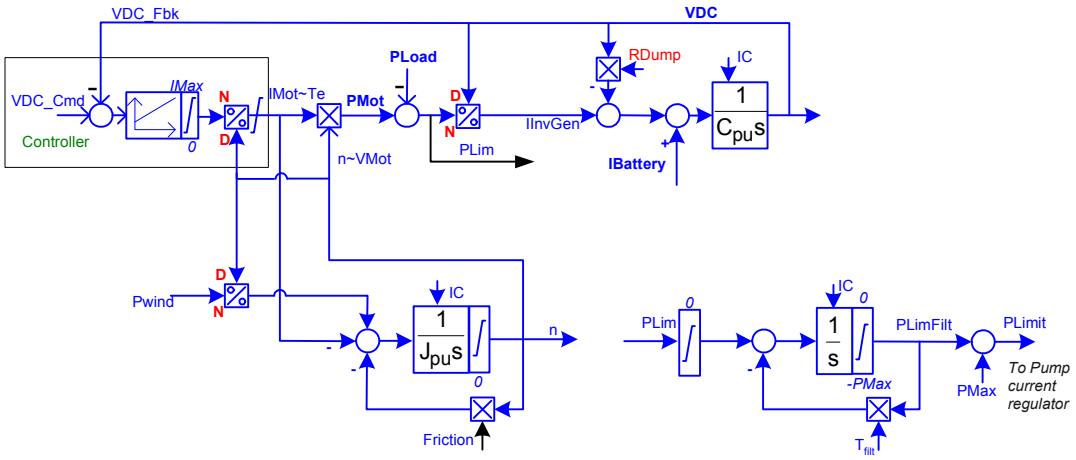

Figure 3-10. Control block diagram of PM generator model

The required sampling time of the simulated system forced a reduction in the order of the machine and inverter simulation. The only state variables considered are the DC link capacitor and the machine shaft mechanical inertia. The machine side inverter current control is represented only through its active current regulator (q-axis), which generates the current that charges or discharges the DC link capacitor as well as the torque generated by the machine. The typical bandwidth for the current regulator is about 1000 radian/s and can be

replaced by a unity gain. The command for this current comes from a DC link voltage controller of much lower bandwidth that was included in the model.

The block diagram shows the computation of the DC link voltage. The integrator that represents the mechanical shaft receives as inputs the torque from wind power and the generator loading. The mechanical speed and the inverter current are used to calculate the power fed from the machine into the DC bus circuit. The active power requested by the load through the grid side inverter is subtracted from this generator power and then divided by the DC link voltage. The result represents the current that flows from the machine and grid side inverter. The other contributors to charge or discharge of the capacitor are the current coming in and out of the battery, and the current to a dump whenever a predetermined overvoltage is reached. This can be reduced to Eq. 3-8. A simplified supervisory control was represented by a power flow limiter that controls the amount of active power sent to the desalination plant.

Several assumptions are made about the grid-isolated WTG model for the wind desalination analysis:

- The same parameters from the grid-connected WTG model are applied for this grid-isolated model to be comparable.
- Fast transients of the control are ignored; only the major states such as voltage regulation and turbine inertia are represented.
- The system represents the WTG response to wind speed variation at steady state (> 0.5 sec.).

STEADY-STATE MODEL VALIDATION

The grid-connected DFIG model was validated against the power curve of GE 1.5-MW WTG. The comparison result is shown in Figure 3-11. Given that the model is greatly simplified, the slight error is acceptable for this study.

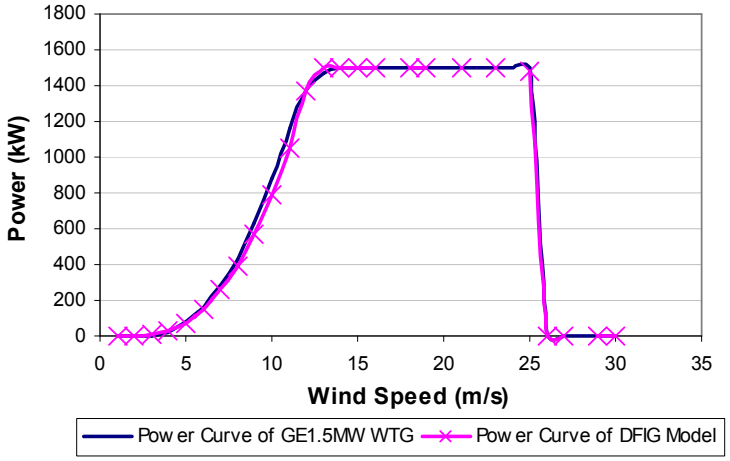

Figure 3-11. Model validation result

The similar power curve was also used for the grid-isolated system model, assuming that the PM WTG gives similar performance.

SUMMARY

This WTG system model includes the major components of a typical wind turbine: DFIG for grid-connected operation and PM generator for stand-alone operation. The DFIG is modeled with parameters that are based on extensive design information and from test data extracted from GE products. The PM generator and the inverter models were developed based on a reduced model that accounts only for the relatively slow electrical transients. They appear to give a realistic approximation of WTG behavior at a sampling time that is suitable for this wind desalination analysis.

3.2.3 Variable Speed Drive and Motor Model

The variable speed drives are major components in the electrical system and are used as prime movers for the desalination water pumps. They are controlled and constrained by the desalination system operation requirements and the WTG power and stability requirements.

A typical AC motor drive includes a rectifier, a large DC link capacitor, and a variable frequency inverter, which regulates the speed (frequency) and torque (current) of the motor. An illustration of this type of variable speed motor drive that uses an induction motor is shown in Figure 3-12.

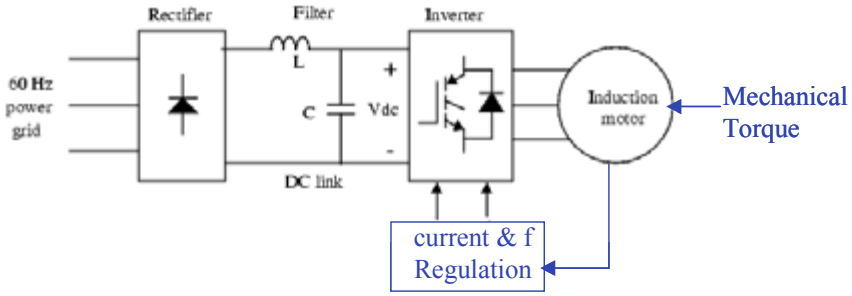

Figure 3-12. Typical variable speed motor drive and induction motor

Since the power electronic controls have very high bandwidth and given the desalination system has a relatively large time constant, fast transients such as the pulse width-modulated switching of the power electronics were simplified to capture only the speed (frequency) and torque (current) control behaviors of the machine. The simplified model is shown in Figure 3-13. The performance indicator control block regulates the speed by measuring the speed feedback from the motor. As already mentioned, the fast-acting current regulator was replaced by a gain with a variable torque limiter, whose value was provided by the WTG. This ensures the motor always operates within the available power supplied by the WTG. The output of the torque regulator is then subtracted from the load torque and the result fed to the integrator that represents the machine and pump inertia. One of the major improvements of this model is that it can consider variable power (current) from the WTG and regulate the current, and in turn control the torque and speed of the motor.

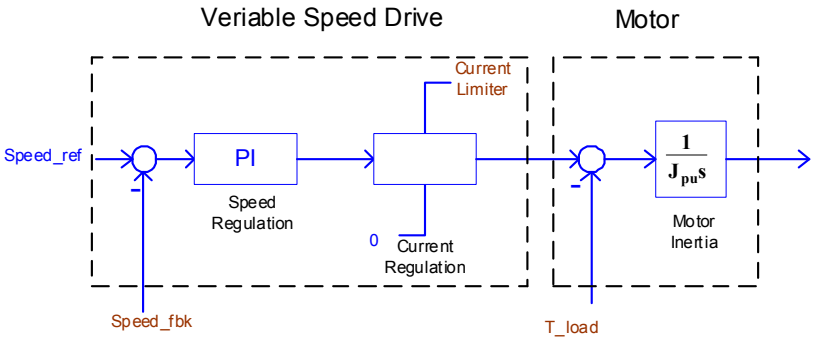

Figure 3-13. Simplified variable speed motor drive and motor model

3.2.4 Reverse Osmosis Membrane Module

The RO membrane module is a spiral-wound arrangement of a polyamide membrane (Figure 3-14), contained in a high-pressure cylindrical vessel (Figure 3-15). In this arrangement, high-salinity water is pressurized to overcome the osmotic pressure against the membrane surface. By means of the RO principle, low-salinity water permeates through the membrane and is collected in the central perforated pipe. For given feedwater state (pressure, concentration, and temperature), the membrane physical characteristics dictate the permeate flow and concentration.

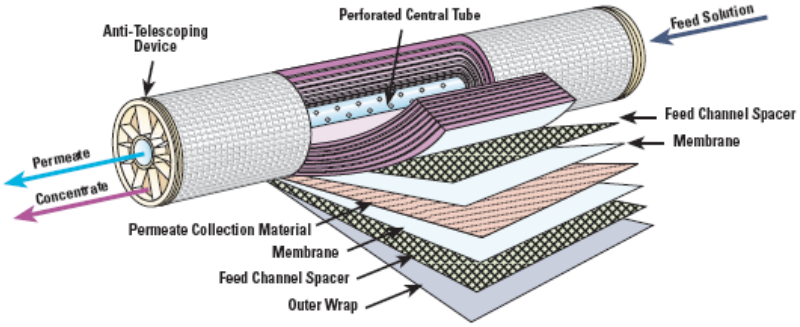

Figure 3-14. RO spiral-wound membrane arrangement

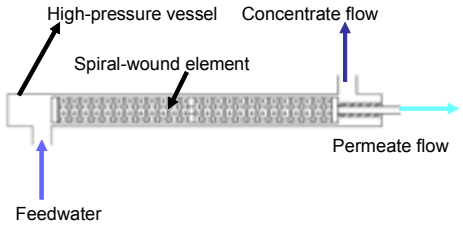

Figure 3-15. RO unit, membrane element contained in a high-pressure vessel

The RO elements are designed for continuous operation, receive a constant stream of feedwater, and generate constant streams of permeate and brine (or concentrate). Standard RO plants use constant operating pressures and flows, and may consider long-term adjustments to accommodate changes in the feedwater properties and changes in the filtration process caused by membrane degradation.

The model developed for the RO element predicts the concentrate pressure flowrates of permeate and concentrate streams and their corresponding concentrations given the feed state (flow rate, concentration, pressure, and temperature) and the permeate pressure. The functional relationship is given in Eq. 3-9 by

[Pc, Qp, Qc, Cp Cc] = RO_element(Qf, Cf, Pf, Pp, T) Eq. 3-9

where

Pc = Concentrate pressure, Pa

Qp = Permeate flow rate, m^3/s

Qc = Concentrate flow rate, m^3/s

Cp = Permeate pressure, Pa

Cc = Concentrate concentration, kg/m^3

Qf = Feed flow rate, m^3/s

Cf = Feed concentration, kg/m^3

Pf = Feed pressure, Pa

Pp = Permeate pressure, Pa

T = Feed temperature, °C

The membrane filtration behavior was predicted by the so called "solution-diffusion" model (see, for example, Meares 1976[10], Odendaal et al. 1996[11], Schwinge et al. 2004[12]). This model takes into account the effect of membrane polarization; that is, the increment of concentration near the membrane interface in the brine channel caused by the salt released by the permeate flow. Our model solves the following solution-diffusion equations (Eq. 3-10) to calculate membrane behavior.

$$
\begin{aligned}
J_w &= A\left\{p_f - p_p - \left[\pi\left(\bar{c}_m\right) - \pi\left(c_p\right)\right]\right\} \\
J_s &= J_w c_p = B\left(\bar{c}_m - c_p\right) \\
\bar{c}_m &= \left(\bar{c} - \bar{c} \cdot psg\right) e^{J_w/k} + psg\ \bar{c}
\end{aligned}
\qquad \text{Eq. 3-10}
$$

where

J_w	=	Water volumetric flux through the membrane, $cm^3/cm^2/s$
J_s	=	Salt mass flux through the membrane, $g/cm^2/s$
A	=	Water permeability, cm/s/atm
B	=	Salt permeability, cm/s
k	=	Mass transfer coefficient, cm/s
c	=	Concentration, g/l
p	=	Pressure, atm
$\bar{c}$	=	$(c_f + c_c)/2$
$\pi(c)$	=	Osmotic pressure corresponding to concentration c, atm
psg	=	c_p / c_m, Salt passage
Subindex f	=	Feed
Subindex p	=	Permeate
Subindex m	=	Membrane interface
Subindex c	=	Concentrate

The solution diffusion model depends critically on the membrane parameters k, A, and B. The mass transfer coefficient k depends on the water properties and the geometric dimensions of spiral-wound design. The permeabilities can be corrected by temperature and pressure. Details on these calculations can be found in Taniguchi et al. 2000[13] and Da Costa et al. 1994[14] and references therein. The model developed under this program incorporates correction of permeabilities by temperature effects.

The model for pressure drop in the brine channel, DP, is described by Eq. 3-11, where K is a constant.

$$DP = K\left(\frac{Q_f + Q_c}{2}\right)^{1.5} \qquad \text{Eq. 3-11}$$

There are several manufacturers of spiral-wound RO modules with similar performance characteristics. The RO models we developed are based on the commercial membrane elements TM820-370 for seawater and TM720-370 for brackish water, both by Toray Membrane America, Inc.

The spiral-wound elements need to satisfy a set of operational constraints to achieve expected performance in terms of product quality, energy efficiency, maintenance costs, and membrane life. Typical operational limits are available from the manufacturers (see, for example, Toray design guidelines in Section 9. Table 3-1 summarizes the set of RO element constraints for seawater application, and Table 3-2 summarize the set of RO

element constraints associated with brackish water that are used for the calculations in this report.

Table 3-1. Operational Limits for a Seawater Membrane Element

Parameter		Limit	Meaning
$c_m / \overline{c}$	<	1.2	Polarization
Pf	<	1200 psi	Feed pressure
Qc	>	15 gpm	Concentrate flow
J_w	<	20.6 gfd	Permeate flux through membrane
DP	<	10 psi	Pressure drop in the brine channel

Table 3-2. Operational Limits for a Brackish Water Membrane Element

Parameter		Limit	*MEANING*
$c_m / \overline{c}$	<	1.2	Polarization
Pf	<	600 psi	Feed pressure
Qc	>	15 gpm	Concentrate flow
J_w	<	28.3 gfd	Permeate flux through membrane
DP	<	10 psi	Pressure drop in the brine channel

The following simplifying assumptions have been used for the RO models:

- The input/output behavior of one spiral-wound module can be predicted in its whole operating range by using the solution-diffusion equations with average water state along the element.
- The flow within the RO element develops instantaneously for changes in the membrane pressure.
- The time response of concentration c to changes in the model inputs can be modeled as in Eq. 3-12, where c_{ss} is the steady-state value for concentration given by the solution-diffusion equations, s is the frequency variable for the Laplace transformation, and T is the time constant in seconds.

$$c = \frac{1}{T\,s + 1}\, c_{ss} \qquad \text{Eq. 3-12}$$

- The permeabilities A and B were assumed to be independent of the membrane pressure. Typical pressure corrections can be found in Taniguchi et al. 2001.[15]
- Membrane degradation effects are not considered.

The RO element model can be used to represent the behavior of membrane elements, since the transport parameters are calculated based on geometric data and nominal permeability values, which are typically available from membrane manufacturers. The current model has been adjusted to represent seawater membranes that are commercialized by GE Water. The predicted input-output behavior was within 2% of the values of pressures, concentrations, and flows given by comparable models used by GE Water at the tested operational points.

3.2.5 Reverse Osmosis Vessels and Banks

Under typical operating conditions, a single RO element produces a permeate flow that is around 7% of the feed flow, that is, the element operates at a 7% recovery. To achieve higher recoveries in a single stage and reduce the impact of pretreatment costs (and to reduce the vessel capital costs), arrangements of several RO elements connected in series are commonly used within the same vessel.

The physical model for a vessel with multiple RO elements is obtained by concatenation of several models of RO elements, and connects the concentrate channel of a given element to the feed channel of the following one. More precisely, a model of an n-element vessel is simply obtained by repeated use of the element model in Eq. 3-9, as follows in Eq. 3-13.

$$[Pc_k, Qp_k, Qc_k, Cp_k, Cc_k] = RO\_element(Qf_k, Cf_k, Pf_k, Pp_k, T) \quad \text{Eq. 3-13}$$

$$\text{with } Qf_k = Qc_{k-1},\ Cf_k = Cc_{k-1},\ Pf_k = Pc_{k-1}$$

The inputs to this vessel model are Qf_1, Cf_1, Pf_1, Pp_1 and T, and the outputs, Pc_n, Qp_n, Qc_n, Cp_n, Cc_n.

The maximum flow a vessel can handle is limited by the maximum diameter of the associated membrane element. Most spiral-wound manufacturers produce modules up to 8 in. diameter. For higher flows, several vessels are connected in parallel to achieve the desired flow (see Figure 3-16).

Figure 3-16. Banks of RO vessels in a seawater desalination plant

Models of an entire bank of RO vessels connected in parallel are obtained from the vessel model in Eq. 3-13. Under the assumption that all the vessels in the same bank have identical input/output behavior, the model for the bank is obtained by multiplying the feed, permeate, and concentrate flows by the number of vessels in the bank.

A seven-element vessel with membranes TM820-370 was developed and tested against the results of Toray software to determine the accuracy of the model in Eq. 3-13[16]. The pressures, concentrations, and flows for the individual elements were all within a 10% discrepancy with the Toray models.

The constraints in Table 3-3 are observed for the RO system (in addition of those in Table 3-1 and Table 3-2):

Table 3-3. RO System Constraints

Parameter		*LIMIT*	*RATIONALE FOR CONSTRAINT*
$\left\lvert \frac{dP_f}{dt} \right\rvert$	<	7.25 psi/s	Feed pressure rate of change at the first element in an RO bank
DP	<	58 psi	Pressure drop across an RO vessel

3.2.6 Energy Recovery

The RO desalination process is characterized by relatively small pressure drops across the vessel brine channel. That is, the concentrate flow conserves a large proportion of the energy available in the feedwater flow. Numerous ERDs have been designed to recover the energy in the concentrate stream and transfer it back to the feed flow stream to reduce the energy expended in feedwater pressurization (and hence, to improve the energy efficiency of RO desalination). These devices are commercially available in a wide range of technologies (see, for example, MacHarg 2001[17] and Liberman 2004[18] for ERD classifications and typical performances).

The most efficient ERDs use positive displacement technology and achieve efficiencies of 92%−96%. In this study, we model a work exchanger, which is a representative member of the positive displacement ERD class manufactured by Calder AG.

The work exchanger transfers energy from the concentrate flow to the feedwater flow via a set of cylindrical vessels and low-friction pistons that travel along the vessel by the pressure difference. Typically, while one vessel is pressurizing the feedwater in work stroke, the other is discarding the concentrate at a low pressure in flush stroke. The work exchanger uses a set of valves and a control system to reverse the piston movements at the end of each stroke to achieve nearly continuous operation (see Figure 3-17).

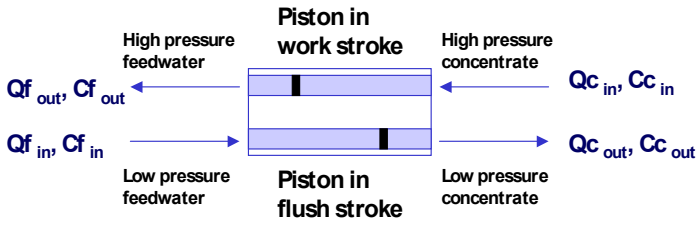

Figure 3-17. Work exchanger ERD

The ERD model calculates the feedwater input and output flows Qf_{in} and Qf_{out}, and feedwater outputs concentration $Cf_{out,}$ and pressure Pf_{out} as a function of the input concentrations Cf_{in}, Cc_{in} and the pressures Pc_{in}, Pf_{in}, Pc_{out}. The functional relationship of this model is given in Eq. 3-14 by

$$[Qc_{in}, Qf_{out}, Cf_{out}, Pf_{out}] = WEER\ (Cc_{in}, Cf_{in}, Pc_{in}, Pf_{in}, Pc_{out}) \qquad \text{Eq. 3-14}$$

The ERD model accounts for leakage flow in the valves, mixing between concentrate and feedwater within the vessel, and overall pressure/flow characteristics, as given by the product specifications[19].

The model in Eq. 3-14 is static, and is assumed that the flow within the ERD develops instantaneously with changes in the input and output pressures.

3.2.7 Water Pumps

Models for the water pumps are necessary to represent the pressure heads obtained by the high-pressure, booster, and interstage pumps at design and off-design conditions, for any given rotational speed and flow. The pump models have the functional representation shown in Eq. 3-15:

$$[H, \eta, P, T] = PMP\_HP(Q,N) \qquad \text{Eq. 3-15}$$

where

H = Pressure head across the pump, psi

η = Pump efficiency

P = Power consumed, W

T = Torque, lb ft

The pump model developed for this program uses a parametric implementation of pump characteristics that is easily adapted for different commercial products and uses standard corrections for speed and flow at off-design conditions (see Veres 1994[20] and Karassik et al. 1976[21]). For the RO configurations presented in the following sections, pump models were developed according to the pump characteristics provided by the pump manufacturer FEDCO.

3.2.8 Energy Storage

A simple battery model was developed to study the impact of energy storage in the operating strategies for grid-connected and grid-isolated wind turbine configuration.

The battery model has only one state, the battery charge x_c and is given by Eq. 3-16:

$$\begin{aligned} \dot{x}_b &= B_p \\ \left|B_p\right| &\le B_{p\max} \\ x_{b\min} &\le x_b < x_{b\max} \end{aligned} \qquad \text{Eq. 3-16}$$

where

B_p = Power drawn from the battery, W

$B_{p\max}$ = Maximum charging and discharging rate for the battery, W

$x_{b\min}$ = Maximum charge, Joul

$x_{b\max}$ = Maximum charge, Joul

The battery model does not account for the effects of temperature, capacity, and efficiency degradation, which affect the performance of the cells.

3.2.9 Valves

The valve model calculates the flow Q as a function of the valve opening y, inlet and outlet pressures P1 and P2, according to Eq. 3-17[22]

$$Q = y\, C_v \sqrt{\frac{\left(P_1 - P_2\right)}{\rho}} \qquad \text{Eq. 3-17}$$

where

C_v = Valve flow coefficient

ρ = Density, kg/m^3

Q = Volumetric flow, m^3/s

3.2.10 Flow Junction

Flow junction models are used to predict the concentration and flow of two or more water streams converging to a single stream by mass balance of water and salt. The functional form is shown in Eq. 3-18:

$$[\text{Qout, Cout}] = \text{FJn(Q1, C1, …, Qn, Cn)} \qquad \text{Eq. 3-18}$$

where

C1 … Cn = Concentration of input streams 1 to n, kg/m^3

Q1 … Qn = Flow of input streams 1 to n, m^3/s

Cout = Concentration of output stream, kg/m^3

Qout = Flow of output stream, m^3/s

All the converging streams are assumed to be at the same pressure and temperature.

3.2.11 Flow Network

The flow network model is used to calculate pressures, flows, and concentrations throughout an RO plant under nominal and off-design conditions. The RO plant consists of a set of RO banks, pumps, valves, and flow junctions that are interconnected through pipes. The operating point of the system is dictated by the environmental variables (pressures, temperatures, and concentrations at the system interface) and by the set points of the available control knobs. Referring to Figure 3-18, for example, the external pressures are feed pressure P0, permeate pressure P15, and brine discharge pressure P16; the control variables are pump speeds N1 and N2, valve opening V1, and the number of active vessels S1.

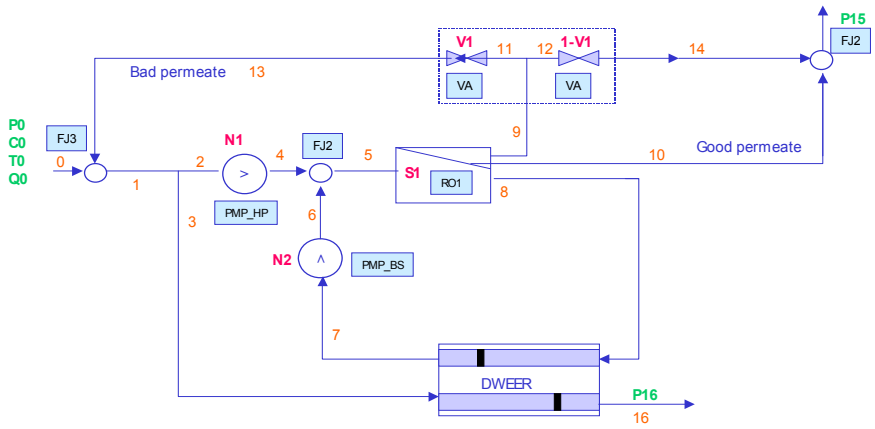

Figure 3-18. Flow network

The network model uses the Newton-Raphson method to solve a set of algebraic equations (the pressure/flow characteristics and the energy and mass balances of every component)[22].

The water temperature is assumed to remain constant throughout the RO system, and the friction losses are assumed to be small enough to neglect temperature changes in the water. The RO network's limits of operation are given by the maximum and minimum speeds of the electrical motors and pumps, maximum and minimum flows in the ERD, water quality requirements, membrane limitations, and maximum number of vessels.

4 Cost of Water Calculation

4.1 Steady-State Cost Model

The cost model for the wind-powered desalination system consists of two major parts, the capital costs associated with purchased equipment and installed facilities required, and the operating costs incurred to produce freshwater permeate. The basis for all capital and operating costs is in year-end 2004 U.S. dollars/m^3 product water. In cases where reference costs were found in previous years' costs, the costs were recalculated in year-end 2004 dollars by applying the Marshall and Swift Index[23]. The cost for a past year is multiplied by the ratio of the Marshall and Swift for 2004 over the Marshall and Swift index for that given year.

Each specific cost model is based on the model analysis of the combined wind-RO system configuration. The wind power is used to drive a 1.5-MW electrical turbine that has a 36% capacity factor, which means that 540 kW of power are generated on average over the course of a year for a standard wind profile. Since each configuration is based on a 1.5-MW wind turbine system with 36% capacity factor, the steady-state analysis of the configuration gives the maximum output of water for that configuration and is the lower bound on the cost per unit water produced.

4.1.1 Capital Costs

4.1.1.1 Reverse osmosis system

The capital cost model for each configuration includes three major sections: the purchased equipment costs, the direct capital costs, and the indirect capital costs. When combined, these form the total capital investment. This is a standard method for capital cost estimation[24]. Purchased equipment sizes are determined from the requirements of each configuration and the associated costs are from several sources. The chemical storage tanks, permeate product tank, and cartridge filter costs come from the Matches Web site (www.matche.com)[25], which is known in the chemical process industry as a source for up-to-date estimates of equipment costs based on size and materials of construction. Pump costs are determined from correlation curves[24] and software calculations[26]. RO membranes and housing costs were determined directly from recent RO system analyses[27,28], and the ERD costs were determined from vendor information[29].

Once the capital costs for the RO, freight, and taxes (2% of purchased equipment costs) and miscellaneous charges (5% of purchased equipment costs) are added[24], the delivered equipment total costs are obtained for the RO system.

4.1.1.2 Energy system

The wind turbine costs were based on the 1.5-MW turbine models and were determined by internal GE cost models for this equipment. The main components of the WTG system are shown in Table 4-1. The battery systems for extra power in low wind conditions were determined from power calculations and costs from internal GE resources. The wind turbine capital costs encompass the cost of electricity produced by the turbine and are amortized over the assumed 20-year lifetime of the turbine system. In this way, no operating costs are

associated with wind-generated electricity, only with grid-connected electricity. Since these energy capital costs include delivery, taxes, installation, and financing, they are added to the direct and indirect capital costs of the RO system. In this way the capital costs for the energy system are separated from those of the RO system.

Table 4-1. Major Cost Components of a Wind Turbine System

Wind turbine cost components
Blades
Aerodynamic control system
Rotor hub
Miscellaneous costs (labor for factory assembly)
Low-speed shaft, bearings, and couplings
Gearbox
Generator
Mechanical braking system
Mainframe (chassis)
Yaw system, including drives, dampers, brakes, and bearings
Nacelle cover
Work platform
Tower
Control and electrical systems

4.1.1.3 Direct capital costs

Next, the direct capital costs are calculated[24] based on correlations for the chemical process industry, using the delivered equipment total costs as the basis. These costs include installation, instrumentation, controls, wiring, piping, valves, and facilities. The feed well development costs are also calculated here based on the flow requirement of feedwater and a 500 m^3/d flow for each well of depth 50 m[30]. Combining the delivered equipment total costs and the direct capital costs gives the total direct capital costs associated with the configuration. Table 4-2 shows the calculations for these costs as a percentage of the delivered equipment total (DET)[24].

4.1.1.4 Indirect capital costs

Indirect capital costs include engineering time, supervision, and contractor construction costs. These are estimated from the total direct capital costs[24]. Engineering, supervision, and contractor construction costs are each 30% of the total direct costs, respectively.

4.1.1.5 Total capital investment

The total of the direct and indirect capital costs, including the wind energy capital costs, is the total direct and indirect capital costs. The total fixed capital investment is found by adding a contingency factor to account for design issues, pricing changes, etc. (10% of the total direct and indirect capital costs). The working capital required for the project is the cash on hand for ongoing expenses incurred during construction and startup. It is 10% of the total fixed capital investment[24], and is added to the total fixed capital investment to yield the total capital investment. This total capital investment represents the sum of all these costs, and is the capital required to design, buy, install, and construct the wind-powered desalination configuration.

Table 4-2 Direct Capital Costs as a Percentage of DET Cost

Direct Capital Expenditure	% of DET
Installation	40
Instruments and Controls	20
Piping and Valves (installed)	30
Electrical	20
Buildings	10
Yard Improvements	20
Service Facilities	5

4.1.2 Operating Costs

The other portion of water costs for desalination is the operating costs incurred during plant operation. The first major component of operating costs is total fixed costs related to interest, taxes, insurance, depreciation, labor, and maintenance. The other major variable is operating cost, which includes raw materials, utilities, and waste disposal costs.

4.1.2.1 Interest on capital

Interest payments for capital are based on the total capital investment and the interest rate using an amortization factor, *a*, shown in Eq. 4-1[30]. The interest rate *i*, is taken as 8%, which is average for this type of cost estimation, and the plant lifetime *n* is taken as 20 years.

$$a = \frac{i(1+i)^n}{(1+i)^n - 1} \qquad \text{Eq. 4-1}$$

4.1.2.2 Labor and maintenance costs

Labor costs were determined from desalination industry standards/m^3 of water[30]. Supplies and general maintenance are taken as 20% and 4%, respectively, of labor costs. Replacement costs for a membrane system, a battery system, and the wind turbine system are accounted for in annual operating costs based on the lifetime of the equipment. The membranes are assumed to last three years, the battery system 10 years, and the wind turbine 20 years. The total cost for

replacement is then divided by the lifetime in years and expensed annually. Routine maintenance on the wind turbine is broken out separately and based on GE average costs for a 1.5-MW turbine system.

4.1.2.3 Taxes, insurance, and depreciation

Taxes and insurance are accounted for as 2% of total capital investment and depreciation is 10% of total capital investment[24].

4.1.2.4 Total fixed costs

Summing all interest, labor, maintenance, replacement, insurance, taxes, and depreciations costs yield the total fixed cost for annual operation. Since these costs are incurred independently of the RO system's production level, they are referred to as fixed costs.

4.1.2.5 Variable costs

Costs that depend on the level of plant production are referred to as variable costs. These include the costs of raw materials, waste disposal, and utilities. The total permeate production is calculated by the number of operating hours in a year and the hourly permeate flowrate determined by the model configuration. This amount of water is the steady-state production basis for the cost model.

The raw materials costs are based on chemical use for pre- and post-treatment of the water. In this model, the costs for a variety of chemicals have been included to meet any specific water treatment option. Sources for chemical costs are given in the references section[28,31–32]. For the configurations presented here, the two pretreatment chemicals used are sulfuric acid for pH adjustment and scale inhibitor to prevent fouling of the membrane system. Configuration model software from Toray Membrane America, Inc. determined the acid use, based on incoming feed and desired product pH of water[33]. Scale inhibitor use was taken as an average value of 0.05g/m^3 of permeate[30].

Waste disposal costs vary from site to site. In some sites, discharge of brine may be feasible (surface or well); in others waste disposal may be required. The model builds in a cost that can vary based on disposal amount and cost. For this model, an average of \$0.018/m^3 is used to estimate these costs based on the volume of brine[34]. Chemical cleaning is sometimes periodically needed, although not desired, as the plant must be shut down. Any waste chemical solutions must be disposed at a cost. This model assumes that at most 0.1% of the volume product water will be used for chemical cleaning purposes. These waste disposal costs are small, even if the volume is 1% of the total product, and represents fractions of a penny per cubic meter of product.

Wind-generated electricity costs are rolled into the wind turbine capital costs. Battery power is also accounted for in the capital costs. The only utility that is used is any grid electricity if the unit is connected to the grid and circumstances dictate that grid power should be used. In this case, the average COE is based on U.S. government statistics[35].

4.1.3 Total Cost

By adding the total fixed costs to the total variable costs (annual operating costs) per cubic meter of permeate water product, the total cost of manufacturing is obtained in U.S.$/m^3 (or alternatively per 1,000 U.S. gallons of water produced). This number is also compared to the costs obtained from several references over the last six years[27,30,34,36,37]. Costs from references are updated to end of year 2004 U.S. dollars by using the Marshal and Swift Index calculation.

4.1.4 Example Calculations

Tables 4-3−4-8 show example capital and manufacturing cost calculations for seawater and brackish water design configurations. The configurations will be described in more detail in section 5. The results shown here are the costs for the steady-state model configurations using a 1.5-MW turbine system as the source of power.

Table 4-3. Capital Costs for Seawater SW-WE-a1 Configuration

Equipment Type	Size	Eng. Units	Size	SI Units	Material	P (PSIG)	Qty	Unit Cost ($)	Total Cost ($)
Vessels									
Chemical Storage Tank 1 - Acids	100	Gallons	379	l	Glass Lined CS	15	1	9,000.00	9,000.00
Chemical Storage Tank 2 - Scale Inhib.	10	Gallons	38	l	316SS	15	1	8,500.00	8,500.00
Permeate Product Tank 3	500,000	Gallons	132	m^3	Lined CS	15	1	194,200.00	194,200.00
CO2 Stripper									
Vessel Sub-Total									**211,700.00**
Filter/RO Membrane									
Bag Filter - Pretreatment	200	Ft^2	18.58	m^2	PE/Duplex SS	35	1	37,840.00	37,840.00
RO-Membrane 1 820-370 50x6	111000	Ft^2	10312.5	m^2	Arom. Polyamide		300	600.00	180,000.00
RO-Membrane 2 820-370 38x6	84,360	Ft^2	7837.5	m^2	Arom. Polyamide		228	600.00	136,800.00
Housings	8	In (D)	20.32	cm	Duplex SS	1200	88	3,000.00	264,000.00
Filter/RO Sub-Total									**618,640.00**
Pumps									
Filter Feed Pump	3000	GPM	681	m^3/hr	Duplex SS	60	1	25,319.47	25,319.47
High Pressure RO Pump 1	650	GPM	148	m^3/hr	Duplex SS	1000	1	47,000.00	47,000.00
High Pressure RO Pump 2	650	GPM	148	m^3/hr	Duplex SS	1000	1	47,000.00	47,000.00
Energy Recovery Turbine 1	1900	GPM	432	m^3/hr	Duplex SS	57	1	144,750.00	144,750.00
Interstage Booster Pump	3000	GPM	681	m^3/hr	Duplex SS	845	1	28,433.63	28,433.63
Chemical Feed Pump 1	5	GPM	1.14	m^3/hr	316SS	60	1	2,030.97	2,030.97
Chemical Feed Pump 2	5	GPM	1.14	m^3/hr	316SS	60	1	2,030.97	2,030.97
Pump Sub-Total									**296,565.04**
Power Generation									
Wind Turbine System			1.502	MW	N/A		1	800,000.00	
Battery System			450	kW-hr	Lead-Acid		1	200.00	90,000.00
Wind Turbine Installation/Financing								700,000.00	
Power Generation Sub-Total								800,200.00	**90,000.00**
Purchased Equipment Total									**1,216,905.04**
Freight & Taxes									24,338.10
Miscellaneous									60,845.25
Delivered Equipment Total									**1,302,088.40**
Direct Costs									**($)**
Delivered Equipment Total									**1,302,088.40**
Installation									520,835.36
Insulation									0.00
Instruments & Controls									260,417.68
Piping/Valves (installed)					Duplex SS				390,626.52
Electrical									260,417.68
Buildings									130,208.84
Yard Improvements									260,417.68
Feed Well Construction							29	35,734.82	1,036,309.74
Service Facilities									65,104.42
Total Direct Cost									**4,226,426.31**
Indirect Costs									**($)**
Engineering & Supervision									1,267,927.89
Construction/Contractor Fees									1,267,927.89
Total Indirect Costs									**2,535,855.79**
Total Direct & Indirect Costs									**7,562,312.10**
Contingencies									756,231.21
Total Fixed Capital Investment									**8,318,543.31**
Working Capital									**924,282.59**
Total Capital Investment									**9,242,825.90**

Table 4-4. Manufacturing Costs for Seawater SW-WE-a1 Configuration

Operating Days			350			
Labor Hrs/yr			1500			
Ro Recovery (%)			40.0%			
Number of RO Stages			2			
RO Membrane Surface Area: m^2 (ft^2)			18150	195360		
Plant Capacity, m^3/day:	(gal/day)		5723	1,512,021		
Feed Water, m^3/day:	(gal/day)		14307.5	3,780,053		
Brine Water, m^3/day:	(gal/day)		8584.5	2,268,032		
Feed Flow Rate, GPM:			2625.0			
Permeate Flow Rate, GPM:			1050.0			
Brine Flow Rate, GPM:			1575.0			
Plant Capacity,MMm^3/yr:	(MM gal/yr)		2.00	529.15		
Total Capital Investment Cost, MM US$:			9,242,825.90			
Plant Lifetime (yrs)			20.0			
Interest rate			8.0%			
Amortization Factor			0.10			
Annual Fixed Charges (MM$/yr)			941,402.23			
Annual Fixed Charges ($/m^3)			0.47			
Marshall & Swift Cost Index for 2004			1224			
					US$/m^3	
LABOR RELATED COSTS:						
RO Specific Cost of operating & maintenance labor					0.0550	
Total Labor Related					0.0550	
		Lifetime (Yrs)	Raw Cost ($)	(%)		
Supplies (% of Operating labor)				20.0%	0.0110	
Genearl Maintenance Material (% of OperatingLabor)				4.0%	0.0022	
Maintenance Battery Replacement Cost ($/m^3)		10			0.00449	
Maintenance Membrane Replacement Cost ($/m		3			0.0527	
Wind Turbine routine Maintenance			14,550.00		0.0073	
Wind turbine Warranty & Non-routine Maintenanc		20	33,230.00		0.0166	
Total					0.0943	
TOTAL MAINTENANCE & LABOR					0.1492	
Taxes & Insurance (%TFI)				2.0%	184,856.52	
Depreciation (%TFI)				10.0%	924,282.59	
CAPITAL RELATED COSTS ($/m^3)					0.5537	
TOTAL FIXED COSTS ($/m^3)					1.1729	
TOTAL MANUFACTURING COSTS ($/m^3) / ($/1000Gal)					1.1960	4.5275
Reference Total Manufacturing Costs ($/m3) / ($/1000Gal)						
Dietrich & Robert (1-10 MM Gal/day permeate scale, 2005)			Max cost is about this		1.51	5.70
Hafez & El Manharawy (4800 m3/day permeate scale, 2002)					1.42	5.37
Ettouney et al (4000 m3/day permeate scale, 1992)					2.68	10.15
Ettouney et al (4546 m3/day permeate scale, 1999)					1.48	5.59
Garcia-Rodriguez et al (3000 m3/day permeate scale, Wind RO system, 2001)					2.01	7.62

				Use	Use		
VARIABLE COSTS:		Density (kg/l)	Conc. wt%	g/m^3 Permeate	(Kg/day)	Matl $/Kg	$/m^3
RAW MATERIALS:							
HCl		1.20	35.0%	0.000	0.000	0.100	0.00000
H2SO4		1.83	93.0%	99.767	571.0	0.099	0.00990
NaOCl		1.00	100.0%	0.000	0.000	3.640	0.00000
Na2CO3		1.00	100.0%	0.000	0.000	0.221	0.00000
Na2S2O5		1.00	100.0%	0.000	0.000	1.544	0.00000
Lime		1.00	100.0%	0.000	0.000	0.077	0.00000
NaOH		1.00	100.0%	0.000	0.000	0.331	0.00000
Scale inhibitor		1.00	100.0%	0.050	0.286	3.440	0.00017
Ferric Sulfate		1.00	100.0%	0.000	0.000	0.210	0.00000
Total Raw Materials ($/m^3)							0.0101
Disposal Costs					m^3/m^3 Perm.	$/m^3	$/m^3
Brine Waste					0.6000	0.0180	0.0108
Chemical Cleaning Waste					0.0010	0.5000	0.0005
Total Waste Disposal							0.0113
TOTAL RAW MATERIALS & WASTE ($/m^3)							0.0214
Power Requirements:		Efficiency (%)	Flow GPM	P (kPA)	P (PSIA)	Power (kW)	Power (hP)
Filter Feed Pump		75.00%	2625	310.3	45	68.53	91.9
RO Feed Pumps		77.30%	1078.4	4833.2	701	425.52	570.6
Booster Pumps		75.00%	1912	289.6	42	46.59	62.5
Chemical Feed Pumps		75.00%	0.06	310.3	45	0.00	0.0018
Totals for Power Calcs				Power		540.6	725.0
Utilities:		(% Usage)	Units	Use (kW)	Total (kW-h)	$/Unit	$/m^3
Electricity	%	1.0%	kw-h	540.6	45,414	0.076	0.0017
Battery	Hours	10.0	kw-h	45.0	450		
TOTAL UTILITIES ($/m^3)							0.0017
TOTAL RAWS & UTILITIES ($/m^3)							0.0231
Wind Turbine Power Requirement							
Power Utilization (%)		36.0%					
Power Output (MW)		1.502					
	Specific Power Comparisons						
	SW-WE-a1 specific energy (kW-hr/m^3)				2.27		
	Ettouney et al (2002)				5		
	Dietrich & Robert (2005)				2-3		
	Garcia-Rodriguez et al (2001)				~4		
	Manth et al (2003)				2-4		
	MacHarg				2.5-3.5		

Table 4-5. Capital Costs for Seawater SW-WE-a3 Configuration

Equipment Type	Size	Eng. Units	Size	SI Units	Material	P (PSIG)	Qty	Unit Cost ($)	Total Cost ($)
Vessels									
Chemical Storage Tank 1 - Acids	100	Gallons	379	l	Glass Lined CS	15	1	9,000.00	9,000.00
Chemical Storage Tank 2 - Scale Inhib.	10	Gallons	38	l	316SS	15	1	8,500.00	8,500.00
Permeate Product Tank 3	500,000	Gallons	132	m^3	Lined CS	15	1	194,200.00	194,200.00
CO2 Stripper									
Vessel Sub-Total									**211,700.00**
Filter/RO Membrane									
Bag Filter - Pretreatment	200	Ft^2	18.58	m^2	PE/Duplex SS	35	1	37,840.00	37,840.00
RO-Membrane 1 820-370 52x7	111000	Ft^2	10312.5	m^2	Arom. Polyamide		364	600.00	218,400.00
Housings	8	In (D)	20.32	cm	Duplex SS	1200	52	3,000.00	156,000.00
Filter/RO Sub-Total									**412,240.00**
Pumps									
Filter Feed Pump	3000	GPM	681	m^3/hr	Duplex SS	60	1	25,319.47	25,319.47
High Pressure RO Pump 1	650	GPM	148	m^3/hr	Duplex SS	1000	1	47,000.00	47,000.00
High Pressure RO Pump 2	650	GPM	148	m^3/hr	Duplex SS	1000	1	47,000.00	47,000.00
Energy Recovery Turbine 1	1900	GPM	432	m^3/hr	Duplex SS	40	1	144,750.00	144,750.00
Dweer Booster Pump	2000	GPM	454	m^3/hr	Duplex SS	50	1	20,309.73	20,309.73
Chemical Feed Pump 1	5	GPM	1.14	m^3/hr	316SS	60	1	2,030.97	2,030.97
Chemical Feed Pump 2	5	GPM	1.14	m^3/hr	316SS	60	1	2,030.97	2,030.97
Pump Sub-Total									**288,441.15**
Power Generation									
Wind Turbine System			1.497	MW	N/A		1	800,000.00	
Battery System			450	kW-hr	Lead-Acid		1	200.00	90,000.00
Wind Turbine Installation/Financing								700,000.00	
Power Generation Sub-Total								800,200.00	**90,000.00**
Purchased Equipment Total									**1,002,381.15**
Freight & Taxes									20,047.62
Miscellaneous									50,119.06
Delivered Equipment Total									**1,072,547.83**
Direct Costs									**($)**
Delivered Equipment Total									**1,072,547.83**
Installation									429,019.13
Insulation									0.00
Instruments & Controls									214,509.57
Piping/Valves (installed)					Duplex SS				321,764.35
Electrical									214,509.57
Buildings									107,254.78
Yard Improvements									214,509.57
Feed Well Construction							27	35,734.82	964,840.10
Service Facilities									53,627.39
Total Direct Cost									**3,592,582.29**
Indirect Costs									**($)**
Engineering & Supervision									1,077,774.69
Construction/Contractor Fees									1,077,774.69
Total Indirect Costs									**2,155,549.37**
Total Direct & Indirect Costs									**7,248,131.66**
Contingencies									724,813.17
Total Fixed Capital Investment									**7,972,944.82**
Working Capital									**885,882.76**
Total Capital Investment ($)									**8,858,827.58**

Table 4-6. Manufacturing Costs for Seawater SW-WE-a3 Configuration

		Lifetime (Yrs)	Raw Cost ($)	(%)	US$/m³	
Operating Days			350			
Labor Hrs/yr			1500			
Ro Recovery (%)			40.0%			
Number of RO Stages			2			
RO Membrane Surface Area: m² (ft²)			10312	111000		
Plant Capacity, m³/day:	**(gal/day)**		5211.2	1,376,803		
Feed Water, m³/day:	**(gal/day)**		13028	3,442,008		
Brine Water, m³/day:	**(gal/day)**		7816.8	2,065,205		
Feed Flow Rate, GPM:			2390.3			
Permeate Flow Rate, GPM:			956.1			
Brine Flow Rate, GPM:			1434.2			
Plant Capacity,MMm³/yr:	**(MM gal/yr)**		1.82	481.82		
Total Capital Investment Cost, MM US$:			8,858,827.58			
Plant Lifetime (yrs)			20.0			
Interest rate			8.0%			
Amortization Factor			0.10			
Annual Fixed Charges (MM$/yr)			902,291.16			
Annual Fixed Charges ($/m³)			0.49			
Marshall & Swift Cost Index for 2004			1224			
LABOR RELATED COSTS:						
RO Specific Cost of operating & maintenance labor					0.0550	
Total Labor Related					0.0550	
Supplies (% of Operating labor)				20.0%	0.0110	
Genearl Maintenance Material (% of OperatingLabor)				4.0%	0.0022	
Maintenance Battery Replacement Cost ($/m³)		10			0.00493	
Maintenance Membrane Replacement Cost ($/m		3			0.0399	
Wind Turbine routine Maintenance			14,560.00		0.0080	
Wind turbine Warranty & Non-routine Maintenanc		20	33,230.00		0.0182	
Total					0.0842	
TOTAL MAINTENANCE & LABOR					0.1392	
Taxes & Insurance (%TFI)				2.0%	177,176.55	
Depreciation (%TFI)				10.0%	885,882.76	
CAPITAL RELATED COSTS ($/m³)					0.5828	
TOTAL FIXED COSTS ($/m³)					1.2168	
TOTAL MANUFACTURING COSTS ($/m³) / ($/1000Gal)					1.2359	4.6784
Reference Total Manufacturing Costs ($/m3) / ($/1000Gal)						
Dietrich & Robert (1-10 MM Gal/day permeate scale, 2005)			**Max cost is about this**		1.51	5.70
Hafez & El Manharawy (4800 m3/day permeate scale, 2002)					1.42	5.37
Ettouney et al (4000 m3/day permeate scale, 1992)					2.68	10.15
Ettouney et al (4546 m3/day permeate scale, 1999)					1.48	5.59
Garcia-Rodriguez et al (3000 m3/day permeate scale, Wind RO system, 2001)					2.01	7.62

VARIABLE COSTS:	Density (kg/l)	Conc. wt%	Use g/m³ Permeate	Use (Kg/day)	Matl $/Kg	$/m³
RAW MATERIALS:						
HCl	1.20	35.0%	0.000	0.0	0.100	0.00000
H2SO4	1.83	93.0%	58.187	303.2	0.099	0.00577
NaOCl	1.00	100.0%	0.000	0.0	3.640	0.00000
Na2CO3	1.00	100.0%	0.000	0.0	0.221	0.00000
Na2S2O5	1.00	100.0%	0.000	0.0	1.544	0.00000
Lime	1.00	100.0%	0.000	0.0	0.077	0.00000
NaOH	1.00	100.0%	0.000	0.0	0.331	0.00000
Scale inhibitor	1.00	100.0%	0.050	0.261	3.440	0.00017
Ferric Sulfate	1.00	100.0%	0.000	0.0	0.210	0.00000
Total Raw Materials ($/m³)						0.0059
Disposal Costs				m³/m³ Perm.	$/m³	$/m³
Brine Waste				0.6000	0.0180	0.0108
Chemical Cleaning Waste				0.0010	0.5000	0.0005
Total Waste Disposal						0.0113
TOTAL RAW MATERIALS & WASTE ($/m³)						0.0172
Power Requirements:	Efficiency (%)	Flow GPM	P (kPA)	P (PSIA)	Power (kW)	Power (hP)
Filter Feed Pump	75.00%	2390	310.3	45	62.40	83.7
RO Feed Pumps	77.20%	981.8	5681.3	824	455.97	611.5
Booster Pumps	75.00%	1408	172.4	25	20.42	27.4
Chemical Feed Pumps	75.00%	0.05	310.3	45	0.00	0.0018
Totals for Power Calcs					538.8	722.5
Utilities:	(Usage)	Units	Use (kW)	Total (kW-h)	$/Unit	$/m³
Electricity %	1.0%	kw-h	538.8	45,258	0.076	0.0019
Battery Hours	10.0	kw-h	45.0	450		
TOTAL UTILITIES ($/m³)						0.0019
TOTAL RAWS & UTILITIES ($/m³)						0.0191
Wind Turbine Power Requirement						
Power Utilization (%)	36.0%					
Power Output (MW)	1.497					
Specific Power (kWh/m³)	6.89					
Specific Power Comparisons						
SW-WE-a3 specific energy (kW-hr/m³)				2.48		
Ettouney et al (2002)				5		
Dietrich & Robert (2005)				2-3		
Garcia-Rodriguez et al (2001)				~4		
Manth et al (2003)				2-4		
MacHarg				2.5-3.5		

Table 4-7. Capital Costs for Brackish Water BW-WE-a1 Configuration

Equipment Type	Size	Eng. Units	Size	SI Units	Material	P (PSIG)	Qty	Unit Cost ($)	Total Cost ($)
Vessels									
Chemical Storage Tank 1 - Acids	1,000	Gallons	3785	l	Glass Lined CS	15	1	5,300.00	5,300.00
Chemical Storage Tank 2 - Scale Inhib.	10	Gallons	38	l	316SS	15	1	9,000.00	9,000.00
Permeate Product Tank 3	1,000,000	Gallons	264	m^3	Lined CS	15	1	246,300.00	246,300.00
CO2 Stripper									
Vessel Sub-Total									**260,600.00**
Filter/RO Membrane									
Bag Filter - Pretreatment	300	Ft^2	27.87	m^2	PE/Duplex SS	35	1	51,700.00	51,700.00
RO-Membrane 1 820-370 82x7	212380	Ft^2	19731.2	m^2	Arom. Polyamide		574	500.00	287,000.00
RO-Membrane 2 820-370 39x7	101,010	Ft^2	9384.4	m^2	Arom. Polyamide		273	500.00	136,500.00
Housings	8	In (D)	20.32	cm	Duplex SS	1200	121	3,000.00	363,000.00
Filter/RO Sub-Total									**838,200.00**
Pumps									
Filter Feed Pump	4000	GPM	909	m^3/hr	Duplex SS	60	1	37,234.51	37,234.51
High Pressure RO Pump 1	1070	GPM	243	m^3/hr	Duplex SS	250	1	41,000.00	41,000.00
High Pressure RO Pump 2	1070	GPM	243	m^3/hr	Duplex SS	250	1	41,000.00	41,000.00
High Pressure RO Pump 2	1070	GPM	243	m^3/hr	Duplex SS	250	1	41,000.00	41,000.00
Energy Recovery Turbine 1	690	GPM	157	m^3/hr	Duplex SS	24.7	1	144,750.00	144,750.00
DWEER BoosterPump	690	GPM	157	m^3/hr	Duplex SS	70	1	13,404.42	13,404.42
Chemical Feed Pump 1	40	GPM	9.09	m^3/hr	316SS	60	1	6,769.91	6,769.91
Chemical Feed Pump 2	5	GPM	1.14	m^3/hr	316SS	60	1	2,030.97	2,030.97
Pump Sub-Total									**327,189.82**
Power Generation									
Wind Turbine System			1.489	MW	N/A		1	800,000.00	
Battery System			450	kW-hr	Lead-Acid		1	200.00	90,000.00
Wind Turbine Installation/Financing								700,000.00	
Power Generation Sub-Total								800,200.00	**90,000.00**
Purchased Equipment Total									**1,515,989.82**
Freight & Taxes									30,319.80
Miscellaneous									75,799.49
Delivered Equipment Total									**1,622,109.11**
Direct Costs									**($)**
Delivered Equipment Total									**1,622,109.11**
Installation									648,843.64
Insulation									0.00
Instruments & Controls									324,421.82
Piping/Valves (installed)					Duplex SS				486,632.73
Electrical									324,421.82
Buildings									162,210.91
Yard Improvements									324,421.82
Well Construction							43	35,734.82	1,536,597.20
Service Facilities									81,105.46
Total Direct Cost									**5,510,764.52**
Indirect Costs									**($)**
Engineering & Supervision									1,653,229.36
Construction/Contractor Fees									1,653,229.36
Total Indirect Costs									**3,306,458.71**
Total Direct & Indirect Costs									**10,317,223.23**
Contingencies									1,031,722.32
Total Fixed Capital Investment									**11,348,945.55**
Working Capital									**1,260,993.95**
Total Capital Investment									**12,609,939.50**

Table 4-8. Manufacturing Costs for Brackish Water BW-WE-a1 Configuration

Operating Days			350			
Labor Hrs/yr			1500			
Ro Recovery (%)			82.0%			
Number of RO Stages			2			
RO Membrane Surface Area: m^2 (ft^2)			29116	313390		
Plant Capacity, m^3/day:	(gal/day)		17,432	4,605,548		
Feed Water, m^3/day:	(gal/day)		21,259	5,616,522		
Brine Water, m^3/day:	(gal/day)		3,827	1,010,974		
Feed Flow Rate, GPM:			3900.4			
Permeate Flow Rate, GPM:			3198.3			
Brine Flow Rate, GPM:			702.1			
Plant Capacity,MMm^3/yr:	(MM gal/yr)		6.10	1611.8		
Total Capital Investment Cost, MM US$:			12,609,939.50			
Plant Lifetime (yrs)			20.0			
Interest rate			8.0%			
Amortization Factor			0.10			
Annual Fixed Charges (MM$/yr)			1,284,350.19			
Annual Fixed Charges ($/m^3)			0.21			
Marshall & Swift Cost Index for 2004			1224			
					US$/m^3	
LABOR RELATED COSTS:						
RO Specific Cost of operating & maintenance labor					0.0550	
Total Labor Related					0.0550	
		Lifetime (Yrs)	Raw Cost ($)	(%)		
Supplies (% of Operating labor)				20.0%	0.0110	
Genearl Maintenance Material (% of OperatingLabor)				4.0%	0.0022	
Maintenance Battery Replacement Cost ($/m^3)		10			0.00148	
Maintenance Membrane Replacement Cost ($/m		3			0.0231	
Wind Turbine routine Maintenance			14,550.00		0.0024	
Wind turbine Warranty & Non-routine Maintenanc		20	33,230.00		0.0054	
Total					0.0456	
TOTAL MAINTENANCE & LABOR					0.1006	
Taxes & Insurance (%TFI)				2.0%	252,198.79	
Depreciation (%TFI)				10.0%	1,260,993.95	
CAPITAL RELATED COSTS ($/m^3)					0.2480	
TOTAL FIXED COSTS ($/m^3)					0.5591	
TOTAL MANUFACTURING COSTS ($/m^3) / ($/1000Gal)					0.5935	2.2468
Reference Total Manufacturing Costs ($/m3) / ($/1000Gal)						
Dietrich & Robert (2005)			Max cost is about this		1.00	3.80
Dietrich & Robert (2005)			Min cost is about this		0.11	0.40
Afonso et al (93,150 m3/day - large scale, 2004)					0.31	1.17

VARIABLE COSTS:	Density (kg/l)	Conc. wt%	Use g/m^3 Permeate	Use (Kg/day)	Mat'l $/Kg	$/m^3
RAW MATERIALS:						
HCl	1.20	35.0%	0.000	0.000	0.100	0.00000
H2SO4	1.83	93.0%	303.1	5,283	0.099	0.03007
NaOCl	1.00	100.0%	0.000	0.000	3.640	0.00000
Na2CO3	1.00	100.0%	0.000	0.000	0.221	0.00000
Na2S2O5	1.00	100.0%	0.000	0.000	1.544	0.00000
Lime	1.00	100.0%	0.000	0.000	0.077	0.00000
NaOH	1.00	100.0%	0.000	0.000	0.331	0.00000
Scale inhibitor	1.00	100.0%	0.010	0.174	3.440	0.00003
Ferric Sulfate	1.00	100.0%	0.000	0.000	0.210	0.00000
Total Raw Materials ($/m^3)						0.0301
Disposal Costs				m^3/m^3 Perm.	$/m^3	$/m^3
Brine Waste				0.1800	0.0180	0.0032
Chemical Cleaning Waste				0.0010	0.5000	0.0005
Total Waste Disposal						0.0037
TOTAL RAW MATERIALS & WASTE ($/m^3)						0.0338
Power Requirements:	Efficiency (%)	Flow GPM	P (kPA)	P (PSIA)	Power (kW)	Power (hP)
Filter Feed Pump	75.00%	3900	310.3	45	101.82	136.5
RO Feed Pumps	77.90%	3211.0	1647.8	239	428.65	574.8
Booster Pumps	61.70%	689	66.9	9.7	4.71	6.3
Chemical Feed Pumps	75.00%	31.00	310.3	45	0.81	1.0853
Totals for Power Calcs					536.0	718.8
Utilities:	(% Usage)	Units	Use (kW)	Total (kW-h)	$/Unit	$/m^3
Electricity %	1.0%	kw-h	536.0	45,023	0.076	0.0006
Battery Hours	10.0	kw-h	45.0	450		
TOTAL UTILITIES ($/m^3)						0.0006
TOTAL RAWS & UTILITIES ($/m^3)						0.0344
Wind Turbine Power Requirement						
Power Utilization (%)	36.0%					
Power Output (MW)	1.489					
Specific Power (kWh/m^3)	2.05					
Specific Power Comparisons						
BW-WE-a1 specific energy (kW-hr/m^3)				0.74		
Afonso et al (2004)				0.83		

4.1.5 Results

The overall costs for seawater and brackish water, respectively, are summarized in Table 4-9 and Table 4-10, along with the specific energy, which is defined as the ratio of the annual energy required to operate the plant to the total amount of permeate water produced. Comparisons to other calculations found in the references are also given. The reference calculations have been updated to year end 2004 U.S. dollars.[23]

The data show that the total manufacturing costs for a 1.5-MW wind-powered seawater desalination system are about $1.22/m^3 of product on the scale of 5200−5700 m^3/d of permeate product water, and using a specific energy of 2.3−2.5 kWh/m^3 of product water. This cost is about $0.20−0.80/m^3 lower than the references cited for nonwind-powered systems[27,30,34] and wind-powered systems[36]. The scale for the wind-powered system is somewhat larger than some of the references, and would thus have a somewhat lower cost. Also, specific factors such as energy costs and site development and waste factors can account

for the deviations from the wind-powered numbers. The specific energy consumption is on par with the references[27,30,36,38,39].

For brackish water, Table 4-10 gives a total manufacturing cost of about \$0.59/m^3, and using a specific energy consumption of 0.74 kWh/m^3 of product water. This is in line with estimates for nonwind-powered systems costs[27,37] and specific energy consumption[37], although there are few data points for comparison.

Table 4-9. Cost Comparisons for Seawater Desalination

Design or Reference	COW (\$/m^3)	Specific Energy (kWh/m^3)
SW-WE-a1	1.20	2.27
SW-WE-a3	1.24	2.48
Dietrich and Robert [27] (1-10 MM gal/d permeate scale, 2005)	1.51	2−3
Hafez and El Manharawy [34] (4800 m^3/d permeate scale, 2002)	1.42	
Ettouney et al. [30] (4000 m^3/d permeate scale, 1992)	2.68	5
Ettouney et al. [30] (4546 m^3/d permeate scale, 1999)	1.48	5
Garcia-Rodriguez et al. [36] (3000 m^3/d permeate scale, Wind RO system, 2001)	2.01	4
Manth et al. [**Error! Bookmark not defined.**] (2003)		2−4
MacHarg [**Error! Bookmark not defined.**]		2.5−3.5

Table 4-10. Cost Comparisons for Brackish Water Desalination

Design or Reference	COW (\$/m^3)	Specific Energy (kWh/m^3)
BW-WE-a1	0.59	0.74
Dietrich and Robert [27] Min Cost	0.11	
Dietrich and Robert [27] Max Cost	1.00	
Afonso et al. [37] (93,150 m^3/d - large scale, 2004)	0.31	0.83

4.2 Cost of Water and Wind Statistical Representation

Because of the stochastic nature and variability of the wind resource (and consequently the variability of the amount of power generated by a wind turbine) the RO water desalination plant is designed to operate at different levels of available power. In particular, for grid-isolated plants, the amount of permeate (freshwater obtained from desalination) will vary with the power available for running the plant, and, evidently, with the speed of the wind available for generating that power. Specifically, at higher wind speeds, when more power is available, a feed stream of higher flowrate can be processed and more permeate can be obtained, and vice-versa. Consequently, the COW produced by the RO desalination plant is to be expected to vary over time, and computing an average/levelized COW over one year of operation is essential to realistically evaluate the economic performance of wind-powered RO desalination.

In light of these facts, the objective of finding an optimal (from a COW point of view) wind-powered RO desalination plant configuration was addressed in two steps:

1. The optimal operating parameters of the RO desalination plant were computed, such that the maximum permeate flow is obtained for a given available power level.
2. The optimization results from step 1 and the cost models presented earlier, along with statistical wind speed data, were used to size the RO plant so the average yearly COW is minimized.

In step 1, the deterministic part of the system (the RO desalination plant) was analyzed, and the optimal operating parameters of the plant were computed, such that the maximum permeate flow is obtained for a given available power level. The input parameters available to control the plant operation are the speeds N (in rpm) of the pumps, the number S of RO vessels used in the RO banks, and the valve opening V of the permeate recycle streams. While we determined the optimal set points for these parameters at each power setting, we took care to satisfy all the economic and physical constraints imposed on the operation of the plant (see below for details particular to each configuration). Thus, the optimization problem in Eq. 4-1

$$\begin{aligned} &\max_{N,S,V} \ Permeate\,Flowrate \\ &subject\ \ to: \\ &\qquad Power = Available\,Power \\ &\qquad Operating\,Constraints \end{aligned} \qquad \text{Eq. 4-1}$$

was solved considering that the available power ranges of 70−1500 kW, and resulted in a table of optimal (from a maximum permeate flow rate point of view) input parameters as a function of the power available for operating the RO plant: Table 4-11 shows the prototype results.

In Table 4-11, index j refers to the equipment or stream number; for example, if several pumps are installed in the plant, each will have its optimal setting: pump 2 at available power P_1 would have the optimal rpm $N_{2,1}$.

Table 4-11. Optimization Data Output Format for RO Plant

Available Power, kW	Optimal N_j rpm	Optimal S_j (vessels)	Optimal recycle V_j	Maximum permeate flow, Q_p, gpm
P_1	$N_{j,1}$	$S_{i,1}$	$V_{i,1}$	$Q_{p,1}$
⋮	⋮	⋮	⋮	⋮
P_n	$N_{j,n}$	$S_{i,n}$	$V_{i,n}$	$Q_{p,n}$

In step 2, the statistical description of the wind resource was used to obtain an average/ levelized SCOW for a plant where S_k RO vessels are installed (Eq. 4-2):

$$SCOW_k = \frac{C_0(S_k) + \sum_{j=1}^{n} C_p(ROPower, \overline{V}_j, \$_e) \cdot w_j}{\overline{Q}_k} + \sum_{j=1}^{n} C_c(ROPower, \overline{V}_j) \cdot w_j \quad \text{Eq. 4-2}$$

where

$C_o(S_k)$ = the annual charges for a plant with S_k vessels, computed as the sum of the yearly fixed charges, capital depreciation, insurance premiums, and maintenance and warranty charges of the plant

$C_c(ROPower, \overline{V}_j)$ = the cost (per cubic meter of permeate) of chemicals, consumables, and labor for a plant operated at a (possibly wind-speed dependent) power consumption *ROPower*

$C_p(ROPower, \overline{V}_j, \$_e)$ = yearly cost of purchasing energy and the gains from selling energy, when the plant is operated at consumption *ROPower,* with the wind turbine producing the amount of power corresponding to the mean wind speed $\overline{V}_j$, and the grid energy prices given by $\$_e$.

$\overline{Q}_k = \sum_{j=1}^{n} Q_j(ROPower, \overline{V}_j) \cdot w_j$ is the average yearly or expected value of the permeate flow rate, computed under the same operating assumptions as above.

$C_o(S_k)$, $C_c(ROPower, \overline{V}_j)$, and $C_p(ROPower, \overline{V}_j, \$_e)$ are functional representations of the specific COW calculation algorithm presented in earlier in this section.

A total number of *n* mean wind speeds $\overline{V}_j$ are considered, with their respective Weibull probabilities $w_j(\overline{V}_j) = f(\overline{V}_j)$ *, so that $\sum_{j=1}^{n} w_j(\overline{V}_j) = 1$. [40] Hence, the average COW is

* $w_j(\overline{V}_j) = f(\overline{V}_j)$ effectively denotes the probability of the mean wind speed taking values in an infinitesimal interval around $\overline{V}_j$.

obtained as the sum of the annual plant charges, the expected values of chemical costs, energy costs, divided by the expected value of yearly permeate flow rate.

To determine the specific cost of water (SCOW), the power P_j generated by the wind turbine, for a given (Weibull-distributed) mean wind speed $\overline{V}_j$, is computed from the turbine power curve. The Weibull probability density function describes the distribution of mean wind speeds at a standard height (10 m); wind speeds are therefore scaled to obtain the corresponding mean speeds at the height of the turbine hub:

$$\overline{V}_{j,hub} = \overline{V}_j \left(\frac{10m}{h_{hub}} \right)^{\alpha} \qquad \text{Eq. 4-3}$$

where

$\alpha = 0.143$ = the vertical shear exponent

The power made available to and consumed by the RO plant, *ROPower,* and the power generated by the wind turbine, P_j, are equal only if a grid-isolated case with no energy storage is considered. For grid-connected configurations, the power consumption of the plant may at times exceed or be surpassed by the amount of power generated. When there is a mismatch between power production and consumption, the difference can be covered by purchasing energy from or selling energy to the grid. Also, energy can be drawn from or spent on charging a battery system. Energy purchases and sales have an impact on the SCOW, depending on the energy purchase and sale prices, $\$_e$, and are duly accounted for in the SCOW function. No cost is associated with disposing of the excess energy generated by the turbine; in case that energy cannot be sold to the grid.

The calculation of the SCOW also takes into account that the plant cost and the SCOW increase as the number of RO vessels installed in the plant, S_k, increases. In the cost calculations, the operation of the plant is assumed to be flexible with respect to the number of RO vessels used. That is, when S_k vessels are in the plant, any number $1<S_{actual}<S_k$ of vessels may be used to achieve the maximum permeate flow rate for *ROPower*, the power available.

When no grid connection is available, the plant will idle when the wind turbine does not generate power and no energy is stored, as the permeate flow rate is reduced to zero. The time intervals when the wind speed is too low for power generation (when the mean wind speed is below the generator cut-in speed) are also accounted for in computing the average SCOW. In such cases, SCOW is reduced to the specific fixed cost of the plant.

4.3 Grid Power Prices

The grid-connected configuration gives the system the flexibility to buy electricity when the wind speed is low, and sell the extra power when the wind speed is high. However, selling power depends on the contractual agreement between the power seller and the utility. The utility usually purchases the excess electricity at the wholesale or "avoided cost" price, which is much lower than the retail price. Some states have legislatures that require at least some utilities to offer net metering, which means that a customer who produces excess electricity can deliver it to the local utility, spinning the utility meter backward and gaining a credit,

which can be used later when power is needed from the grid. This provides the customer with full retail value for all the electricity produced. So far most net metering applies only to small wind turbine, PV or other generation sources.[41] This study assumed no net metering and that the extra power will be sold back to the grid at a negotiated price, which is assumed to be a small percentage of the buying price.

5 Wind Desalination Configurations

5.1 Overall System Requirements

Wind desalination may be a viable alternative for increasing the availability of potable water in inland and coastal regions. As such, different desalination topologies must be evaluated for these two cases. In the inland application, wind desalination will primarily be dedicated to the purification of brackish water, which is is typically defined to be less than 10,000 ppm of TDS. A potential complicating factor for inland and coastal areas is grid connectivity. Hence, understanding the operational impact on the desalination system under various scenarios is important. One configuration described in this section will be analyzed further with regard to the following grid connectivity scenarios:

- Wind turbine and desalination plant grid connected
- Wind turbine and desalination plant coupled with the capability to purchase energy from the grid
- Grid independence with energy storage.

To effectively examine these system variants, a set of topologies for seawater and brackish water conditions is investigated in this work. For the seawater case, a single-stage and a two-stage system are investigated. For brackish water, a two-stage system is investigated. Based on the design analysis, a single configuration is selected for further design with respect to plant sizing and operations. The methodology that is developed for the selected configuration is applicable to other configurations and presents a general framework for defining a wind desalination facility.

5.1.1 Design Goals and Design Process Overview

The main criteria for each wind-RO design are that it provides reasonable RO system parameters, is flexible to model inputs, and matches the power outputs of the wind turbine to the power requirements of the RO system. The design begins with the wind power available to accomplish these tasks. In this case a 1.5-MW wind turbine was chosen as the base-case power source because it is a standard GE model that is deployed in field applications and it allows for easy scale-up by employing a series of these turbines to produce the desired power. The output power of these turbine systems varies depending on the wind profile. For this case, a class II wind profile is assumed, which gives a turbine capacity factor of 36%. This means that the 1.5-MW turbine will provide on average 540 kW of power for the RO system.

Standard single- and two-stage systems were considered for the RO model. The single-stage system takes a saline feed and provides product permeate to meet specifications in a single pass; the two-stage system takes brine output from the first stage and further removes water from it to increase product output. Pumps are used at each stage to achieve proper pressures for RO. In addition, an ERD (dual work exchanger energy recovery [DWEER] or turbine type) is used to recover the output energy of the waste brine and pressurize feed into the membranes. Schematic designs of the two systems are shown in Figure 5-1 and Figure 5-2.

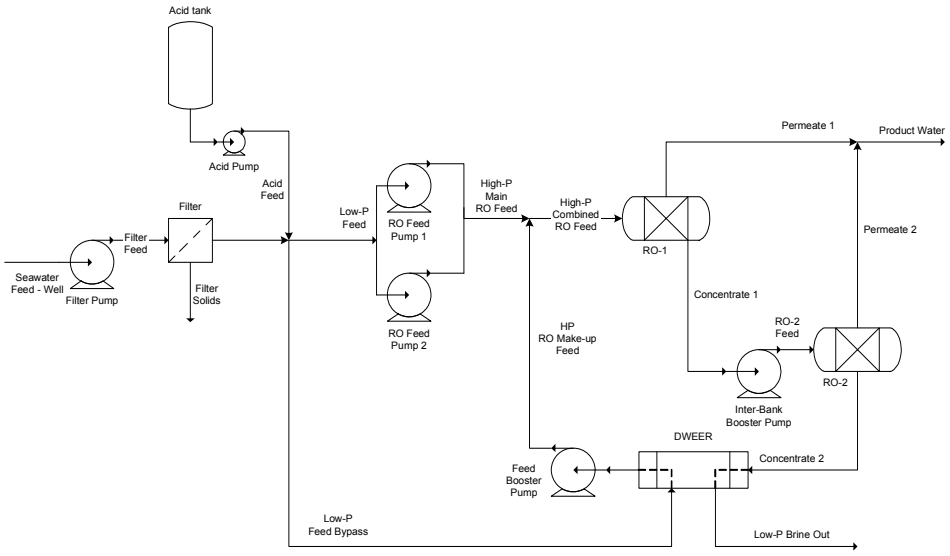

Figure 5-1. Schematic diagram of two-stage RO membrane system

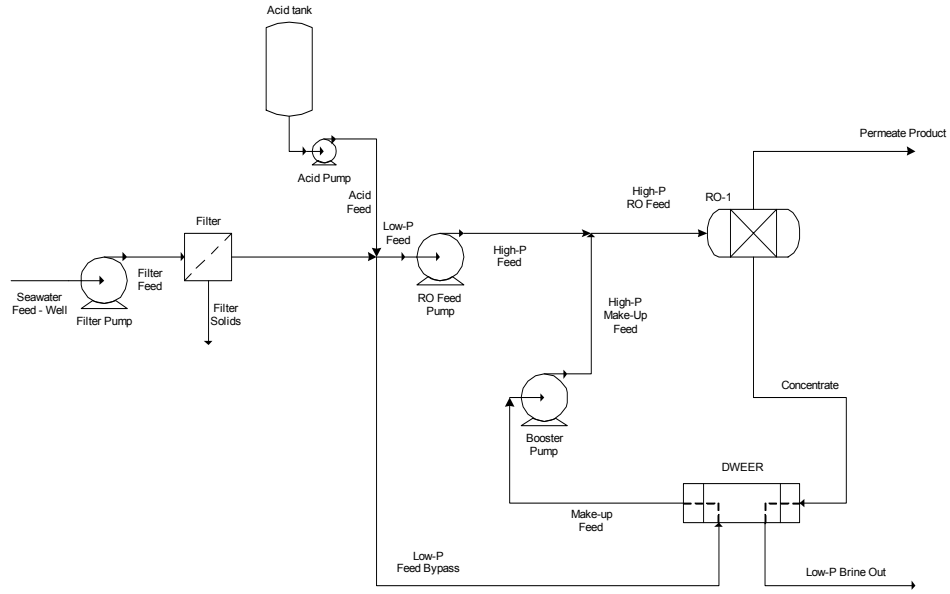

Figure 5-2. Schematic diagram of a single-stage RO membrane system

Power calculations on the pumps determine the amount of power required to pump a given flow through the RO system. The flow rates and pressures are set to nominal values that are in the ranges necessary for the RO to operate, with typical membrane recoveries of 35%−45% for seawater and 75%−85% for brackish water. This power is then compared to the available power from the wind turbine. The system flow is then adjusted and the power recalculated. This iteration is continued until the power requirements of the pumps in the RO system match the wind turbine output. The overall pump power calculation is given in Eq. 5-1.

$$P = \frac{H\,Q}{\varepsilon} \qquad \text{Eq. 5-1}$$

where

P = the power

H = the head pressure difference between the inlet and outlet streams

Q = the stream flow-rate

ε = the overall pump efficiency

The schematic energy iteration calculation is given in Figure 5-3. Once the nominal values are obtained from this power calculation, they are applied to specific steady-state design configurations and optimized with RO system calculation software[33] to arrive at a specific RO design that meets the design parameters for water quality and power requirements. When the design is optimized to meet these criteria, a capital and operating cost model is applied (see Section 4 of this report) to obtain an overall COW for this steady-state configuration.

With this baseline design and cost complete, the configuration is then simulated with the combined wind-RO system model to develop a transient configuration model that accounts for variations in wind, water output, and optimization strategies. A cost for each strategy is then developed.

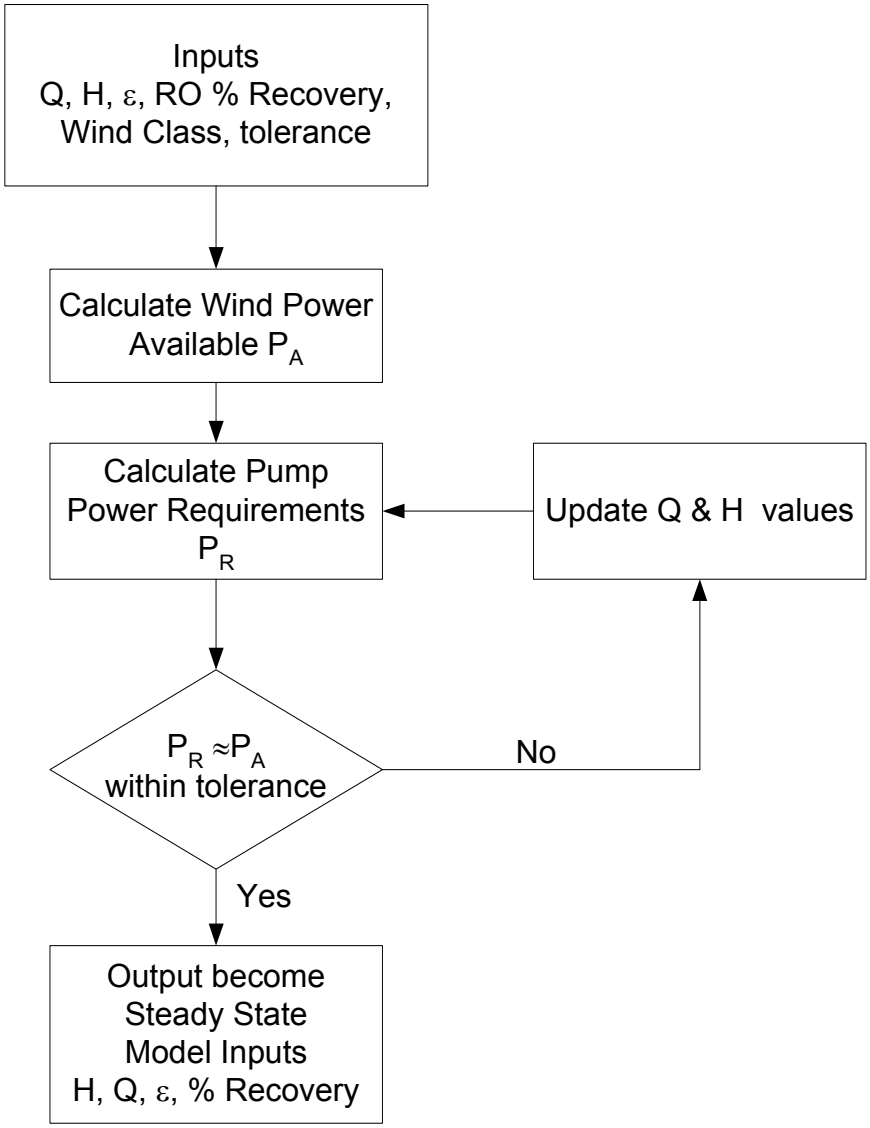

Figure 5-3. Flow chart for determining RO configuration inputs

5.1.2 Constraint Description

The analysis that follows explicitly accounts for the physical and operational constraints in the wind desalination system, including the power generation constraints in the wind turbine (Section 3.2.2), RO constraints (Table 3-1, Table 3-2, and Table 3-3), and speed limitations for the electrical drives and pumps. Some design parameters like maximum number of RO vessels were left unlimited, because the purpose of this section is to obtain entitlement analysis; sizing of these parameters is handled in Section 6.

5.2 Seawater

The seawater RO design objective is to obtain a viable commercial wind/RO system configuration that can provide purified product water at a cost that is competitive with traditionally powered RO systems. Because there is a plentiful supply of seawater in many

areas of the world where there is no power infrastructure, or where energy costs are high, designing a wind-powered RO system that can produce competitively priced water is desirable. The challenges are that seawater dissolved solids can vary greatly. Other solid contaminants also pose an issue, as they must be removed by settling or filtration before RO treatment. Also, the corrosiveness of seawater requires attention to materials of construction in system design. For the seawater systems to be considered, the TDS of the feed seawater is taken as ~35,100 ppm. Table 5-1 shows the breakdown of cations and anions in the model seawater considered, which is taken as typical seawater from the Toray RO model program[33].

Table 5-1. Model Seawater Feed Composition

Component	Concentration (ppm)
CATIONS	
Calcium	408
Magnesium	1,298
Sodium	10,768
Potassium	388
ANIONS	
Bicarbonate	143
Chlorine	19,380
Sulfate	2,702
Boron	1.1
Phosphate	0.5
Carbonate	2.29
NON-VALENT	
Silicon Dioxide	15
Carbon Dioxide	2.4
TDS	**35,106**
pH	**7.8**

Taking this input and the methodology outlined in section 5.1.1, steady-state models for the single-stage and two-stage RO systems were developed. The design goals were to provide the maximum amount of water for the given power input (product yield) and the water quality to meet World Health Organization (WHO) standards[42] (product quality). Because product yield and quality typically are at odds with one another, some different RO system sizes and pressure and pumping schemes were considered for the given power requirements.

5.2.1 SW-WE-a1 System Design

The first design considered was a two-stage RO system, with energy recovery and the option of interstage pumping to boost pressure in the second stage. This model is designated SW-WE-a1. The SW refers to seawater, the WE is for work exchanger (energy recovery) and the a1 design is a two-stage system (Figure 5-1). In performing the power calculations outlined in section 5.1.1, two design options concerned the interstage boost and the DWEER described in section 3.2.6. The first option was to provide a pump to boost the brine outlet pressure from the first stage before entering the second stage. The second was to provide a booster pump to the feed, which has already recovered energy from the DWEER, but is still at a lower pressure than the main feed system to the RO unit. Based on a power and pressure study of each of these possible configurations, there were only two viable alternatives: (1) to provide an interstage booster pump (Figure 5-4), which precludes the necessity of a post-DWEER booster pump, since the brine pressure out of the second stage is high enough to power the DWEER so the DWEER feed pressure is equal to that of the main feed pressure; and (2) to use no interstage boost, and therefore, a booster pump is needed after the DWEER to provide the necessary makeup feed pressure (Figure 5-5).

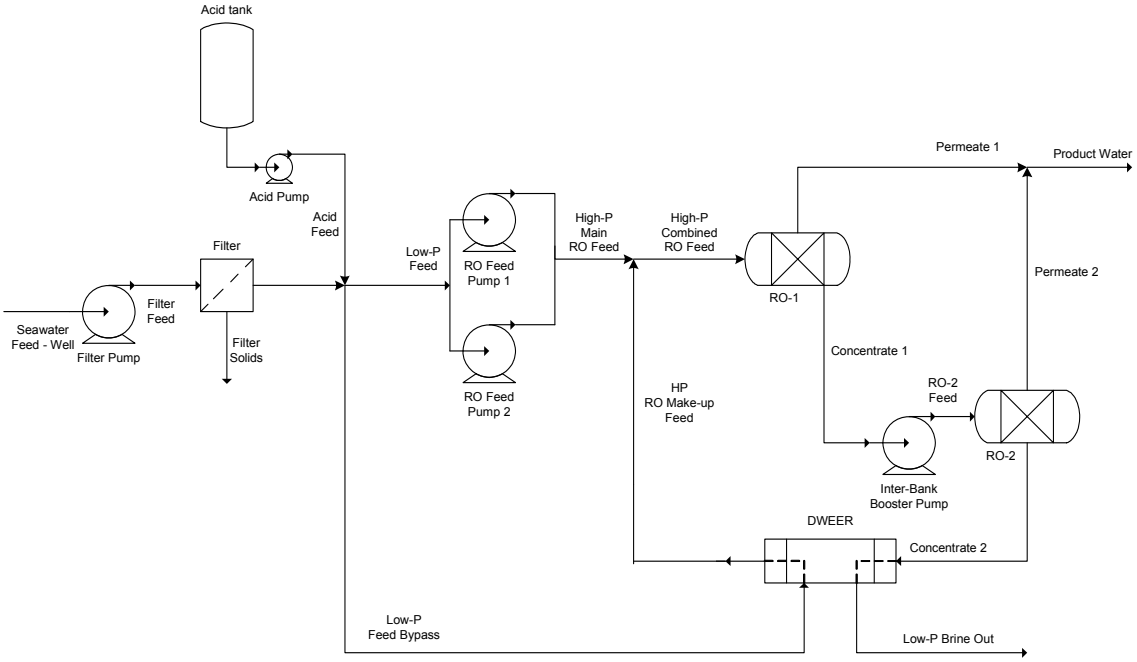

Figure 5-4. SW-WE-a1 configuration with interstage boost

Power is then calculated with nominal values for pressure and flow until a value for the total power is about 540 kW. This gives a baseline for the configuration.

Next, the RO membrane steady-state model[33] is applied to determine the appropriate configuration for the RO part of the configuration. This model uses the feed described in section 5.2, and is optimized with the constraints detailed in Table 5-2. These constraints have been determined by industry design standards, and the capabilities of the membranes manufactured by Toray Membrane America, Inc.[33]

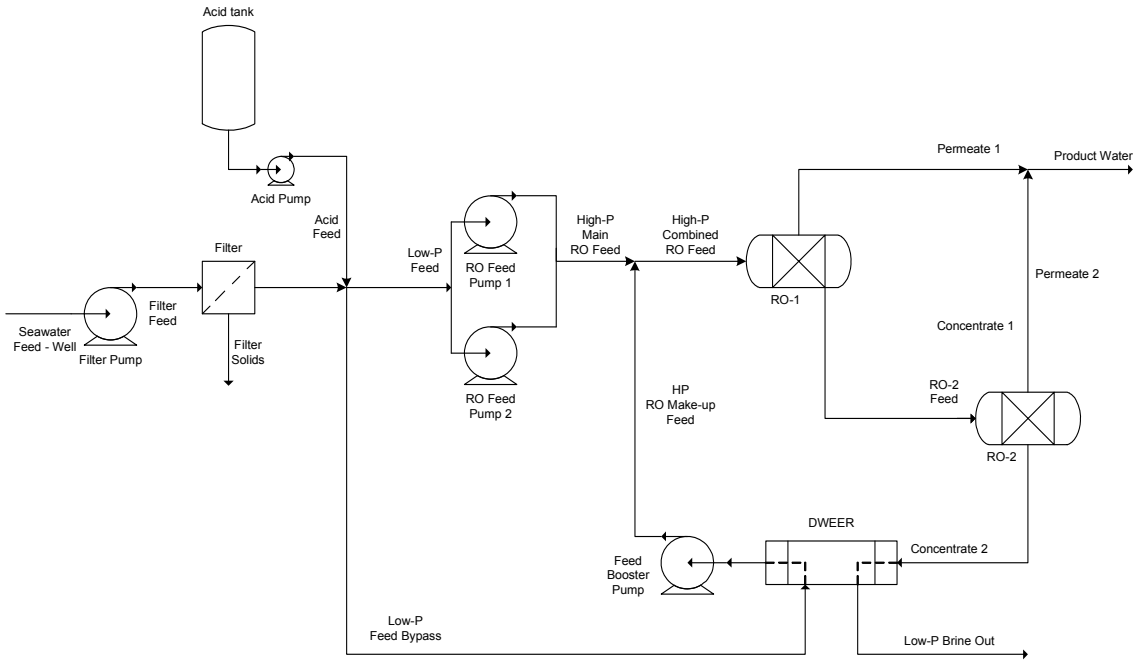

Figure 5-5. SW-WE-a1 configuration with DWEER feed boost

Table 5-2. Membrane Design Parameters

Parameter	Value/Range	*REMARKS*
Feed Flow	Lower limit > 15 gpm on the last element in the train	gpm = gal/min
Permeate Flux	Seawater: 8 < gfd <12 (13−21 lmh) Brackish: 10 < gfd < 16 (17−27 lmh)	gfd = gal/ft^2/d; lmh = liter/m^2/h Limits: scaling, feed P and osmotic P
Feed Pressure	Seawater: 1000 psig/70 bar Brackish: 600 psig/41 bar	
Pressure Drop	< 20 psi (1.4 bar)/module < 60 psi (4.0 bar)/vessel	Limitation by membrane structure
Permeate	< 500 ppm TDS-250 NaCl-0.5 ppm Boron	WHO limits[42]
RO Recovery	Seawater: 35%−45% Brackish: 70%−80%	
Temperature	< 45°C (113°F) for operation	Element limitations
Fouling	10% permeate flux decline per year	
Membrane Lifetime	3−5 years	

5.2.1.1 Filter model

In both designs, the primary feed is from a seawater well, which required filtration of any suspended solids. This filter is modeled with a standard design equation[24], which is detailed in Eq. 5-2.

$$V^2 + 2AV_F V = \frac{2A^2(\Delta P)^{(1-s)}\theta'}{\alpha' W \mu} \qquad \text{Eq. 5-2}$$

Inputs

V	=	Filtrate volume – amount of water to be pretreated by filter (m^3)
ΔP	=	Pressure drop – determined by feed pump power draw as the input pressure, and assumes atmospheric pressure after filter. Design based on maximum ΔP(N/m^2)
ρ_c	=	Filter cake density (dry solids per volume we filter cake, kg/m^3)
W	=	Solids conc. in solution (dry solids per volume solid–free liquid, kg/m^3)
μ	=	Solution viscosity ($N\text{-}s/m^2$)
θ’	=	Filtration time – Determined by time for a given filtration. Design based on minimum time for filtration (s)

Constants – Empirically Determined or Use Industrial Correlations

V_F	=	Filtrate volume constant related to filter cake thickness (m^3/m^2
s	=	Compressibility exponent of filter cake (dimensionless)
α’	=	Cake resistance constant = $(\alpha)/(\Delta P)^s$ ($s\ m^2/kg$)
α	=	Specific filter cake resistance = C/ρ_c ($s\ m^2/kg$)
C	=	Proportionality constant for cake resistance and cake thickness

Outputs

A	=	Filter area (m^2)
Cost	=	Capital cost for the filter ($)

The solution to Eq. 5-2 is typically accomplished in two stages. The first is to use empirical data from the fluid/solid system to be filtered to determine some of the model parameters. Typically, this is done in a laboratory with a small-scale test. In this case, numbers from typical filtration systems were used[24,43] with the method described in Figure 5-6.

- For at least two or three values of constant ΔP experimental data, plot $\theta'\Delta P/(V/A)$ versus (V/A) to give slope $\alpha' w\mu(\Delta P)^s/2$ and intercept $\alpha' w\mu V_F(\Delta P)^s$
- Log (slope) = s Log ΔP + Log $(\alpha' w\mu/2)$
- Log (intercept) = s Log ΔP + Log $(\alpha' w\mu V_F)$
- Plot ΔP versus Slope to get experimental values of s and $\alpha' w\mu/2$
- Plot ΔP versus Intercept to get experimental values of s and $\alpha' w\mu V_F$
- Check data for consistency and arrive at values of s, α’, and V_F

Figure 5-6. Algorithm for solving first stage of filtration model equation

The next step is to then apply the known values of variables and constants to Eq. 5-2, and then rearrange the equation to solve for the area, A, of the filter required to separate solids at a given concentration in a feed fluid, using a defined pressure gradient. This rearrangement is shown in Eq. 5-3, where the right-hand term of the equation is subtracted from both slides, leading to a quadratic equation, whose solution is given in Eq. 5-4.

$$[(2(\Delta P)^{(1-s)}\theta')/(\alpha' w\mu)]\,A^2 - (2V_F V)A - V^2 = 0 \qquad \text{Eq. 5-3}$$

$$A = \frac{(4V_F^2V^2) \pm \sqrt{\{(4V_F^2V^2) + 4V^2[(2(\Delta P)^{(1-s)}\theta')/(\alpha' w\mu)]\}}}{[4(\Delta P)^{(1-s)}\theta'/(\alpha' w\mu)]} \qquad \text{Eq. 5-4}$$

The positive value for A is taken as the real solution to the model equation. From the power calculations for the SW-WE-a1 configuration, the volumetric flow rate V is given. In turn, the surface area, A, of the filter can be calculated from the above equation, and then the capital cost of the filter can be determined[24,25]. This cost is then included in the cost model of section 4.1.

5.2.1.2 Power and reverse osmosis model optimization

We used the design parameters from Table 5-2 and the flows from the power calculations to optimize the steady-state membrane model, which uses software developed by Toray Membrane America, Inc.[33]. Feed inputs are the composition of the feed, the feed flow rate, and any feed pretreatment (pH adjustment, scale inhibitor, etc.). The RO unit inputs are the type of membrane, the RO recovery, the number of stages, the number of RO elements per vessel, the membrane fouling factor, the salt passage rate per year, the age of the membrane, and the permeate backpressure. The model then converges to a solution for the ion concentrations in the brine and permeate streams by use of the flux equation across a membrane shown in Eq. 5-5 and Eq. 5-6.

$$J_{sol} = \frac{K_{sol}}{t_m}(Mc_b - c_p) \qquad \text{Eq. 5-5}$$

$$M = c_w / c_b \qquad \text{Eq. 5-6}$$

where

J_{sol} = the flux across the membrane

K_{sol} = the permeability of the membrane to the solvent

t_m = the membrane thickness

M = the polarization modulus

c_b = the bulk ion concentration

c_p = the permeate ion concentration

c_w = the ion concentration at the membrane wall

The membrane flux, ion concentrations, and stream pressures are determined for each element and each stage of the model. Once converged, the model gives a steady-state output from the system. These outputs include the overall flows and pressures of each stream, the ion concentrations in each stream, and the individual and overall fluxes for the RO membrane system.

At each convergence of the RO model, the output flows and pressures from the membrane model were plugged back into the pump power calculations to see if the power was still optimal at about 540 kW. Since the feed flow is the largest power draw on the system, if the power was too low, the feed flow to the membrane model was increased. If the power was too high, the feed flow was decreased. This cycle was iterated until the maximum flow for the given power input through an RO system was achieved. Figure 5-7 and Figure 5-8 show the results of this optimization for the power calculations that represent the configurations in Figure 5-4 and Figure 5-5, respectively. The RO steady-state model outputs are found in Appendix A, which refers to the interstage boost case, and data from the DWEER boost case.

The interstage boost design of Figure 5-4 was optimized for the first stage of 50 vessels by six elements per vessel, followed by a second stage of 38 vessels by six elements per vessel. Each stage uses a Toray Membrane America, Inc. Model 820-370 seawater membrane. Appendix A details the specifications of this type of membrane. The DWEER boost design of Figure 5-5 was similarly optimized to 50 x 6 and 38 x 6 model configurations. Both design scenarios obtain the same optimal RO configuration, as the placement of the boost before the second stage or after the DWEER does not affect the overall design. In the case of interstage boost, the second stage operates at a higher pressure, with slightly greater recovery of permeate from this stage, but since the constraints on the input energy, the membrane flux and feed pressure limit the amount of permeate in the second stage, the optimization shows that there is no design difference in the RO elements for the two design cases (interstage boost or DWEER boost).

SW-WE-a1 40% Recovery 2-Stage with DWEER, Interstage Boost, no DWEER Boost									
Capacity Information				Input cells					
Operating Days/yr	350			Output cells					
Plant Capacity (MM m^3/yr) / (MM gal/yr)	2.00	529.2							
Plant Capacity (m^3/day) / (MM gal/day)	5723.6	1.512							
Permeate Flow (m3/Hr) / (GPM)	238.5	1,050.0							
Overall System Recovery (%)	40.0%								
Wind turbine Efficiency (%)	36.0%								
Specific Energy (kW-Hr/m^3)	2.26								
Toray Model and DWEER Information	Vessels	Elements	Type	Element Area (ft^2)	Total Area (ft^2)	Total Area (m^2)	Recovery (%)	Flux (GFD)	Flux (LMH)
1st Stage Membrane Configuration	50	6	820-370	370	111,000	10,312	27.2%	9.27	15.74
2nd Stage Membrane Configuration	38	6	820-370	370	84,360	7,837	17.6%	5.76	9.78
Filter Outlet Pressure (PSIA) / (Bar)	30	2.07							
RO Feed Pressure (PSIA) / (Bar)	731	50.40							
Concentrate Flow (GPM) / (m^3/hr)	1575.0	357.7							
Concentrate Pressure (PSIA) / (Bar)	742	51.16							
DWEER Brine Outlet P (PSIA) / (Bar)	15	1.03							
DWEER Water Out P (PSIA)	733	50.56							
DWEER Leakage (%)	1.00%								
Calculate Pump Energy Requirments base on Toray Models & Fedco Design Specifications									
Design Conditions	Efficiency (%)	Flow (m^3/hr)	Flow (GPM)	ΔP (kPa)	ΔP (PSIA)	Power (kW)	Power (hP)	Speed (RPM)	~ Cost ($)
Filter Feed Pump	75.00%	596.2	2625	310.3	45	68.53	91.9	3600	30,000.00
RO Feed Pump-1	77.40%	122.5	539.18	4833.2	701	212.48	284.9	3858	48,000.00
RO Feed Pump-2	77.40%	122.5	539.18	4833.2	701	212.48	284.9	3858	48,000.00
Interstage Booster Pump	75.00%	434.3	1912	289.6	42	46.59	62.5		
DWEER Booster Pump	75.00%	351.3	1546.65	0.0	0	0.00	0.0	3600	30,000.00
ERD - DWEER	95.00%	351.3	1546.65	5056.0	733	468.82	628.7		
Total Power Requirements						540.1	724.2		
Wind Turbine Power Requirement						1500.2	2011.8		

Figure 5-7. Power calculations for SW-WE-a1 design with interstage boost

SW-WE-a1 40% Recovery 2-Stage with DWEER, No Interstage Boost, DWEER Boost									
Capacity Information				Input cells					
Operating Days/yr	350			Output cells					
Plant Capacity (MM m^3/yr) / (MM gal/yr)	1.98	524.2							
Plant Capacity (m^3/day) / (MM gal/day)	5669.1	1.498							
Permeate Flow (m3/Hr) / (GPM)	236.2	1,040.0							
Overall System Recovery (%)	40.0%								
Wind turbine Efficiency (%)	36.0%								
Specific Energy (kW-Hr/m^3)	2.27								
Toray Model and DWEER Information	Vessels	Elements	Type	Element Area (ft^2)	Total Area (ft^2)	Total Area (m^2)	Recovery (%)	Flux (GFD)	Flux (LMH)
1st Stage Membrane Configuration	50	6	820-370	370	111,000	10,312	28.6%	9.66	16.40
2nd Stage Membrane Configuration	38	6	820-370	370	84,360	7,837	16.0%	5.08	8.62
Filter Outlet Pressure (PSIA) / (Bar)	30	2.07							
RO Feed Pressure (PSIA) / (Bar)	753	51.92							
Concentrate Flow (GPM) / (m^3/hr)	1560.0	354.3							
Concentrate Pressure (PSIA) / (Bar)	723	49.85							
DWEER Brine Outlet P (PSIA) / (Bar)	15	1.03							
DWEER Water Out P (PSIA)	715	49.29							
DWEER Leakage (%)	1.00%								
Calculate Pump Energy Requirments base on Toray Models & Fedco Design Specifications									
Design Conditions	Efficiency (%)	Flow (m^3/hr)	Flow (GPM)	ΔP (kPa)	ΔP (PSIA)	Power (kW)	Power (hP)	Speed (RPM)	~ Cost ($)
Filter Feed Pump	75.00%	590.5	2600	310.3	45	67.88	91.0	3600	30,000.00
RO Feed Pump-1	77.30%	121.3	534.0	4984.9	723	217.34	291.5	3887	48,000.00
RO Feed Pump-2	77.30%	121.3	534.0	4984.9	723	217.34	291.5	3887	48,000.00
Interstage Booster Pump	75.00%	0.0	0	0.0	0	0.00	0.0		
DWEER Booster Pump	75.00%	347.9	1531.9	262.5	38	33.84	45.4	3600	30,000.00
ERD - DWEER	95.00%	347.9	1531.9	4929.2	715	452.72	607.1		
Total Power Requirements						536.4	719.3		
Wind Turbine Power Requirement						1490.0	1998.1		

Figure 5-8. Power calculations for SW-WE-a1 design with DWEER boost

We used the RO membrane design reports and the power calculations to develop an overall process flow diagram for each SW-WE-a1 configuration. The interstage boost case is shown in Figure 5-9 with calculations shown in both English and metric units. A similar flow diagram is shown for the DWEER boost case in Figure 5-10. English units for flow, pressure, and flux are gal/min (gpm), pound-force/in^2 (psia), and gal/ft^2/d (gfd), respectively. Corresponding metric units are m^3/h (cmh), bar, and liter/m^2/h (lmh).

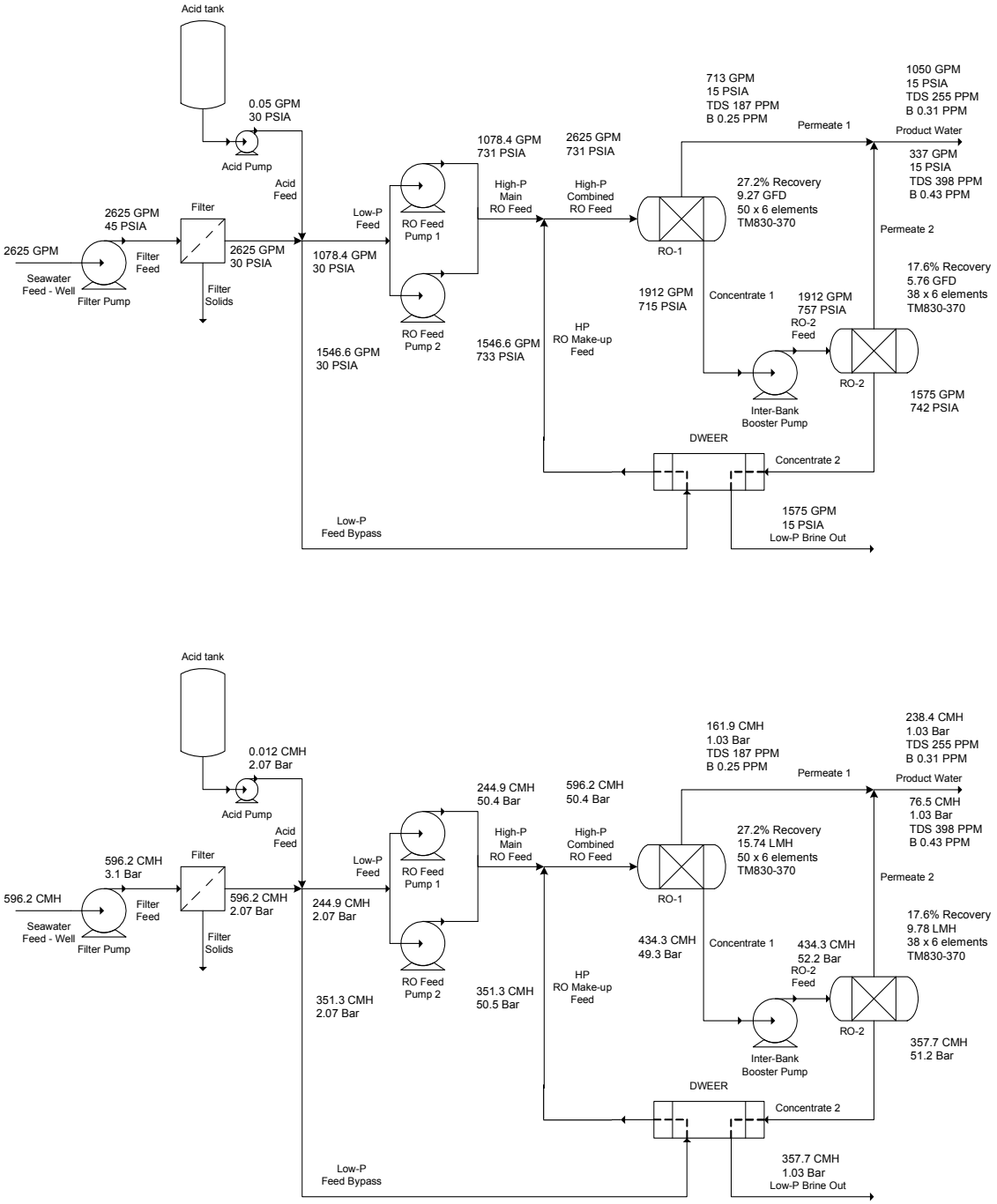

Figure 5-9. SW-WE-a1 interstage boost flow diagram

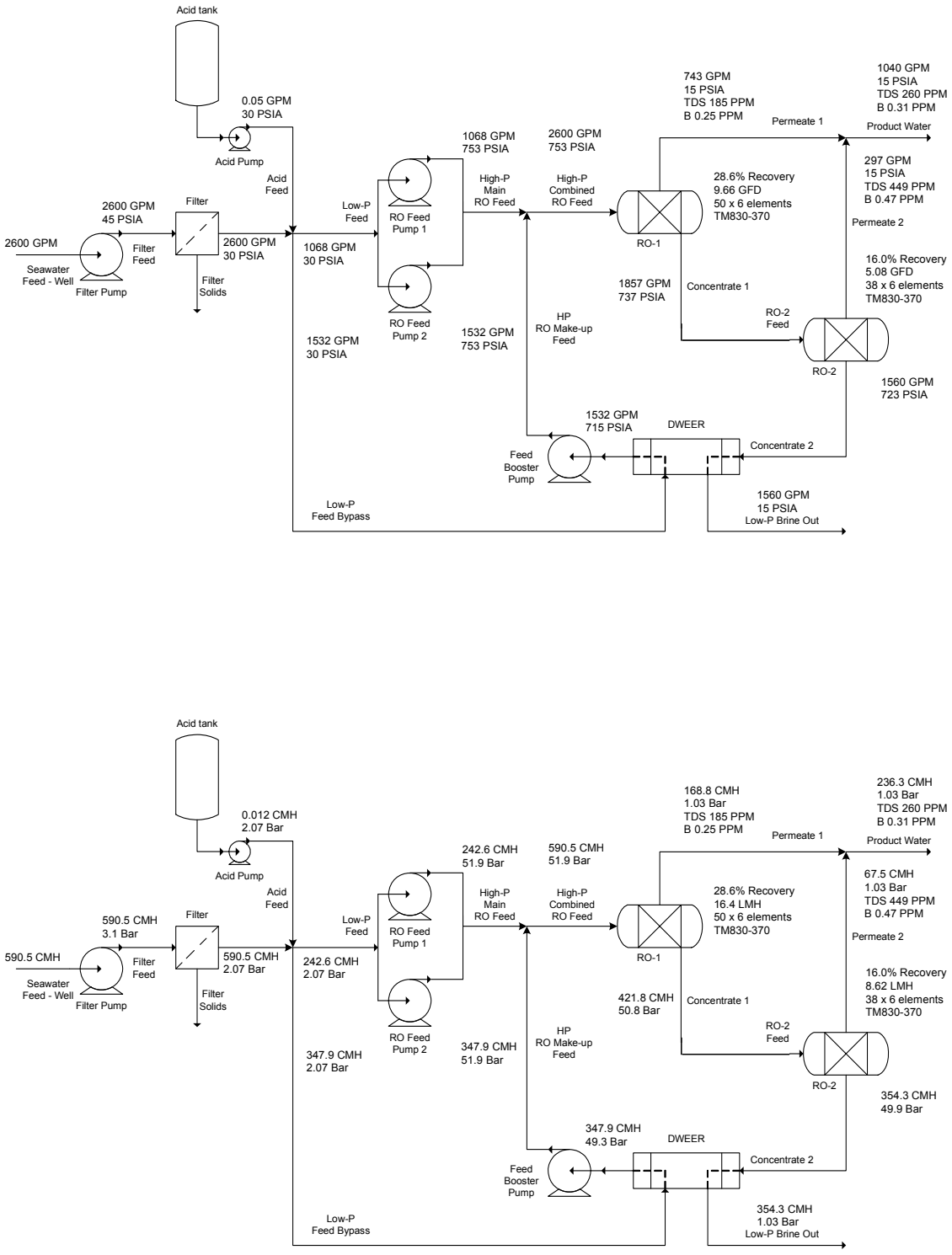

Figure 5-10. SW-WE-a1 DWEER boost flow diagram

Based on a comparison of the two configurations, the interstage boost configuration produces about 68% of the product in the first stage and 32% in the second stage. In the DWEER boost configuration, the first stage produces 71% of the product, with 29% in the second stage. The results indicate nearly equal performance of the two configurations in both production amount and product quality.

5.2.1.3 Boron sensitivity analysis

The level of Boron in permeate water is now set to 0.3-0.5 ppm by WHO[42]. To understand the sensitivity of this configuration to Boron, we increased its feed level to determine what level of Boron in the feed would cause it to break through in the permeate to a level of 0.5 ppm . We used the steady-state RO membrane model[33] to determine that the level of Boron in the feed that results in a 0.5-ppm level in the product permeate is 1.8 ppm for the interstage boost and DWEER boost designs. Since there is large variation in seawater Boron levels, any feedwater with Boron levels higher than 1.8 ppm would require a redesign of the system for a specific situation.

One way is to lower recovery on the current configurations to increase salt rejection, which will lower product output. This is the quality/productivity trade-off. For example, lowering the overall recovery of the current configurations from 40% to 30% (a 10% decrease), and reducing the array configuration to 45 x 6 on the first stage and 30 x 6 on the second stage allows for the same permeate flow and power use as the base configurations. In this type of configuration, the increase in the feed Boron level is only to about 2 ppm (11% increase) to still meet the 0.5 ppm limit. There is little room for improvement in the current design to higher Boron levels. Therefore, if Boron levels are higher than 2 ppm, the best design option would be to have another RO Boron removal stage for the permeate only. This would require extra capital costs and increase energy consumption. Either a smaller production plant or larger wind turbine would be required to compensate for the increased energy use. Those trade-offs in capital and operating expenses versus productivity would have to be assessed on specific high-Boron feed cases.

5.2.2 Cost of Water Analysis

Based on the above design, an overall COW is determined by calculating capital and operating costs for the configuration as outlined in detail in section 4.1. Because the only real difference between the SW-WE-a1 interstage boost configuration and the DWEER boost configuration is the placement and size of the booster pump, the capital and operating costs for these two configurations are virtually identical. A cost summary that outlines the relevant capital and operating costs for the steady state model is shown in Figure 5-11. The model assumes an operating year is 350 days, with a permeate flow rate of 5723 m^3/d (1,050 gpm). This yields an annual production of 2 x 10^6 m^3/yr of product water. Rolling up all the capital and operating costs for this production level gives an overall steady-state COW of about \$1.20/m^3. This cost can vary for a site-specific situation, where well construction costs, feed concentrations, and waste disposal costs can vary. The steady-state cost model, however, is flexible and can make provisions for these cost variances (see section 4.1).

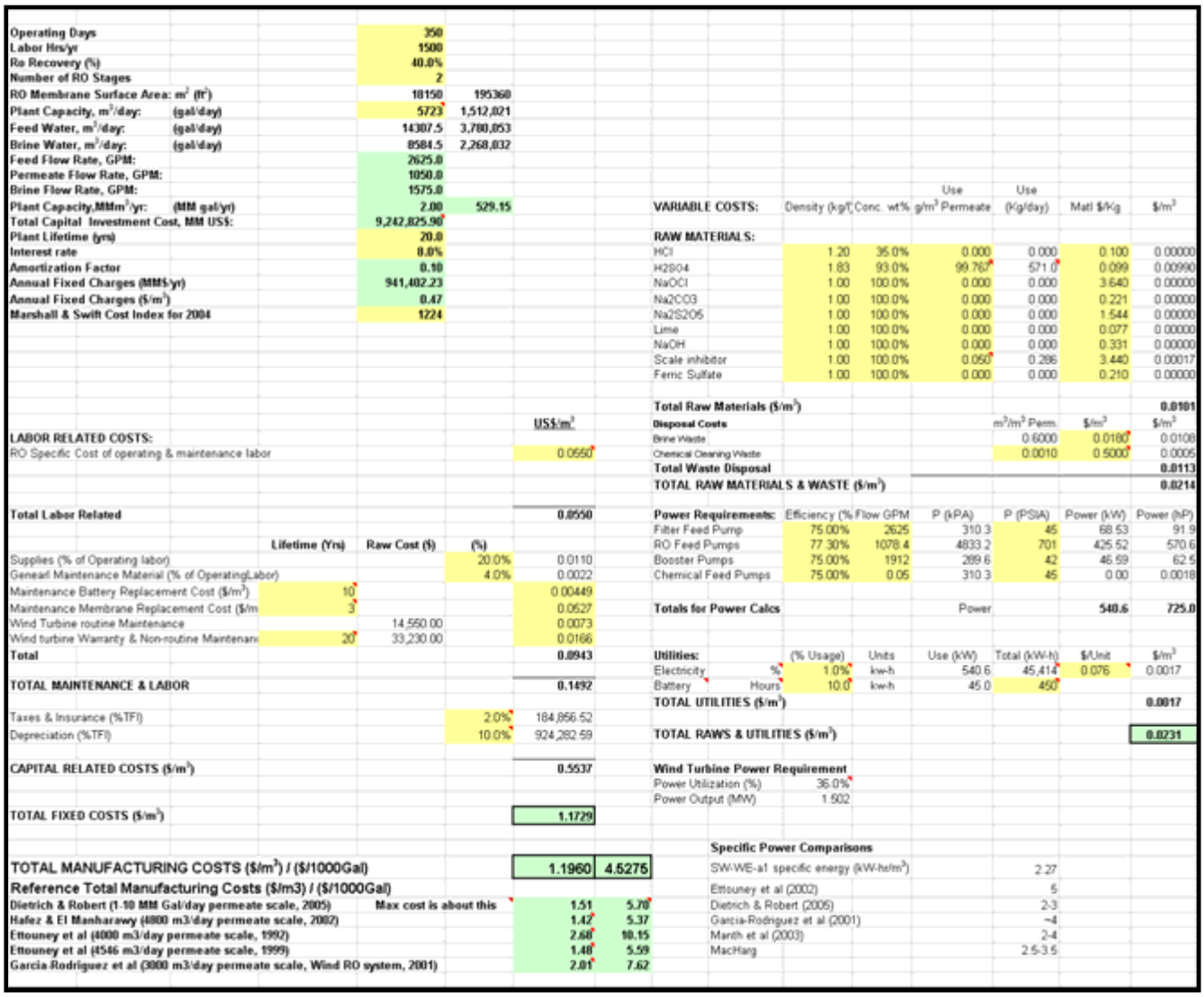

Operating Days		350	
Labor Hrs/yr		1500	
Ro Recovery (%)		40.0%	
Number of RO Stages		2	
RO Membrane Surface Area: m^2 (ft^2)		18150	195360
Plant Capacity, m^3/day:	(gal/day)	5723	1,512,021
Feed Water, m^3/day:	(gal/day)	14307.5	3,780,053
Brine Water, m^3/day:	(gal/day)	8584.5	2,268,032
Feed Flow Rate, GPM:		2625.0	
Permeate Flow Rate, GPM:		1050.0	
Brine Flow Rate, GPM:		1575.0	
Plant Capacity,MMm^3/yr:	(MM gal/yr)	2.00	529.15
Total Capital Investment Cost, MM US$:		9,242,825.90	
Plant Lifetime (yrs)		20.0	
Interest rate		8.0%	
Amortization Factor		0.10	
Annual Fixed Charges (MM$/yr)		941,402.23	
Annual Fixed Charges ($/m^3)		0.47	
Marshall & Swift Cost Index for 2004		1224	

VARIABLE COSTS:	Density (kg/L)	Conc. wt%	Use g/m^3 Permeate	Use (Kg/day)	Matl $/Kg	$/m^3
RAW MATERIALS:						
HCl	1.20	35.0%	0.000	0.000	0.100	0.00000
H2SO4	1.83	93.0%	99.767	571.0	0.099	0.00990
NaOCl	1.00	100.0%	0.000	0.000	3.640	0.00000
Na2CO3	1.00	100.0%	0.000	0.000	0.221	0.00000
Na2S2O5	1.00	100.0%	0.000	0.000	1.544	0.00000
Lime	1.00	100.0%	0.000	0.000	0.077	0.00000
NaOH	1.00	100.0%	0.000	0.000	0.331	0.00000
Scale inhibitor	1.00	100.0%	0.050	0.286	3.440	0.00017
Ferric Sulfate	1.00	100.0%	0.000	0.000	0.210	0.00000
Total Raw Materials ($/m^3)						**0.0101**

	US$/m^3
LABOR RELATED COSTS:	
RO Specific Cost of operating & maintenance labor	0.0550
Total Labor Related	**0.0550**

	Lifetime (Yrs)	Raw Cost ($)	(%)	
Supplies (% of Operating labor)			20.0%	0.0110
General Maintenance Material (% of OperatingLabor)			4.0%	0.0022
Maintenance Battery Replacement Cost ($/m^3)	10			0.00449
Maintenance Membrane Replacement Cost ($/m	3			0.0527
Wind Turbine routine Maintenance		14,550.00		0.0073
Wind turbine Warranty & Non-routine Maintenanc	20	33,230.00		0.0166
Total				**0.0943**
TOTAL MAINTENANCE & LABOR				**0.1492**
Taxes & Insurance (%TFI)			2.0%	184,856.52
Depreciation (%TFI)			10.0%	924,282.59
CAPITAL RELATED COSTS ($/m^3)				**0.5537**
TOTAL FIXED COSTS ($/m^3)				**1.1729**

Disposal Costs			m^3/m^3 Perm.	$/m^3	$/m^3
Brine Waste			0.6000	0.0180	0.0108
Chemical Cleaning Waste			0.0010	0.5000	0.0005
Total Waste Disposal					**0.0113**
TOTAL RAW MATERIALS & WASTE ($/m^3)					**0.0214**

Power Requirements:	Efficiency (%	Flow GPM	P (kPA)	P (PSIA)	Power (kW)	Power (hP)
Filter Feed Pump	75.00%	2625	310.3	45	68.53	91.9
RO Feed Pumps	77.30%	1078.4	4833.2	701	425.52	570.6
Booster Pumps	75.00%	1912	289.6	42	46.59	62.5
Chemical Feed Pumps	75.00%	0.05	310.3	45	0.00	0.0018
Totals for Power Calcs			Power		**540.6**	**725.0**

Utilities:		(% Usage)	Units	Use (kW)	Total (kW-h)	$/Unit	$/m^3
Electricity	%	1.0%	kw-h	540.6	45,414	0.076	0.0017
Battery	Hours	10.0	kw-h	45.0	450		
TOTAL UTILITIES ($/m^3)							**0.0017**
TOTAL RAWS & UTILITIES ($/m^3)							**0.0231**

Wind Turbine Power Requirement	
Power Utilization (%)	36.0%
Power Output (MW)	1.502

TOTAL MANUFACTURING COSTS ($/m^3) / ($/1000Gal)	**1.1960**	**4.5275**
Reference Total Manufacturing Costs ($/m3) / ($/1000Gal)		
Dietrich & Robert (1-10 MM Gal/day permeate scale, 2005) Max cost is about this	**1.51**	**5.70**
Hafez & El Manharawy (4800 m3/day permeate scale, 2002)	**1.42**	**5.37**
Ettouney et al (4000 m3/day permeate scale, 1992)	**2.68**	**10.15**
Ettouney et al (4546 m3/day permeate scale, 1999)	**1.48**	**5.59**
Garcia-Rodriguez et al (3000 m3/day permeate scale, Wind RO system, 2001)	**2.01**	**7.62**

Specific Power Comparisons	
SW-WE-a1 specific energy (kW-hs/m^3)	2.27
Ettouney et al (2002)	5
Dietrich & Robert (2005)	2-3
Garcia-Rodriguez et al (2001)	~4
Manth et al (2003)	2-4
MacHarg	2.5-3.5

Figure 5-11. Summary costs for the steady-state SW-WE-a1 configuration

5.2.3 Design Space Analysis

We conducted a design space analysis to understand the extent of the operating envelope associated with the configuration described in Section 5.2.1. The main purpose of this study is to investigate the points in the input space at which the system fails to satisfy all the component and system constraints. If the system were operated at these points, where the constraints were not met, the potential for membrane degradation through fouling or scaling or membrane destruction caused by increased stresses may result. In addition to understanding where constraints are violated, the design space study provides some insight into how system quantities of interest such as recovery ratio, specific energy consumption, total power and permeate flow vary with the choice of input parameters. The qualitative understanding that the design space study provides is critical for understanding the potential for system optimization.

For the two-stage configuration shown in Figure 5-12, the input space is defined by the parameters listed in Table 5-3.

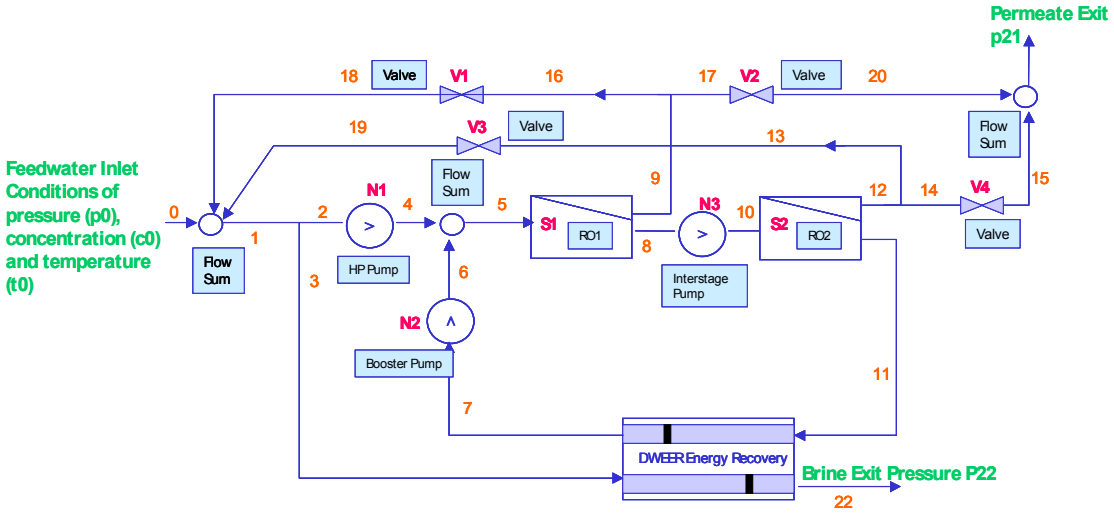

Figure 5-12. RO system configuration SWWE-a1

Table 5-3. Input Parameters for Configuration SWWE-a1

Parameter	Description
S1	Number of vessels in stage 1
S2	Number of vessels in stage 2
N1	High-pressure pump speed
N2	Booster pump speed
N3	Interstage pump speed
V1	Stage 1 permeate recycle valve position
V2	Stage 1 permeate output valve position
V3	Stage 2 permeate recycle valve position
V4	Stage 2 permeate output valve position

Since the valve positions V1−V4 are mainly used to initiate a recycle flow for very low wind power capture conditions, the design space analysis fixes these quantities V1 = V3 = 0 (valve closed) and V2 = V4 = 1 (valve fully opened). The aforementioned valve positions indicate that there is no recycle of the permeate flow.

Table 5-4 lists the parameter values investigated in the design space analysis for this configuration.

The steady-state constraints for the RO system are highlighted in Section 5.1.2 and listed in Table 5-5. Table 5-5 also lists the index associated with each constraint; this index reference is used in the figures associated with the design space analysis to highlight which constraints, if any, are being violated at a given point in the input space.

Table 5-4. Input Space Parameter Ranges for Configuration SWWE-a1

Parameter	Description	Units	Variation Range
S1	Vessels in stage 1	-	15–75
S2	Vessels in stage 2	-	15− 55
N1	High-pressure pump speed	rpm	3000–3900
N2	Booster pump speed	rpm	3000–3900
N3	Interstage pump speed	rpm	3000–3900
V1	Stage 1 permeate recycle valve	% open	0 (fully closed)
V2	Stage 1 permeate output valve	% open	1 (fully open)
V3	Stage 2 permeate recycle valve	% open	0 (fully closed)
V4	Stage 2 permeate output valve	% open	1 (fully open)
p0	Feedwater pressure	psid	20
p21	Permeate exit pressure	psid	15
p22	Brine exit pressure	psid	15
T0	Feedwater temperature	°C	25
c0	Feedwater dissolved salt concentration	kg/m^3	29.6

Table 5-5. Constraint Definition for Configuration SWWE-a1

Parameter	Value/Range	Index Used in Plots
Element polarization	$C_m / C_{avg} < 1.2$	1 – Stage 1 2 – Stage 2
Element concentration flow	$Q_c > 15$ gpm	3 – Stage 1 4 – Stage 2
Feedwater pressure	$P_f < 1{,}200$ psi	5
Element pressure drop	$\Delta P_{elm} < 10$ psid	6 – Stage 1 8 – Stage 2
Vessel pressure drop	$\Delta P_{vessel} < 58$ psid	7 – Stage 1 9 – Stage 2
Permeate quality	$C_p < 500$ ppm	10
Element flux	Flux < 20.6 gfd	11 – Stage 1 12 – Stage 2

The results of the design space analysis are shown in Figure 5-13–Figure 5-37 for system parameters such as permeate flow, total power, specific energy consumption, and recovery ratio. The figures associated with these parameters also highlight the constraints violated in brackets and the system parameter value at each data point in the analysis. Finally, for each combination of input parameters that are presented, the distance to the constraint is identified in terms of percentage. The distance in terms of percentage from maximum constraints is given in Eq. 5-7 by

$$Distance\ to\ constraint = \frac{Constraint\ Value - Parameter\ Value}{Constraint\ Value} * 100 \qquad \text{Eq. 5-7}$$

and the distance in terms of percentage from minimum constraints is given in Eq. 5-8 by

$$Distance\ to\ constraint = \frac{Parameter\ Value - Constraint\ Value}{Constraint\ Value} * 100 \qquad \text{Eq. 5-8}$$

Positive numbers in these figures indicate that there are no limiting constraints, and the number shown in the figure is the distance to the most restrictive constraint. Negative numbers shown in the figures indicate that at least one constraint is being violated, and the number shown in the figure indicates the maximum constraint violation.

Consider the results shown in Figure 5-13–Figure 5-27 for the case where the booster pump speed (N2) and interstage pump speed (N3) are set to 3000 rpm, and the number of vessels in the second stage, S2, is varied from 15 to 39 to 55. For each value of S2, data associated with permeate flow, total power, specific power, recovery ratio, and distance from the constraint are shown as a function of high-pressure pump speed (N1) and the number of vessels in stage 1 (S1). When the number of vessels in the second stage is 15, S2 = 15, the only viable operating point is when the number of vessels in stage 1 is large and the high-pressure pump speed is at a minimum (Figure 5-13). In fact, in most cases, the constraints associated with a membrane element and vessel pressure drop in the second stage are being violated (Figure 5-16). Also, when the number of vessels in stage 1 is low, the pressure drop constraint (element and vessel) is violated (Figure 5-16).

As the number of vessels in the second stage increases, the available design space that meets all the constraints greatly increases (Figure 5-14 and Figure 5-15). However, the distance from the constraint in the viable operating space does not change significantly. This would suggest that the robustness associated with a particular design point does not improve as the number of vessels in stage 2 increases. The results for permeate flow (Figure 5-16–Figure 5-18) show that as the high-pressure pump speed or the number of vessels in the first stage is increased, the permeate flow also increases. However, the rate of increase is higher at larger high pressure pump speeds. In addition, the increase rate of permeate flow as a function of high-pressure pump speed is larger as the number of stages in S1 increases. With regard to total power consumed, the results in Figure 5-19−Figure 5-21 show that at a given N2, N3 combination, the total power is primarily dictated by the high pressure pump speed. This result is expected given that the high pressure pump dominates the system energy consumption.

By coupling the permeate flow results with the total power results, we can investigate the variation in specific energy consumption (Figure 5-22–Figure 5-23). The specific energy consumption decreases as the number of vessels in the second stage increases, going from a minimum value of 2.4 kWh/m^3 to 2.0 kWh/m^3. In addition, as the number of vessels in the second stage increases, the minimum point for specific energy consumption moves to lower high pressure pump speeds. Finally, with regard to recovery ratio (Figure 5-25–Figure 5-27), the achievable recovery ratio increases with the number of vessels in the second stage. In addition, as the number of vessels in the second stage increases, a line of constant recovery ratio would move to the left in the S1–N1 range.

To consider the impact of changes in the booster pump speed (N2), consider the changes in system parameters as booster pump speed is varied from 3,000 rpm to 3,540 rpm for a fixed number of vessels in the second stage, S2 = 39, and a fixed interstage pump speed of 3,000 rpm. The distance from the limiting constraints is not significantly different in the acceptable regions of the design space (Figure 5-28). In fact, variations in N2 have little impact on the permeate flow of the system or the recovery ratio (Figure 5-29 and Figure 5-32). As expected, there is an increase in the total power consumed because of the higher booster pump speed (Figure 5-30), which in turn leads to a higher specific energy consumption (Figure 5-31). The minimum point for specific energy consumption moves to greater high-pressure pump speeds as booster pump speed is increased (Figure 5-31). Although not plotted, similar results were obtained at other stage two vessel configurations and other interstage pump speeds.

To understand the impact of changes in the interstage pump speed (N3), consider the changes in the system parameters as the interstage pump speed is varied from 3,000 rpm to 3,540 rpm for a fixed number of vessels in the second stage, S2 = 39 and a fixed booster speed of 3,000 rpm. As in the above case where the booster pump speed is varied, the results with regard to the system parameters of interest are similar. The distance from the limiting constraints is not significantly different in the acceptable regions of the design space (Figure 5-33). Variations in N3 have little impact on the permeate flow of the system and the recovery ratio (Figure 5-34 and Figure 5-37). As expected, there is an increase in the total power consumed because of the higher interstage pump speed (Figure 5-35), which in turn leads to a higher specific energy consumption (Figure 5-36). As in the case of N2 variation, the minimum point for specific energy consumption moves to greater high-pressure pump speeds as interstage pump speed is increased (Figure 5-36). Although not plotted, similar results were obtained at other stage two vessel configurations and other booster pump speeds.

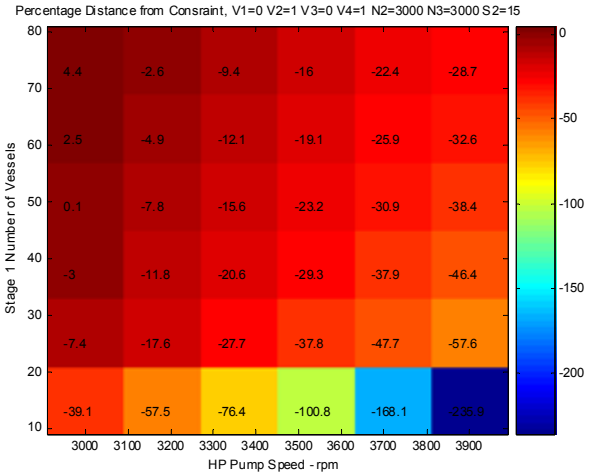

Figure 5-13. Percentage distance from constraint at N2 = 3,000 rpm, N3 = 3,000 rpm, and S2 = 15

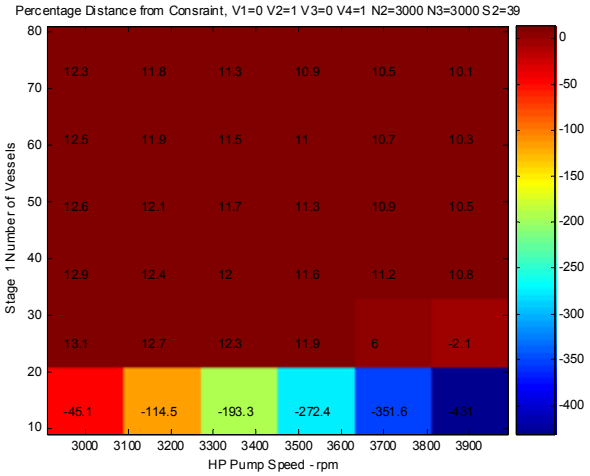

Figure 5-14. Percentage distance from constraint at N2 = 3,000 rpm, N3 = 3,000 rpm, and S2 = 39

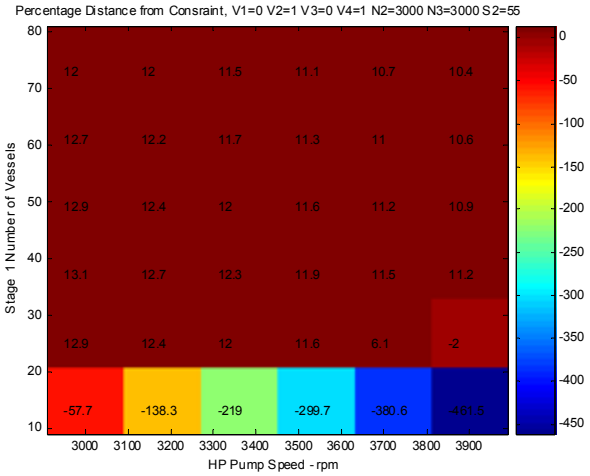

Figure 5-15. Percentage distance from constraints at N2 = 3,000 rpm,

N3 = 3,000 rpm, and S2 = 55

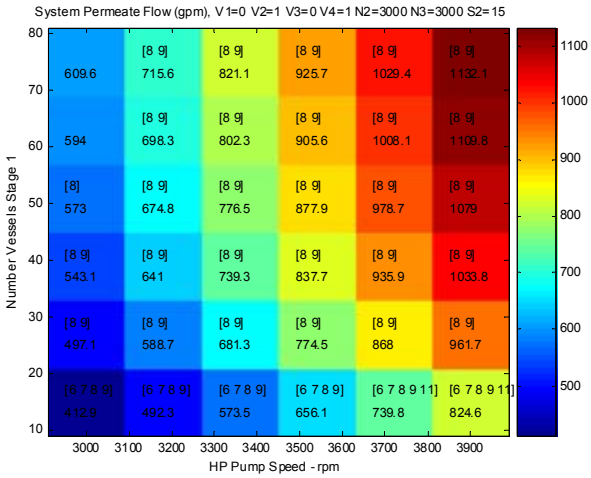

Figure 5-16. Permeate flow for N2 = 3,000 rpm, N3 = 3,000 rpm, and S2 = 15

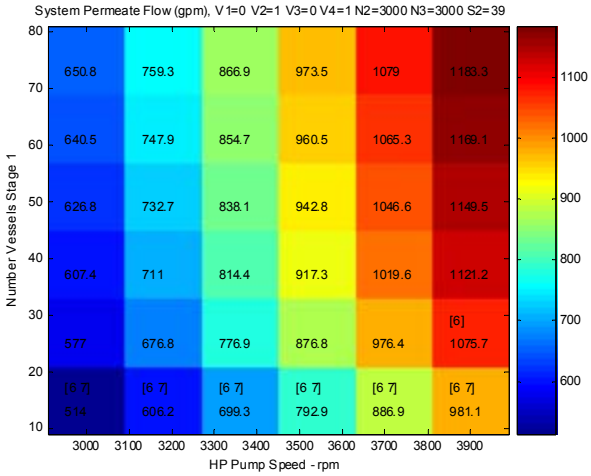

Figure 5-17. Permeate flow for N2 = 3,000 rpm, N3 = 3,000 rpm, and S2 = 39

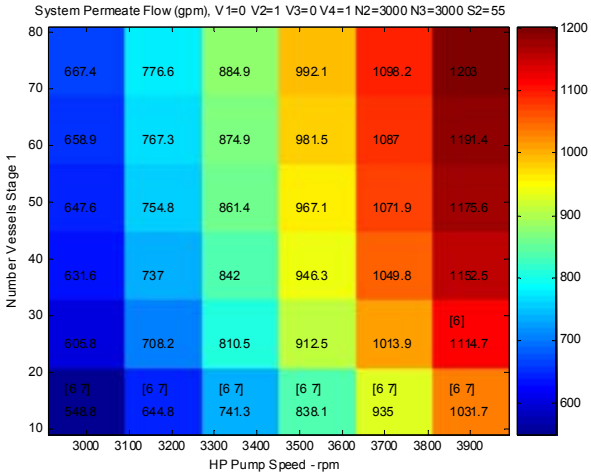

Figure 5-18. Permeate flow for N2 = 3,000 rpm, N3 = 3,000 rpm, and S2 = 55

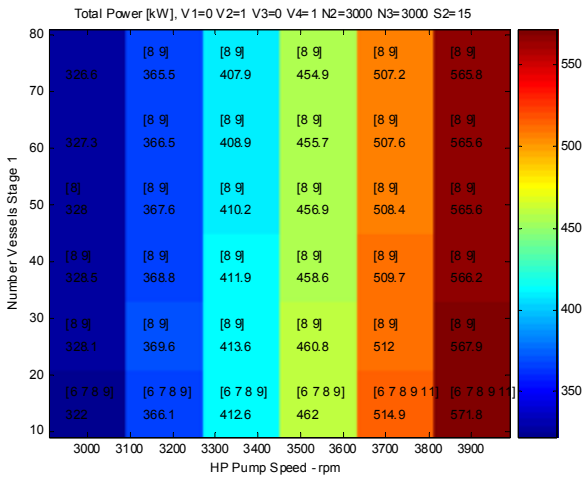

Figure 5-19. Total power for N2 = 3,000 rpm, N3 = 3,000 rpm, and S2 = 15

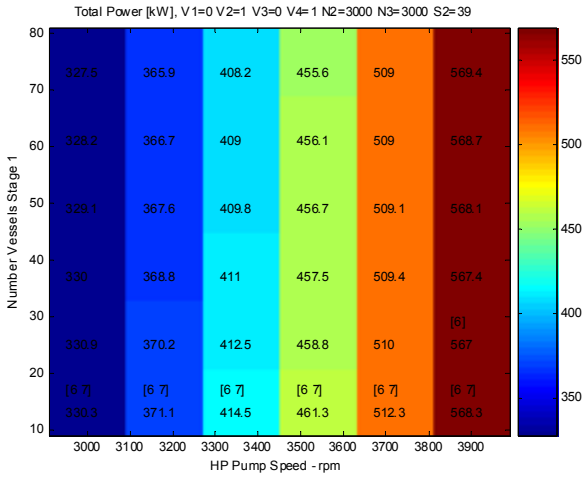

Figure 5-20. Total power for N2 = 3,000 rpm, N3 = 3,000 rpm, and S2 = 39

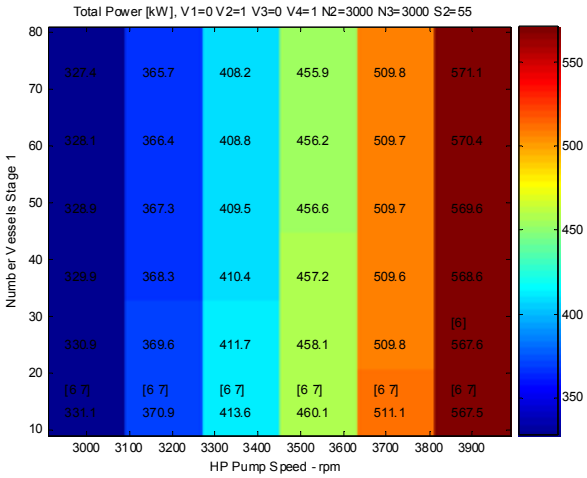

Figure 5-21. Total power for N2 = 3000 rpm, N3 = 3000 rpm, and S2 = 55

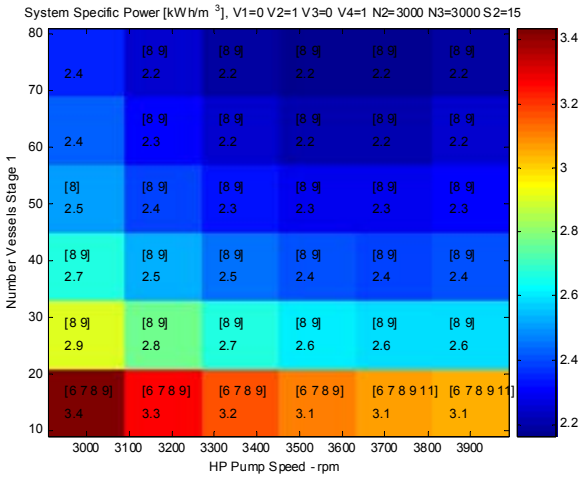

Figure 5-22. Specific power for N2 = 3,000 rpm, N3 = 3,000 rpm, and S2 = 15

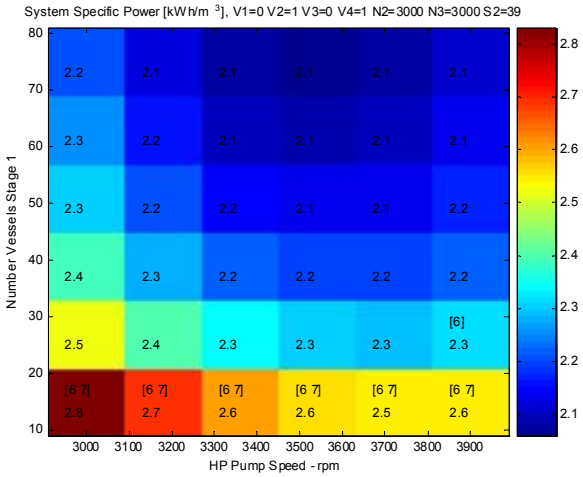

Figure 5-23. Specific power for N2 = 3,000 rpm, N3 = 3,000 rpm, and S2 = 39

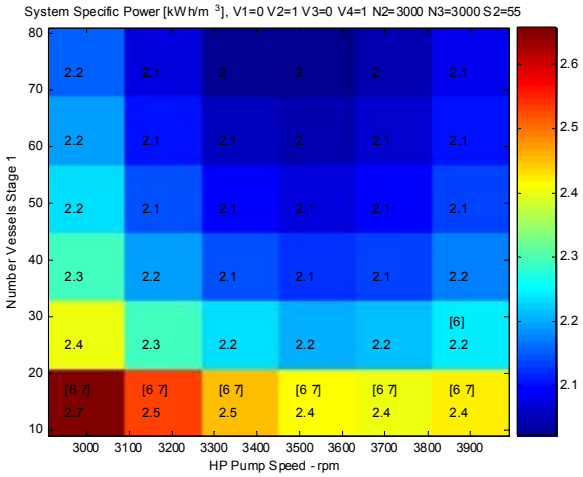

Figure 5-24. Specific power for N2 = 3,000 rpm, N3 = 3,000 rpm, and S2 = 55

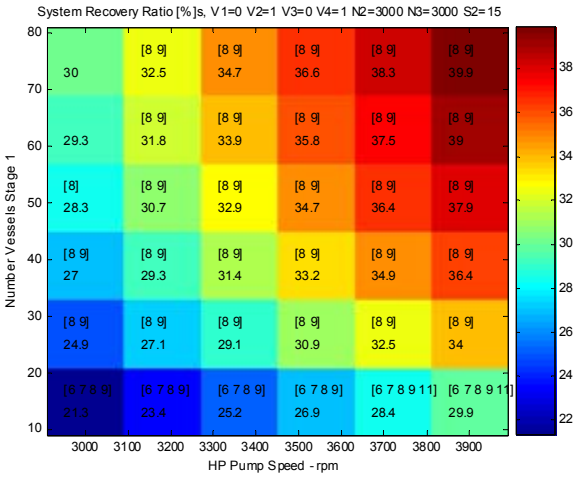

Figure 5-25: Recovery ratio for N2 = 3,000 rpm, N3 = 3,000 rpm, and S2 = 15

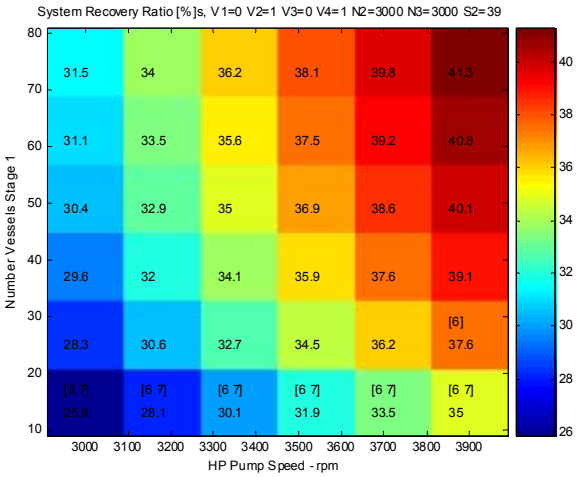

Figure 5-26. Recovery ratio for N2 = 3,000 rpm, N3 = 3,000 rpm, and S2 = 39

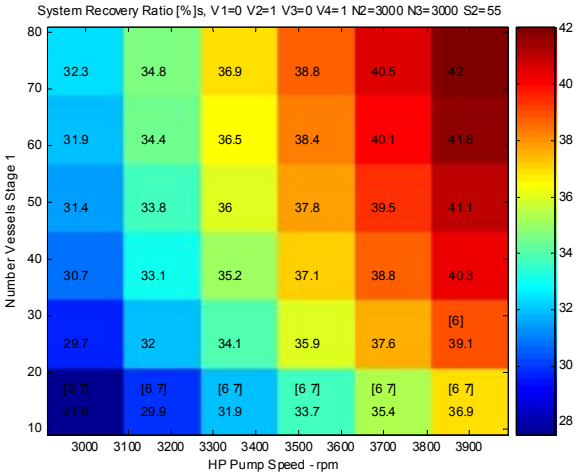

Figure 5-27. Recovery ratio for N2 = 3,000 rpm, N3 = 3,000 rpm, and S2 = 55

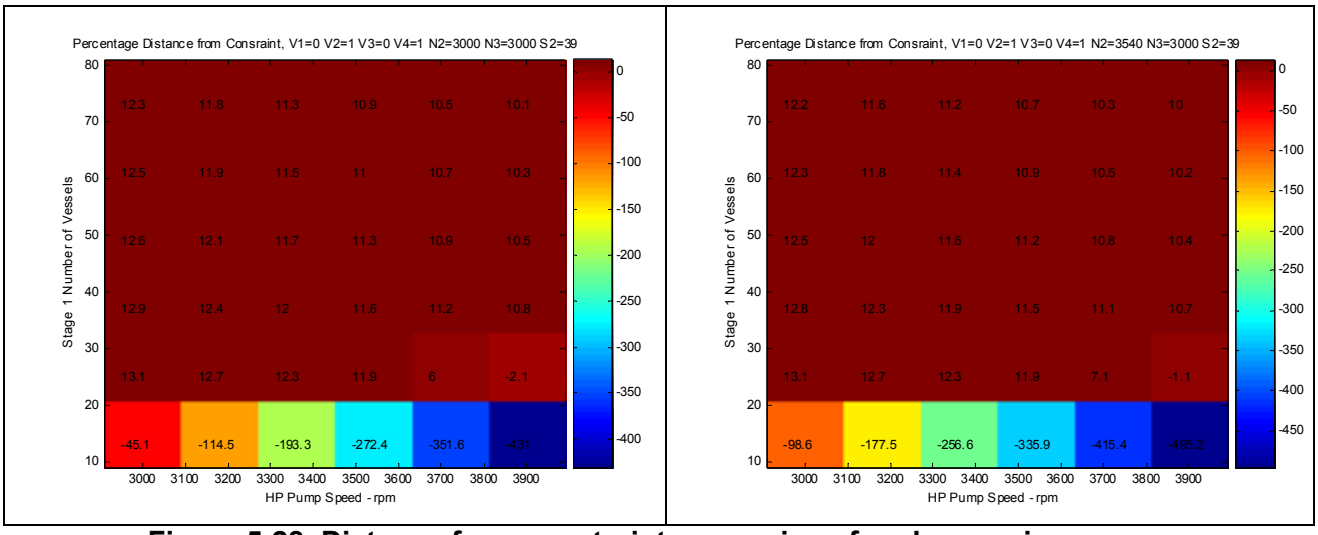

Figure 5-28. Distance from constraint comparison for changes in N2 for fixed N3 and S2

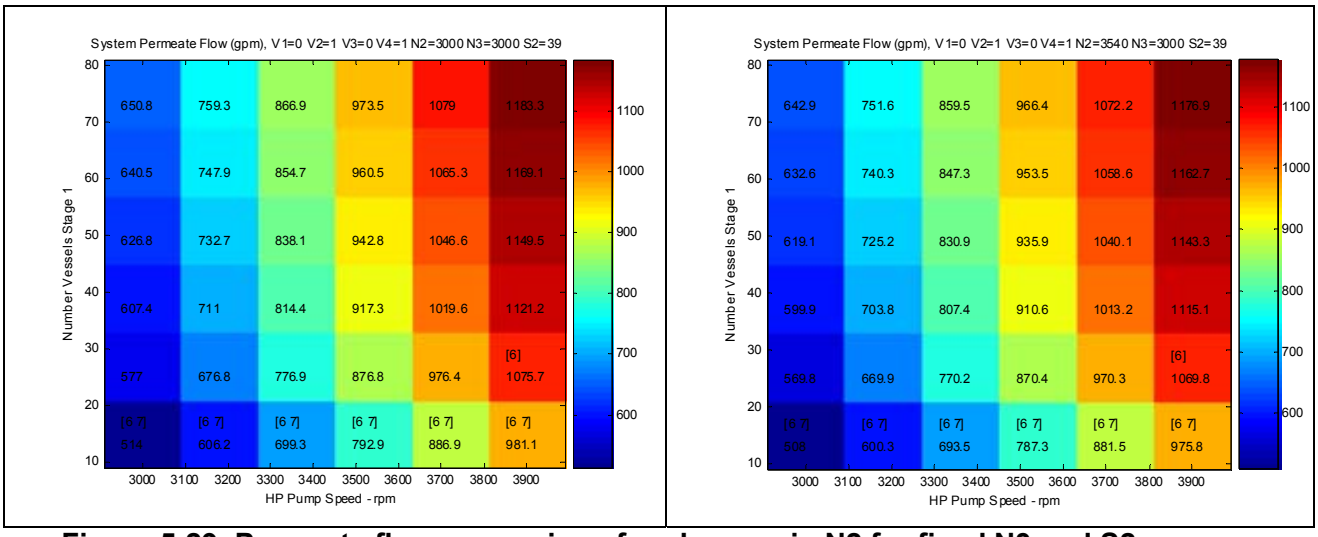

Figure 5-29. Permeate flow comparison for changes in N2 for fixed N3 and S2

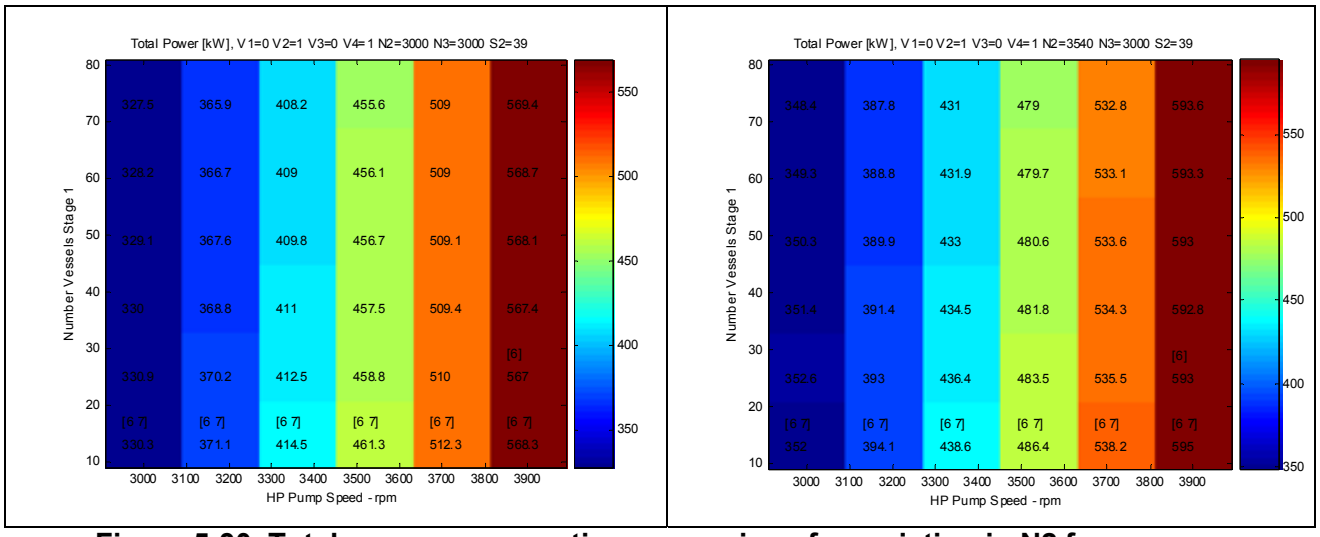

Figure 5-30. Total power consumption comparison for variation in N2 for fixed N3 and S2

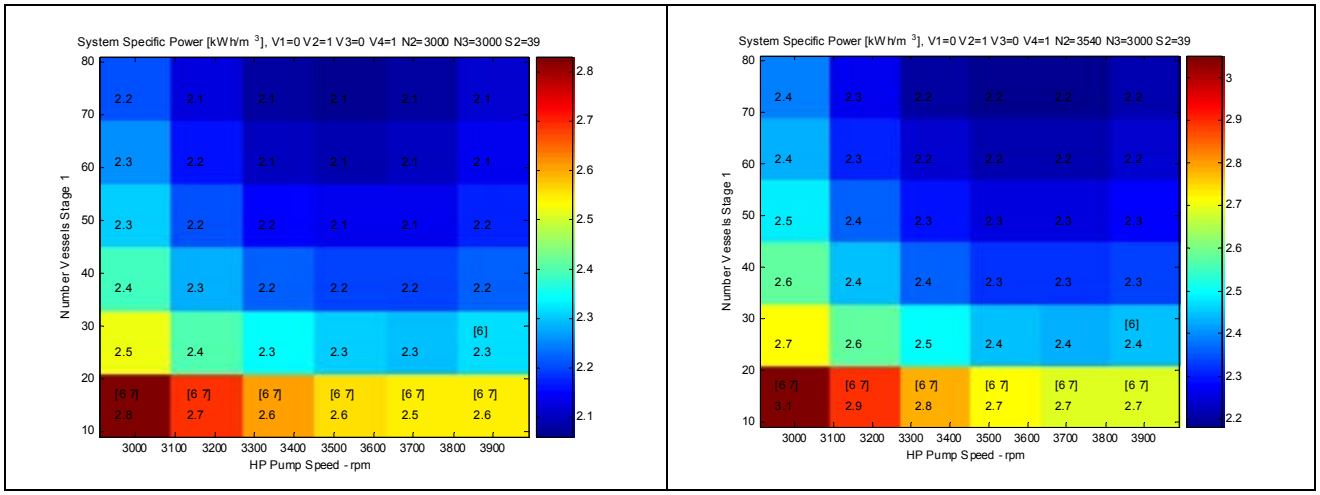

Figure 5-31. Specific power consumption comparison for variation in N2 for fixed N3 and S2

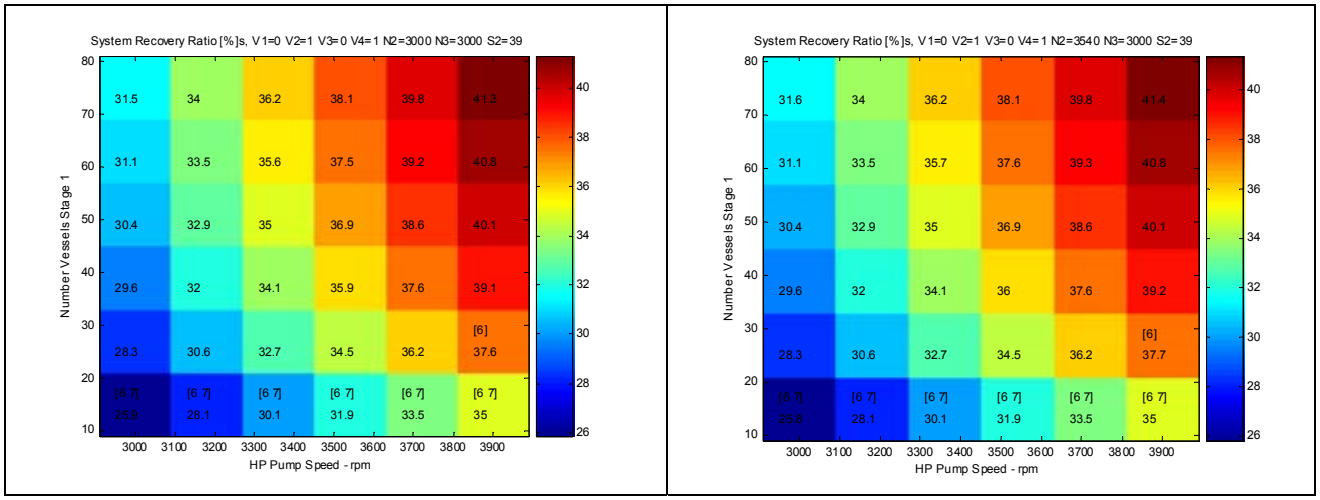

Figure 5-32: Recovery ratio comparison for variation in N2 for fixed N3 and S2

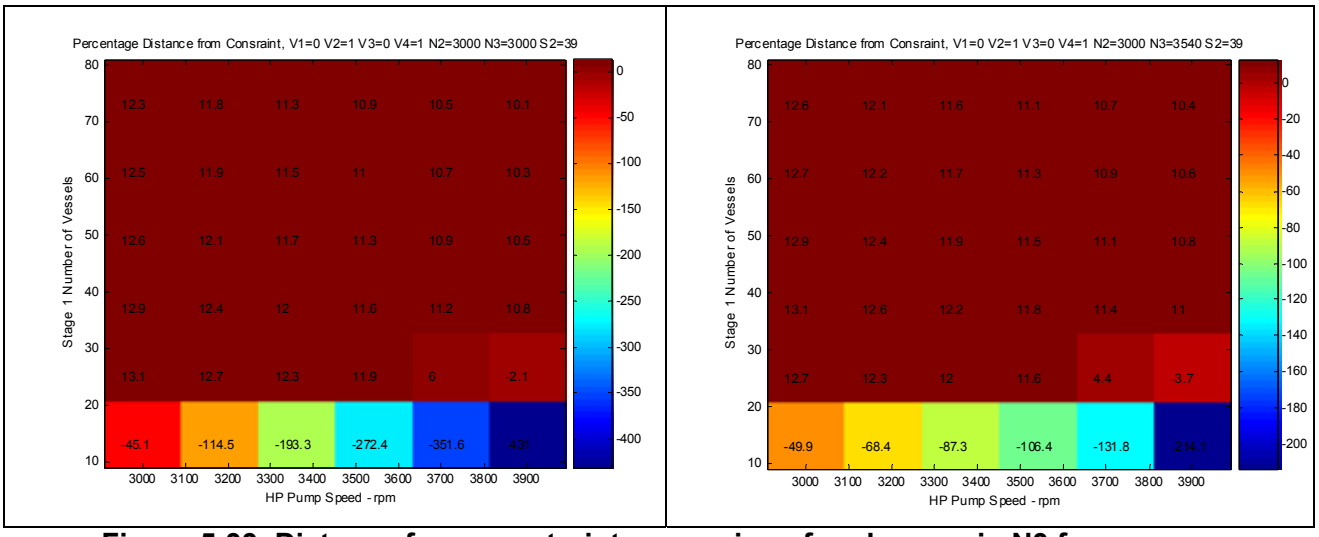

Figure 5-33. Distance from constraint comparison for changes in N3 for fixed N2 and S2

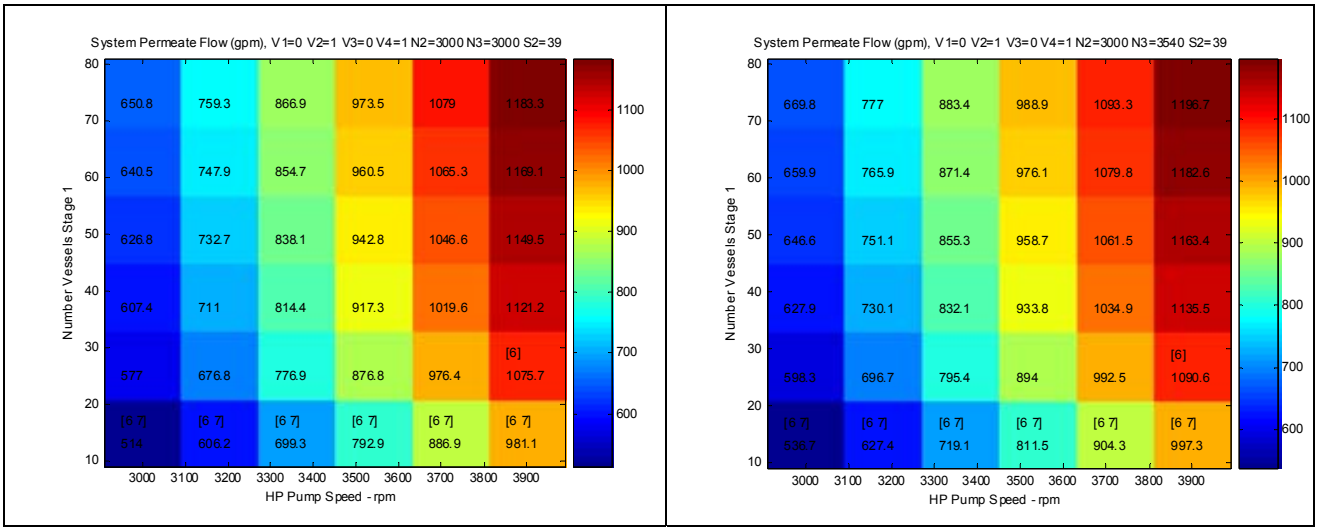

Figure 5-34. Permeate flow comparison for changes in N3 for fixed N2 and S2

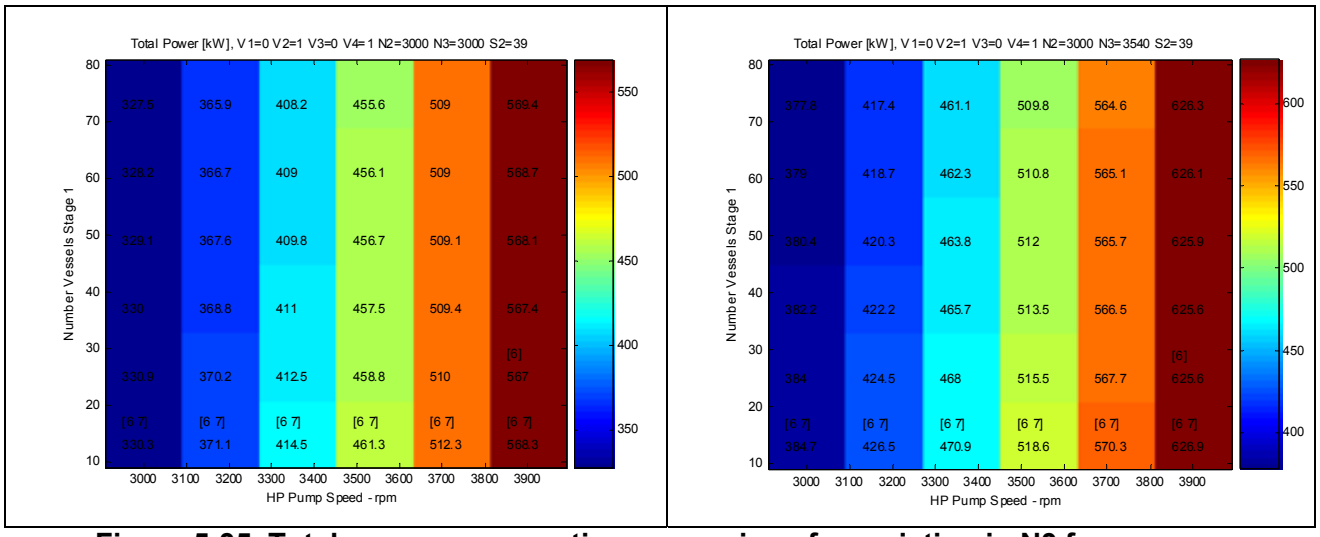

Figure 5-35. Total power consumption comparison for variation in N3 for fixed N2 and S2

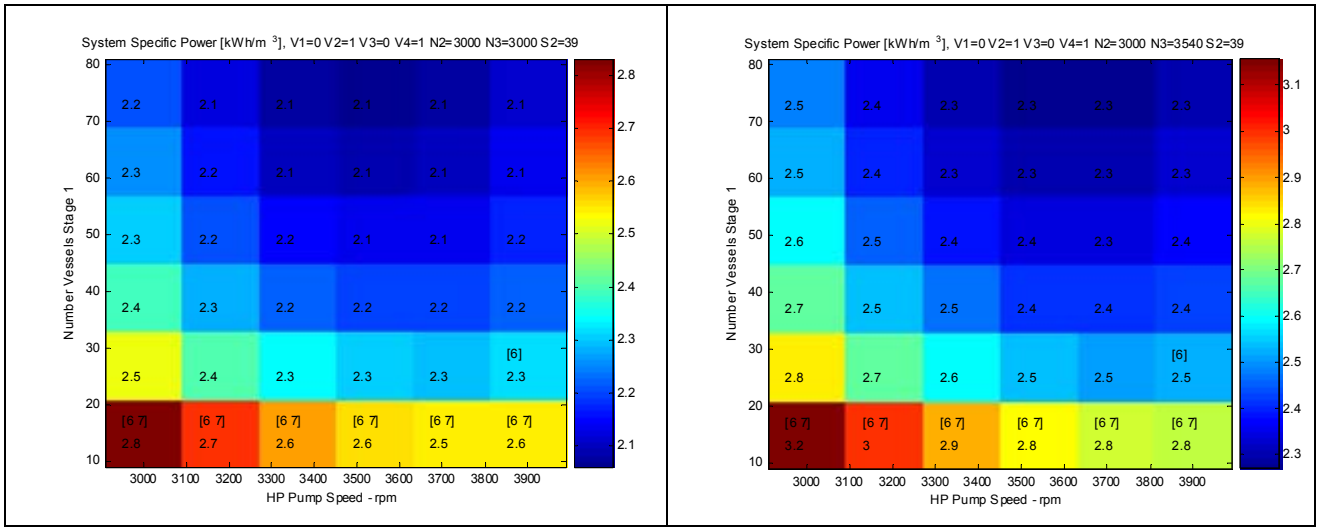

Figure 5-36. Specific power consumption comparison for variation in N3 for fixed N2 and S2

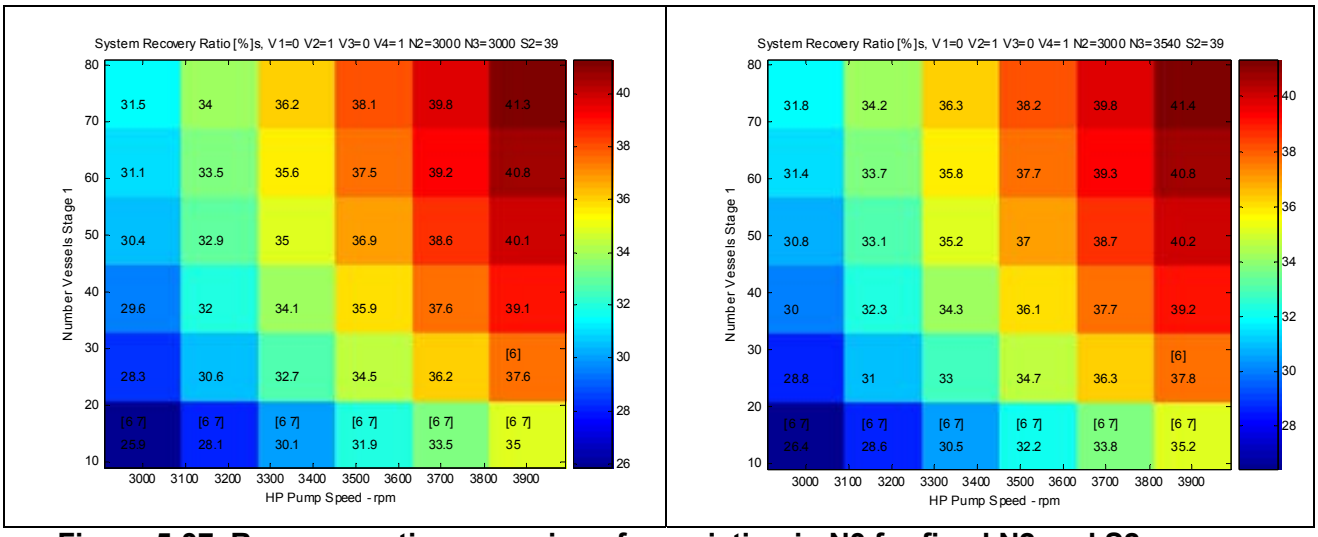

Figure 5-37. Recovery ratio comparison for variation in N3 for fixed N2 and S2

5.2.4 SWWE-a3 Nominal Design

In the SW-We-a3 configuration, a single-stage RO system is analyzed to determine the optimal design for the given energy and membrane constraints as applied to the SE-WE-a1 configuration. In this case, since there is only a single stage, there is no interstage boost pump. This means the system needs to be a DWEER boost pump, since the brine outlet pressure will always be below the feed inlet pressure to the RO system. This configuration is shown schematically in Figure 5-38.

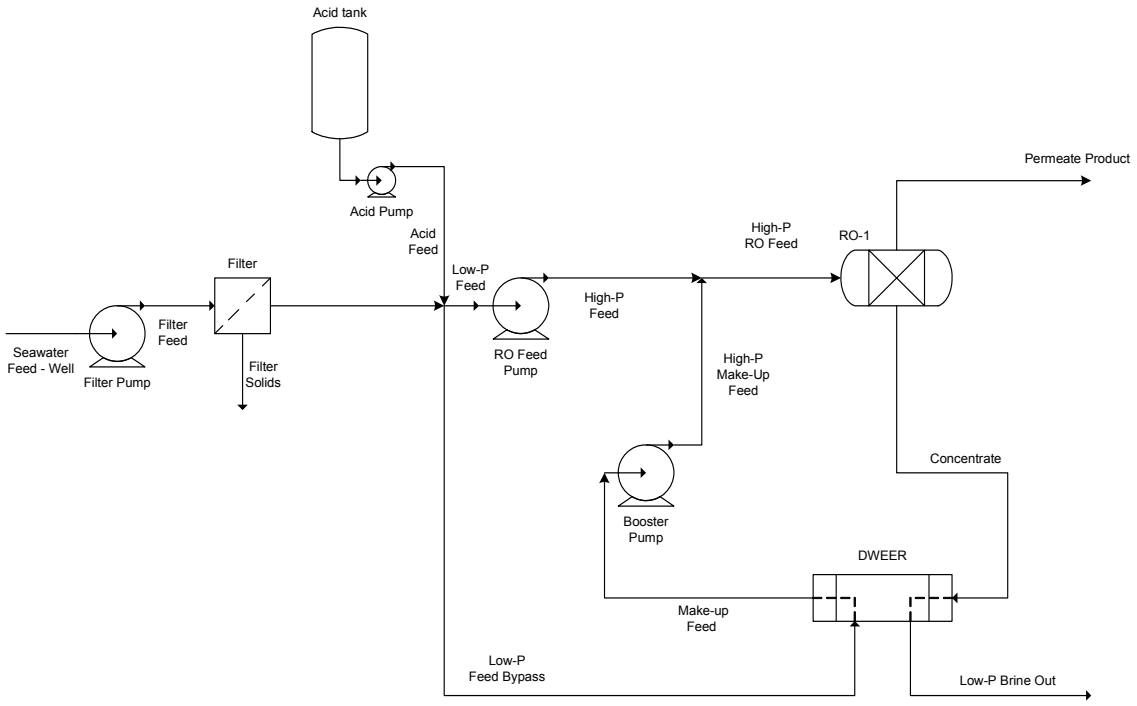

Figure 5-38. SW-WE-a3 configuration with DWEER feed boost

5.2.4.1 Power and reverse osmosis model optimization

As with SW-WE-a1, power is calculated with nominal values for pressure and flow until a value for the total power is about 540 kW. This gives a baseline for the configuration. We used the design parameters from Table 5-2 and the flows from the power calculations to optimize the steady-state membrane model.

At each convergence of the RO model, the output flows and pressures from the membrane model were plugged back into the pump power calculations to see if the power was still optimal at about 540 kW. Since the feed flow is the largest power draw on the system, if the power was too low, the feed flow to the membrane model was increased. If the power was too high, the feed flow was decreased. This cycle was iterated until the maximum flow for the given power input through an RO system was achieved. Figure 5-39 shows the results of this optimization for the power calculations representing the configurations in Figure 5-38. The

RO steady state model outputs are found in Appendix A, which refers to the data from the DWEER boost case.

SW-WE-a3 40% Recovery 1 Pass with DWEER & DWEER Boost									
Capacity Information				Input cells					
Operating Days/yr	350			Output cells					
Plant Capacity (MM m^3/yr) / (MM gal/yr)	1.82	481.8							
Plant Capacity (m^3/day) / (MM gal/day)	5211.2	1.377							
Permeate Flow (m3/Hr) / (GPM)	217.1	956.0							
Overall System Recovery (%)	40.0%								
Wind turbine Efficiency (%)	36.0%								
Specific Energy (kW-Hr/m^3)	2.40								
Toray Model and DWEER Information	Vessels	Elements	Type	Element Area (ft^2)	Total Area (ft^2)	Total Area (m^2)	Recovery (%)	Flux (GFD)	Flux (LMH)
1st Pass Membrane Configuration	52	7	820-370	370	134,680	12,512	40.0%	10.2	17.31
2nd Pass Membrane Configuration									
Filter Outlet Pressure (PSIA) / (Bar)	30	2.07							
RO Feed Pressure (PSIA) / (Bar)	854	58.88							
Concentrate Flow (GPM) / (m^3/hr)	1434.0	325.7							
Concentrate Pressure (PSIA) / (Bar)	841	57.98							
DWEER Brine Outlet P (PSIA) / (Bar)	15	1.03							
DWEER Water Out P (PSIA)	829	57.16							
DWEER Leakage (%)	1.80%								
Calculate Pump Energy Requirments base on Toray Models & Fedco Design Specifications									
Design Conditions	Efficiency (%)	Flow (m^3/hr)	Flow (GPM)	ΔP (kPa)	ΔP (PSIA)	Power (kW)	Power (hP)	Speed (RPM)	~ Cost ($)
Filter Feed Pump	75.00%	542.8	2390	310.3	45	62.40	83.7	3800	30,000.00
RO Feed Pump-1	77.20%	111.5	490.9	5681.3	824	227.99	305.7	3899	56,000.00
RO Feed Pump-2	77.20%	111.5	490.9	5681.3	824	227.99	305.7	3899	56,000.00
Interstage Booster Pump	75.00%	0.0	0	0.0	0	0.00	0.0		
DWEER Booster Pump	75.00%	319.8	1408.2	171.8	25	20.36	27.3	3800	30,000.00
ERD - DWEER	95.00%	319.8	1408.2	5716.3	829	482.60	647.2		
Total Power Requirements						**538.7**	**722.4**		
Wind Turbine Power Requirement						**1496.5**	**2006.8**		

Figure 5-39. Power calculations for SW-WE-a3 design with DWEER boost

We used the RO membrane design reports and the power calculations to develop an overall process flow diagram for the SW-WE-a3 configuration. A flow diagram is shown for the DWEER boost case in Figure 5-40. English units for flow, pressure, and flux are gpm, psia, and gfd, respectively. Corresponding metric units are cmh, bar, and lmh.

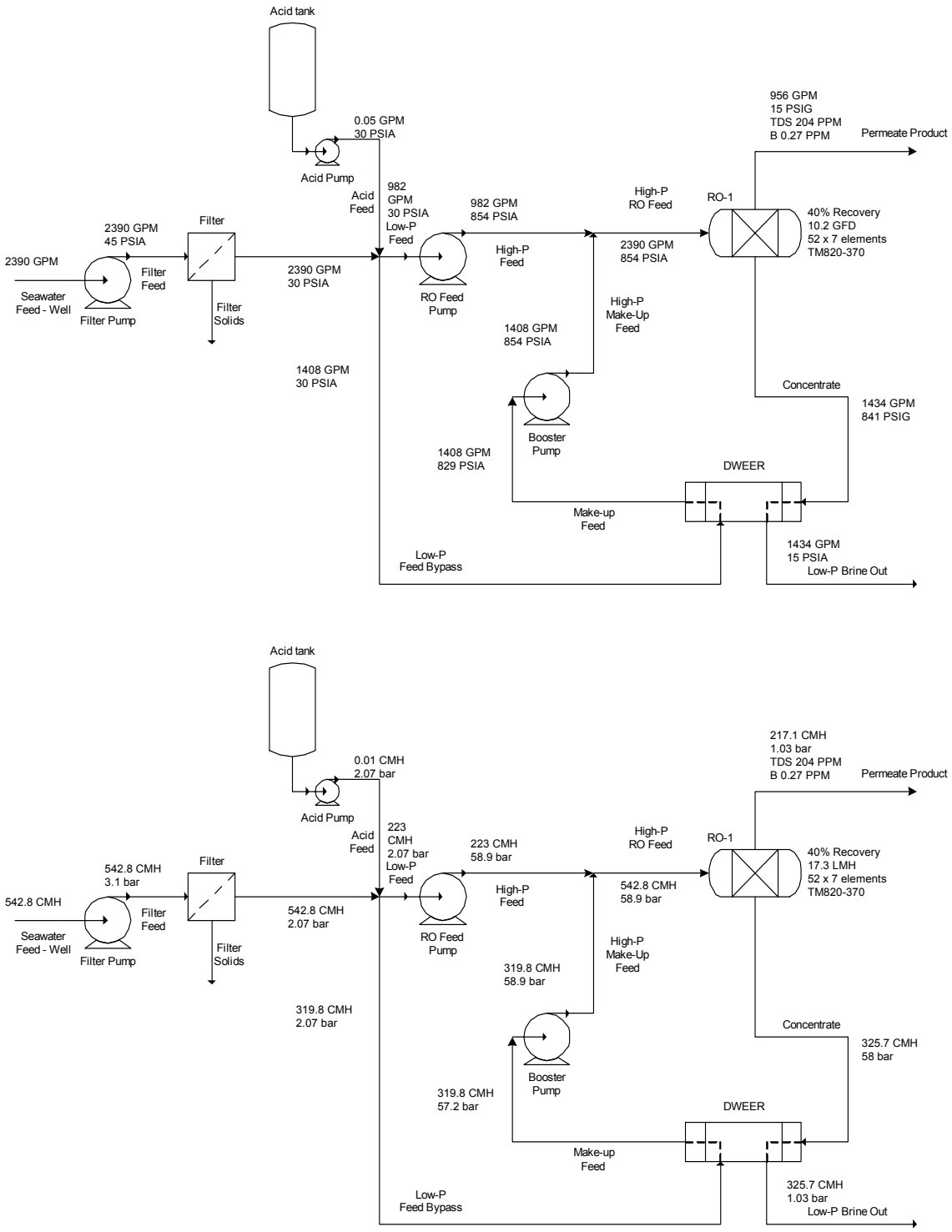

Figure 5-40. SW-WE-a3 DWEER boost flow diagram

5.2.4.2 Boron sensitivity analysis

The level of Boron in permeate water is now set to 0.3−0.5 ppm by WHO[42]. To understand the sensitivity of this configuration to Boron, we increased its feed level to determine what its level in the feed would cause it to break through in the permeate to a level of 0.5 ppm. We used the steady-state RO membrane model[33] to determine that the level of Boron in the feed that results in a 0.5-ppm level in the product permeate is 2.05 ppm. Since there is large variation in seawater Boron levels, any feedwater with Boron levels higher than 2 ppm would require a redesign of the system for a specific situation.

In this single-stage case, reducing the recovery to 30% for the 52 x 7 element configuration, and keeping the same production rate, the feed rate can be increased to 3,187 gpm (724 cmh). The energy consumption remains at about 540 kW, as the feed pressure drops to 785 psia (54.1 bar) from 854 psia (58.9 bar). The feed level of Boron can be raised to 2.3 ppm (12.2% increase), and the product permeate will remain at 0.5 ppm. There is some room for improvement in the current design to higher Boron levels. Therefore, if Boron levels are higher than 2.3 ppm, the best design option would be to have another RO Boron removal stage for the permeate only. This would require extra capital costs and increase energy consumption. Either a smaller production plant or a larger wind turbine would be required to compensate for the increased energy use. Those trade-offs in capital and operating expenses versus productivity would have to be assessed on specific high-Boron feed cases.

5.2.5 Cost of Water Analysis

Based on the above design, an overall COW is determined by calculating capital and operating costs for the configuration as outlined in detail in section 4.1. This configuration has only one stage, so the capital costs for the membrane system are much lower than those of the SW-WE-a1 configuration. A summary of the cost is shown in Figure 5-41, which outlines the relevant capital and operating costs for the steady-state model. The model assumes an operating year is 350 days, with a permeate flow rate of 5,211 m^3/day (956 gpm). This yields an annual production of 1.82 x 10^6 m^3/yr of product water. This single-stage configuration produces about 10% less water than the two-stage SW-WE-a1 configuration. Since the first stage of the SW-WE-a1 configuration (50 vessels x 6 elements, 15.7 lmh flux) is similar to the SW-WE-a3 stage (52 vessels x 7 elements, 17.3 lmh flux), the costs reduced capital costs of the single-stage SW-WE-a3 are offset by a 10% lower production rate of water.

Rolling up all the capital and operating costs for this production level gives an overall steady-state COW of about \$1.24/m^3. This cost can vary for a site-specific situation, where well construction costs, feed concentrations, and waste disposal costs can vary. The steady-state cost model, however, is flexible and can make provisions for these variances (see section 4.1).

Operating Days		350	
Labor Hrs/yr		1500	
Ro Recovery (%)		40.0%	
Number of RO Stages		2	
RO Membrane Surface Area: m^2 (ft^2)		10312	111000
Plant Capacity, m^3/day:	(gal/day)	5211.2	1,376,803
Feed Water, m^3/day:	(gal/day)	13028	3,442,008
Brine Water, m^3/day:	(gal/day)	7816.8	2,065,205
Feed Flow Rate, GPM:		2390.3	
Permeate Flow Rate, GPM:		956.1	
Brine Flow Rate, GPM:		1434.2	
Plant Capacity,MMm^3/yr:	(MM gal/yr)	1.82	481.82
Total Capital Investment Cost, MM US$:		8,858,827.58	
Plant Lifetime (yrs)		20.0	
Interest rate		8.0%	
Amortization Factor		0.10	
Annual Fixed Charges (MM$/yr)		902,291.16	
Annual Fixed Charges ($/m^3)		0.49	
Marshall & Swift Cost Index for 2004		1224	

	Lifetime (Yrs)	Raw Cost ($)	(%)	US$/m^3	
LABOR RELATED COSTS:					
RO Specific Cost of operating & maintenance labor				0.0550	
Total Labor Related				0.0550	
Supplies (% of Operating labor)			20.0%	0.0110	
Genearl Maintenance Material (% of OperatingLabor)			4.0%	0.0022	
Maintenance Battery Replacement Cost ($/m^3)	10			0.00493	
Maintenance Membrane Replacement Cost ($/m	3			0.0399	
Wind Tubine routine Maintenance		14,560.00		0.0080	
Wind turbine Warranty & Non-routine Maintenanc	20	33,230.00		0.0182	
Total				0.0842	
TOTAL MAINTENANCE & LABOR				0.1392	
Taxes & Insurance (%TFI)			2.0%	177,176.55	
Depreciation (%TFI)			10.0%	885,882.76	
CAPITAL RELATED COSTS ($/m^3)				0.5828	
TOTAL FIXED COSTS ($/m^3)				1.2168	
TOTAL MANUFACTURING COSTS ($/m^3) / ($/1000Gal)				1.2359	4.6784
Reference Total Manufacturing Costs ($/m3) / ($/1000Gal)					
Dietrich & Robert (1.10 MM Gal/day permeate scale, 2005)		Max cost is about this		1.51	5.70
Hafez & El Manharawy (4800 m3/day permeate scale, 2002)				1.42	5.37
Ettouney et al (4000 m3/day permeate scale, 1992)				2.68	10.15
Ettouney et al (4546 m3/day permeate scale, 1999)				1.48	5.59
Garcia-Rodriguez et al (3000 m3/day permeate scale, Wind RO system, 2001)				2.01	7.62

VARIABLE COSTS:	Density (kg/l)	Conc. wt%	Use g/m^3 Permeate	Use (Kg/day)	Matl $/Kg	$/m^3
RAW MATERIALS:						
HCl	1.20	35.0%	0.000	0.0	0.100	0.00000
H2SO4	1.83	93.0%	58.187	303.2	0.099	0.00577
NaOCl	1.00	100.0%	0.000	0.0	3.640	0.00000
Na2CO3	1.00	100.0%	0.000	0.0	0.221	0.00000
Na2S2O5	1.00	100.0%	0.000	0.0	1.544	0.00000
Lime	1.00	100.0%	0.000	0.0	0.077	0.00000
NaOH	1.00	100.0%	0.000	0.0	0.331	0.00000
Scale inhibitor	1.00	100.0%	0.050	0.261	3.440	0.00017
Ferric Sulfate	1.00	100.0%	0.000	0.0	0.210	0.00000
Total Raw Materials ($/m^3)						0.0059
Disposal Costs				m^3/m^3 Perm.	$/m^3	$/m^3
Brine Waste				0.6000	0.0180	0.0108
Chemical Cleaning Waste				0.0010	0.5000	0.0005
Total Waste Disposal						0.0113
TOTAL RAW MATERIALS & WASTE ($/m^3)						0.0172

Power Requirements:	Efficiency (%	Flow GPM	P (kPA)	P (PSIA)	Power (kW)	Power (hP)
Filter Feed Pump	75.00%	2390	310.3	45	62.40	83.7
RO Feed Pumps	77.20%	981.8	5681.3	824	455.97	611.5
Booster Pumps	75.00%	1408	172.4	25	20.42	27.4
Chemical Feed Pumps	75.00%	0.06	310.3	45	0.00	0.0018
Totals for Power Calcs					538.8	722.5

Utilities:		(Usage)	Units	Use (kW)	Total (kW-h)	$/Unit	$/m^3
Electricity	%	1.0%	kw-h	538.8	45,258	0.076	0.0019
Battery	Hours	10.0	kw-h	45.0	450		
TOTAL UTILITIES ($/m^3)							0.0019
TOTAL RAWS & UTILITIES ($/m^3)							0.0191

Wind Turbine Power Requirement	
Power Utilization (%)	36.0%
Power Output (MW)	1.497
Specific Power (kWh/m^3)	6.89

Specific Power Comparisons	
SW-WE-a3 specific energy (kW-hr/m^3)	2.48
Ettouney et al (2002)	5
Dietrich & Robert (2005)	2-3
Garcia-Rodriguez et al (2001)	~4
Manth et al (2003)	2-4
MacHarg	2.5-3.5

Figure 5-41 Summary costs for the steady-state SW-WE-a3 configuration

5.2.6 Design Space Analysis

We conducted a design space analysis to understand the extent of the operating envelope associated with the configuration described in Section 5.2.2. As in the previous configurations, the main purpose of this study is to investigate the points in the input space at which the system fails to satisfy all the component and system constraints. If the system were operated at these points, where the constraints were not met, the potential for membrane degradation through fouling or scaling or membrane destruction from increased stresses may result. In addition to understanding where constraints are violated, the design space study provides some insight into how system quantities of interest such as recovery ratio, specific energy consumption, total power, and permeate flow vary with the choice of input parameters. The qualitative understanding that the design space study provides is critical for understanding the potential for system optimization.

For the single stage configuration shown in Figure 5-42, the input space is defined by the parameters listed in Table 5-6.

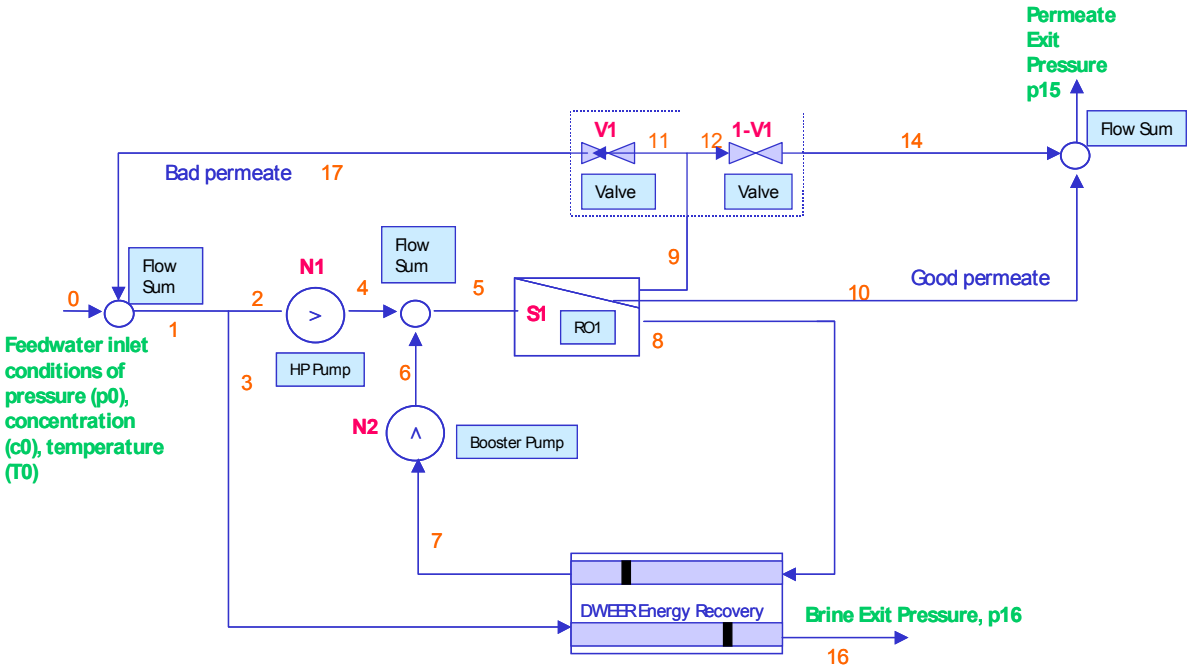

Figure 5-42. RO system configuration SWWE-a3

Table 5-6. Input Parameters for Configuration SWWE-a3

Parameter	Description
S1	Number of vessels in stage 1
N1	High-pressure pump speed
N2	Booster pump speed
V1	Bad permeate recycle valve position

Since the valve position V1 is mainly used to initiate a recycle flow for low wind power capture conditions, the design space analysis considers only small amounts of recycle given by valve positions in the range of 0%–20%. Table 5-7 lists the parameter values investigated in the design space analysis for this configuration.

The steady-state constraints for the RO system were highlighted in Section 5.1.2 and are repeated in Table 5-8. Table 5-8 also lists the index associated with each constraint; this index reference is used in the design space plots to highlight which constraints, if any, are being violated at a given point in the input space.

Table 5-7. Input Space Parameter Ranges for Configuration SWWE-a3

Parameter	Description	Units	Variation Range
S1	Vessels in stage 1	-	15−125
N1	High pressure pump speed	rpm	3,000–3900
N2	Booster pump speed	rpm	3,000–3,900
V1	Stage 1 permeate recycle valve	% open	0%–20%
p0	Feedwater pressure	psid	20
p15	Permeate exit pressure	psid	15
p16	Brine exit pressure	psid	15
T0	Feedwater temperature	°C	25
c0	Feedwater dissolved salt concentration	kg/m^3	29.6

Table 5-8. Constraint definition for configuration SWWE-a3

Parameter	Value/range	Index Used in Plots
Element polarization	$C_m / C_{avg} < 1.2$	1
Element concentration flow	$Q_c > 15$ gpm	2
Feedwater pressure	$P_f < 1200$ psi	3
Element pressure drop	$\Delta P_{elm} < 10$ psid	4
Vessel pressure drop	$\Delta P_{vessel} < 58$ psid	5
Permeate quality	$C_p < 500$ ppm	6
Element flux	Flux < 20.6 gfd	7

The results of the design space analysis for the seawater configuration SWWE-a3 are shown in Figure 5-43−Figure 5-57 for system parameters such as permeate flow, total power, specific energy consumption, and recovery ratio. The figures associated with these parameters also highlight the constraints violated in brackets and the system parameter value at each data point in the analysis. Finally, for each combination of input parameters that are presented, the distance to the constraint is identified in terms of percentage. The distance in terms of percentage from maximum constraints is given in Eq. 5-9 by

$$Distance\ to\ constraint = \frac{Constraint\ Value - Parameter\ Value}{Constraint\ Value} * 100 \qquad \text{Eq. 5-9}$$

and the distance in terms of percentage from minimum constraints is given in Eq. 10 by

$$Distance\ to\ constraint = \frac{Parameter\ Value - Constraint\ Value}{Constraint\ Value} * 100 \qquad \text{Eq. 5-10}$$

Positive numbers in these figures indicate that there are no limiting constraints, and the number shown in the figure is the distance to the most restrictive constraint. Negative numbers shown in the figures indicate that at least one constraint is being violated, and the number shown in the figure indicates the maximum constraint violation.

Consider the results shown in Figure 5-43–Figure 5-57 for the case where the booster pump speed (N2) is varied from 3,000 rpm to 3,900 rpm, and the recycle valve, V1, is varied between a fully closed position (V1 = 0) to a partially opened position (V1 = 20%). For each value of N2, data associated with permeate flow, total power, specific power, recovery ratio, and distance from the constraint are shown as functions of high-pressure pump speed (N1) and the number of vessels in RO stage (S1). Considering the results in Figure 5-43, the operating points that meet the constraints of the system lie on a diagonal in the S1-N1 input space. Essentially, as the high-pressure pump speed is increased, the number of vessels should also increase. Figure 5-43−Figure 5-45 show that as the booster pump speed is increased, the allowable design space shifts downward toward a lower number of vessels. The impact on the design space variation when permeate recycle is introduced is slight. For example, consider Figure 5-43 where N2 = 3,000 rpm and the recycle valve is opened from a fully closed position to a partially open position. The area of the S1-N1 input space that sees the most impact is the lower right hand corner, small number of vessels and larger high pressure pump speeds. For this region of the input space, recycle reduces the allowable design space and drives the system further away from meeting the constraints. This behavior is also observed at other booster speeds (Figure 5-44 and Figure 5-45).

To better understand the limiting constraints and the impact on additional system parameters, consider the permeate flow results shown in Figure 5-46–Figure 5-48. Figure 5-46 shows that the primary constraint being violated at large number of vessels is the minimum concentration flow. The fact that concentration flow is the limiting factor is reasonable given that the feedwater is divided across a larger number of vessels without a significant increase in recovery ratio (Figure 5-55). The result is a lower concentration flow in each element, which results in a violation of the minimum concentration flow constraint. When the high-pressure pump speed is great and the number of vessels is small, the limiting constraint is the flux in an element. This behavior is reasonable in that at greater high-pressure pump speeds for a specified pressure rise, the larger inlet flow is split across fewer vessels. Hence, the flux in each element of the vessel will be larger and result in a violation of the flux constraint. The trend in permeate flow for a given booster pump speed depends on the speed of the high-pressure pump. At lower speeds, the gradient with number of vessels is approximately 5 gpm/vessel. However, at higher speeds, the gradient is on the order of 15 gpm/vessel. The impact of booster pump speed on permeate flow is that as booster speed is increased, the permeate flow decreases by approximately 3%-4% for a 500-rpm increase in booster speed.

The results in Figure 5-49–Figure 5-51 show that the total power consumed is primarily dictated by the high-pressure pump speed. This result is expected given that the high pressure pump dominates the system energy consumption. The increase in power consumed for a given high-pressure pump speed that is caused by an increase in the number of vessels is on the order of 2 kW/vessel at lower values of high-pressure pump speed and approximately 7 kW/vessel at higher pump speeds. The power consumption per vessel differences at low and high speeds is primarily driven by the increased flow capacity at the higher speeds, which corresponds to higher permeate flows at larger high

pressure pump speeds. By coupling the permeate flow results with the total power consumption results, the variation in specific energy consumption can be investigated (Figure 5-52−Figure 5-54). The specific energy consumption decreases slightly when the number of vessels is increased. In addition, as the booster speed is increased, the area in the S1-N1 region that corresponds to minimum specific energy consumption shifts to the right, i.e., greater high-pressure pump speeds. The impact of permeate recycle is to slightly increase the specific energy consumption that is caused by a reduction in overall permeate flow.

Finally, with regard to system recovery ratio (Figure 5-55−Figure 5-57), the relationship between number of vessels and high-pressure pump speed is nonlinear. For example, consider the results in Figure 5-55 for a booster pump speed of 3,000 rpm. At each high-pressure pump speed, the system recovery ratio initially increases as the number of vessels is increased. However, with a large number of vessels, the system recovery ratio does not change significantly with further increases in the number of vessels. This behavior would suggest that initially the throughput of the system is easily increased with an increasing number of vessels without a substantial increase in feedwater flow. However, there is a point of diminishing returns where changes in recovery ratio are not easily made. In this case, an increase in feedwater flow rates is required for an increase in permeate flow. The number of vessels at which the recovery ratio stabilizes is lower as the high-pressure pump speed is increased. The impact of booster pump speed on the recovery ratio is to slightly decrease the system recovery and incur an increase in power consumption. As expected, the impact of the permeate recycle is to drop the overall system recovery rate.

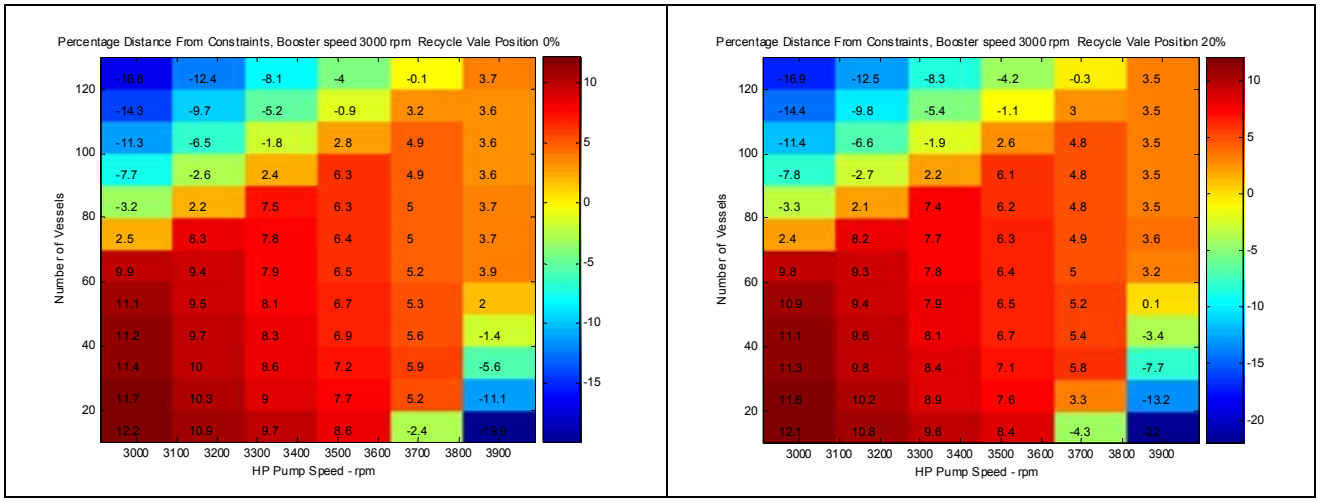

Figure 5-43. Percentage distance from constraint for N2 = 3,000 rpm, recycle valve at 0% and 20% opening

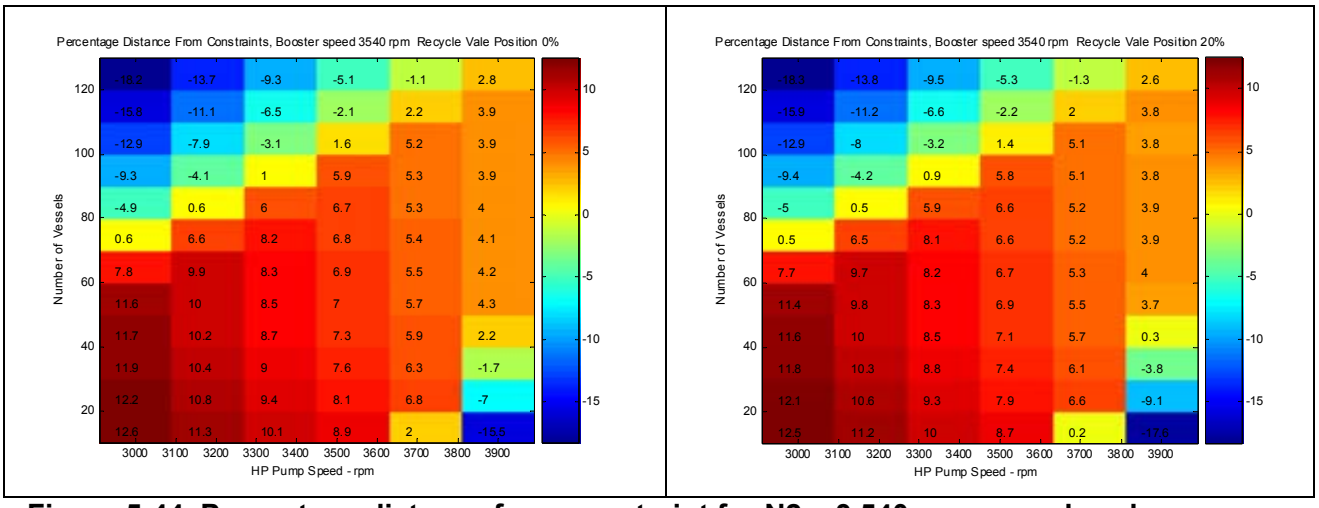

Figure 5-44. Percentage distance from constraint for N2 = 3,540 rpm, recycle valve at 0% and 20% opening

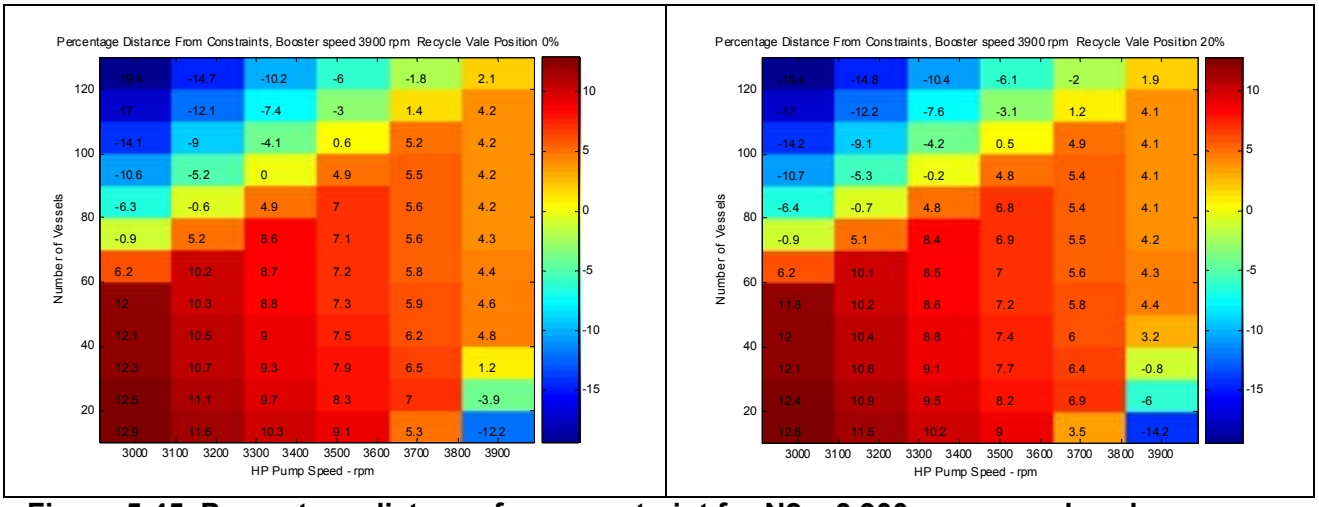

Figure 5-45. Percentage distance from constraint for N2 = 3,900 rpm, recycle valve at 0% and 20% opening

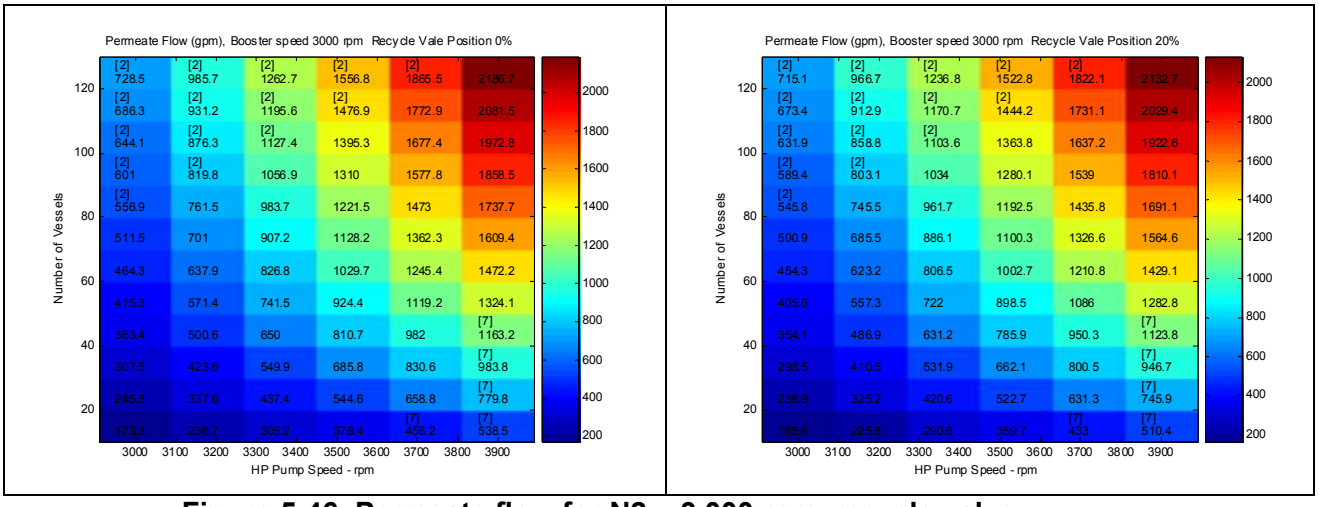

Figure 5-46. Permeate flow for N2 = 3,000 rpm, recycle valve at 0% and 20% opening

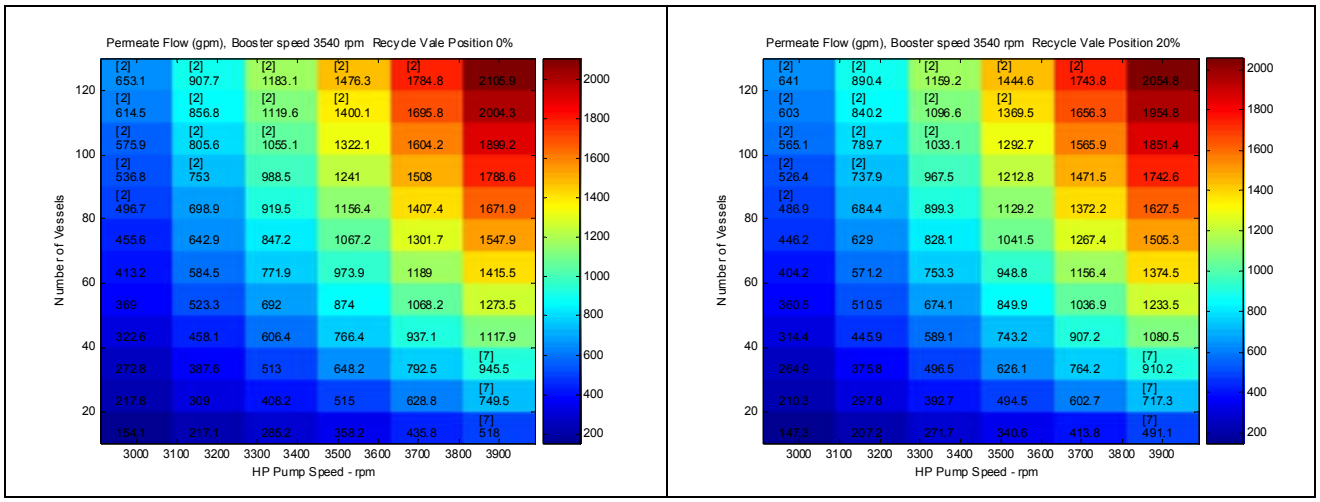

Figure 5-47. Permeate flow for N2 = 3,540 rpm, recycle valve at 0% and 20% opening

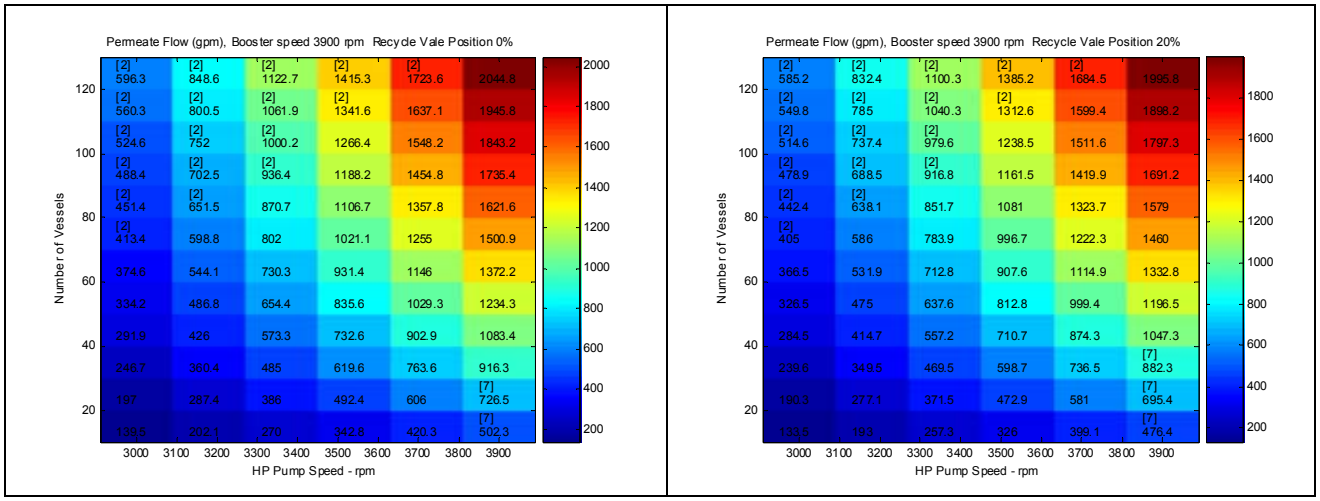

Figure 5-48. Permeate flow for N2 = 3,900 rpm, recycle valve at 0% and 20% opening

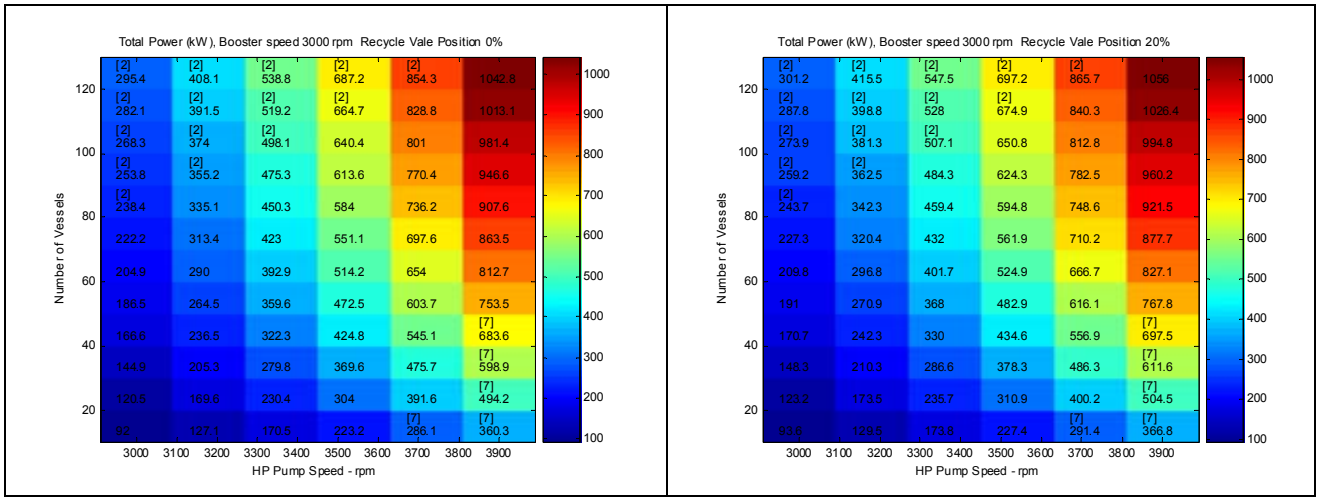

Figure 5-49. Total power for N2 = 3,000 rpm and recycle valve position at 0% and 20% opening

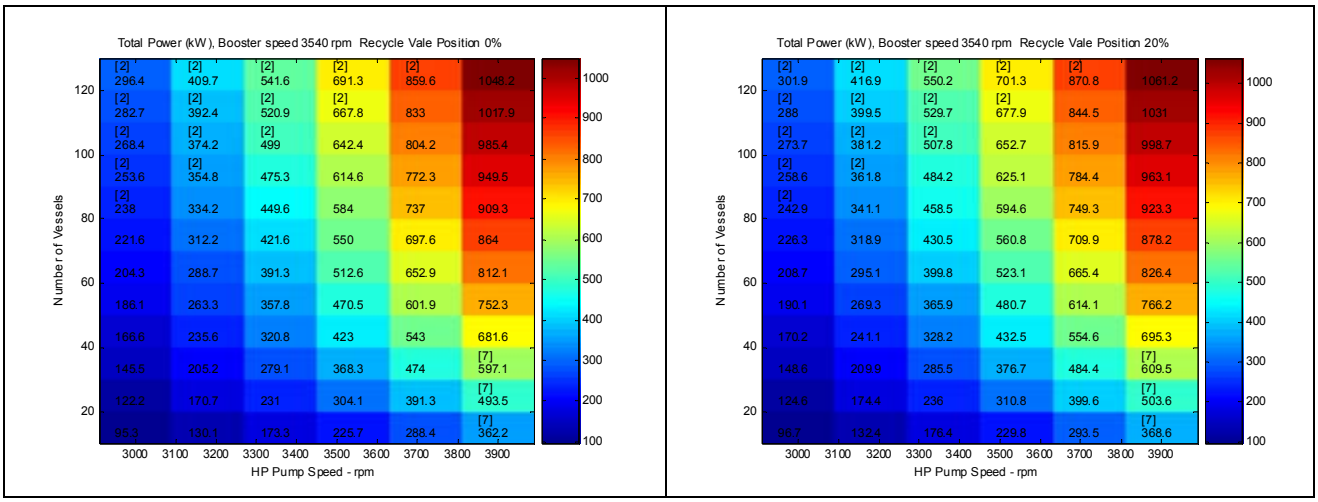

Figure 5-50. Total power for N2 = 3,540 rpm and recycle valve position at 0% and 20% opening

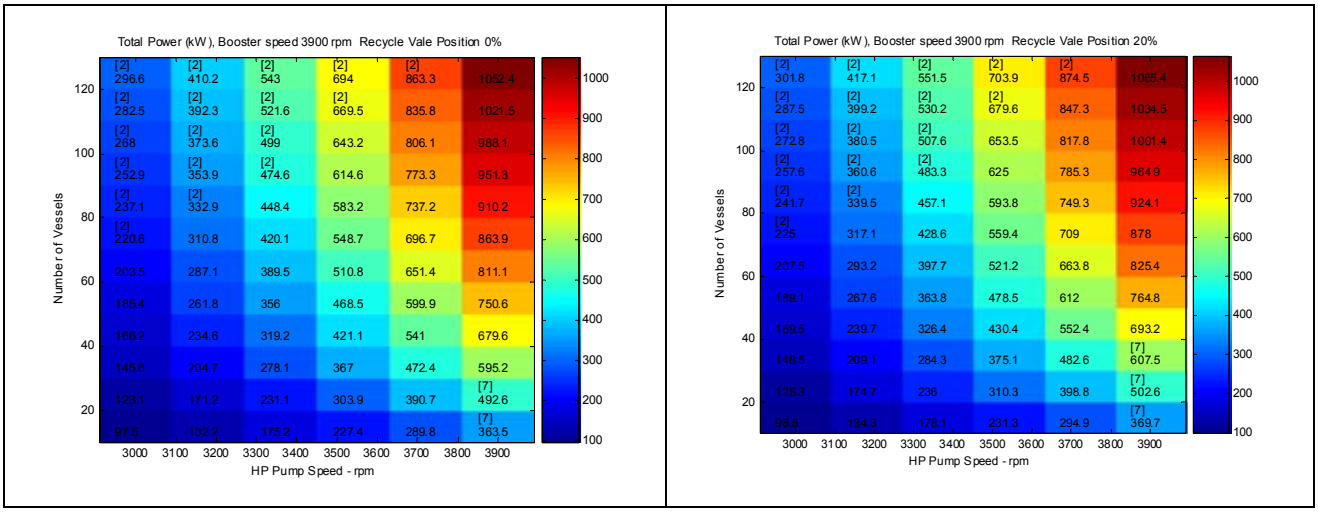

Figure 5-51. Total power for N2 = 3,900 rpm and recycle valve position at 0% and 20% opening

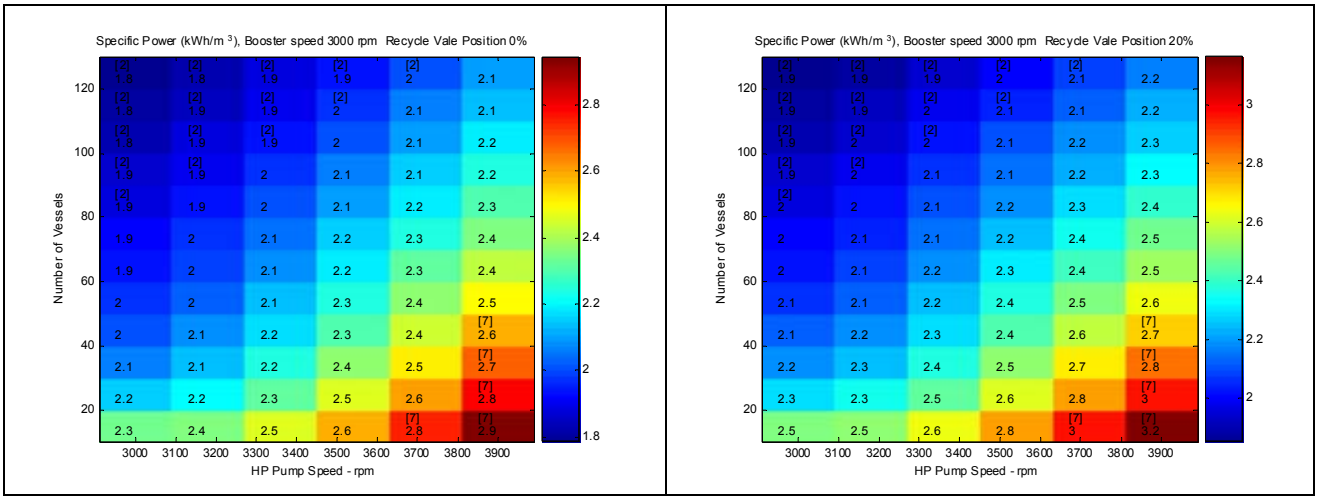

Figure 5-52. Specific energy consumption for N2 = 3,000 rpm and recycle valve position at 0% and 20% opening

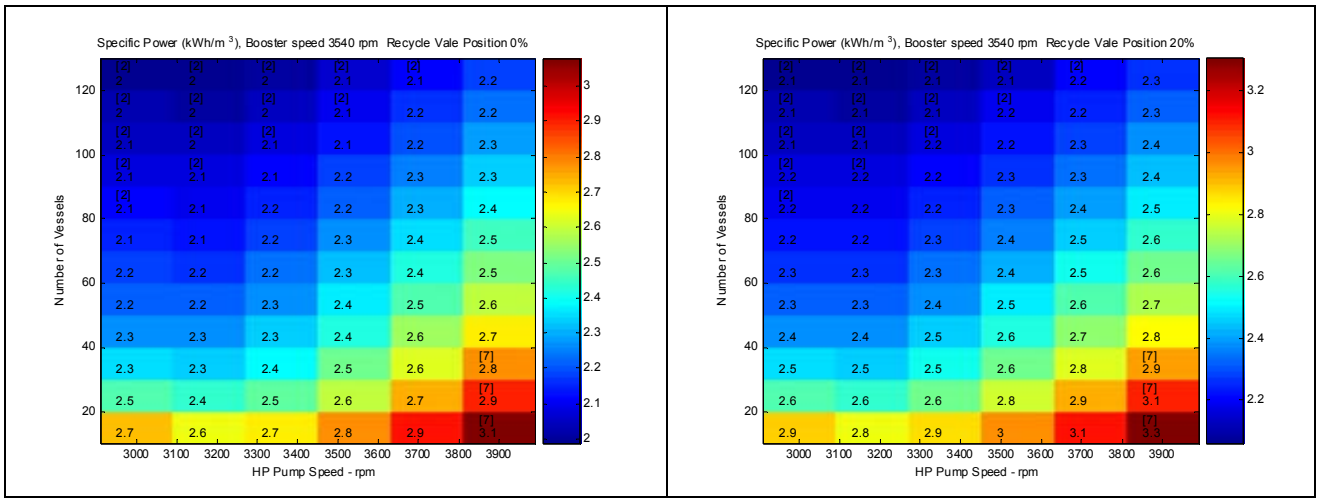

Figure 5-53. Specific energy consumption for N2 = 3,540 rpm and recycle valve position at 0% and 20% opening

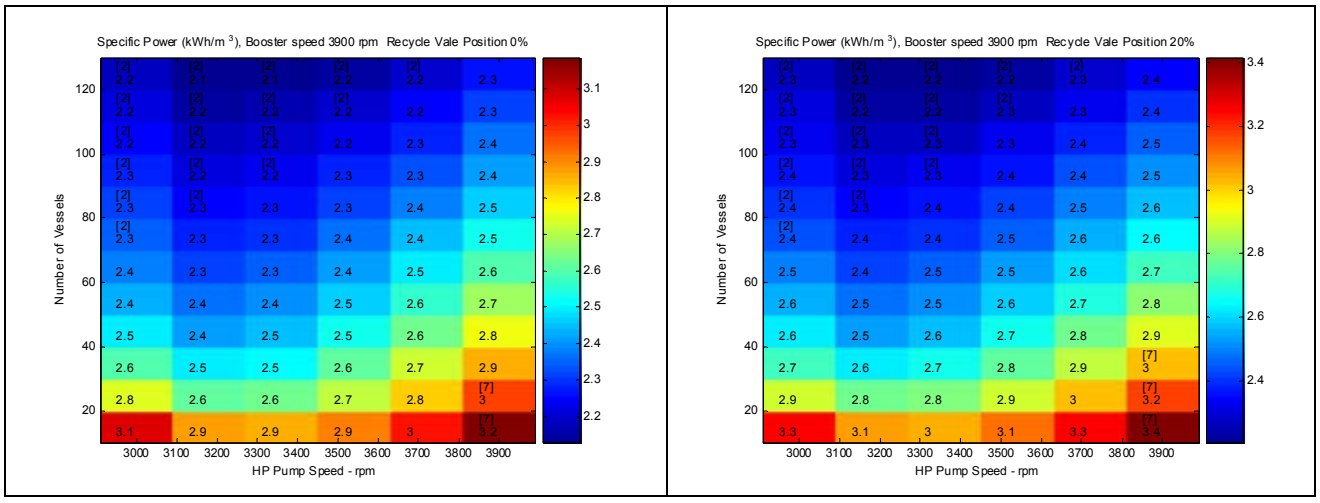

Figure 5-54. Specific energy consumption for N2 = 3,900 rpm and recycle valve position at 0% and 20% opening

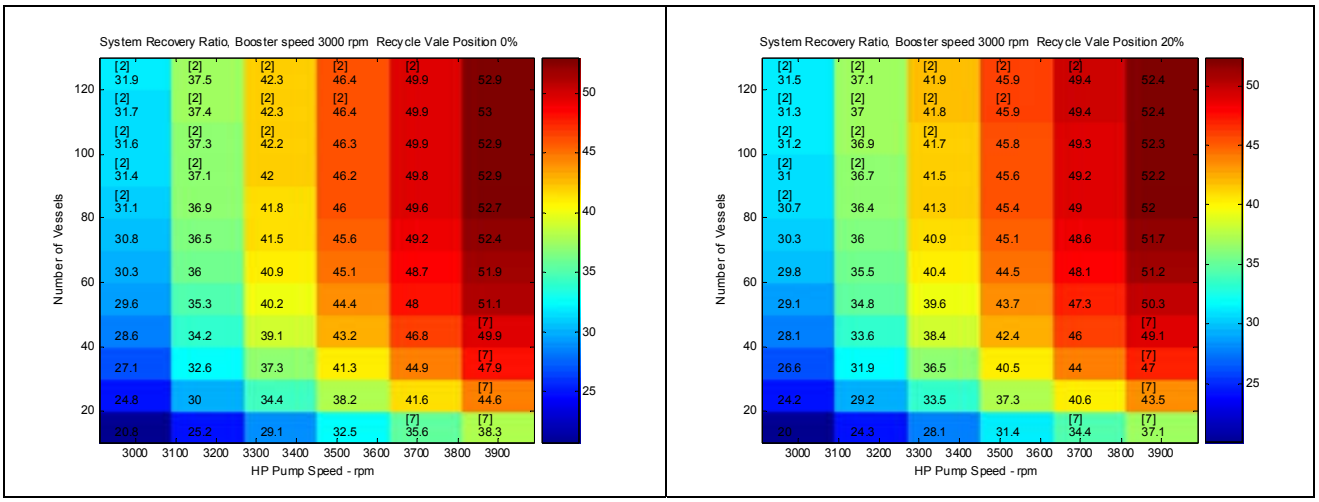

Figure 5-55. System recovery ratio for N2 = 3,000 rpm and recycle valve position at 0% and 20% opening

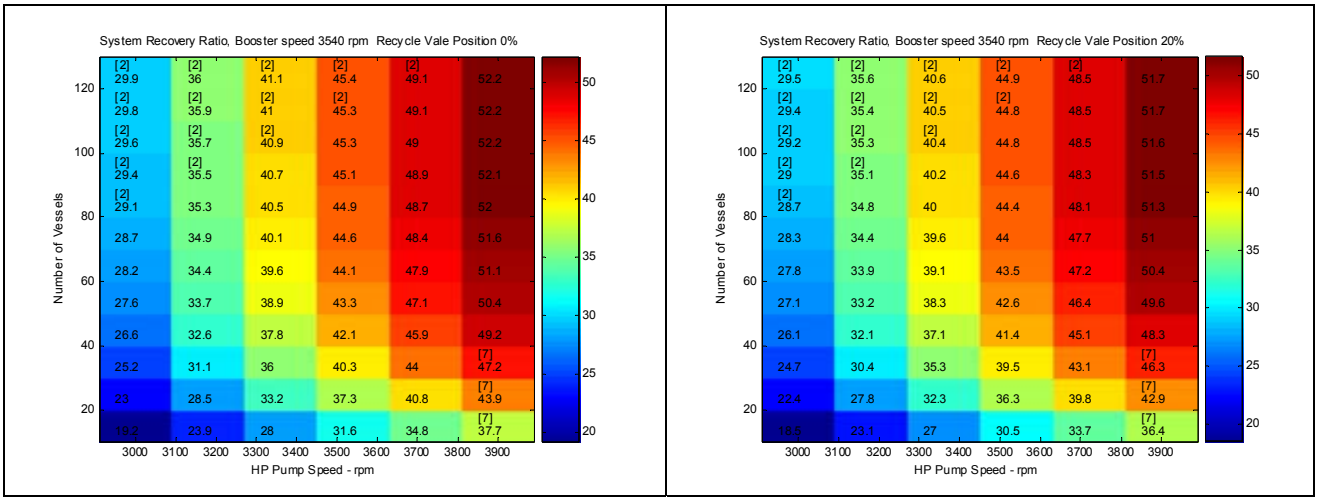

Figure 5-56. System recovery ratio for N2 = 3,540 rpm and recycle valve position at 0% and 20% opening

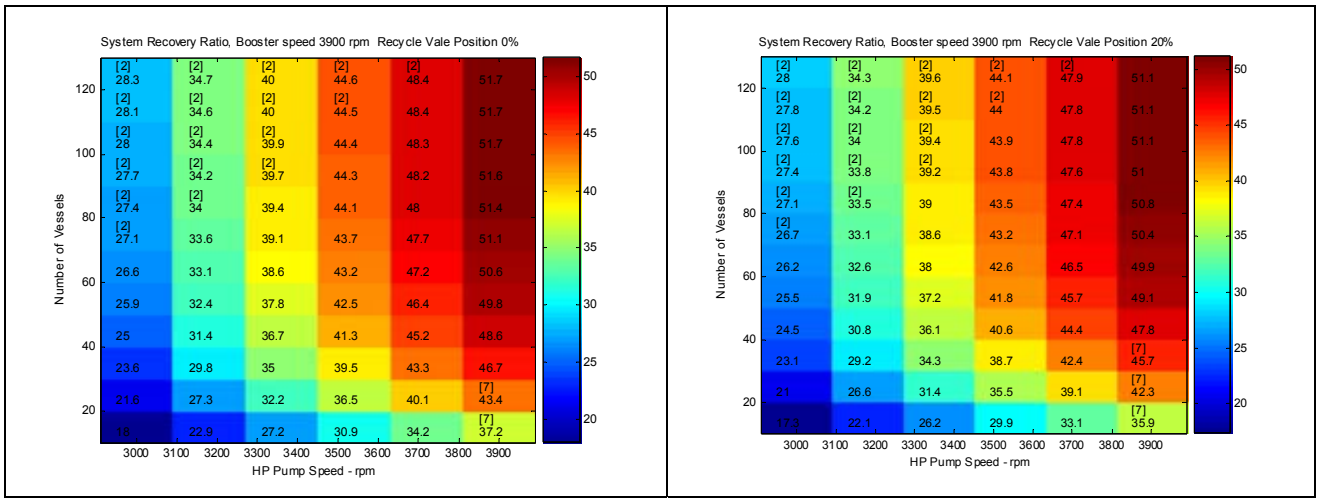

Figure 5-57. System recovery ratio for N2 = 3,900 rpm and recycle valve position at 0% and 20% opening

5.3 Brackish Water

The seawater RO design objective is to obtain a viable commercial wind-RO system configuration that can provide purified product water at a cost that is competitive with traditionally powered RO systems. Because there is a plentiful supply of brackish water in many remote areas that have no power infrastructure or where energy costs are high, a wind-powered RO system that can produce competitively priced water is desirable. The challenges are that brackish water dissolved solids can vary even more than those of seawater; other solid contaminants also pose an issue, as they must be removed by settling or filtration before RO treatment. Because of the great variation in brackish feedwater, the model configuration represents an example case study. Since the model is robust to the feedwater input concentrations, it can easily be adjusted to optimize a configuration for a site-specific application of the wind-powered RO system. Even on a specific site, individual well sources of brackish water may vary greatly in composition. For these specific cases, a homogenizing feed tank may be desirable to average the concentration of the feed so the membrane does not incur wide swings in ionic feed concentrations. This would require additional capital.

In addition, brackish water is moderately corrosive and has varying compositions of brackish water, so construction materials are important. For the brackish water system to be considered, the TDS of the feedwater is taken as ~5,000 ppm. Table 5-9 shows the breakdown of cations and anions in the model brackish water considered.

Table 5-9. Model Brackish Water Feed Composition

Component	Concentration (ppm)
CATIONS	
Sodium	1,370
ANIONS	
Bicarbonate	3,626
Chlorine	0.41
Carbonate	3.61
NON-VALENT	
Carbon Dioxide	486
TDS	**5,000**
pH	**7.0**

We took this input and the methodology outlined in section 5.1.1 to develop a steady-state model for a two-stage RO system. The design goals were to provide the maximum amount of water for the given power input (product yield) and to meet WHO standards[42] for product quality. Because product yield and quality typically are at odds with one another, several RO system sizes and pressure and pumping schemes were considered for the power requirements.

5.3.1 BW-WE-a1 Nominal Design

Based on the single- and two-stage analysis and optimization for seawater, the two-stage system can maximize production of a given feed stream. Because brackish water has typically six to seven times less TDS, the two-stage RO system was chosen as the base design. The first design considered was a two-stage RO system, with energy recovery and the option of interstage pumping to boost pressure in the second stage. This model is designated BW-WE-a1. The BW refers to brackish water, the WE is for work exchanger (energy recovery), and the a1 design is a two-stage system. The system is depicted schematically in Figure 5-58. In performing the power calculations as outlined in section 5.1.1, two design options concerned the interstage boost and the ERD DWEER described in section 3.2.6: (1) provide a pump to boost the brine outlet pressure from the first stage before it enters the second stage; and (2) provide a booster pump to the feed, which has already recovered energy from the DWEER, but is still at a lower pressure than the main feed system to the RO unit. Based on a power and pressure study of each of these possible configurations, we determined that there were only two viable alternatives. Because the brackish water is much lower in brine content, the TDS of the brine outlet from the first stage is at high enough pressure for further recovery of permeate. Since the seawater model showed little difference in the SW-WE-a1 and SW-WE-a3 configurations, we decided to look at the DWEER boost case for brackish water as the viable option.

Power was calculated with nominal values for pressure and flow until a value for the total power is about 540 kW. This gives a baseline for the configuration.

Next, the RO membrane steady-state model[33] is applied to determine the appropriate configuration for the RO portion of the configuration. This model uses the feed described earlier in this section and is optimized using the constraints detailed in Table 5-10. These constraints have been determined by industry design standards, and the capabilities of the membranes manufactured by Toray Membrane America, Inc.[33].

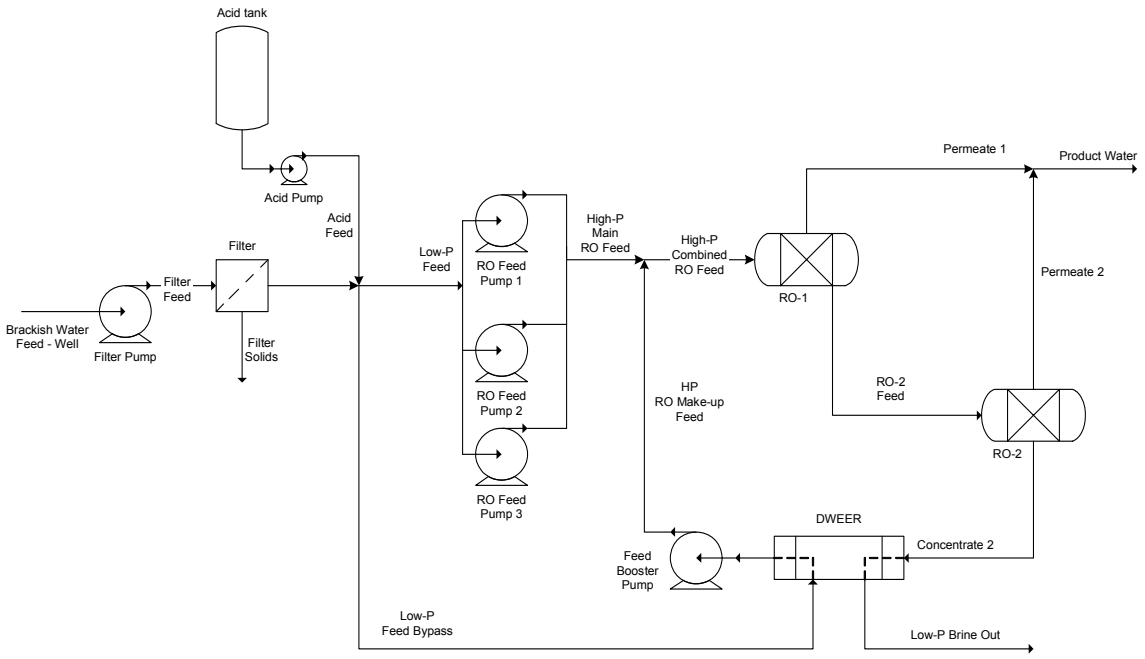

Figure 5-58. BW-WE-a1 configuration with DWEER boost

Table 5-10. Membrane Design Parameters

Parameter	Value/Range	*REMARKS*
Feed Flow	Lower limit > 15 gpm on the last element in the train	gpm = gal/min
Permeate Flux	Brackish: 10 < gfd <16 (17−27 lmh)	gfd = gal/ft^2/d; lmh = l/m^2/h Limits: scaling, feed P, and osmotic P
Feed Pressure	Brackish: 600 psig/41 bar	
Pressure Drop	< 20 psi (1.4 bar)/module < 60 psi (4.0 bar)/vessel	Limitation by membrane structure
Permeate	< 500 ppm TDS, 250 Na, Cl-0.5 ppm Boron	WHO limits[42]
RO Recovery	Brackish: 70%−80%	
Temperature	< 45°C (113°F) for operation	Element limitations
Fouling	10% permeate flux decline per year	
Membrane Lifetime	3−5 years	

5.3.1.1 Filter model

In this design, the primary feed is from a brackish water well, which required suspended solids to be filtrated. This filter is modeled with a standard design equation[24], which is detailed in section 5.2.1. The volumetric flow rate V is given from the power calculations for

the BW-WE-a1 configuration. In turn, the surface area, A, of the filter can be calculated from this equation, then the capital cost of the filter can be determined[24,25]. This cost is then included in the cost model of section 4.1.

5.3.1.2 Power and reverse osmosis model optimization

We used the design parameters from Table 5-10 and the flows from the power calculations to optimize the steady-state membrane model. The steady-state model for the RO membranes uses software developed by Toray Membrane America, Inc.[33]. Feed inputs are composition, feed, flow rate, and any pretreatment (pH adjustment, scale inhibitor, etc). The RO unit inputs are the type of membrane, the RO recovery, the number of stages, the number of RO elements per vessel, the membrane fouling factor, the salt passage rate per year, the age of the membrane, and the permeate backpressure. The model then converges a solution for the ion concentrations in the brine and permeate streams by use of the flux equation across a membrane shown in Eq. 5-5 and Eq. 5-6.

The membrane flux, ion concentrations, and stream pressures are determined for each element and each stage of the model. Once converged, the model gives a steady-state output form the system. These outputs include the overall flows and pressures of each stream, the ion concentrations in each stream, and the individual and overall fluxes for the RO membrane system.

At each convergence of the RO model, the output flows, and pressures from the membrane model were plugged back into the pump power calculations to see if the power was still optimal at about 540 kW. Since the feed flow is the largest power draw on the system, if the power was too low, the feed flow to the membrane model was increased. If the power was too high, the feed flow was decreased. This cycle was iterated until the maximum flow for the given power input through an RO system was achieved. Figure 5-59 shows the results of this optimization for the power calculations representing the configurations in Figure 5-58. The RO steady-state model outputs are found in Appendix A, which shows data from the DWEER boost case.

The DWEER boost design of Figure 5-58 was optimized for the first stage of 82 vessels by seven elements per vessel, followed by a second stage of 39 vessels by seven elements per vessel. Each stage uses a Toray Membrane America, Inc. Model 720-370 seawater membrane. Appendix A details the specifications of this type of membrane.

BW-WE-a1 82% Recovery 2-Stage with DWEER, No Interstage Boost, DWEER Boost									
Capacity Information				Input cells					
Operating Days/yr	350			Output cells					
Plant Capacity (MM m^3/yr) / (MM gal/yr)	6.10	1611.8							
Plant Capacity (m^3/day) / (MM gal/day)	17432.4	4.605							
Permeate Flow (m3/Hr) / (GPM)	726.4	3,198.0							
Overall System Recovery (%)	82.0%								
Wind turbine Efficiency (%)	36.0%								
Specific Energy (kW-Hr/m^3)	0.74								
Toray Model and DWEER Information	Vessels	Elements	Type	Element Area (ft^2)	Total Area (ft^2)	Total Area (m^2)	Recovery (%)	Flux (GFD)	Flux (LMH)
1st Stage Membrane Configuration	82	7	720-370	370	212,380	19,731	68.9%	18.3	31.06
2nd Stage Membrane Configuration	39	7	720-370	370	101,010	9,384	42.1%	7.28	12.36
Filter Outlet Pressure (PSIA) / (Bar)	30	2.07							
RO Feed Pressure (PSIA) / (Bar)	269	18.55							
Concentrate Flow (GPM) / (m^3/hr)	702	159.4							
Concentrate Pressure (PSIA) / (Bar)	252	17.37							
DWEER Brine Outlet P (PSIA) / (Bar)	15	1.03							
DWEER Water Out P (PSIA)	259	17.88							
DWEER Leakage (%)	1.80%								
Calculate Pump Energy Requirments base on Toray Models & Fedco Design Specifications									
Design Conditions	Efficiency (%)	Flow (m^3/hr)	Flow (GPM)	ΔP (kPa)	ΔP (PSIA)	Power (kW)	Power (hP)	Speed (RPM)	~ Cost ($)
Filter Feed Pump	75.00%	885.8	3900	310.3	45	101.82	136.5	3800	30,000.00
RO Feed Pump-1	77.90%	243.1	1070.2	1647.8	239	142.87	191.6	3818	41,000.00
RO Feed Pump-2	77.90%	243.1	1070.2	1647.8	239	142.87	191.6	3818	41,000.00
RO Feed Pump-3	77.90%	243.1	1070.2	1647.8	239	142.87	191.6	3818	41,000.00
Interstage Booster Pump	75.00%	0.0	0	0.0	0	0.00	0.0		
DWEER Booster Pump	61.70%	156.6	689.4	67.0	9.7	4.73	6.3	2257	21,000.00
ERD - DWEER	95.00%	156.6	689.4	1787.6	259	73.88	99.1		
Total Power Requirements						535.1	717.6		
Wind Turbine Power Requirement						1486.5	1993.4		

Figure 5-59. Power calculations for BW-WE-a1 design with DWEER boost

We used the RO membrane design reports and the power calculations to develop an overall process flow diagram of the BW-WE-a1 configuration. A flow diagram is shown for the DWEER boost case in Figure 5-60. English units for flow, pressure, and flux are gpm, psia, and gfd, respectively. Corresponding metric units are cmh, bar, and lmh.

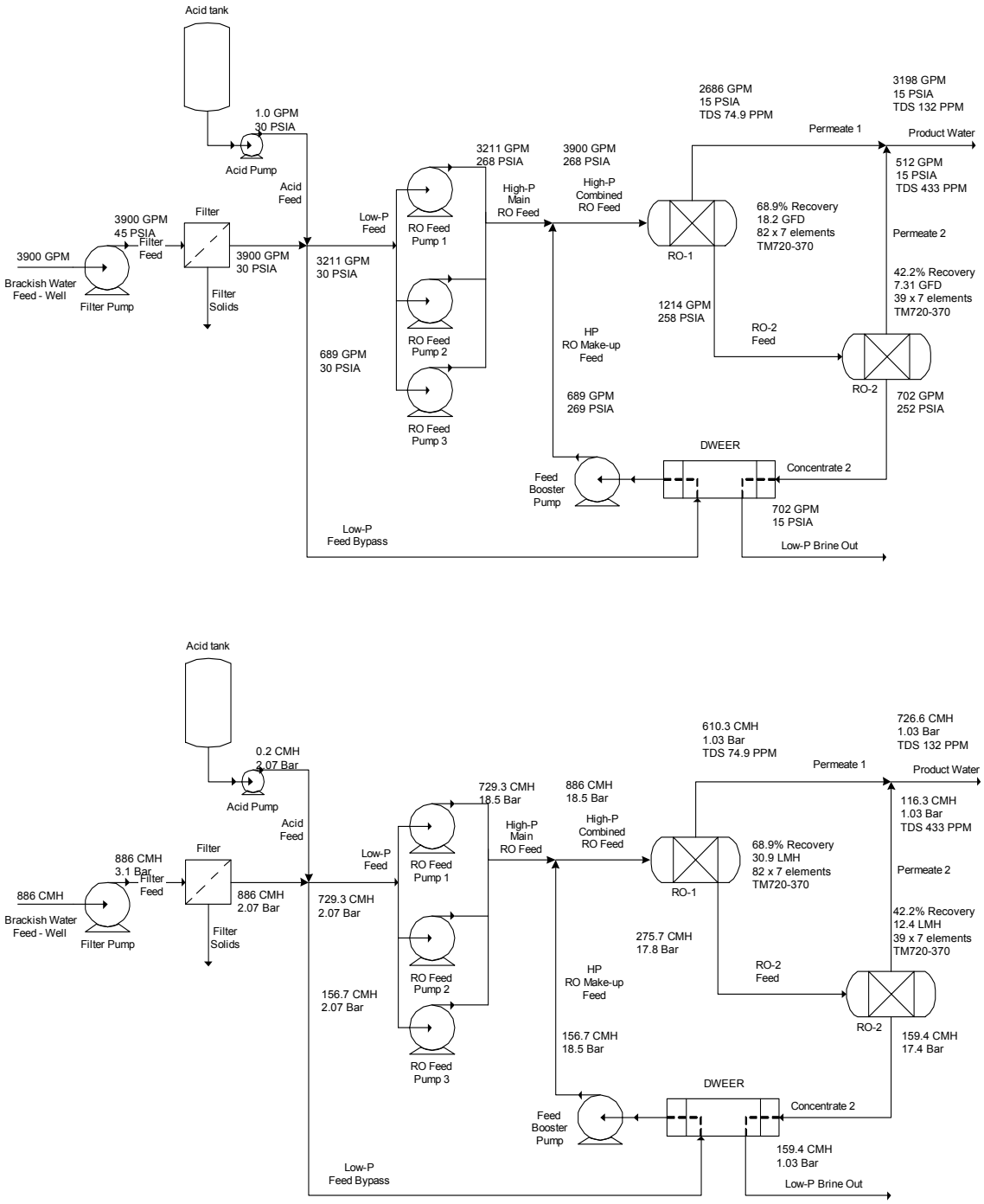

Figure 5-60. BW-WE-a1 DWEER boost flow diagram

5.3.1.3 Boron sensitivity analysis

The level of Boron in permeate water is now set to 0.3−0.5 ppm by WHO[42]. To understand the sensitivity of this configuration to Boron, we increased its feed level to determine what its level in the feed would cause it to break through in the permeate to a level of 0.5 ppm. We used the steady-state RO membrane model[33] to determine that the level of Boron in the feed that results in a 0.5-ppm level in the product permeate is 0.7 ppm. Since there is large

variation in brackish water Boron levels, any feedwater with Boron levels higher than 0.7 ppm would require a redesign of the system for a specific situation.

One way is to lower recovery on the current configurations to increase salt rejection, which lowers product output. This is the quality/productivity trade-off. For example, lowering the overall recovery of the current configurations from 82% to 70% (12% decrease), and allowing for the same permeate flow and power use as the base configurations, the increase in the feed Boron level is only to about 0.8 ppm (14% increase) to still meet the 0.5-ppm limit. There is little room for improvement in the current design to higher Boron levels. Therefore, if Boron levels are higher than 0.8 ppm, the best design option would be to have another RO Boron removal stage for the permeate only. This would require extra capital costs and increase energy consumption. Either a smaller production plant or a larger wind turbine would be required to compensate for the increased energy use. Those trade-offs in capital and operating expenses versus productivity would have to be assessed for specific high-Boron feed cases.

5.3.2 Cost of Water Analysis

Based on the above design, an overall COW is determined by calculating capital and operating costs for the configuration as outlined in detail in section 4.1. A summary of the cost is shown in Figure 5-61, which outlines the relevant capital and operating costs for the steady-state model. The model assumes an operating year of 350 days, with a permeate flowrate of 17,432 m^3/day (3,198 gpm). This yields an annual production of 6.1 x 10^6 m^3/yr of product water. Rolling up all the capital and operating costs for this production level gives an overall steady-state COW of about \$0.60/m^3. This cost can vary for a site-specific situation, where well construction costs, feed concentrations, and waste disposal costs can vary. The steady-state cost model, however, is flexible and can make provisions for these cost variances.

Operating Days		350	
Labor Hrs/yr		1500	
Ro Recovery (%)		82.0%	
Number of RO Stages		2	
RO Membrane Surface Area: m² (ft²)		29116	313390
Plant Capacity, m³/day:	(gal/day)	17,432	4,605,548
Feed Water, m³/day:	(gal/day)	21,259	5,616,522
Brine Water, m³/day:	(gal/day)	3,827	1,010,974
Feed Flow Rate, GPM:		3900.4	
Permeate Flow Rate, GPM:		3198.3	
Brine Flow Rate, GPM:		702.1	
Plant Capacity,MMm³/yr:	(MM gal/yr)	6.10	1611.8
Total Capital Investment Cost, MM US$:		12,609,939.50	
Plant Lifetime (yrs)		20.0	
Interest rate		8.0%	
Amortization Factor		0.10	
Annual Fixed Charges (MM$/yr)		1,284,350.19	
Annual Fixed Charges ($/m³)		0.21	
Marshall & Swift Cost Index for 2004		1224	

	Lifetime (Yrs)	Raw Cost ($)	(%)	US$/m³	
LABOR RELATED COSTS:					
RO Specific Cost of operating & maintenance labor				0.0550	
Total Labor Related				0.0550	
Supplies (% of Operating labor)			20.0%	0.0110	
Genearl Maintenance Material (% of OperatingLabor)			4.0%	0.0022	
Maintenance Battery Replacement Cost ($/m³)	10			0.00148	
Maintenance Membrane Replacement Cost ($/m	3			0.0231	
Wind Turbine routine Maintenance		14,550.00		0.0024	
Wind turbine Warranty & Non-routine Maintenanc	20	33,230.00		0.0054	
Total				0.0456	
TOTAL MAINTENANCE & LABOR				0.1006	
Taxes & Insurance (%TFI)			2.0%	252,198.79	
Depreciation (%TFI)			10.0%	1,260,993.95	
CAPITAL RELATED COSTS ($/m³)				0.2480	
TOTAL FIXED COSTS ($/m³)				0.5591	
TOTAL MANUFACTURING COSTS ($/m³) / ($/1000Gal)				0.5935	2.2468
Reference Total Manufacturing Costs ($/m3) / ($/1000Gal)					
Dietrich & Robert (2005)		Max cost is about this		1.00	3.80
Dietrich & Robert (2005)		Min cost is about this		0.11	0.40
Afonso et al (93,150 m3/day - large scale, 2004)				0.31	1.17

VARIABLE COSTS:	Density (kg/l)	Conc. wt%	Use g/m³ Permeate	Use (Kg/day)	Mat'l $/Kg	$/m³
RAW MATERIALS:						
HCl	1.20	35.0%	0.000	0.000	0.100	0.00000
H2SO4	1.83	93.0%	303.1	5,283	0.099	0.03007
NaOCl	1.00	100.0%	0.000	0.000	3.640	0.00000
Na2CO3	1.00	100.0%	0.000	0.000	0.221	0.00000
Na2S2O5	1.00	100.0%	0.000	0.000	1.544	0.00000
Lime	1.00	100.0%	0.000	0.000	0.077	0.00000
NaOH	1.00	100.0%	0.000	0.000	0.331	0.00000
Scale inhibitor	1.00	100.0%	0.010	0.174	3.440	0.00003
Ferric Sulfate	1.00	100.0%	0.000	0.000	0.210	0.00000
Total Raw Materials ($/m³)						0.0301
Disposal Costs				m³/m³ Perm.	$/m³	$/m³
Brine Waste				0.1800	0.0180	0.0032
Chemical Cleaning Waste				0.0010	0.5000	0.0005
Total Waste Disposal						0.0037
TOTAL RAW MATERIALS & WASTE ($/m³)						0.0338

Power Requirements:	Efficiency (%)	Flow GPM	P (kPA)	P (PSIA)	Power (kW)	Power (hP)
Filter Feed Pump	75.00%	3900	310.3	45	101.82	136.5
RO Feed Pumps	77.90%	3211.0	1647.8	239	428.65	574.8
Booster Pumps	61.70%	609	66.9	9.7	4.71	6.3
Chemical Feed Pumps	75.00%	31.00	310.3	45	0.81	1.0863
Totals for Power Calcs					536.0	710.8

Utilities:		(% Usage)	Units	Use (kW)	Total (kW-h)	$/Unit	$/m³
Electricity	%	1.0%	kw-h	536.0	45,023	0.076	0.0006
Battery	Hours	10.0	kw-h	45.0	450		
TOTAL UTILITIES ($/m³)							0.0006
TOTAL RAWS & UTILITIES ($/m³)							0.0344

Wind Turbine Power Requirement	
Power Utilization (%)	36.0%
Power Output (MW)	1.489
Specific Power (kWh/m³)	2.05

Specific Power Comparisons	
BW-WE-a1 specific energy (kW-hr/m³)	0.74
Afonso et al (2004)	0.83

Figure 5-61. Summary costs for the steady-state BW-WE-a1 configuration

5.3.3 Design Space Analysis

We conducted a design space analysis to understand the extent of the operating envelope associated with the configuration described in Section 5.3.1. As in the previous configurations, the main purpose of this study is to investigate the points in the input space at which the system fails to satisfy all the component and system constraints. If the system were operated at these points, the potential for membrane degradation through fouling or scaling or membrane destruction caused by increased stresses may result. In addition to helping us understand where constraints are violated, the design space study provides some insight into how recovery ratio, specific energy consumption, total power, and permeate flow vary with the choice of input parameters. The qualitative understanding that the design space study provides is critical for understanding the potential for system optimization.

For the two-stage configuration shown in Figure 5-62, the input space is defined by the parameters listed in Table 5-11.

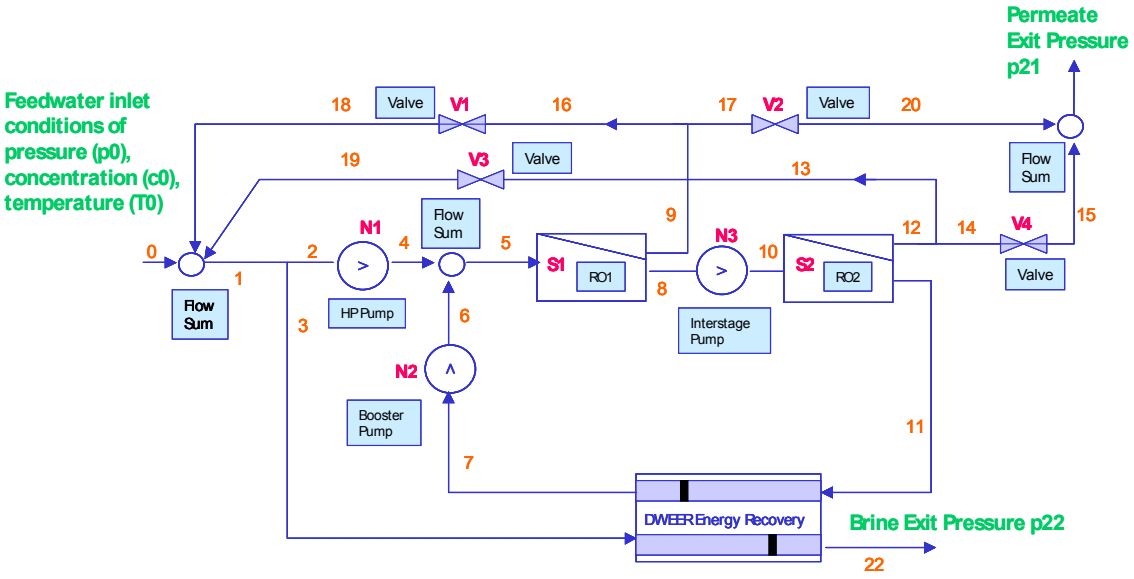

Figure 5-62. RO system configuration BWWE-a1

Table 5-11. Input Parameters for Configuration BWWE-a1

Parameter	Description
S1	Number of vessels in stage 1
S2	Number of vessels in stage 2
N1	High pressure pump speed
N2	Booster pump speed
N3	Interstage pump speed
V1	Stage 1 permeate recycle valve position
V2	Stage 1 permeate output valve position
V3	Stage 2 permeate recycle valve position
V4	Stage 2 permeate output valve position

Since the valve positions V1−V4 are mainly used to initiate a recycle flow for very low wind power capture conditions, the design space analysis fixes these quantities V1 = V3 = 0 (valve closed) and V2 = V4 = 1 (valve fully opened). These valve positions indicate that there is no recycle of the permeate flow.

Table 5-12 lists the parameter values investigated in the design space analysis for this configuration.

Table 5-12. Input Space Parameter Ranges for Configuration BWWE-a1

Parameter	Description	Units	Variation Range
S1	Vessels in stage 1	-	40–120
S2	Vessels in stage 2	-	20–70
N1	High pressure pump speed	rpm	3,000–3,900
N2	Booster pump speed	rpm	3,000–3,900
N3	Interstage pump speed	rpm	3,000–3,900
V1	Stage 1 permeate recycle valve	% open	0 (fully closed)
V2	Stage 1 permeate output valve	% open	1 (fully open)
V3	Stage 2 permeate recycle valve	% open	0 (fully closed)
V4	Stage 2 permeate output valve	% open	1 (fully open)
p0	Feedwater pressure	psid	20
p21	Permeate exit pressure	psid	15
p22	Brine exit pressure	psid	15
T0	Feedwater temperature	°C	25
c0	Feedwater dissolved salt concentration	kg/m^3	4.8

The steady-state constraints for the RO system are highlighted in Section 5.1.2 and listed in Table 5-13, which also lists the index associated with each constraint. This index reference is used in the figures associated with the analysis to highlight which constraints, if any, are being violated at a given point in the input space.

Table 5-13. Constraint Definition for Configuration BWWE-a1

Parameter	Value/Range	Index Used in Plots
Element polarization	$C_m / C_{avg} < 1.2$	1 – Stage 1 2 – Stage 2
Element concentration flow	$Q_c > 15$ gpm	3 – Stage 1 4 – Stage 2
Feedwater pressure	$P_f < 600$ psi	5
Element pressure drop	$\Delta P_{elm} < 10$ psid	6 – Stage 1 8 – Stage 2
Vessel pressure drop	$\Delta P_{vessel} < 58$ psid	7 – Stage 1 9 – Stage 2
Permeate quality	$C_p < 500$ ppm	10
Element flux	Flux < 28.3 gfd	11 – Stage 1 12 – Stage 2

The results of the design space analysis for the brackish water configuration BWWE-a1 are shown in Figure 5-63–Figure 5-87 for system parameters such as permeate flow, total power, specific energy consumption, and recovery ratio. The figures associated with these parameters also highlight the constraints violated in brackets and the system parameter value at each data point in the analysis. Finally, for each combination of input parameters that are presented, the distance to the constraint is identified in terms of percentage. The distance in terms of percentage from maximum constraints is given in Eq. 5-11 by

$$Distance\ to\ constraint = \frac{Constraint\ Value - Parameter\ Value}{Constraint\ Value} * 100 \qquad \text{Eq. 5-11}$$

and the distance in terms of percentage from minimum constraints is given in Eq. 5-12 by

$$Distance\ to\ constraint = \frac{Parameter\ Value - Constraint\ Value}{Constraint\ Value} * 100 \qquad \text{Eq. 5-12}$$

Positive numbers in these figures indicate that there are no limiting constraints, and the number shown in the figure is the distance to the most restrictive constraint. Negative numbers shown in the figures indicate that at least one constraint is being violated, and the number shown in the figure indicates the maximum constraint violation.

Consider the results shown in Figure 5-63–Figure 5-77 for the case where the booster pump speed (N2) and interstage pump speed (N3) are set to 3,000 rpm, and the number of vessels in the second stage, S2, is varied from 20 to 40 to 60. For each value of S2, data associated with permeate flow, total power, specific power, recovery ratio, and distance from the constraint are shown as a function of high-pressure pump speed (N1) and the number of vessels in stage 1 (S1). Figure 5-63 shows that when the number of vessels in the second stage is 20, S2 = 20, the available design space that meets all the constraints lies in a diagonal band across the N1, S1 input space. In particular, the results indicate that at low high-pressure pump speeds, the number of vessels in S1 must be limited to the lower values. As the high-pressure pump speed is increased, the region in which there is an allowable design space increases with the number of vessels in S1. At very large N1, e.g., 3,900 rpm, constraint violation occurs with a small number of vessels in stage 1. As the number of vessels in stage 2 increases, S2 = 40, the design space is slightly reduced at low high-pressure pump speeds (Figure 5-64). At larger values of N1, the number of vessels in S1 that fall into the allowable design space increases compared to the case when S2 = 20. Hence, as the number of vessels is increased from 20 to 40, there is an increase in the allowable operating envelope of the configuration. Finally, at S2 = 60 (Figure 5-65), there are no viable operating points in the N1-S1 input space for N2 = 3,000 rpm, N3 = 3,000 rpm. Thus, as the number of stages is increased from 20 to 40 to 60, there is a potential for defining an optimal configuration that maximizes the allowable operating envelope.

To better understand the limiting constraints, and the impact on additional system parameters, consider the permeate flow results shown in Figure 5-66−Figure 5-68. Figure 5-66 shows that the primary constraint being violated is the minimum concentration flow in the first stage. To understand this behavior, consider the situation when N1 = 3,000 rpm. For the range of S1, the total permeate flow is not vastly different. If the recovery ratio were essentially the same,

Figure 5-75, the larger number of vessels would indicate a reduction in the feedwater flow to each vessel. Consequently, as the number of vessels in S1 is increased, the concentration flow at each vessel is expected to decrease. At great high-pressure pump speeds, N1 = 3,900 rpm, the maximum flux constraint is violated in the second stage. This would suggest that the number of vessels in the second stage is too small for the system flow that results from the values of N1, N2, N3, S1 and S2. As the number of vessels in S2 is increased from 20 to 40 to 60, Figure 5-67 and Figure 5-68, the limiting constraints are the concentration flow requirements for both stage 1 and stage 2. Again the previous argument can be used to understand this trend. With regard to the permeate flow itself, for a given N1 the magnitude of the change in permeate flow with an increase in S1 vessels diminishes. Finally, for a given S1, permeate flow increases with increased N1 because of the higher flow capabilities of the pump at higher speeds for the same pressure rise. However, the magnitude of the change in flow is greater for an increased number of vessels.

The results in Figure 5-69–Figure 5-71 show that at a given N2, N3 combination, the total power consumed is primarily dictated by the high-pressure pump speed. This result is expected given that the high-pressure pump dominates the system energy consumption. The increase in the power consumed for a given N1 caused by an increase in S1 is slight. In fact the power consumption decreases slightly at first and then increases. At large S1, the power consumption levels off. By coupling the permeate flow results with the total power consumption results, the variation in specific energy consumption can be investigated (Figure 5-72–Figure 5-74). The specific energy consumption decreases slightly, approximately 0.1 kWh/m^3, at some S1-N1 combinations as the number of vessels in the second stage increases. In addition, as the number of vessels in the second stage increase, the range of S1−N1 combinations where specific energy consumption is low increases. Finally, with regard to recovery ratio (Figure 5-75–Figure 5-77), the achievable recovery ratio increases with the number of vessels in the second stage. In addition, as the number of vessels in the second stage increases, a line of constant recovery ratio moves to the lower right in the S1–N1 range.

To understand the impact of changes in the booster pump speed (N2), consider the changes in system parameters as booster pump speed is varied from 3,000 rpm to 3,540 rpm for a fixed number of vessels in the second stage, S2 = 40, and a fixed interstage pump speed of 3,000 rpm. The distance from the limiting constraints is not significantly different in the acceptable regions of the design space (Figure 5-78). However, at the limiting boundary between the allowable and nonallowable design space, an increase in the constraint violation is observed. When considering permeate flow (Figure 5-79) as well as recovery ratio (Figure 5-82), variations in N2 have little impact. As expected, there is an increase in the total power consumed caused by the higher booster pump speed (Figure 5-80), which in turn leads to a higher specific energy consumption (Figure 5-81). The S1-N1 region with lower specific energy consumption expands into regions associated with larger high pressure pump speeds as booster pump speed is increased (Figure 5-81). Although not plotted, similar results were obtained at other interstage pump speeds and the two-stage vessel size.

To understand the impact of changes in the interstage pump speed (N3), consider the changes in the system parameters as the interstage pump speed is varied from 3,000 rpm to 3,540 rpm for a fixed number of vessels in the second stage, S2 = 40 and a fixed booster speed of 3,000 rpm. As the interstage pump speed is increased, the applicable design space increases; however, at each viable operating point, the degree of robustness is reduced (Figure 5-83),

which is evident from a reduction in the distance from the limiting constraint. Variation in N3 also impacts the permeate flow in that the permeate flow is increased anywhere from approximately 3% at great high-pressure pump speeds to 5% at low high-pressure pump speeds (Figure 5-84). The increase in permeate flow, however, comes at a price of higher power consumption of approximately 50–60 kW over the S1−N1 input space (Figure 5-85). The recovery ratio, on the other hand, increases slightly, typically 0.1%, at most combinations of S1-N1 (Figure 5-87). The recovery is increases slightly, but the increase in power consumption offsets the increased permeate flow translating into a slight increase in the specific energy consumption as N3 is increased (Figure 5-86). Although not plotted, similar results were obtained at other two-stage vessel configurations and other booster pump speeds.

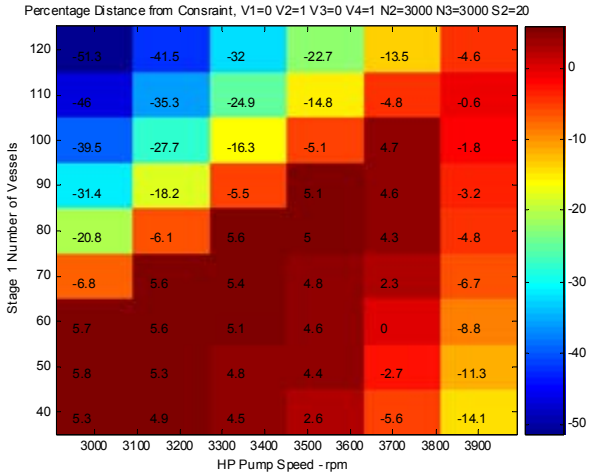

Figure 5-63. Percentage distance from constraint at N2 = 3,000 rpm, N3 = 3,000 rpm, and S2 = 20

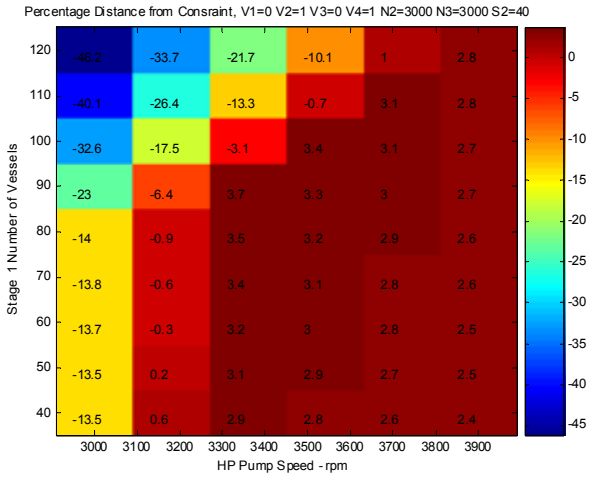

Figure 5-64. Percentage distance from constraint at N2 = 3,000 rpm, N3 = 3,000 rpm, and S2 = 40

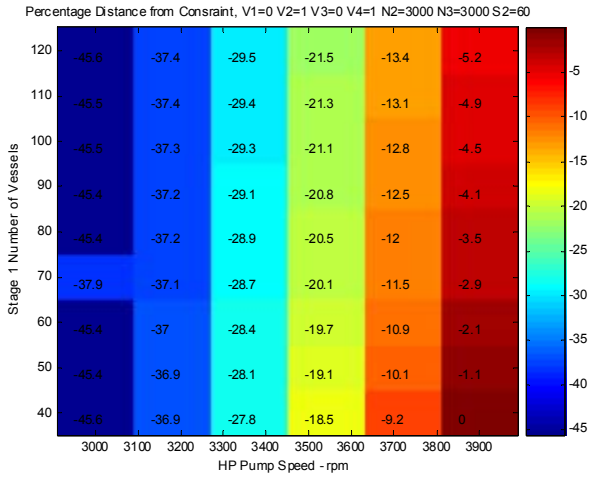

Figure 5-65. Percentage distance from constraint at N2 = 3,000 rpm, N3 = 3,000 rpm, and S2 = 60

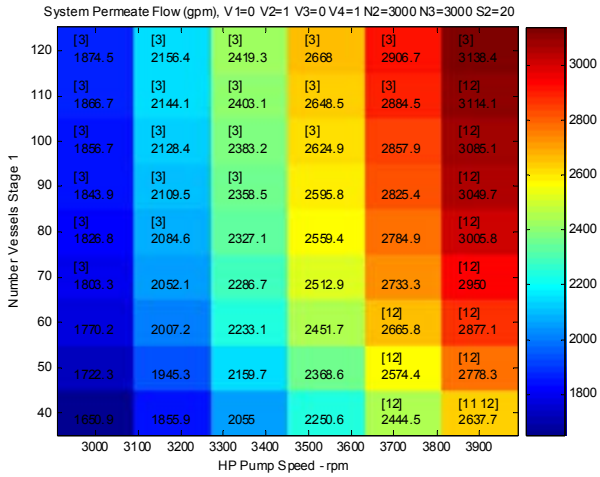

Figure 5-66. Permeate flow for N2 = 3,000 rpm, N3 = 3,000 rpm, and S2 = 20

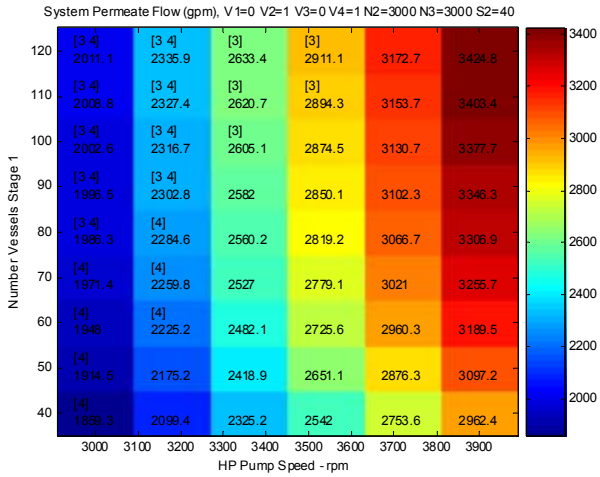

Figure 5-67. Permeate flow for N2 = 3,000 rpm, N3 = 3,000 rpm, and S2 = 40

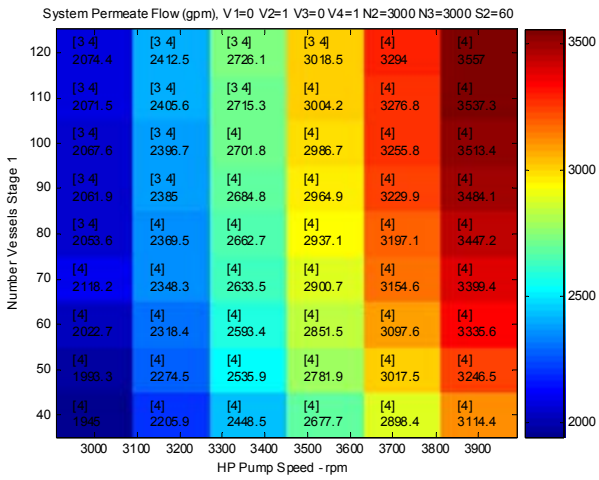

Figure 5-68. Permeate flow for N2 = 3,000 rpm, N3 = 3,000 rpm, and S2 = 60

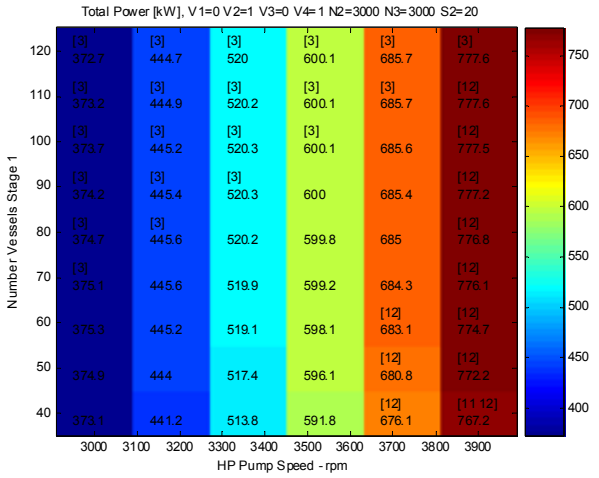

Figure 5-69. Total power consumed at N2 = 3,000 rpm, N3 = 3,000 rpm, and S2 = 20

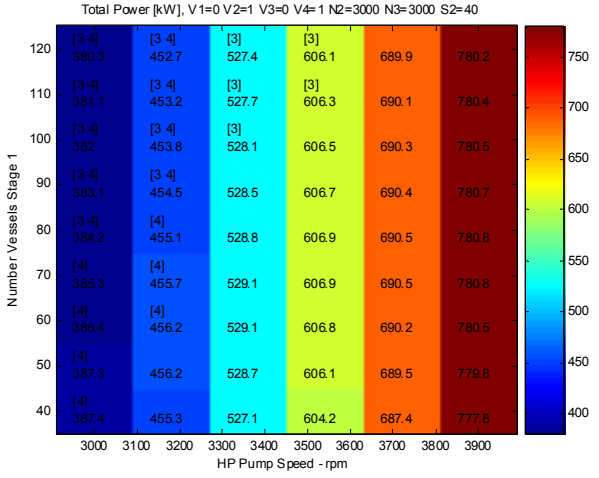

Figure 5-70. Total power consumed at N2 = 3,000 rpm, N3 = 3,000 rpm, and S2 = 40

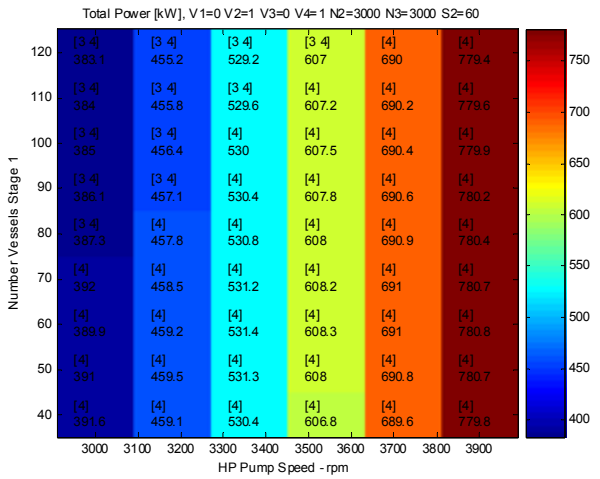

Figure 5-71. Total power consumed at N2 = 3,000 rpm, N3 = 3,000 rpm, and S2 = 60

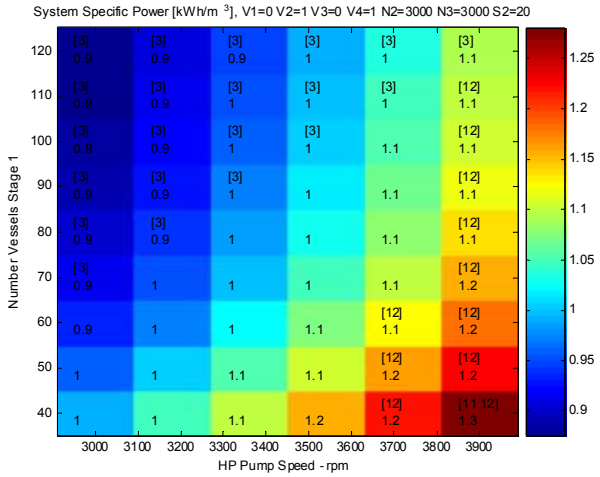

Figure 5-72: Specific power consumption at N2 = 3,000 rpm, N3 = 3,000 rpm, and S2 = 20

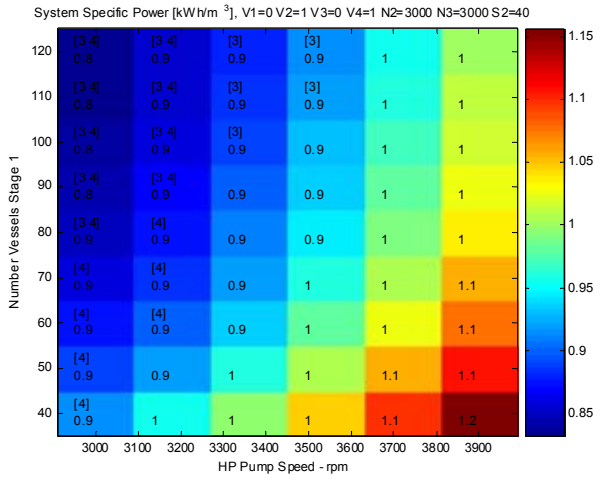

Figure 5-73. Specific power consumption at N2 = 3,000 rpm, N3 = 3,000 rpm, and S2 = 40

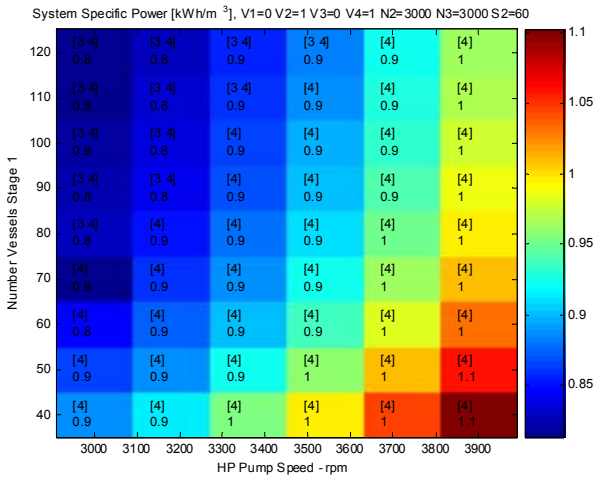

Figure 5-74. Specific power consumption at N2 = 3,000 rpm, N3 = 3,000 rpm, and S2 = 60

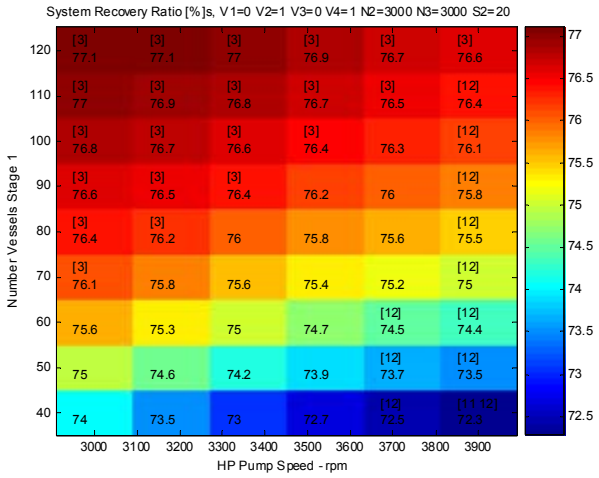

Figure 5-75. System recovery ratio for N2 = 3,000 rpm, N3 = 3,000 rpm, and S2 = 20

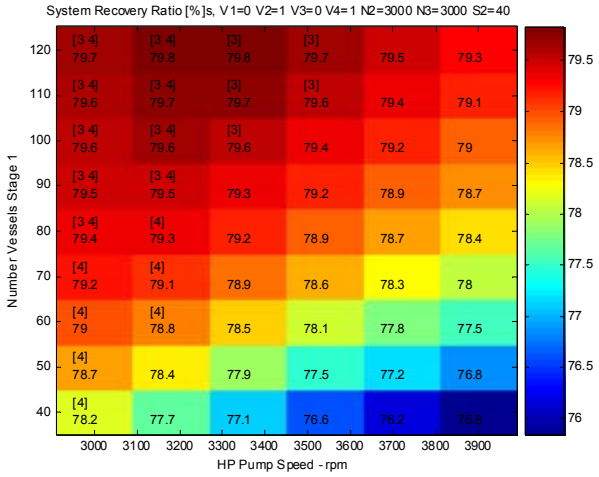

Figure 5-76. System recovery ratio for N2 = 3,000 rpm, N3 = 3,000 rpm, and S2 = 40

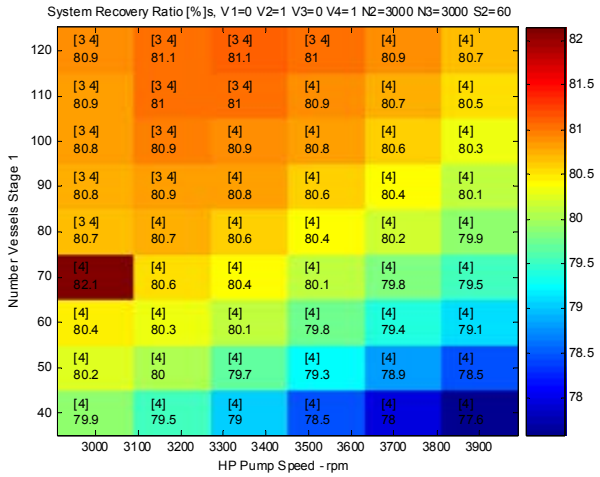

Figure 5-77. System recovery ratio for N2 = 3,000 rpm, N3 = 3,000 rpm, and S2 = 60

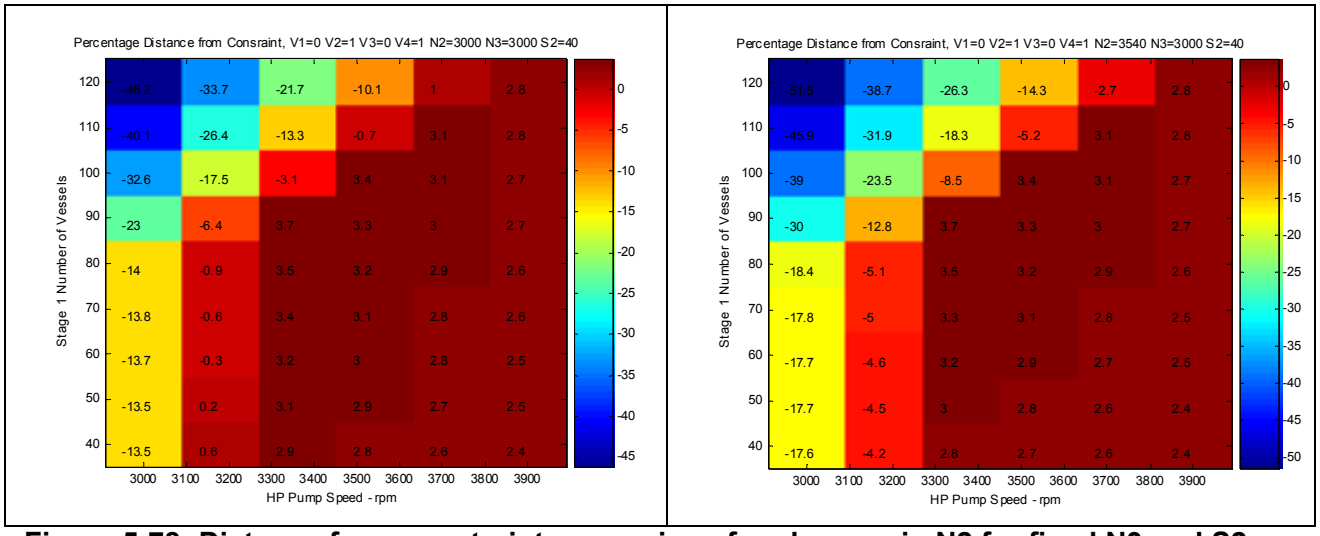

Figure 5-78: Distance from constraint comparison for changes in N2 for fixed N3 and S2

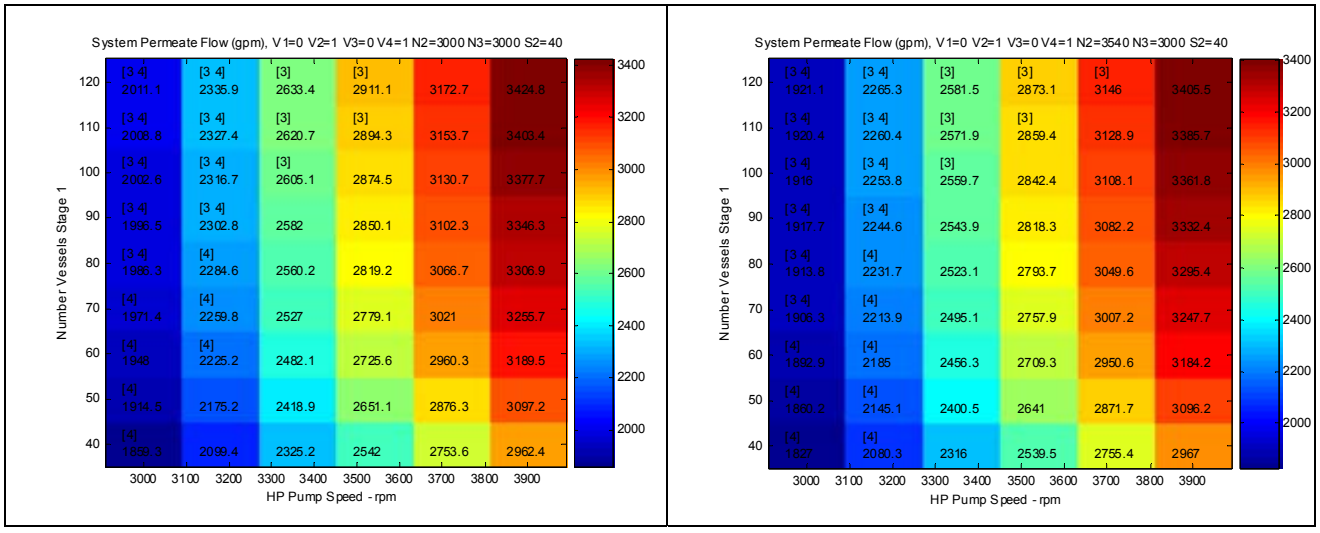

Figure 5-79. Permeate flow comparison for changes in N2 for fixed N3 and S2

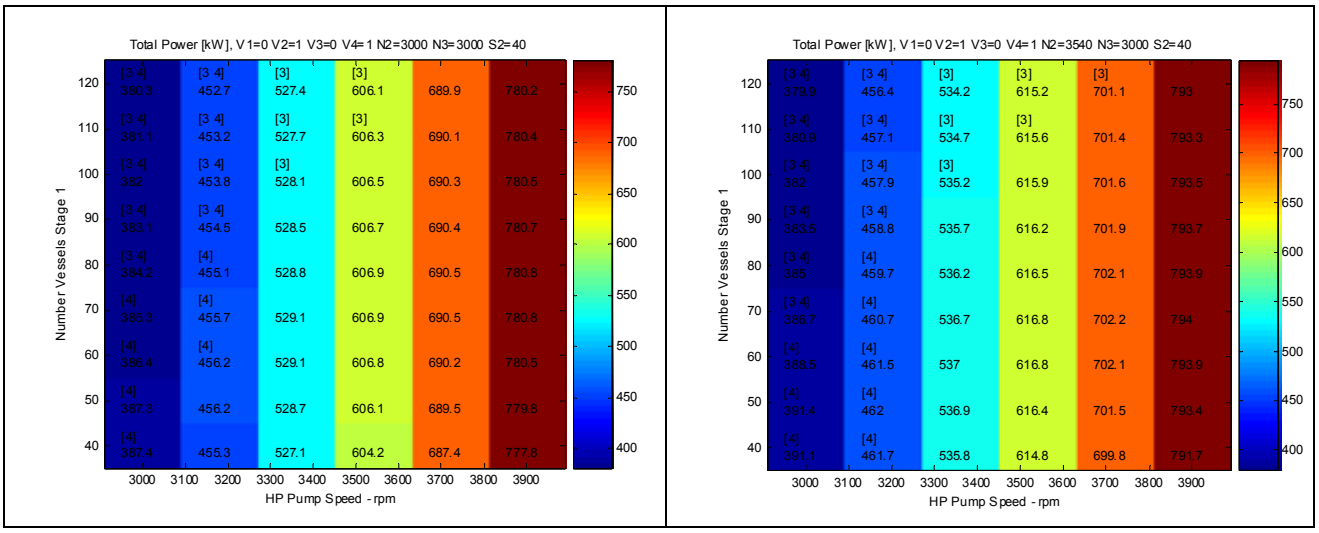

Figure 5-80. Total power consumption comparison for variation in N2 for fixed N3 and S2

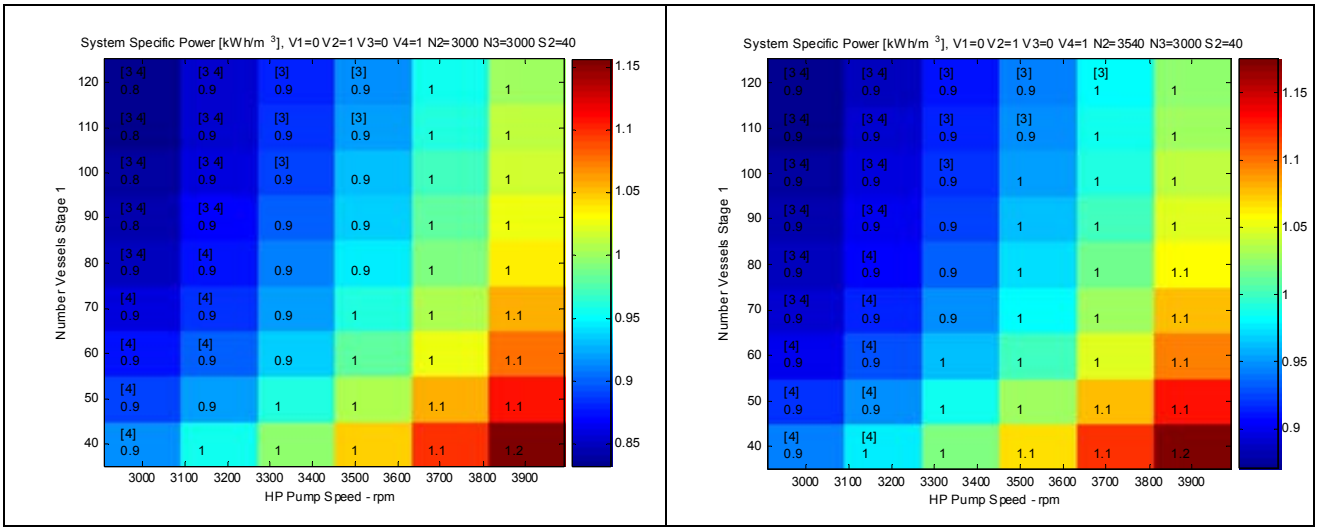

Figure 5-81. Specific power consumption comparison for variation in N2 for fixed N3 and S2

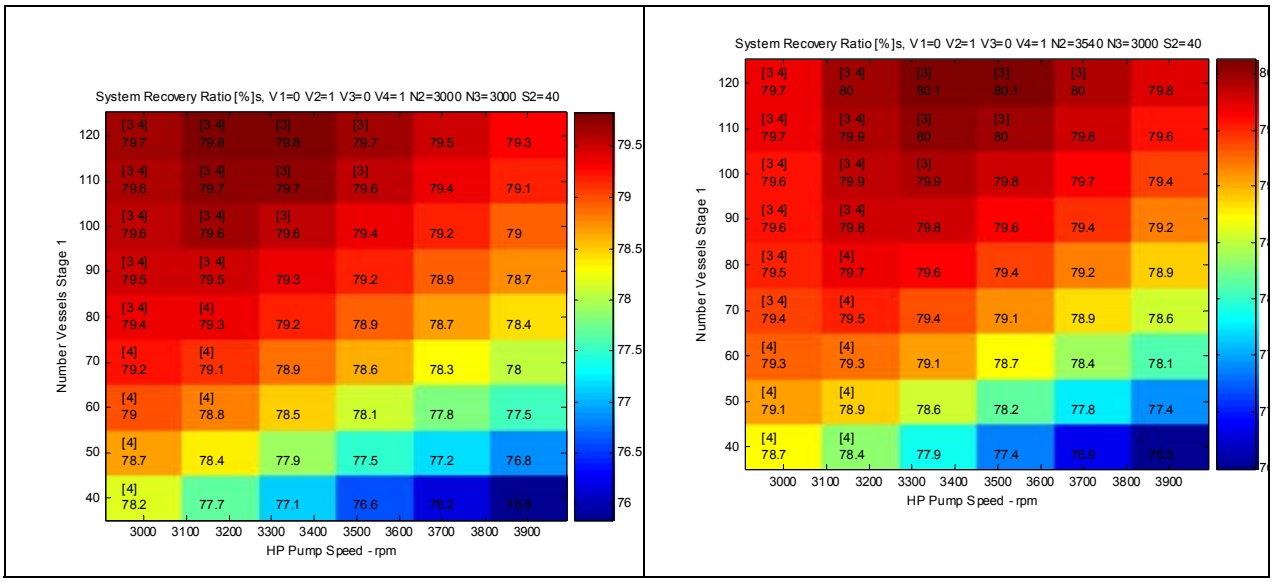

Figure 5-82. Recovery ratio comparison for variation in N2 for fixed N3 and S2

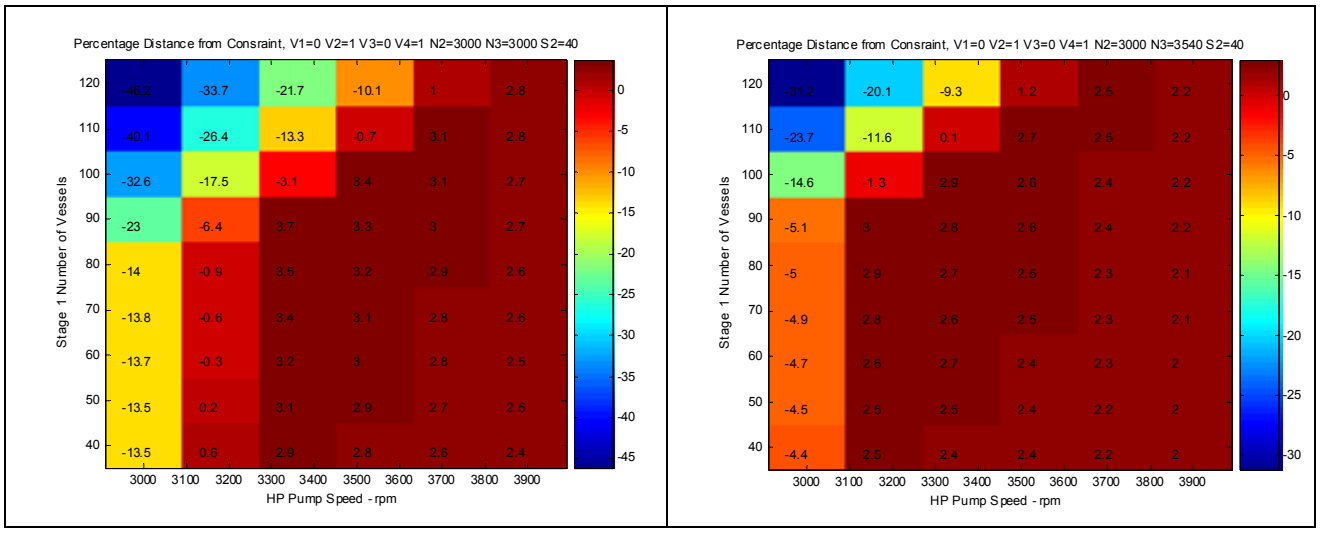

Figure 5-83. Distance from constraint comparison for changes in N3 for fixed N2 and S2

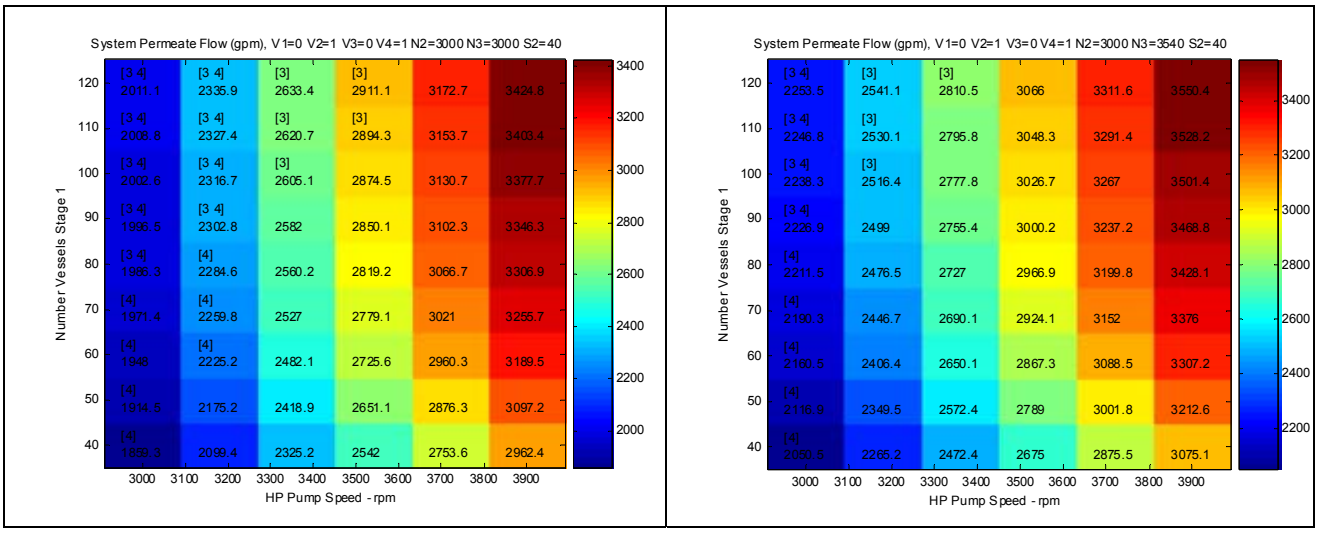

Figure 5-84. Permeate flow comparison for changes in N3 for fixed N2 and S2

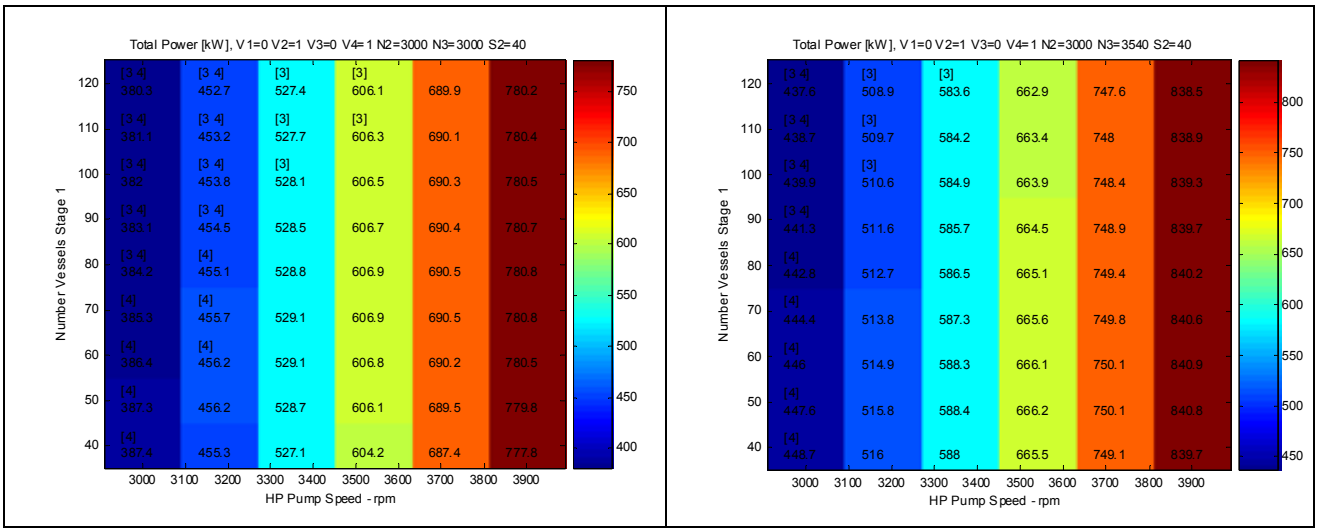

Figure 5-85. Total power consumption comparison for variation in N3 for fixed N2 and S2

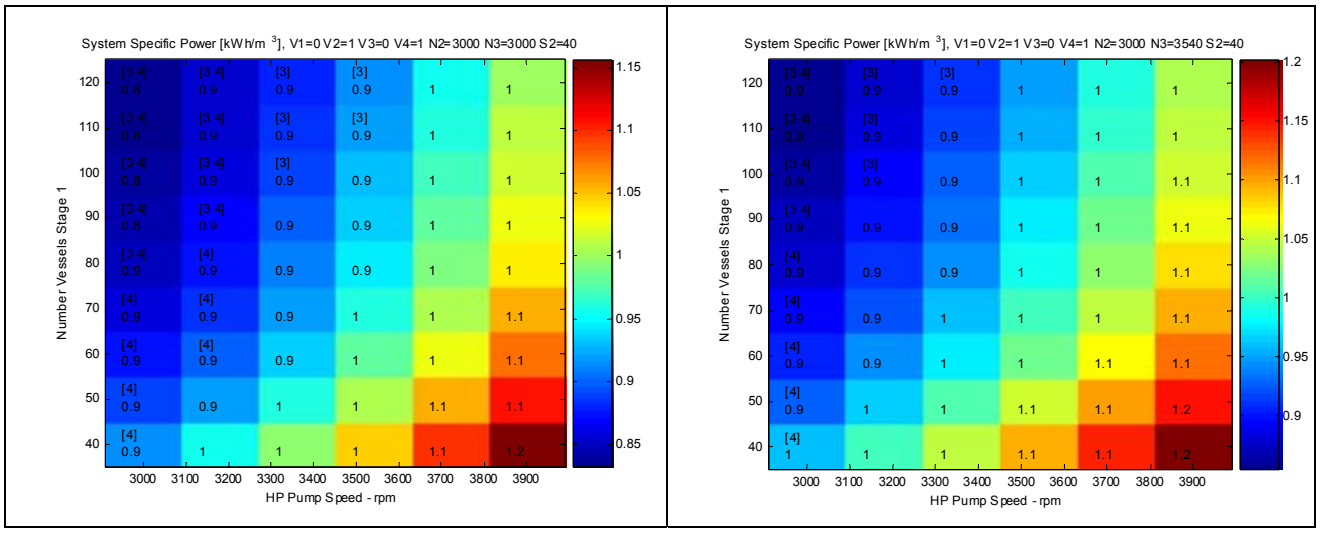

Figure 5-86. Specific power consumption comparison for variation in N3 for fixed N2 and S2

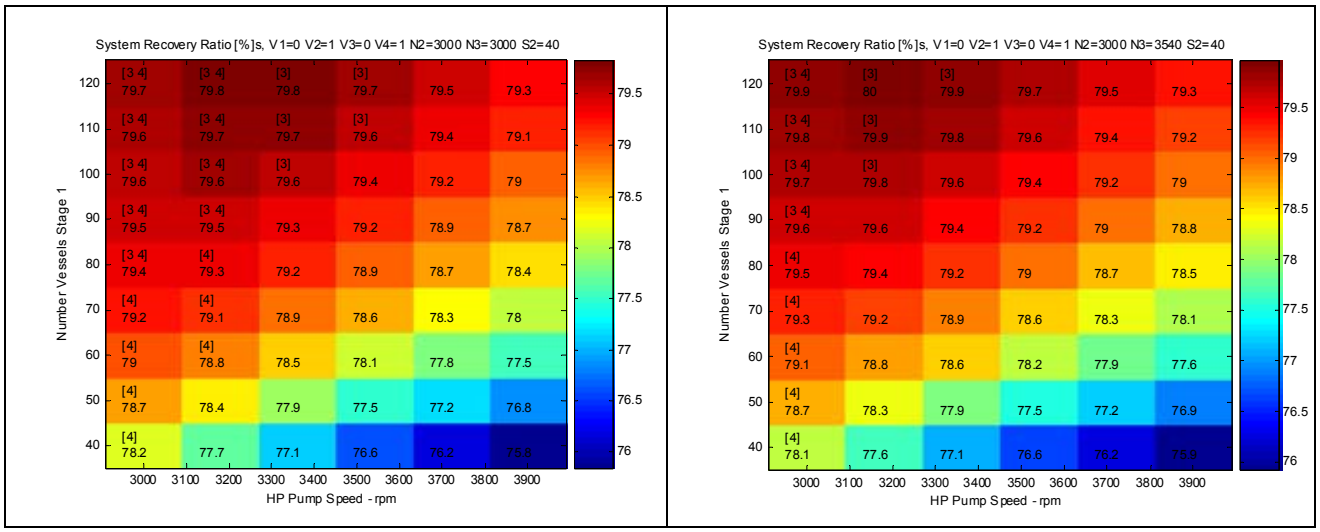

Figure 5-87. Recovery ratio comparison for variation in N3 for fixed N2 and S2

6 Wind Desalination Design Optimization

Typically, RO desalination technology has been developed for operation at nearly constant conditions, except for trimming plant set points to account for long-term variations in membrane degradation and changes in water temperature and salinity.

Where grid power is not available or is cost prohibitive, the hybrid RO system uses only wind energy and needs to operate under wide variations in available power. The economic viability of the wind desalination technology in a grid-isolated topology largely depends on the ability of the RO plant to produce water efficiently in most of this range.

The configurations proposed in the previous section are meant to provide a great degree of flexibility to operate the wind desalination system in a wide range of conditions dictated by available power and feedwater state. In this section we use the physical and economic models, in combination with optimization techniques, to define plant size and the location in the operating space to minimize the resulting COW. For example, we provide a rigorous method to address a fundamental design problem: to define the relative size of the power generation subsystem with respect to the desalination subsystem. Also, since the proposed configurations rely on the ability to change the desalination capacity by partially activating RO banks, we propose methodologies to calculate optimal RO capacities and the corresponding pump speeds as a function of the available power.

6.1 Overview of Wind Desalination Topologies

The grid topologies analyzed in this section are grid isolated, where the RO system operates with the wind power and, occasionally, from energy storage devices; and a grid-connected topology where the RO system operates with wind power, grid power, or both.

The analysis has focused on two problems that are fundamental in the design and operation of a wind desalination plant:

1. Given the available energy for desalination, calculate the RO set points for maximum water production.
2. Given an RO plant and local grid energy prices, decide whether wind power is economically viable to produce water.

The optimization studies were performed for the single-stage seawater configuration (SWWE-a3) only, although the same techniques can be applied to the other two configurations proposed in Section 2.

6.1.1 Grid-Isolated and Design Choices/Optimization Opportunities

The grid-isolated configuration consists in the RO configuration SWWE-a3 (see Figure 5-40) powered by a 1.5-MW wind turbine that operates with class II winds. To evaluate the COW for this configuration, the size of the RO subsystem, operating strategy, and energy storage size have to be defined, for which we have taken the following steps.

1. Solved an optimization problem for the range of possible power levels from a 1.5-MW wind turbine to obtain the maximum water production subject to all the operating

constraints. As a result, the upper bound of number of RO vessels was obtained, as well as the optimal set points for associated operating strategies.

2. Obtained the optimal number of vessels by calculating the COW for every RO plant size (assuming an optimal operation as given by step 1, assuming an energy storage size), and selecting the lowest one.
3. Suggested a procedure to size the energy storage based on wind statistical information.

6.1.2 Grid-Connected and Design Choices/Optimization Opportunities

Given the greater flexibility of a grid-connected topology, there are many opportunities for optimal design and optimal operation calculations. For the grid-connected case, we focused on analyzing viability of a wind-powered RO technology and understanding its preferred conditions over an RO plant that is powered with grid energy only. We chose a simple operating strategy to compute a detailed COW for this topology. In addition, we suggested an optimal operation strategy for dealing with the energy management between wind power, grid power, and the energy storage subsystem.

6.2 Grid-Isolated Results

6.2.1 Plant Sizing Analysis with Regard to Cost of Water

We analyzed a single-stage RO water desalination plant (configuration SWWE-a3). This analysis assumed that the wind turbine is the sole energy source for the plant; i.e., that the plant is isolated from the power grid, and that no energy storage is available. In this case, the size of the plant is of interest, in terms of RO vessels installed, that leads to a minimum average SCOW over one year of operation, taking into account the variability of the energy source. Detailed COW evaluations for two-stage configurations (like SWWE-a1 and BWWE-a1) can be evaluated with the same methodology.

6.2.1.1 Design Process

The size of the RO plant, given by the maximum number of RO vessels, has been defined to obtain the minimal COW when the power is produced for a 1.5-MW wind turbine. For this purpose, we:

1. Defined the generic operation of the RO plant at different power levels.
2. Given the generic operation in step 1, computed the expected COW (taking into account the wind speed statistics) that correspond to RO plants in a range of possible sizes.
3. Selected the size for which minimum COW is achieved.

Generic Operation of Reverse Osmosis Plant

Defining the plant operation consists of calculating the set points of the available control knobs that will lead to minimal COW at all possible power levels. Regarding RO configuration, this involves calculating the optimal number of active RO vessels in the RO bank, *S*, the optimal speed of the high-pressure pump, N_1, and of the booster pump, N_2, the optimal valve opening for permeate recycle, V_1 in the range of 70 kW to 1500 kW of

consumed power. To achieve minimum COW, we used the maximization of water production as the optimization criterion. Therefore, the RO operating set points were defined by maximizing the permeate flow-rate subject to the following constraints:

- RO operational constraints as described in Section 5.1.2.
- The power consumed by the pumps is fixed.

This optimization problem has been solved for a set of power levels of 70−1500 kW. The results of these calculations are presented in Figure 6-1−Figure 6-7 and Table 6-1. For most values of available power, the maximum permeate flow is achieved when the last element concentrate flow has the lowest value allowed by the constraints. This is consistent with the analysis of the operational space presented in Section 5.2.6 (see Figure 5-52).

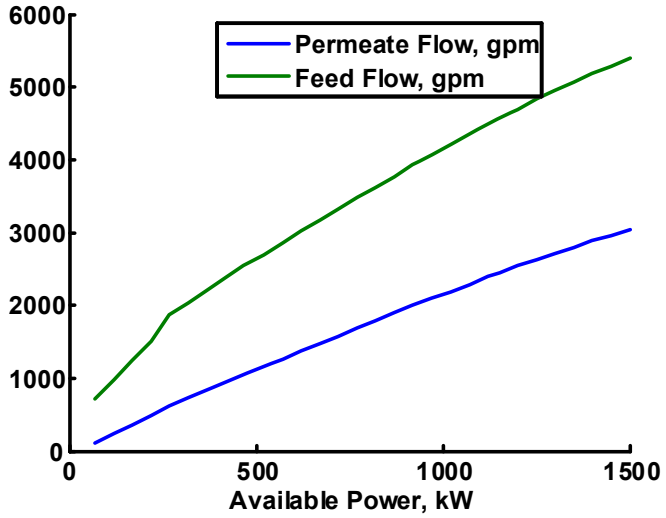

Figure 6-1. Maximum permeate flow as a function of available power for plant SWWE-a3

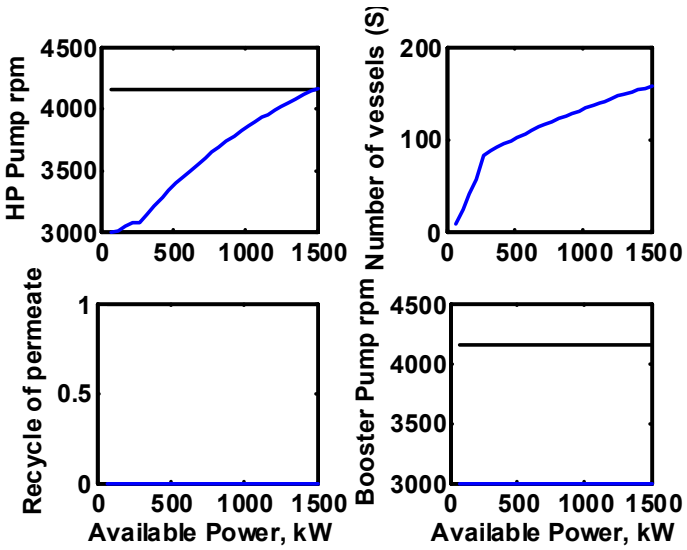

Figure 6-2. Optimal operating parameters as a function of available power, plant SWWE-a3; dotted lines represent the available parameter variation ranges

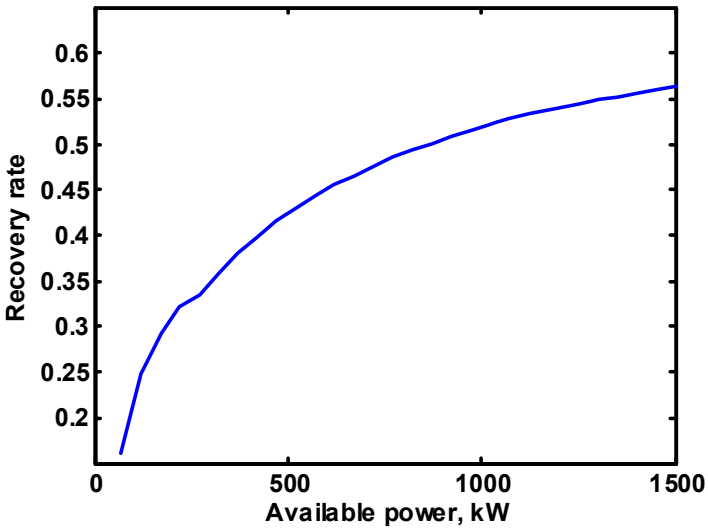

Figure 6-3. Recovery of a function of available power for optimal results (configuration SWWE-a3)

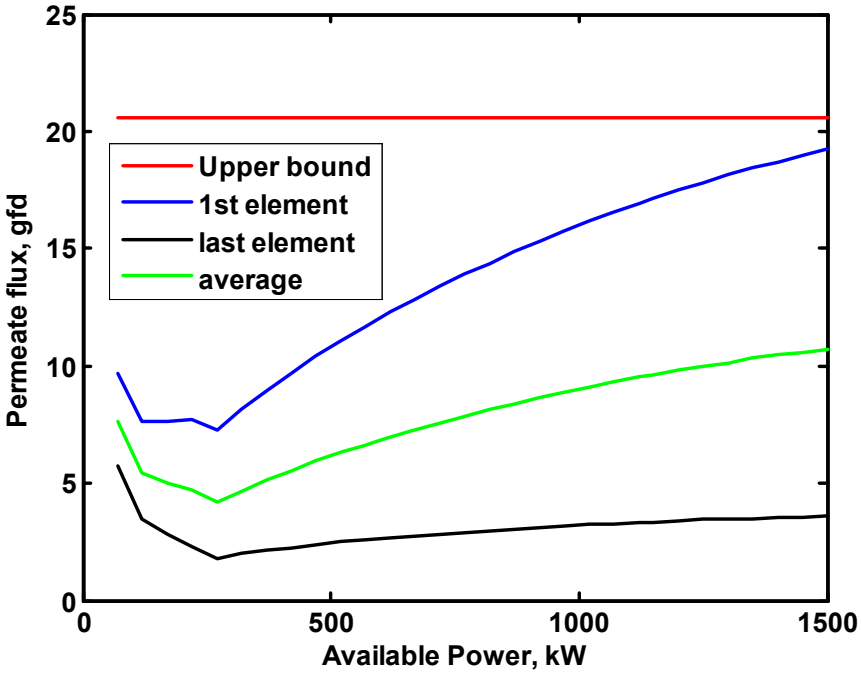

Figure 6-4. Permeate flux for optimal results on configuration SWWE-a3

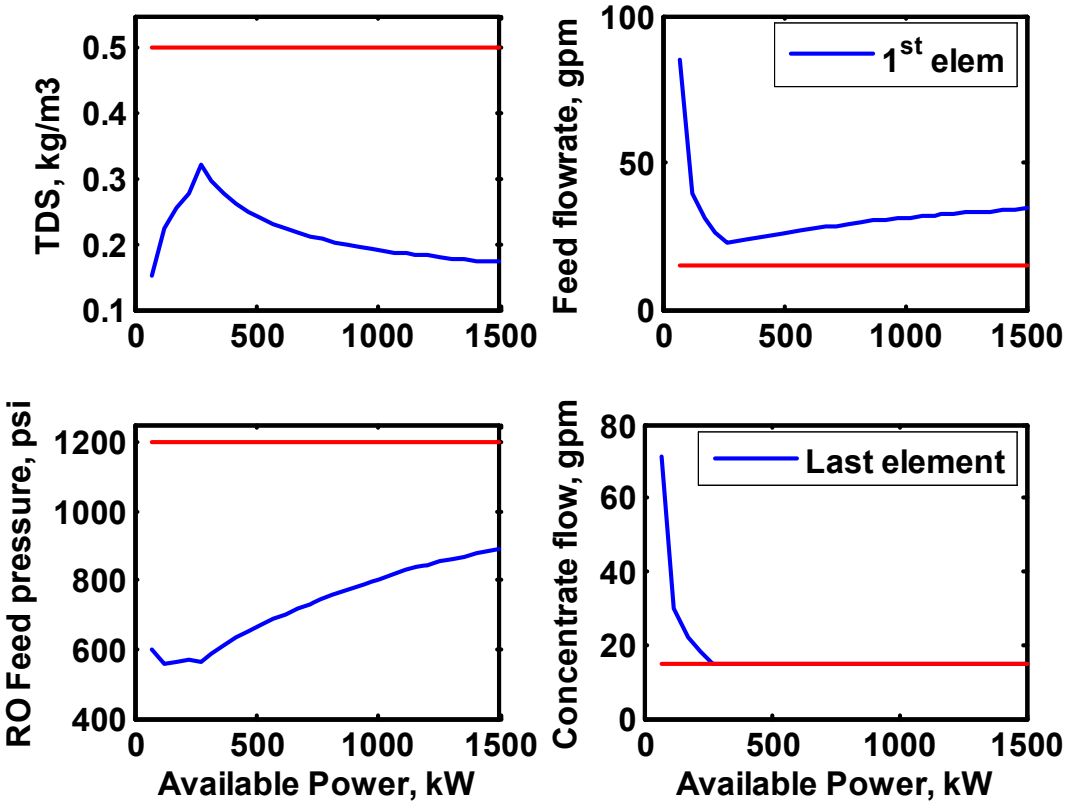

Figure 6-5. Constrained variables for optimal results on configuration SWWE-a3

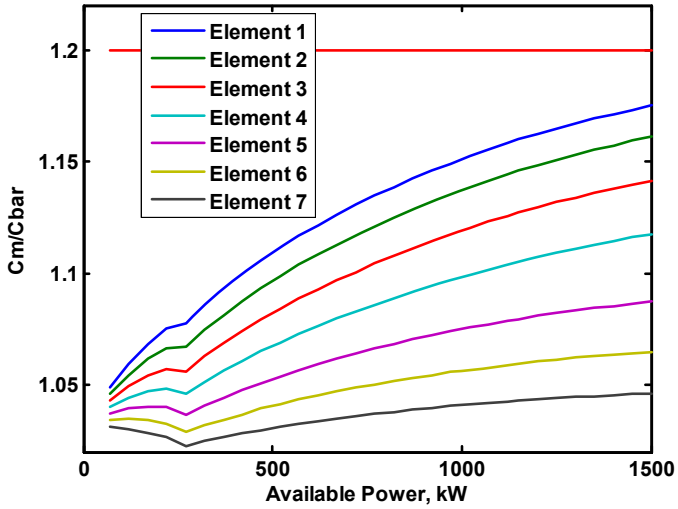

Figure 6-6. Concentration polarization for optimal results on RO configuration SWWE-a3

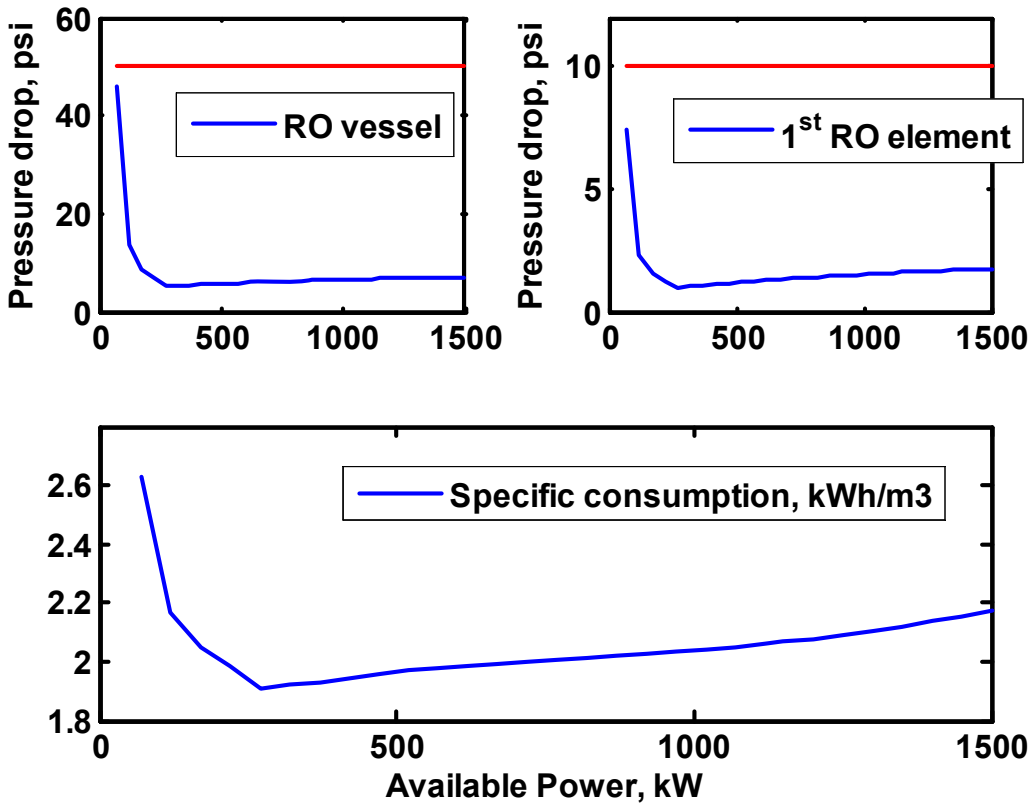

Figure 6-7. RO pressure drop and specific energy consumption for optimal results on configuration SWWE-a3

Table 6-1. Optimal Operating Parameters for Plant SWWE-a3

Available Power, kW	Optimal N1, rpm	Optimal N2, rpm	Optimal S (vessels)	Optimal Recycle	Maximum Permeate Flow, gpm	Optimal Recovery
70	3,000.0	3,000	9	0	117.37	0.16168
120	3,000.0	3,000	25	0	244.16	0.24751
170	3,040.3	3,000	41	0	364.94	0.29296
220	3,072.0	3,000	58	0	487.22	0.32123
270	3,070.6	3,000	83	0	623.15	0.33394
320	3,146.8	3,000	88	0	734.04	0.35931
370	3,216.1	3,000	92	0	842.85	0.38077
420	3280.2	3,000	96	0	950.15	0.39927
470	3,340.0	3,000	100	0	1,056.8	0.41567
520	3,396.7	3,000	103	0	1,162.7	0.43022
570	3,450.7	3,000	107	0	1,268.2	0.44332
620	3,502.4	3,000	110	0	1,373.4	0.4552
670	3,552.2	3,000	113	0	1,478.5	0.46605
720	3,600.2	3,000	117	0	1,583.2	0.476
770	3,646.6	3,000	120	0	1,687.7	0.48517
820	3,691.5	3,000	123	0	1,791.6	0.49363
870	3,735.0	3,000	126	0	1,894.9	0.50147
920	3,777.1	3,000	129	0	1,997.2	0.50872
970	3,817.9	3,000	132	0	2,098.4	0.51545
1,020	3,857.3	3,000	135	0	2,198.2	0.52169
1,070	3,895.4	3,000	138	0	2,296.2	0.52748
1,120	3,932.1	3,000	140	0	2,392.3	0.53285
1,150	3,953.5	3,000	142	0	2,449.0	0.53589
1,200	3,988.0	3,000	144	0	2,541.5	0.54066
1,250	4,021.2	3,000	147	0	2,631.6	0.54508
1,300	4,053.0	3,000	149	0	2,719.1	0.54919
1,350	4,083.4	3,000	152	0	2,803.9	0.55301
1,400	4,112.5	3,000	154	0	2,885.9	0.55656
1,450	4,140.2	3,000	156	0	2,965.2	0.55986
1,500	4,166.7	3,000	158	0	3,041.8	0.56294

This calculation assumed that the capacity of the ERD depends linearly on the number of RO vessels, according to the relation in Eq. 6-1:

$$C_{pe} = 1 + 0.0087(S - 51) \qquad \text{Eq. 6-1}$$

This law of variation was determined by accounting for the capacity of the pressure exchanger used at the nominal design point of the plant (where 35% of the nominal power of the turbine is available) and the capacity of the ERD necessary to cope with the maximum capacity of the plant (when the turbine generates 1.5 MW). The increased cost incurred by using a larger capacity ERD is accounted for in the cost model.

Expected Cost of Water for Reverse Osmosis Plants of Different Sizes

As a second step in determining the optimal plant RO size, the expected COW was calculated for all plant sizes (ranging from nine vessels to 158 vessels) with the COW model described in Section 4.2.

We considered a location with a yearly average wind speed (at a 10-m standard height) of 7 m/s (Class II wind). The parameters characterizing the Weibull probability density function for mean wind speeds at standard height are in this case $A_{10m} = 7.9$ and k = 2. At hub height, $h_{hub} = 70m$ (corresponding to the GE 1.5-MW turbine), the yearly average wind speed is 9.24 m/s (Eq. 4-3), and the parameters of the Weibull probability density function are $A_{hub} = 10.43$ and k = 2. The probabilities of $n = 28$ mean wind speeds (0−27 m/s) at hub height, occurring in a one year period, as computed from the Weibull probability density function, are presented in Figure 6-8.

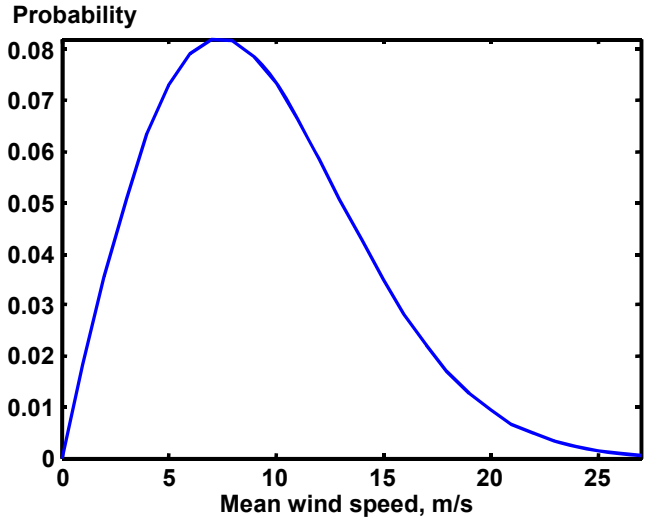

Figure 6-8. Probability of mean wind speeds at turbine hub height, A = 10.43, k = 2

The available power at each wind speed was calculated with a GE 1.5 turbine power curve (Section 3.2.2). A plot of the available power at different (hub height) wind speeds is presented in Figure 6-9.

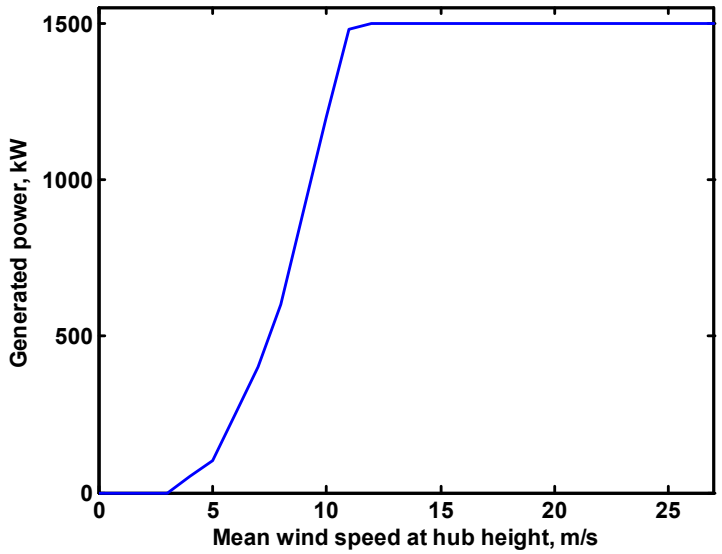

Figure 6-9. Generated power as a function of wind speed (measured at 70 m above the ground)

Once the available power for each wind speed was computed, the optimal operating points for each wind speed were determined by using the results in Table 6-1.

The average yearly SCOW considering plants with different numbers of installed RO vessels, was computed following the procedure presented in Section 4. In this case (Eq. 4-2), $ROPower = P_j$., i.e., the power available to the RO plant varies in time and is, in fact, the power generated by the wind turbine, corresponding to the mean wind speed $\overline{V}_j$.

A plot of the SCOW as a function of the number of RO vessels installed in the plant is presented in Figure 6-10.

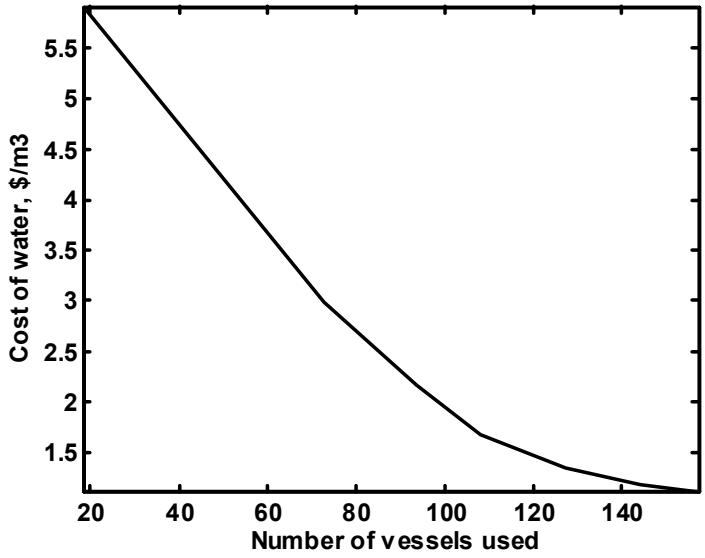

Figure 6-10. Annual average COW for plant SWWE-a3, operated as grid isolated, as a function of the number of RO vessels installed

Optimal Plant Size

From results in Figure 6-10, the average COW is minimized for a plant size of 158 vessels.

6.2.1.2 Results

The optimal plant size for RO configuration SWWE-a3 is given by 158 vessels. The corresponding performance indexes, computed using weighted averaging calculations similar to those in Section 4.2, are given in Table 6-2.

Table 6-2. Performance of Optimal Wind-RO Plant

Maximum wind turbine power	1,500 kW
RO plant size	158 vessels
Average COW	1.111 $/m^3
Average recovery rate	39.45%
Average permeate flow rate	1,686 gpm
Average permeate flow per maximum power	1.12 gpm/kW

Even though $S_{\min COW} = 158$ vessels are physically installed in the plant, they may not be used at all times. Depending on the level of power available to operate the plant, vessels may be connected and disconnected; the speed of the pumps and the recycle rate may also be adjusted to ensure a maximum flow rate of permeate for the power available. The above calculations indicate that on average over one year (the period considered in computing the Weibull distribution) the SCOW produced by a plant that has 158 vessels installed is the lowest of all the plant configurations considered (see also Table 6-1).

The contributions of the factors considered in developing the cost model (Section 4) to the SCOW produced by the optimal grid-isolated desalination plant (operating at full capacity), 158 vessels connected to a 1,500-kW wind turbine are presented in Figure 6-11.

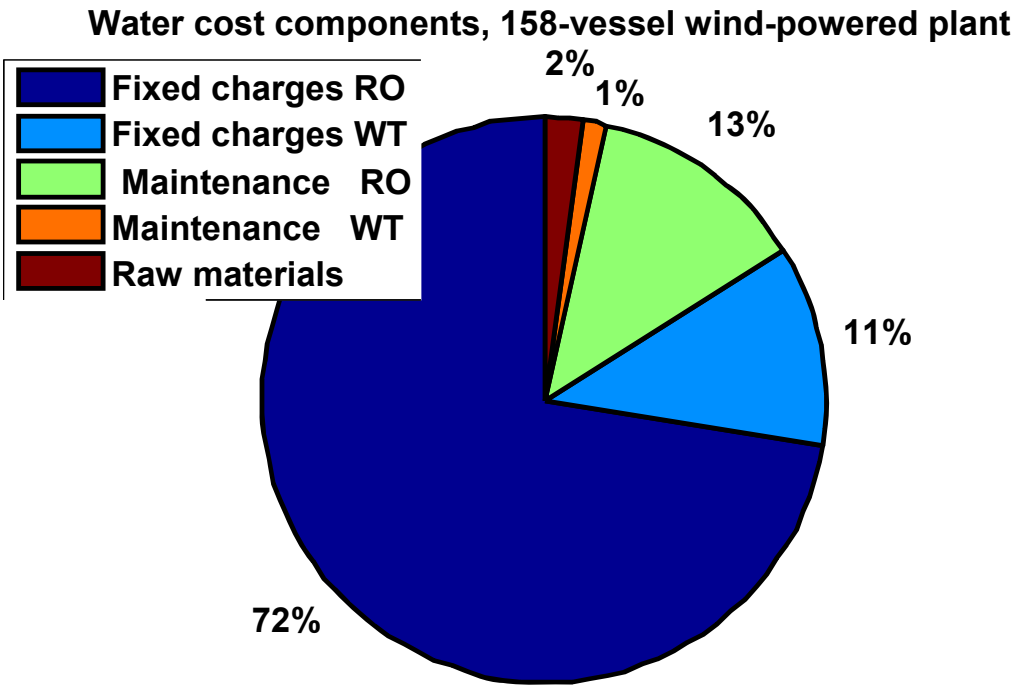

Figure 6-11. Contribution to the COW for an optimal grid-isolated RO plant powered by a wind turbine

The design procedure and results in this section assume that the plant operator would produce as much water as possible for the available wind power. There was no attempt to deal with changes in water demand or distributions constraints. If this assumption is not satisfied, the design procedure can be adjusted accordingly, and the optimal size and performance may differ from those presented in this section.

6.2.2 Sizing energy storage

Energy storage is useful in a grid-isolated topology to keep the RO system in operation even without wind power. The following parameters should be understood to quantify the economic benefits of using a battery to reduce shutdowns:

- Statistical information on the period of time for which the RO plant lacks power to be operative. This magnitude depends on the local wind characteristics and in the minimum number of vessels that can be active in the RO plant.
- The effect of an RO shutdown on the COW, including effects of lack of water production during shutdown and increased use of chemicals.

A preliminary battery size can be determined from the maximum period of time to operate the minimum set of vessels in the RO plant. This consideration leads to the minimum battery power rating and the maximum battery capacity.

The wind statistical description can be used to find an optimal battery sizing. In fact, we can use wind statistics to determine the effect of "blackouts" on battery life as a function of battery size (smaller batteries will cycle more often and will exhaust their lives sooner than larger batteries). An optimal battery size can be calculated by a trade-off analysis between a battery's size and its economic impact on the COW.

Since the required wind statistical description for optimal battery sizing is not available, we sized the battery so it provides 100 kW during four hours of continuous operation, which is enough to operate at least nine vessels during that time (according to Table 6-1).

6.2.3 Plant operation concepts

The operational strategy suggested by the optimization results in Section 6.2.1 indicates that, whenever the available wind power is 70−1500 kW, the plant set points should be as close as possible to the optimal values in Table 6-1. If the wind is such that the available power is outside this range, the following operational modes should be taken into account.

- If the wind power is below 70 kW, the plant can operate if the battery charge is above the minimum charge level. A threshold on minimum wind speed should be defined to bring the RO plant up again. This threshold should be greater than the cut-in wind speed.
- When wind power is available, it can be used to produce water and charge the energy storage device, if it is not at full charge. A possible strategy to operate the plant is to use a threshold on wind speeds (or wind power) for battery charging. If wind power is below the threshold, the wind power will be used only to produce water. If wind power exceeds the threshold and battery is not at full capacity, the excess of power will be used to charge the battery until it is at full capacity. If wind power is above a threshold and battery is full, all the wind power will be used to produce water. The optimal value for the power threshold depends on the local wind statistics, the local water demand, or constraints in the water distribution. The optimal set point could be calculated with the methods outlined in Section 6.3.3.

Using the optimal operating set points given in the previous section would require the ability to switch individual vessels on and off. Building an RO plant with this capability may be impractical; in a more likely scenario, the RO plant will be able to connect groups of vessels instead of individual vessels.

If the RO vessels can only be connected in groups, the optimal set points can be calculated with the methodology described earlier, but must explicitly include the limitations on the RO operation. Irrespective of the restrictions in the vessel connections, Table 6-1 gives the maximum number of vessels that can be connected for any given power. That is, if the current wind power is such that the optimal number of vessels cannot be used, the plant should operate with fewer vessels (most available, fewer than the optimal). For example, if the wind turbine is producing 1 MW and the RO vessels can be connected only in groups of 20, only 120 vessels should be active. Connecting 140 vessels would lead to violations of constraints

on minimum concentrate. The interaction between specific energy consumption, number of active vessels, and constraint violation should be clear from the design space analysis in Section 5.2.6 (see, for example, Figure 5-52) and the results in Section 6.2.

Because of membrane degradation considerations, vessels should avoid being inactive and filled of seawater for more than 12 hours. To handle this constraint, the plant operation should cycle the active vessels if the wind power is not enough to operate all the available vessels.

6.3 Grid-Connected Results

6.3.1 Wind-Reverse Osmosis Viability Analysis

The availability of a power grid connection increases the flexibility of an RO water desalination plant design. We analyzed two possible designs with the same RO capital expenditure (given by a size of 158 vessels) to evaluate the viability of the wind-RO technology in a grid-connected topology:

- The RO plant is operated at full capacity solely with grid power (in which case capital expenditures decrease without a wind turbine).
- The RO plant is operated at full capacity with both grid and wind power.

In designing a grid-connected wind-RO plant, the goal was to improve on the operation of the grid-isolated plant described in Section 6.2. Thus, we considered that the plant is operated at a constant set point, namely, using the plant parameters that lead to the lowest average COW in the grid-isolated case. During periods of low wind speeds, when the wind power is not enough to operate the RO plant at full capacity, the remaining power is purchased from the grid. This operating strategy is "robust" with respect to grid blackouts, since in the case unavailable grid power, the plant can be operate on wind power alone, and water would be, even under these circumstances, produced at a minimum cost.

Specifically, parameters chosen for the operation of the plant are (also, see Table 6-1).

Number of RO vessels	$S_{\min COW} = 158$
HP pump speed	$N_{1,\min COW} = 4{,}166$ rpm
Booster pump speed	$N_{2,\min\ COW} = 3{,}000$ rpm
Power	$P_{\min COW} = 1{,}500$ Kw
Permeate flow	$Q_{p,\min COWl} = 3{,}041.8$ gpm

To maintain the plant operation at the constant set point above, energy is assumed to be purchased from the grid at a price $\$_{buy}$ when the generated power P_{gen} is less than $P_{\min COW}$.

The average SCOW was computed according to the method presented in Section 4, considering that the energy purchase price is \$0.02/kWh−\$0.2/kWh.

6.3.2 COW Results

The SCOW obtained for the two RO plants described in the previous sections and summarized in Figure 6-12 presents COW for wind-powered and grid-connected wind-powered plants for various energy purchase prices.

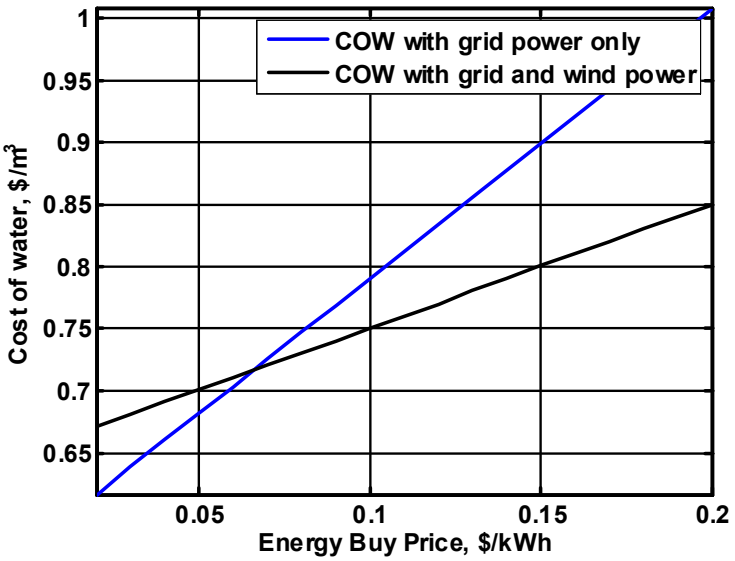

Figure 6-12. Comparison of the SCOW for a grid-connected wind-powered desalination plant and its grid-powered counterpart

The SCOW generated with grid power only is lower at low energy costs, and becomes higher than that of the water generated by the grid-connected wind-powered RO desalination plant as the cost of buying energy from the grid increases. The "break even" point (where the cost of water generated by the two plants considered is the same) occurs when the energy buy price is $\$_{buy} = 0.0664\$/kWh$. In this price range it can be understood by considering that the COE generated by the wind-turbine considered in the present project (GE 1.5 MW, in a Class II wind location) is \$0.0664/kWh. As such, the wind-powered grid-connected plant is expected to become a viable alternative to the grid-only plant when the cost of grid energy exceeds the COE generated by the wind turbine. Since the plant is designed to operate at the maximum power provided by the wind turbine (1.5 MW), no power is sold to the grid; hence, the energy sale price does not influence the COW. The SCOW generated by the grid-connected wind-powered plant is less dependent on the cost of energy purchased from the grid. Specifically, the COW produced by the grid-connected wind-powered plant exhibits a change of less than 30% over the range of variation of energy prices considered; the variation of the specific COW produced by the grid-powered plant is close to 65% over the same range. Thus, when high fluctuations in the grid energy purchase price are anticipated, resorting to a wind-powered grid connected desalination plant would lead to smaller fluctuations in the production COW than in the case of a grid-powered plant.

Table 6–3 and Table 6–4 summarize the performance of the two plants analyzed in this section. Figure 6-13 gives the structure of COW for a grid-connected wind-RO plant, assuming an average cost of grid energy of \$0.08/kWh. Figure 6-14 gives COW structure for

the 158-vessel desalination plant, powered only with grid energy, assuming a $0.08/kWh energy cost.

Table 6-3. Performance of a Grid-Connected Wind-RO Plant

Maximum wind turbine power	1,500 kW
RO plant size	158 vessels
Average cost of water (COE at $0.04/kWh)	0.69 $/m^3
Average cost of water (COE at $0.12/kWh)	0.77 $/m^3
Average recovery rate	56.3 %
Average permeate flow rate	3,042 gpm
Average permeate flow per maximum power	2.03 gpm/kW

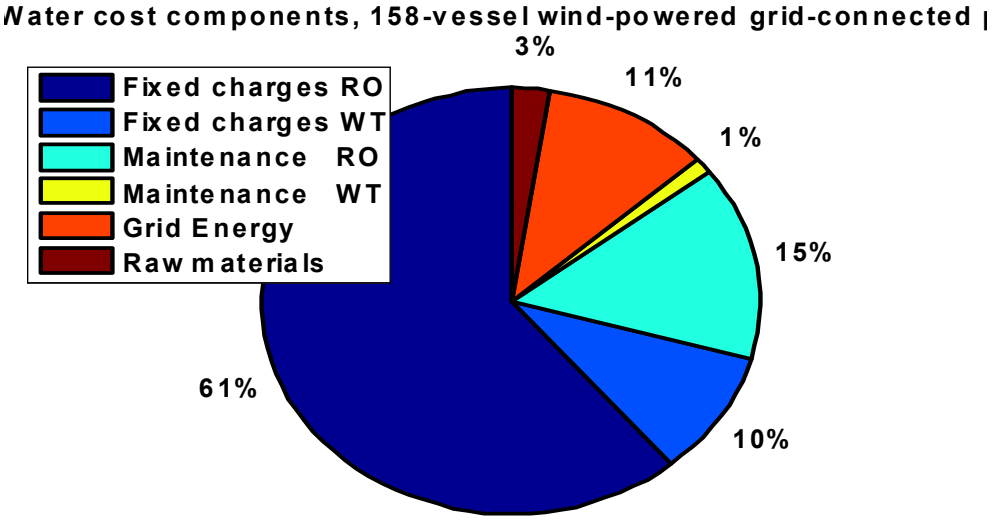

Figure 6-13. COW structure for the 158-vessel grid-connected wind-RO desalination plant, assuming $0.08/kWh grid energy cost

Table 6-4. Performance of an RO Plant Using Only Grid Power

Maximum wind turbine power	1,500 kW
RO plant size	158 vessels
Average COW (COE at $0.04/kWh)	0.66 $/m^3
Average COW (COE at $0.12/kWh)	0.83 $/m^3
Average recovery rate	56.3 %
Average permeate flow rate	3,042 gpm
Average permeate flow per maximum power	2.03 gpm/kW

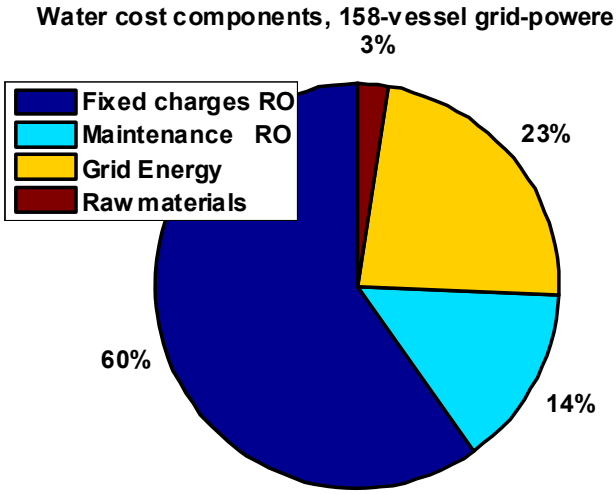

Figure 6-14. COW structure for the 158-vessel desalination plant, powered only with grid energy, assuming a $0.08/kWh energy cost

The average SCOW in the case of a grid-connected wind-powered desalination plant is lower than that in the similar plant operated in a grid-isolated mode (considered in Section 6.2). This reduction is owed to the more efficient use of equipment; namely, the cost of power purchased from the grid to run the plant at full capacity (with no RO vessels idling at any time) is smaller than the fixed (annualized) cost of the RO vessels that would remain unused when the power generated by the turbine is insufficient for running the RO plant at full capacity. This occurs for any (currently reasonable) cost of the energy purchased from the grid. However, for a very large COE, this balance may not stay true, and operating a grid-connected wind-powered RO desalination plant will become less advantageous than the operation of a similar, but grid-isolated configuration.

6.3.3 Plant operation concepts

The constant operation of a wind-RO plant analyzed in Section 6.3.1 is one of many possible operating strategies. Clearly, for the same capital expenditure, the plant operator may prefer to produce less water when grid power is expensive (decreasing the operating costs) and increase water production when wind is available. Accordingly, the "optimal" size of RO plant is closely dependent on the chosen strategy.

For a grid-connected operation, the plant set points include not only the grid-isolated topology set points (water pump speeds, number of active vessels, recirculation flows), but also those that correspond to the power management: power used by the RO plant, power bought or sold to the grid, and power drawn from or stored in the batteries (if available).

The operation of a wind-RO plant can take into account the forecast for wind speeds, and energy prices to make well-informed decisions to manage the energy storage. One possible way to achieve this is to use receding horizon techniques that continuously correct the operating set points to maximize a performance criterion. In the context of a grid-connected wind-RO plant this strategy can be defined by solving optimization problems in Table 6-5.

Table 6-5. Receding Horizon Approach for Wind-RO Operating Strategies

Minimize	$\sum_{k=1}^{N} COW_k$
Subject to	RO operational constraints (Sections 3.2.4−3.2.5)
	Energy storage constraints (Section 3.2.8)
	S < Smax (RO plant size)
	$\overline{Q}_p$ > $\overline{Q}_p$ demand
	$\overline{C}_p$ < $\overline{C}_p$ max

Where the optimization is performed with respect to the wind-RO plant set points, during a period of time spanning N steps, COW_k is the SCOW at the step k, Smax is the maximum number of vessels in the RO plant, $\overline{Q}_p$ and $\overline{C}_p$ are respectively, the average permeate flow and permeate concentration during the following N steps, and the limits $\overline{Q}_p$ min and $\overline{C}_p$ max depend on the local water regulations.

Model predictive control strategies as defined in Table 6-5 have been subjected to extensive use in industry for process control (see Rossiter 2003[44] and Maciejowski 2002[45]).

7 Conclusions

A systematic approach to address fundamental problems in the integration of wind energy and desalination systems was presented. The basic technological challenge for integrating RO desalination with renewable energy sources relies on the interaction between a power generation characterized by significant time fluctuations with a desalination technology that is typically designed for a steady operation and possesses a multiplicity of restrictive operational limits.

The design of a wind-RO system and its operational strategy requires an understanding of the physical limits that constrain the desalination operation and the way they are affected by power variations. To address this issue, a physics-based model has been developed to simulate the integrated wind-desalination system accounting effects such as:

- Changes in pressures, concentrations, and flows throughout the RO plant generated by changes in pump speeds, feedwater concentration, pressure and temperature, valve openings, and connection of RO vessels during operation
- Changes in the pump efficiencies caused by changes in water flows and pump speeds
- Changes in the electrical motor loads caused by changes in pump speed and flow rates
- Changes in the available power caused by changes in wind speeds
- Analyzing physical constraints (of all the components in the system) for any value of pump speed, valve position, vessel connection, and feedwater properties.

An integrated COW model was developed to evaluate the economic viability of various wind-desalination configurations and perform trade-off analyses. The integrated model accounts for the stochastic nature of wind and its economic effects on water production.

The operational flexibility is regarded as an important concern to operate RO plants in a wide range of available powers. This issue has been addressed first, by defining a set of desalination configurations with the ability to operate in a wide range of settings; then, a rigorous analysis has been performed using the physical models, to obtain the actual operating space allowed by the system constraints and to understand the trade-offs between operational constraints and desalination performance.

A preliminary cost analysis has been presented for two seawater desalination configurations and one brackish water configuration, which showed that the resulting COW had the potential to be viable. These configurations were defined considering that a 1.5-MW wind turbine provides the power.

One RO configuration was selected for further analysis to understand its performance and economics in grid-connected and grid-isolated electrical topologies. The detailed analyses include:

- The definition and calculation of an optimal operational strategy for a grid-isolated topology

- Definition and calculation of optimal plant size
- Detailed COW calculation of the resulting grid-isolated topology
- Definitions and calculation of an operating strategy for grid-connected topology
- Detailed COW calculation for resulting grid-connected topology, including a sensitivity analysis with respect to the cost of grid energy
- Definition of optimal operating strategies for grid-connected topologies.

The results showed that a wind-RO-integrated technology can produce water at competitive prices. For example, the analysis of seawater desalination powered by a 1.5-MW wind turbine, predicted a levelized annual cost of $\$1.11/m^3$ in a grid-isolated topology, and a cost of $\$0.77/m^3$ for a grid-connected topology with energy prices of \$0.12/kWh.

The systematic approach presented in this report should prove useful to pursue more detailed system design, trade-off analysis, and optimal operation strategies definition on similar systems and to analyze other hybrid desalination system with renewable energy sources.

8 Future Work

Many problems that can be considered as parts of a natural continuation of the approach presented in this report, and can benefit the understanding and design procedures for wind/RO systems. Some of them are listed here.

1. Use the physics and economical models in the proposed approach to investigate the potential technological improvements that have the largest impact on the COW for wind/RO desalination (or other hybrid desalination technologies). Methods to reduce the CO include
    a. Improve pump efficiencies.
    b. Improve energy recovery efficiencies.
    c. Relax RO membrane constraints by redesigning spiral wound elements.
    d. Augment the operational flexibility of ERDs.
2. Calculate optimal strategies to account for switching behavior of vessels and ERDs. The current strategy (as indicated in section 6.2.3) assumes that vessels can be individually activated or deactivated. An optimal strategy that accounts for restrictions in vessel and ERD operation should be used for more detailed analysis. As a by-product, a method to determine the optimal size of membrane and energy recovery banks will be obtained.
3. Define optimal operating strategies for efficient operation of wind-RO plants, taking into account local water distribution constraints. The approach, which was outlined in Section 6.3.3, takes into account the dynamics of the energy storage system and forecasted wind speeds and energy prices (if connected to the grid).
4. Obtain control strategies that account for damaging effects of membrane pressure fluctuations. This problem is more critical with grid-isolated configurations, and requires a good understanding of membrane degradation as a function of pressure fluctuations. The fluctuation in membrane caused by changes in wind speed (and electrical power fed to the water pumps) could be absorbed by the energy storage system.
5. Operating strategy will not follow exactly the table of optimal results. Instead the pump speed command should use a filter to mitigate pressure fluctuations in the range of frequencies that most affect membrane life. In this case the mismatch between wind power and used power can be absorbed by the energy storage.
6. Trip design: in cases when the fluctuations in power are large enough so that there is not time to implement switching strategies in RO banks or even dissipate extra power, there should be protective logic to prevent membrane damage. Threshold on the wind fluctuations can be defined to trigger a plant shutdown.

9 Toray Membrane America Design Guidelines

DESIGN GUIDELINES

Operating Parameters	RO Permeate	Well Water / Softened Water	Surface Water		Tertiary Effluent		Seawater, Beach Well	Seawater, Open Inlet
			MF/UF Pretreated	Filtered	MF/UF Pretreated	Filtered		
SDI_{15}	< 1	< 3	< 3	< 4	< 3	< 4	< 3	< 4
Maximum Recovery 40 Inch Element	30	20	17	15	14	12	12	10

Maximum Permeate Flow Rate, per element, gpd(m^3/d)

Four inch elements

TM710	1900 (7.2)	1580 (6.0)	1370 (5.2)	1240 (4.7)	1000 (3.8)	830 (3.1)		
TMG10	1900 (7.2)	1580 (6.0)	1370 (5.2)	1240 (4.7)	1000 (3.8)	830 (3.1)		
TM810	1825 (6.9)	1520 (5.8)	1310 (5.0)	1190 (4.5)	970 (3.7)	790 (3.0)	1520 (5.8)	1250 (4.7)

Eight inch elements

TM720-370	9300 (35)	7700 (29)	6600 (25)	6000 (23)	4900 (19)	4000 (15)		
TM720-400	10000 (38)	8300 (31)	7200 (27)	6500 (25)	5300 (20)	4400 (16)		
TM720-430	10800 (41)	9000 (34)	7700 (29)	7000 (26)	5700 (22)	4700 (18)		
TMG20-400	10000 (38)	8300 (31)	7200 (27)	6500 (25)	5300 (20)	4400 (16)		
TMG20-430	10080 (41)	9000 (34)	7700 (29)	7000 (26)	5700 (22)	4700 (18)		
TML20-370	9300 (35)	7700 (29)	6600 (25)	6000 (23)	4900 (19)	4000 (15)		
TML20-400	10000 (38)	8300 (31)	7200 (27)	6500 (25)	5300 (20)	4400 (16)		
TM820-370	9300 (35)	7700 (29)	6600 (25)	6000 (23)	4900 (19)	4000 (15)	7700 (29)	6300 (23.8)
TM820-400	10000 (38)	8300 (31)	7200 (27)	6500 (25)	5300 (20)	4400 (16)	8300 (31)	

Maximum Feed Flow Rate, gpm(m^3/d)

Four Inch Diameter	15 (55)	15 (55)	15 (55)	15 (55)	15 (55)	15 (55)	15 (55)	15 (55)
Eight Inch Diameter	70 (380)	65 (350)	60 (330)	55 (300)	55 (300)	55 (300)	60 (330)	55 (300)

Minimum Concentrate Flow Rate, gpm(m^3/d)

Four Inch Diameter	2 (11)	3 (16)	3 (16)	3 (16)	3 (16)	3 (16)	3 (16)	3 (16)
Eight Inch Diameter	10 (55)	15 (82)	15 (82)	15 (82)	15 (82)	15 (82)	15 (82)	15 (82)

TORAY Industries, Inc. Membrane Products Department.
8-1, Mihama 1-Chome, Urayasu, Chiba 279-8555, Japan
Tel : +81 (47) 350 6030
Fax : +81 (47) 350 6066

TORAY Membrane America, Inc.
USA, South America, Canada & Mexico
12520 High Bluff Drive, Suite 120,
San Diego, CA 92130, USA
Tel : +1 (858) 523 0476
Fax : +1 (858) 523 0861

ROPUR AG
Europe, Middle East and Africa
Grabenackerstrasse 8
CH-4142 Münchenstein 1, Switzerland
Tel : +41 (61) 415 87 10
Fax : +41 (61) 415 87 20

10 References

[1] U.S. Bureau of Reclamation and Sandia National Laboratories. *Desalination and Water Purification Technology Roadmap, A Report of the Executive Committee*, Jan. 2003.

[2] Economic and Social Commission for Western Asia. *Water Desalination Technologies in the ESCWA Member Countries*, July 27, 2001.

[3] Lawrence Livermore National Laboratory. *Helping Water Managers Ensure Clean and Reliable Supplies*, S&TR Report July/August 2004.

[4] Thomson M, Miranda MS, Infield D. "A small-scale seawater reverse-osmosis system with excellent energy efficiency over a wide operating range," *Desalination* 153, pp. 229–36 (2002).

[5] Carta JA, Gonzales J, Subiela V. "The SDAWES project: an ambitious R&D prototype for wind-powered desalination," *Desalination* 161, pp. 33–48 (2004).

[6] Miranda M, Infield D. "A wind-powered seawater reverse-osmosis system without batteries," *Desalination* 153, pp. 9–16 (2002).

[7] Colangelo A, Marano D, Spagna G, Sharma VK. "Photovoltaic powered reverse osmosis seawater desalination systems," *Applied Energy* 64, pp. 289–305 (1999).

[8] Pestana I, Latorre F, Espinoza C, Gotor A. "Optimization of RO desalination systems powered by renewable energies. Part I Wind energy," *Desalination* 160, pp. 293–99 (2004).

[9] Manth T, Gabor M, Oklejas E. "Minimizing RO energy consumption under variable conditions of operation," *Desalination* 157, pp. 9–21 (2003).

[10] Kershman, Sultan A, Rheinlander J, Neumann T, Goebel O. "Hybrid wind / PV and conventional power for desalination in Libya – GECOL's facility for medium and small scale research at Ras Ejder," *Desalination* 183, pp. 519−529 (2005).

[7] Burton T, Sharpe D, Jenkins N, Bossanyi E. *Wind Energy Handbook*, Chichester: J. Wiley and Sons (2001).

[8] Ong C-M. *Dynamic Simulation of Electric Machinery*, Englewood, NJ: Prentice-Hall, Inc. (1998).

[9] Ong C-M. *Dynamic Simulation of Electric Machinery*, Englewood, NJ: Prentice-Hall, Inc. (1998).

[10] Meares P (ed). *Membrane Separation Processes*, chapter 4, Elsevier (1976).

[11] Odendaal PE, Wiesner MR, and Mallevialle J. (eds). *Water Treatment Membrane Processes*, New York: McGraw-Hill (1996).

[12] Schwinge J, Neal P, Wiley D, Fletcher D, Fane A. "Spiral wound modules and spacers. Review and analysis," *Journal of Membrane Science*, 242, pp 129−153 (2004).

[13] Taniguchi M, Kimura S. "Estimation of transport parameters of RO membranes for seawater desalination," *AIChE Journal*, 46(10) (2000).

[14] Da Costa A, Fane A, Wiley D. "Spacer characterization and pressure drop modeling in spacer-filled channels for ultrafiltration," *Journal of Membrane Science* 87, pp. 79−98 (1994).

[15] Taniguchi M, Kurihara M, Kimura S. "Behavior of reverse osmosis plant adopting a brine conversion two-stage process and its computer simulation," *Journal of Membrane Science* 183, pp. 149−257 (2001).

[16] Toray RO. Membrane System Software, Version 2.28, Toray Membrane America, Inc., 12520 High Bluff Drive, Suite 120, San Diego, CA 92130 (858) 523-0476.

[17] MacHarg J. "Comparative study, the evolution of SWRO energy recovery systems," *Desalination and Water Reuse* 11(3), pp. 49−53 (2001).

[18]Liberman B. "The importance of energy recovery devices in reverse osmosis desalination," *The Future of Desalination in Texas*, Vol 2, Biennial report on seawater desalination, Texas Water Development Board (December 2004).

[19] Product specifications for the work exchanger DWEER 1100 from CALDER AG, www.calder.ch.

[20] Veres J. "Centrifugal and axial pump design and off-design performance prediction," NASA Technical Memorandum 106745 (1994).

[21] Karassik I, Krutzsch W, Fraser W, Messina J. *Pump Handbook*, 2nd Edition, McGraw-Hill (1976).

[22] Thomas P. *Simulation of Industrial Processes for Control Engineers*, Butterworth-Heinemann (1999).

[23] Web site for Chemical Engineering Magazine, using the Economic Indicators information regarding the Marshall & Swift Index for various years, www.che.com.

[24] Peters M, Timmerhaus K. *Plant Design and Economics for Chemical Engineers*, 4th Ed., New York: McGraw-Hill (1991).

[25] Web site of Matches Engineering Company, 2005 N Mistletoe Lane, Edmond, OK 73034-6054, (405) 340-2673, www.matche.com.

[26] FEDCO Product Selection Software, Version 04-01-05, Fluid Development Company, 914 Huber Drive, Monroe, MI 48162, (734) 241-3935.

[27] Dietrich J, Robert C. *Cost Guidance for Seawater Desalination Facilities in Texas*, Reiss Environmental Inc. Report (2005).

[28] GE-Osmonics Membrane System Software, WinFlows/CashFlows, Version 2.0.14.

[29] Calder AG. DWEER Model 1100 Quote 7-11-05, Calder AG Industrie Nord CH-5704 Egliswil, Switzerland +041(0) 62-769-60-60, www.calder.ch.

[30] Ettouney H, et al. "Evaluating the economics of desalination," *CEP*, 98(12) (2002).

[31] Web site for the Chemical Market Reporter, Costs from March 2005, www.chemicalmarketreporter.com.

[32] Web site for eChinaChem.com, 1091 Industrial Road, Suite 240, San Carlos, CA 94070, (650) 598-0328, www.echinachem.com.

[33] Toray RO. Membrane System Software, Version 2.28, Toray Membrane America, Inc., 12520 High Bluff Drive, Suite 120, San Diego, CA 92130, (858) 523-0476.

[34] Hafez A, El-Manharawy S. "Economics of seawater RO desalination in the Red Sea region, Egypt. Part 1. A case study," *Desalination* 153, pp. 335−347 (2002).

[35] Web site of the U.S. Department of Energy, Energy Information Administration www.eia.doe.gov/cneaf/electricity/epm/epm_sum.html.

[36] Garcia-Rodriguez L, et al. "Economic analysis of wind-powered desalination," *Desalination* 137, pp. 259−265 (2001).

[37] Afonso MD, Jaber JO, Mohsen MS. "Brackish groundwater treatment by reverse osmosis in Jordan," *Desalination* 164, pp. 157−171 (2004).

[38] Manth T, Gabor M, Oklejas E. "Minimizing RO energy consumption under variable conditions of operation," *Desalination* 157, pp. 9−21 (2003).

[39] MacHarg J. "The evolution of SWRO energy-recovery systems," *Desalination & Water Reuse* 11/3, 49−53.

[40] Helstrom CW. *Probability and Stochastic Processes for Engineers*, 2nd Edition, New York: Macmillan (1990).

[41] www.awea.org/faq/netbdef.html

[42] *WHO Guidelines for Drinking Water Quality*, 2nd ed., Geneva (1993).

[43] Perry RH, Green DW. *Perry's Chemical Engineers' Handbook,* 7th Edition, New York: McGraw-Hill, Chapter 18.

[44] Rossiter J. *Model-Based Predictive Control: A Practical Approach*, CRC Press, Control Series (2003).

[45] Maciejowski J. *Predictive Control with Constraints*, Addison Wesley Longman (2002).

Appendix A
Toray Reverse Osmosis, Brackish Water, and Seawater Elements

The following documents are used with permission from Toray Membrane America, Inc.

ROMEMBRA
TORAY REVERSE OSMOSIS ELEMENTS

Project:
Comments:

Prepared For:
Location:
Prepared By:
Date Prepared:

System Results

Flow Rates	Gal/min	Concentrations	mg/l
RO Feed	2600	RO Feed TDS	35098
Permeate	1040	Permeate TDS	260
Concentrate	1560	Concentrate TDS	58323
Total Feed	2600	Total Feed TDS	35106
Total Product	1040	Total Product TDS	260

System Details **Single Stage Design**

Temperature: 25.0 Deg C Water Type: Seawater -well
System Recovery: 40.0 %

Pass 1 **Units: Pressure - Psi** **Flow - Gal/min** **TDS - mg/l**

Array 1 Recovery: 40.0% Concentrate TDS: 58323 Concentrate Flow: 1560

Bank	Total Vessels	Total Elements	Element Model	Feed Flow	Perm Flow	Feed Press	Delta Press	Perm TDS
1	50	300	TM820-370	2600	743	753	14.2	185
2	38	228	TM820-370	1857	297	737	14.5	449
Total	**88**	**528**		**2600**	**1040**			**260**

Concentration, Saturation and pH Data **mg/l**

Ion	Permeate	Treated Feed	Feed	Concentrate
Ca	0.96	408	408	679
Mg	3.07	1298	1298	2161
Na	92.6	10768	10768	17885
K	3.77	388	388	644
Ba	0.0	0.0	0.0	0.0
Sr	0.0	0.0	0.0	0.0
NH4	0.0	0.0	0.0	0.0
Fe	0.0	0.0	0.0	0.0
HCO3	1.26	101	143	168
Cl	149	19380	19380	32200
SO4	8.6	2738	2702	4558
NO3	0.0	0.0	0.0	0.0
F	0.0	0.0	0.0	0.0
B	0.31	1.1	1.1	1.63

Ion	Permeate	Treated Feed	Feed	Concentrate
SiO2	0.16	15.0	15.0	24.9
PO4	0.0011	0.5	0.5	0.83
CO3	4.12E-06	0.0814	2.29	0.26
CO2	34.0	34.0	2.4	34.0
TDS	260	35098	35106	58323
pH	4.76	6.5	7.8	6.7
Saturation Data (%)				
CaSO4	0.0027	21.8	21.5	41.6
CaPO4	0.0	0.0732	10000	174
CaF2	0.0	0.0	0.0	0.0
BaSO4	0.0	0.0	0.0	0.0
SiO2	0.12	14.0	11.7	23.8
SrSO4	0.0	0.0	0.0	0.0
LSI	-7.62	-0.74	0.72	0.0899
SDSI	-6.56	-1.57	-0.11	-1.08

System Summary

System Configuration

System Type:	
Feed Predosing?:	Yes
Feed Afterdosing?:	No
Interpass Dosing?:	No
Product Dosing?:	No
Feed CO2 Stripping?:	No
Interpass CO2 Stripping?:	No
Product CO2 Stripping?:	No
Raw Feed Bypass?:	No
First Pass Recycle?:	No
Interpass Pumping?:	No

Feed Information

Water Type:	Seawater -well
Temperature, Deg C:	25.0
Feed pH:	7.8
Silt Density Index:	5.5

Feed Ion Concentration (mg/l)

Ca	408
Mg	1298
Na	10768
K	388
Ba	0.0
Sr	0.0
NH4	0.0
Fe	0.0
HCO3	143
Cl	19380
SO4	2702
NO3	0.0
F	0.0
B	1.1
SiO2	15.0
PO4	0.5
CO3	2.29
CO2	2.4

System Flux, Flows and Recoveries

Average System Flux:	7.68 Gal/ft2/day
Feed Flow:	2,600.00 Gal/min
Product Flow:	1,040.00 Gal/min
Concentrate Flow:	1,560.00 Gal/min
First Pass Recovery:	40.0 %
System Recovery:	40.0 %

First Pass Array

Interbank Pressure Drop:	2.0 Psi
Interbank Pressure Boost Bank 1-2:	0.0 Psi
Bank 1 Back Pressure:	15.0 Psi
Bank 2 Back Pressure:	15.0 Psi

Number of Banks: 2 Total Elements: 528

Bank	# Vessels	# Elements/Vessel	Element Type	Element Age
1	50	6	TM820-370	3
2	38	6	TM820-370	3

Chemical Treatment

Station	Chemical	Target pH
Feed Pre-Treat	Sulfuric Acid	6.5

Process Data

Flow Units: Gal/min
Pressure Units: psi

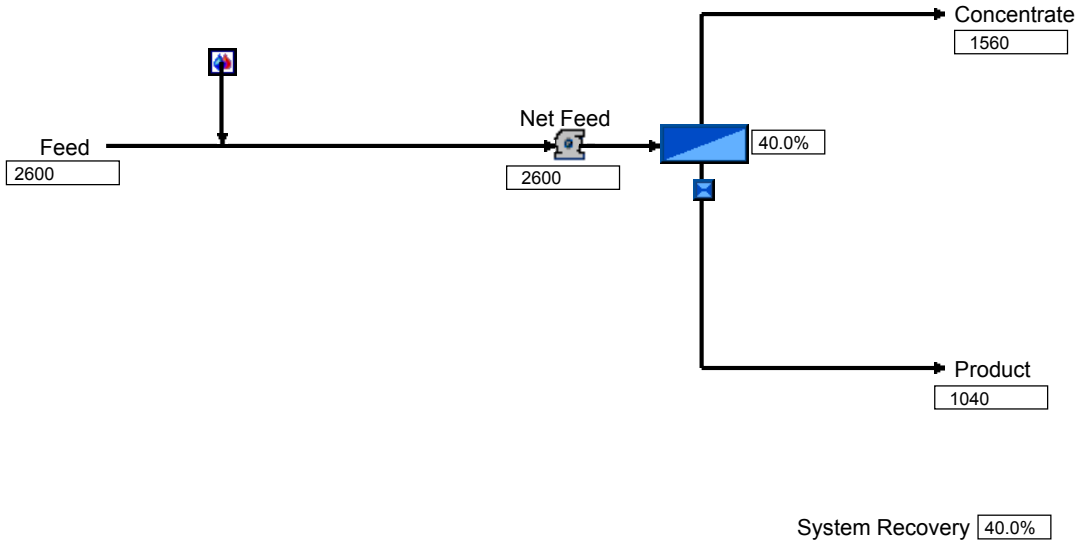

Flow Rates	Gal/min	Concentrations	mg/l
RO Feed	2600	RO Feed TDS	35098
Permeate	1040	Permeate TDS	260
Concentrate	1560	Concentrate TDS	58323
Total Feed	2600	Total Feed TDS	35106
Total Product	1040	Total Product TDS	260

System Data **Single Stage Design**

Temperature: 25.0 Deg C

	Stage 1	
Fouling Allowance	85.0	%
Salt Passage Increase Per Year	10.0	%
Feed Pressure	753	Psi
Interbank Loss	2.0	Psi
Element Age	3.0	Years

Interbank Boost Pressure	Stage 1	
Banks 1-2	0.0	Psi

Chemical Usage	Chemical	lb/day	kg/day	Target pH
Feed Pre-Treat	Sulfuric Acid	1156	525	6.5

Stream Data

Units: Pressure - psi Flow - Gal/min TDS - mg/l Saturation - %

Stream --->	System Feed	Predosed Feed	1st Pass Feed	Total Permeate	System Product
Ca	408	408	408	0.96	0.96
Mg	1298	1298	1298	3.07	3.07
Na	10768	10768	10768	92.6	92.6
K	388	388	388	3.77	3.77
Ba	0.0	0.0	0.0	0.0	0.0
Sr	0.0	0.0	0.0	0.0	0.0
NH4	0.0	0.0	0.0	0.0	0.0
Fe	0.0	0.0	0.0	0.0	0.0
HCO3	143	101	101	1.26	1.26
Cl	19380	19380	19380	149	149
SO4	2702	2738	2738	8.6	8.6
NO3	0.0	0.0	0.0	0.0	0.0
F	0.0	0.0	0.0	0.0	0.0
B	1.1	1.1	1.1	0.31	0.31
SiO2	15.0	15.0	15.0	0.16	0.16
PO4	0.5	0.5	0.5	0.0011	0.0011
CO3	2.29	0.0814	0.0814	4.12E-06	4.12E-06
CO2	2.4	34.0	34.0	34.0	34.0
TDS	35106	35098	35098	260	260
pH	7.8	6.5	6.5	4.76	4.76
LSI	0.72	-0.74	-0.74	-7.62	-7.62
Stiff-Davis	-0.11	-1.57	-1.57	-6.56	-6.56
BaSO4 Sat	0.0	0.0	0.0	0.0	0.0
CaSO4 Sat	21.5	21.8	21.8	0.0027	0.0027
CaPO4 Sat	10000	0.0732	0.0732	0.0	0.0
CaF2 Sat	0.0	0.0	0.0	0.0	0.0
SrSO4 Sat	0.0	0.0	0.0	0.0	0.0
SiO2 Sat	11.7	14.0	14.0	0.12	0.12
Flow	2600	2600	2600	1040	1040
Temp, Deg C	25.0	25.0	25.0	25.0	25.0
Pressure	753	753	753	0.0	0.0
Osm Pressure	368	368	368	3.07	3.07

Units: Pressure - psi Flow - Gal/min TDS - mg/l Saturation - %

Stream --->	System Concentrate
Ca	679
Mg	2161
Na	17885
K	644
Ba	0.0
Sr	0.0
NH4	0.0
Fe	0.0
HCO3	168
Cl	32200
SO4	4558
NO3	0.0
F	0.0
B	1.63
SiO2	24.9
PO4	0.83
CO3	0.26
CO2	34.0
TDS	58323
pH	6.7
LSI	0.0899
Stiff-Davis	-1.08
BaSO4 Sat	0.0
CaSO4 Sat	41.6
CaPO4 Sat	174
CaF2 Sat	0.0
SrSO4 Sat	0.0
SiO2 Sat	23.8
Flow	1560
Temp, Deg C	25.0
Pressure	723
Osm Pressure	603

Element Data

Pass 1, Bank 1 **Units: Pressure - psi, Flow - Gal/min, TDS - mg/l, Saturation - %, Flux - gal/ft2/day**

Bank Permeate Back Pressure: 15.0

	Elem 1	Elem 2	Elem 3	Elem 4	Elem 5	Elem 6
Permeate Ions						
Ca	0.48	0.55	0.63	0.73	0.85	1.02
Mg	1.53	1.75	2.02	2.33	2.72	3.24
Na	46.5	53.1	61.0	70.6	82.1	97.8
K	1.89	2.16	2.48	2.87	3.34	3.98
Ba	0.0	0.0	0.0	0.0	0.0	0.0
Sr	0.0	0.0	0.0	0.0	0.0	0.0
NH4	0.0	0.0	0.0	0.0	0.0	0.0
Fe	0.0	0.0	0.0	0.0	0.0	0.0
HCO3	0.63	0.72	0.83	0.96	1.12	1.33
Cl	74.9	85.6	98.4	114	133	158
SO4	4.3	4.91	5.65	6.54	7.61	9.08
NO3	0.0	0.0	0.0	0.0	0.0	0.0
F	0.0	0.0	0.0	0.0	0.0	0.0
B	0.19	0.21	0.23	0.26	0.3	0.34
SiO2	0.0807	0.0925	0.11	0.12	0.14	0.17
PO4	0.0005	0.0006	0.0007	0.0008	0.0009	0.0011
CO3	9.82E-07	1.30E-06	1.73E-06	2.34E-06	3.21E-06	4.63E-06
CO2	34.0	34.0	34.0	34.0	34.0	34.0
TDS	130	149	171	198	231	275
pH	4.47	4.52	4.58	4.64	4.71	4.78
LSI	-9.4	-9.29	-9.17	-9.06	-8.94	-7.23
Stiff-Davis	-7.43	-7.26	-7.09	-6.9	-6.71	-6.49
Conc Saturation						
BaSO4 Sat	0.0	0.0	0.0	0.0	0.0	0.0
CaSO4 Sat	23.5	25.3	27.2	29.1	31.2	33.2
CaF2 Sat	0.0	0.0	0.0	0.0	0.0	0.0
SrSO4 Sat	0.0	0.0	0.0	0.0	0.0	0.0
SiO2 Sat	14.9	15.8	16.8	17.8	18.9	19.9
Flow						
Feed	52.0	48.9	46.1	43.5	41.1	39.0
Permeate	3.07	2.83	2.59	2.35	2.12	1.89
Pressure						
Feed	753	751	748	746	743	741
Net Driving	330	305	279	253	227	202
Pressure Drop	2.83	2.62	2.43	2.27	2.12	1.99
Feed Osmotic	368	390	413	437	462	486
Other Parameters						
% Recovery	5.9	5.79	5.63	5.41	5.15	4.84
B Conc Pol	1.08	1.08	1.07	1.07	1.06	1.06
A Value	2.56E-09	2.57E-09	2.58E-09	2.58E-09	2.59E-09	2.60E-09
B Value	2.06E-08	2.06E-08	2.05E-08	2.04E-08	2.04E-08	2.07E-08
Flux	12.0	11.0	10.1	9.18	8.26	7.37

Pass 1, Bank 2 **Units: Pressure - psi, Flow - Gal/min, TDS - mg/l, Saturation - %, Flux - gal/ft2/day**

Bank Permeate Back Pressure: 15.0
Bank Boost Pressure: 0.0

	Elem 1	Elem 2	Elem 3	Elem 4	Elem 5	Elem 6
Permeate Ions						
Ca	1.17	1.35	1.57	1.83	2.13	2.49
Mg	3.72	4.31	5.0	5.82	6.78	7.91
Na	112	130	151	175	204	238
K	4.57	5.29	6.13	7.12	8.29	9.65
Ba	0.0	0.0	0.0	0.0	0.0	0.0
Sr	0.0	0.0	0.0	0.0	0.0	0.0
NH4	0.0	0.0	0.0	0.0	0.0	0.0
Fe	0.0	0.0	0.0	0.0	0.0	0.0
HCO3	1.53	1.77	2.05	2.38	2.77	3.22
Cl	182	210	244	283	330	384
SO4	10.4	12.1	14.0	16.3	19.0	22.2
NO3	0.0	0.0	0.0	0.0	0.0	0.0
F	0.0	0.0	0.0	0.0	0.0	0.0
B	0.37	0.41	0.46	0.5	0.56	0.61
SiO2	0.19	0.22	0.26	0.29	0.34	0.39
PO4	0.0013	0.0015	0.0017	0.002	0.0023	0.0027
CO3	6.21E-06	8.43E-06	1.15E-05	1.58E-05	2.18E-05	3.02E-05
CO2	34.0	34.0	34.0	34.0	34.0	34.0
TDS	316	365	424	493	573	668
pH	4.84	4.9	4.96	5.02	5.08	5.15
LSI	-6.75	-6.42	-6.16	-5.92	-5.7	-5.5
Stiff-Davis	-6.31	-6.13	-5.94	-5.76	-5.57	-5.38
Conc Saturation						
BaSO4 Sat	0.0	0.0	0.0	0.0	0.0	0.0
CaSO4 Sat	34.7	36.3	37.7	39.1	40.4	41.6
CaF2 Sat	0.0	0.0	0.0	0.0	0.0	0.0
SrSO4 Sat	0.0	0.0	0.0	0.0	0.0	0.0
SiO2 Sat	20.6	21.3	22.0	22.7	23.3	23.8
Flow						
Feed	48.9	47.2	45.6	44.3	43.1	42.0
Permeate	1.71	1.53	1.36	1.21	1.07	0.94
Pressure						
Feed	737	735	732	730	727	725
Net Driving	183	165	148	132	117	104
Pressure Drop	2.65	2.54	2.44	2.36	2.28	2.21
Feed Osmotic	510	528	545	561	576	590
Other Parameters						
% Recovery	3.49	3.24	2.99	2.73	2.48	2.24
B Conc Pol	1.05	1.04	1.04	1.03	1.03	1.03
A Value	2.59E-09	2.59E-09	2.57E-09	2.56E-09	2.54E-09	2.53E-09
B Value	2.09E-08	2.10E-08	2.11E-08	2.13E-08	2.14E-08	2.16E-08
Flux	6.65	5.96	5.31	4.71	4.16	3.67

Errors & Warnings

Warning - High LSI. LSI > zero. Concentrate CaCO3 greater than saturation. Scale inhibitor required.
The feed water analysis was balanced with added Na or Cl.

Database version used for design : 2.028

TORAY

Toray Industries, Inc. Membrane Products Dept.
8-1, Mihama 1-chome, Urayasu, Chiba 279-8555, Japan
TEL: (+81) 47-350-6030
Fax: (+81) 47-350-6066

TORAY Membrane America, Inc.
USA, South America, Canada
12520 High Bluff Drive, Suite 120
San Diego, CA 92130, USA
Tel: +1 (858) 523 0476
Fax: +1 (858) 523 0861

ROPUR AG
Europe, Middle East and Africa
Grabenackerstrasse 8
CH-4142 Munchenstein 1, Switzerland
Tel: +41 (61) 415 87 10
Fax: +41 (61) 415 87 20

ROMEMBRA
TORAY REVERSE OSMOSIS ELEMENTS

Project:
Comments:

Prepared For:
Location:
Prepared By:
Date Prepared:

System Results

Flow Rates	Gal/min	Concentrations	mg/l
RO Feed	2625	RO Feed TDS	35098
Permeate	1050	Permeate TDS	255
Concentrate	1575	Concentrate TDS	58327
Total Feed	2625	Total Feed TDS	35106
Total Product	1050	Total Product TDS	255

System Details **Single Stage Design**

Temperature: 25.0 Deg C Water Type: Seawater -well
System Recovery: 40.0 %

Pass 1 **Units: Pressure - Psi** **Flow - Gal/min** **TDS - mg/l**

Array 1 Recovery: 40.0% Concentrate TDS: 58327 Concentrate Flow: 1575

Bank	Total Vessels	Total Elements	Element Model	Feed Flow	Perm Flow	Feed Press	Delta Press	Perm TDS
1	50	300	TM820-370	2625	713	731	14.6	187
2	38	228	TM820-370	1912	337	757	14.9	398
Total	**88**	**528**		**2625**	**1050**			**255**

Concentration, Saturation and pH Data **mg/l**

Ion	Permeate	Treated Feed	Feed	Concentrate
Ca	0.94	408	408	679
Mg	3.0	1298	1298	2161
Na	90.7	10768	10768	17886
K	3.69	388	388	644
Ba	0.0	0.0	0.0	0.0
Sr	0.0	0.0	0.0	0.0
NH4	0.0	0.0	0.0	0.0
Fe	0.0	0.0	0.0	0.0
HCO3	1.23	101	143	168
Cl	146	19380	19380	32202
SO4	8.42	2738	2702	4558
NO3	0.0	0.0	0.0	0.0
F	0.0	0.0	0.0	0.0
B	0.31	1.1	1.1	1.63

Ion	Permeate	Treated Feed	Feed	Concentrate
SiO2	0.16	15.0	15.0	24.9
PO4	0.001	0.5	0.5	0.83
CO3	3.95E-06	0.0814	2.29	0.26
CO2	34.0	34.0	2.4	34.0
TDS	255	35098	35106	58327
pH	4.75	6.5	7.8	6.7
Saturation Data (%)				
CaSO4	0.0026	21.8	21.5	41.6
CaPO4	0.0	0.0732	10000	175
CaF2	0.0	0.0	0.0	0.0
BaSO4	0.0	0.0	0.0	0.0
SiO2	0.12	14.0	11.7	23.8
SrSO4	0.0	0.0	0.0	0.0
LSI	-7.88	-0.74	0.72	0.09
SDSI	-6.58	-1.57	-0.11	-1.08

System Summary

System Configuration

System Type:	
Feed Predosing?:	Yes
Feed Afterdosing?:	No
Interpass Dosing?:	No
Product Dosing?:	No
Feed CO2 Stripping?:	No
Interpass CO2 Stripping?:	No
Product CO2 Stripping?:	No
Raw Feed Bypass?:	No
First Pass Recycle?:	No
Interpass Pumping?:	No

Feed Information

Water Type:	Seawater -well
Temperature, Deg C:	25.0
Feed pH:	7.8
Silt Density Index:	5.5

Feed Ion Concentration (mg/l)

Ca	408
Mg	1298
Na	10768
K	388
Ba	0.0
Sr	0.0
NH4	0.0
Fe	0.0
HCO3	143
Cl	19380
SO4	2702
NO3	0.0
F	0.0
B	1.1
SiO2	15.0
PO4	0.5
CO3	2.29
CO2	2.4

System Flux, Flows and Recoveries

Average System Flux:	7.75 Gal/ft2/day
Feed Flow:	2,625.00 Gal/min
Product Flow:	1,050.00 Gal/min
Concentrate Flow:	1,575.00 Gal/min
First Pass Recovery:	40.0 %
System Recovery:	40.0 %

First Pass Array

Interbank Pressure Drop: 2.0 Psi

Interbank Pressure Boost
Bank 1-2: 42.0 Psi

Bank 1 Back Pressure: 15.0 Psi
Bank 2 Back Pressure: 15.0 Psi

Number of Banks: 2 Total Elements: 528

Bank	# Vessels	# Elements/Vessel	Element Type	Element Age
1	50	6	TM820-370	3
2	38	6	TM820-370	3

Chemical Treatment

Station	Chemical	Target pH
Feed Pre-Treat	Sulfuric Acid	6.5

Process Data

Flow Units: Gal/min
Pressure Units: psi

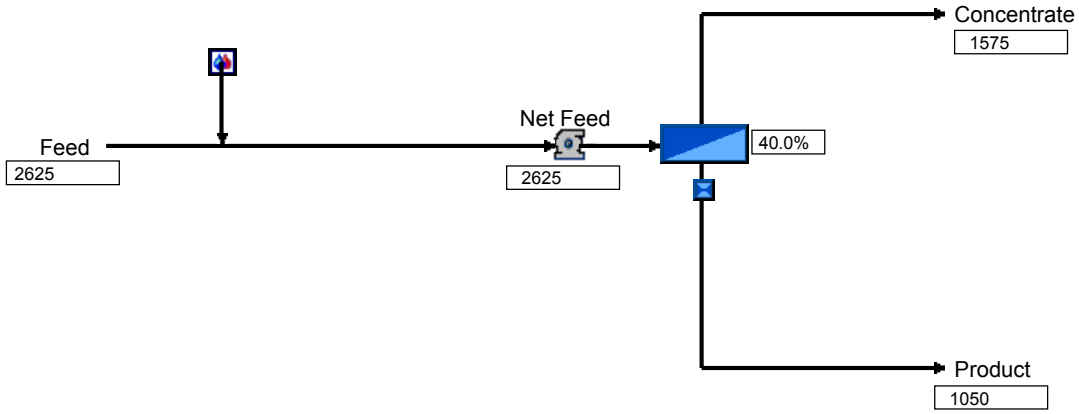

System Recovery 40.0%

Flow Rates	Gal/min	Concentrations	mg/l
RO Feed	2625	RO Feed TDS	35098
Permeate	1050	Permeate TDS	255
Concentrate	1575	Concentrate TDS	58327
Total Feed	2625	Total Feed TDS	35106
Total Product	1050	Total Product TDS	255

System Data **Single Stage Design**

Temperature: 25.0 Deg C

	Stage 1	
Fouling Allowance	85.0	%
Salt Passage Increase Per Year	10.0	%
Feed Pressure	731	Psi
Interbank Loss	2.0	Psi
Element Age	3.0	Years

Interbank Boost Pressure	Stage 1	
Banks 1-2	42.0	Psi

Chemical Usage	Chemical	lb/day	kg/day	Target pH
Feed Pre-Treat	Sulfuric Acid	1167	531	6.5

Stream Data

Units: Pressure - psi Flow - Gal/min TDS - mg/l Saturation - %

Stream --->	System Feed	Predosed Feed	1st Pass Feed	Total Permeate	System Product
Ca	408	408	408	0.94	0.94
Mg	1298	1298	1298	3.0	3.0
Na	10768	10768	10768	90.7	90.7
K	388	388	388	3.69	3.69
Ba	0.0	0.0	0.0	0.0	0.0
Sr	0.0	0.0	0.0	0.0	0.0
NH4	0.0	0.0	0.0	0.0	0.0
Fe	0.0	0.0	0.0	0.0	0.0
HCO3	143	101	101	1.23	1.23
Cl	19380	19380	19380	146	146
SO4	2702	2738	2738	8.42	8.42
NO3	0.0	0.0	0.0	0.0	0.0
F	0.0	0.0	0.0	0.0	0.0
B	1.1	1.1	1.1	0.31	0.31
SiO2	15.0	15.0	15.0	0.16	0.16
PO4	0.5	0.5	0.5	0.001	0.001
CO3	2.29	0.0814	0.0814	3.95E-06	3.95E-06
CO2	2.4	34.0	34.0	34.0	34.0
TDS	35106	35098	35098	255	255
pH	7.8	6.5	6.5	4.75	4.75
LSI	0.72	-0.74	-0.74	-7.88	-7.88
Stiff-Davis	-0.11	-1.57	-1.57	-6.58	-6.58
BaSO4 Sat	0.0	0.0	0.0	0.0	0.0
CaSO4 Sat	21.5	21.8	21.8	0.0026	0.0026
CaPO4 Sat	10000	0.0732	0.0732	0.0	0.0
CaF2 Sat	0.0	0.0	0.0	0.0	0.0
SrSO4 Sat	0.0	0.0	0.0	0.0	0.0
SiO2 Sat	11.7	14.0	14.0	0.12	0.12
Flow	2625	2625	2625	1050	1050
Temp, Deg C	25.0	25.0	25.0	25.0	25.0
Pressure	731	731	731	0.0	0.0
Osm Pressure	368	368	368	3.01	3.01

Units: Pressure - psi Flow - Gal/min TDS - mg/l Saturation - %

Stream --->	System Concentrate
Ca	679
Mg	2161
Na	17886
K	644
Ba	0.0
Sr	0.0
NH4	0.0
Fe	0.0
HCO3	168
Cl	32202
SO4	4558
NO3	0.0
F	0.0
B	1.63
SiO2	24.9
PO4	0.83
CO3	0.26
CO2	34.0
TDS	58327
pH	6.7
LSI	0.09
Stiff-Davis	-1.08
BaSO4 Sat	0.0
CaSO4 Sat	41.6
CaPO4 Sat	175
CaF2 Sat	0.0
SrSO4 Sat	0.0
SiO2 Sat	23.8
Flow	1575
Temp, Deg C	25.0
Pressure	742
Osm Pressure	603

Element Data

Pass 1, Bank 1 **Units: Pressure - psi, Flow - Gal/min, TDS - mg/l, Saturation - %, Flux - gal/ft2/day**

Bank Permeate Back Pressure: 15.0

	Elem 1	Elem 2	Elem 3	Elem 4	Elem 5	Elem 6
Permeate Ions						
Ca	0.49	0.56	0.65	0.74	0.86	1.02
Mg	1.57	1.79	2.05	2.37	2.75	3.24
Na	47.7	54.3	62.2	71.7	83.0	98.0
K	1.94	2.21	2.53	2.92	3.38	3.98
Ba	0.0	0.0	0.0	0.0	0.0	0.0
Sr	0.0	0.0	0.0	0.0	0.0	0.0
NH4	0.0	0.0	0.0	0.0	0.0	0.0
Fe	0.0	0.0	0.0	0.0	0.0	0.0
HCO3	0.65	0.74	0.85	0.98	1.13	1.33
Cl	76.8	87.5	100	116	134	158
SO4	4.4	5.02	5.76	6.64	7.7	9.09
NO3	0.0	0.0	0.0	0.0	0.0	0.0
F	0.0	0.0	0.0	0.0	0.0	0.0
B	0.19	0.21	0.24	0.27	0.3	0.34
SiO2	0.0837	0.0956	0.11	0.13	0.15	0.17
PO4	0.0005	0.0006	0.0007	0.0008	0.0009	0.0011
CO3	1.03E-06	1.36E-06	1.80E-06	2.42E-06	3.29E-06	4.65E-06
CO2	34.0	34.0	34.0	34.0	34.0	34.0
TDS	134	152	175	201	233	275
pH	4.48	4.53	4.59	4.65	4.71	4.78
LSI	-9.38	-9.27	-9.16	-9.05	-8.93	-7.23
Stiff-Davis	-7.4	-7.24	-7.06	-6.88	-6.69	-6.49
Conc Saturation						
BaSO4 Sat	0.0	0.0	0.0	0.0	0.0	0.0
CaSO4 Sat	23.4	25.1	26.8	28.7	30.5	32.4
CaF2 Sat	0.0	0.0	0.0	0.0	0.0	0.0
SrSO4 Sat	0.0	0.0	0.0	0.0	0.0	0.0
SiO2 Sat	14.8	15.7	16.7	17.6	18.5	19.5
Flow						
Feed	52.5	49.6	46.8	44.3	42.1	40.1
Permeate	2.95	2.72	2.49	2.26	2.04	1.82
Pressure						
Feed	731	729	726	723	721	719
Net Driving	310	286	262	237	214	191
Pressure Drop	2.86	2.67	2.49	2.33	2.18	2.05
Feed Osmotic	368	389	411	433	456	478
Other Parameters						
% Recovery	5.61	5.48	5.31	5.1	4.84	4.55
B Conc Pol	1.08	1.07	1.07	1.06	1.06	1.05
A Value	2.62E-09	2.63E-09	2.63E-09	2.64E-09	2.64E-09	2.65E-09
B Value	2.04E-08	2.03E-08	2.03E-08	2.02E-08	2.01E-08	2.04E-08
Flux	11.5	10.6	9.7	8.81	7.94	7.1

Pass 1, Bank 2 **Units: Pressure - psi, Flow - Gal/min, TDS - mg/l, Saturation - %, Flux - gal/ft2/day**

Bank Permeate Back Pressure: 15.0
Bank Boost Pressure: 42.0

	Elem 1	Elem 2	Elem 3	Elem 4	Elem 5	Elem 6
Permeate Ions						
Ca	1.03	1.2	1.39	1.61	1.88	2.2
Mg	3.29	3.8	4.41	5.14	5.99	7.0
Na	99.5	115	133	155	180	211
K	4.05	4.67	5.41	6.29	7.33	8.56
Ba	0.0	0.0	0.0	0.0	0.0	0.0
Sr	0.0	0.0	0.0	0.0	0.0	0.0
NH4	0.0	0.0	0.0	0.0	0.0	0.0
Fe	0.0	0.0	0.0	0.0	0.0	0.0
HCO3	1.35	1.56	1.81	2.11	2.45	2.86
Cl	161	185	215	250	292	340
SO4	9.23	10.7	12.4	14.4	16.8	19.6
NO3	0.0	0.0	0.0	0.0	0.0	0.0
F	0.0	0.0	0.0	0.0	0.0	0.0
B	0.34	0.38	0.42	0.46	0.51	0.57
SiO2	0.17	0.19	0.22	0.26	0.3	0.35
PO4	0.0011	0.0013	0.0015	0.0018	0.0021	0.0024
CO3	4.80E-06	6.49E-06	8.86E-06	1.22E-05	1.68E-05	2.34E-05
CO2	34.0	34.0	34.0	34.0	34.0	34.0
TDS	279	323	374	435	507	592
pH	4.79	4.85	4.91	4.97	5.03	5.1
LSI	-7.15	-6.69	-6.38	-6.11	-5.88	-5.66
Stiff-Davis	-6.47	-6.28	-6.1	-5.91	-5.72	-5.53
Conc Saturation						
BaSO4 Sat	0.0	0.0	0.0	0.0	0.0	0.0
CaSO4 Sat	34.0	35.7	37.2	38.8	40.2	41.6
CaF2 Sat	0.0	0.0	0.0	0.0	0.0	0.0
SrSO4 Sat	0.0	0.0	0.0	0.0	0.0	0.0
SiO2 Sat	20.3	21.0	21.8	22.5	23.2	23.8
Flow						
Feed	50.3	48.4	46.7	45.1	43.7	42.5
Permeate	1.92	1.73	1.55	1.38	1.22	1.08
Pressure						
Feed	757	754	751	749	747	744
Net Driving	209	189	170	153	136	121
Pressure Drop	2.75	2.62	2.51	2.41	2.32	2.24
Feed Osmotic	500	519	538	556	573	589
Other Parameters						
% Recovery	3.81	3.57	3.31	3.05	2.79	2.53
B Conc Pol	1.05	1.05	1.04	1.04	1.03	1.03
A Value	2.55E-09	2.54E-09	2.53E-09	2.52E-09	2.50E-09	2.48E-09
B Value	2.10E-08	2.11E-08	2.13E-08	2.15E-08	2.16E-08	2.18E-08
Flux	7.47	6.73	6.03	5.36	4.75	4.19

Errors & Warnings

Warning - High LSI. LSI > zero. Concentrate CaCO3 greater than saturation. Scale inhibitor required.
The feed water analysis was balanced with added Na or Cl.

Database version used for design : 2.028

TORAY

Toray Industries, Inc. Membrane Products Dept.
8-1, Mihama 1-chome, Urayasu, Chiba 279-8555, Japan
TEL: (+81) 47-350-6030
Fax: (+81) 47-350-6066

TORAY Membrane America, Inc.
USA, South America, Canada
12520 High Bluff Drive, Suite 120
San Diego, CA 92130, USA
Tel: +1 (858) 523 0476
Fax: +1 (858) 523 0861

ROPUR AG
Europe, Middle East and Africa
Grabenackerstrasse 8
CH-4142 Munchenstein 1, Switzerland
Tel: +41 (61) 415 87 10
Fax: +41 (61) 415 87 20

Project: SW-WE-a3
Comments:

Prepared For:
Location:
Prepared By:
Date Prepared: 08 June 2005

System Results

Flow Rates	Gal/min	Concentrations	mg/l
RO Feed	2390	RO Feed TDS	35102
Permeate	956	Permeate TDS	204
Concentrate	1434	Concentrate TDS	58367
Total Feed	2390	Total Feed TDS	35106
Total Product	956	Total Product TDS	204

System Details **Single Stage Design**

Temperature: 77.0 Deg F Water Type: Seawater -well
System Recovery: 40.0 %

Pass 1 **Units: Pressure - Psi** **Flow - Gal/min** **TDS - mg/l**

Array 1 Recovery: 40.0% Concentrate TDS: 58367 Concentrate Flow: 1434

Bank	Total Vessels	Total Elements	Element Model	Feed Flow	Perm Flow	Feed Press	Delta Press	Perm TDS
1	52	364	TM820-370	2390	956	854	12.8	204
Total	**52**	**364**		**2390**	**956**			**204**

Concentration, Saturation and pH Data **mg/l**

Ion	Permeate	Treated Feed	Feed	Concentrate
Ca	0.76	408	408	679
Mg	2.4	1298	1298	2162
Na	72.7	10768	10768	17898
K	2.96	388	388	645
Ba	0.0	0.0	0.0	0.0
Sr	0.0	0.0	0.0	0.0
NH4	0.0	0.0	0.0	0.0
Fe	0.0	0.0	0.0	0.0
HCO3	1.17	120	143	200
Cl	117	19380	19380	32221
SO4	6.69	2723	2702	4534
NO3	0.0	0.0	0.0	0.0
F	0.0	0.0	0.0	0.0
B	0.27	1.1	1.1	1.66
SiO2	0.12	15.0	15.0	24.9

Ion	Permeate	Treated Feed	Feed	Concentrate
PO4	0.0008	0.5	0.5	0.83
CO3	5.88E-06	0.19	2.29	0.62
CO2	20.2	20.2	2.4	20.2
TDS	204	35102	35106	58367
pH	4.95	6.8	7.8	7.0
Saturation Data (%)				
CaSO4	0.0017	21.6	21.5	41.4
CaPO4	0.0	5.04	10000	9994
CaF2	0.0	0.0	0.0	0.0
BaSO4	0.0	0.0	0.0	0.0
SiO2	0.0915	14.6	11.7	24.9
SrSO4	0.0	0.0	0.0	0.0
LSI	-6.89	-0.36	0.72	0.47
SDSI	-6.49	-1.19	-0.11	-0.7

System Summary

System Configuration

System Type:	
Feed Predosing?:	Yes
Feed Afterdosing?:	No
Interpass Dosing?:	No
Product Dosing?:	No
Feed CO2 Stripping?:	No
Interpass CO2 Stripping?:	No
Product CO2 Stripping?:	No
Raw Feed Bypass?:	No
First Pass Recycle?:	No
Interpass Pumping?:	No

Feed Information

Water Type:	Seawater -well
Temperature, Deg F:	77.0
Feed pH:	7.8
Silt Density Index:	5.5

Feed Ion Concentration (mg/l)

Ca	408
Mg	1298
Na	10768
K	388
Ba	0.0
Sr	0.0
NH4	0.0
Fe	0.0
HCO3	143
Cl	19380
SO4	2702
NO3	0.0
F	0.0
B	1.1
SiO2	15.0
PO4	0.5
CO3	2.29
CO2	2.4

System Flux, Flows and Recoveries

Average System Flux:	10.2 Gal/ft2/day
Feed Flow:	2,390.00 Gal/min
Product Flow:	956.00 Gal/min
Concentrate Flow:	1,434.00 Gal/min
First Pass Recovery:	40.0 %
System Recovery:	40.0 %

First Pass Array

Interbank Pressure Drop: 0.0 Psi
Bank 1 Back Pressure: 15.0 Psi

Number of Banks: 1 Total Elements: 364

Bank	# Vessels	# Elements/Vessel	Element Type	Element Age
1	52	7	TM820-370	3

Chemical Treatment

Station	Chemical	Target pH
Feed Pre-Treat	Sulfuric Acid	6.8

Process Data

Flow Units: Gal/min
Pressure Units: psi

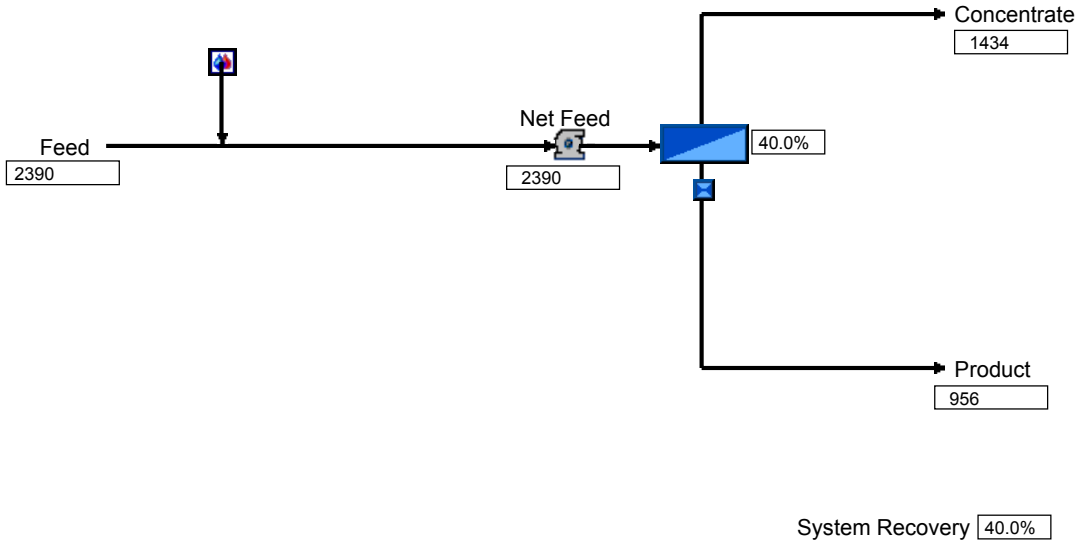

System Recovery 40.0%

Flow Rates	Gal/min	Concentrations	mg/l
RO Feed	2390	RO Feed TDS	35102
Permeate	956	Permeate TDS	204
Concentrate	1434	Concentrate TDS	58367
Total Feed	2390	Total Feed TDS	35106
Total Product	956	Total Product TDS	204

System Data **Single Stage Design**

Temperature: 77.0 Deg F

	Stage 1	
Fouling Allowance	85.0	%
Salt Passage Increase Per Year	10.0	%
Feed Pressure	854	Psi
Interbank Loss	0.0	Psi
Element Age	3.0	Years

Interbank Boost Pressure	Stage 1

Chemical Usage	Chemical	lb/day	kg/day	Target pH
Feed Pre-Treat	Sulfuric Acid	619	282	6.8

Stream Data

Units: Pressure - psi Flow - Gal/min TDS - mg/l Saturation - %

Stream --->	System Feed	Predosed Feed	1st Pass Feed	Total Permeate	System Product
Ca	408	408	408	0.76	0.76
Mg	1298	1298	1298	2.4	2.4
Na	10768	10768	10768	72.7	72.7
K	388	388	388	2.96	2.96
Ba	0.0	0.0	0.0	0.0	0.0
Sr	0.0	0.0	0.0	0.0	0.0
NH4	0.0	0.0	0.0	0.0	0.0
Fe	0.0	0.0	0.0	0.0	0.0
HCO3	143	120	120	1.17	1.17
Cl	19380	19380	19380	117	117
SO4	2702	2723	2723	6.69	6.69
NO3	0.0	0.0	0.0	0.0	0.0
F	0.0	0.0	0.0	0.0	0.0
B	1.1	1.1	1.1	0.27	0.27
SiO2	15.0	15.0	15.0	0.12	0.12
PO4	0.5	0.5	0.5	0.0008	0.0008
CO3	2.29	0.19	0.19	5.88E-06	5.88E-06
CO2	2.4	20.2	20.2	20.2	20.2
TDS	35106	35102	35102	204	204
pH	7.8	6.8	6.8	4.95	4.95
LSI	0.72	-0.36	-0.36	-6.89	-6.89
Stiff-Davis	-0.11	-1.19	-1.19	-6.49	-6.49
BaSO4 Sat	0.0	0.0	0.0	0.0	0.0
CaSO4 Sat	21.5	21.6	21.6	0.0017	0.0017
CaPO4 Sat	10000	5.04	5.04	0.0	0.0
CaF2 Sat	0.0	0.0	0.0	0.0	0.0
SrSO4 Sat	0.0	0.0	0.0	0.0	0.0
SiO2 Sat	11.7	14.6	14.6	0.0915	0.0915
Flow	2390	2390	2390	956	956
Temp, Deg F	77.0	77.0	77.0	77.0	77.0
Pressure	854	854	854	0.0	0.0
Osm Pressure	368	368	368	2.41	2.41

Units: Pressure - psi Flow - Gal/min TDS - mg/l Saturation - %

Stream --->	System Concentrate
Ca	679
Mg	2162
Na	17898
K	645
Ba	0.0
Sr	0.0
NH4	0.0
Fe	0.0
HCO3	200
Cl	32221
SO4	4534
NO3	0.0
F	0.0
B	1.66
SiO2	24.9
PO4	0.83
CO3	0.62
CO2	20.2
TDS	58367
pH	7.0
LSI	0.47
Stiff-Davis	-0.7
BaSO4 Sat	0.0
CaSO4 Sat	41.4
CaPO4 Sat	9994
CaF2 Sat	0.0
SrSO4 Sat	0.0
SiO2 Sat	24.9
Flow	1434
Temp, Deg F	77.0
Pressure	841
Osm Pressure	604

Element Data

Pass 1, Bank 1 **Units: Pressure - psi, Flow - Gal/min, TDS - mg/l, Saturation - %, Flux - gal/ft2/day**

Bank Permeate Back Pressure: 15.0

	Elem 1	Elem 2	Elem 3	Elem 4	Elem 5	Elem 6	Elem 7
Permeate Ions							
Ca	0.45	0.52	0.62	0.74	0.91	1.14	1.44
Mg	1.42	1.66	1.96	2.35	2.9	3.63	4.59
Na	42.9	50.2	59.4	71.0	87.8	110	138
K	1.75	2.04	2.42	2.89	3.57	4.46	5.63
Ba	0.0	0.0	0.0	0.0	0.0	0.0	0.0
Sr	0.0	0.0	0.0	0.0	0.0	0.0	0.0
NH4	0.0	0.0	0.0	0.0	0.0	0.0	0.0
Fe	0.0	0.0	0.0	0.0	0.0	0.0	0.0
HCO3	0.69	0.81	0.96	1.15	1.42	1.77	2.23
Cl	69.1	80.9	95.7	114	142	177	223
SO4	3.94	4.62	5.46	6.53	8.09	10.1	12.8
NO3	0.0	0.0	0.0	0.0	0.0	0.0	0.0
F	0.0	0.0	0.0	0.0	0.0	0.0	0.0
B	0.18	0.2	0.23	0.27	0.31	0.37	0.43
SiO2	0.0715	0.084	0.0996	0.12	0.14	0.18	0.22
PO4	0.0005	0.0006	0.0007	0.0008	0.001	0.0013	0.0016
CO3	1.97E-06	2.73E-06	3.87E-06	5.60E-06	8.73E-06	1.39E-05	2.27E-05
CO2	20.2	20.2	20.2	20.2	20.2	20.2	20.2
TDS	120	141	167	199	247	308	389
pH	4.73	4.8	4.87	4.94	5.03	5.13	5.22
LSI	-9.16	-9.03	-7.78	-6.96	-6.49	-6.12	-5.78
Stiff-Davis	-7.16	-6.96	-6.75	-6.52	-6.25	-5.97	-5.68
Conc Saturation							
BaSO4 Sat	0.0	0.0	0.0	0.0	0.0	0.0	0.0
CaSO4 Sat	23.9	26.4	29.1	32.0	35.1	38.3	41.4
CaF2 Sat	0.0	0.0	0.0	0.0	0.0	0.0	0.0
SrSO4 Sat	0.0	0.0	0.0	0.0	0.0	0.0	0.0
SiO2 Sat	15.8	17.2	18.7	20.2	21.8	23.4	24.9
Flow							
Feed	46.0	42.4	39.2	36.2	33.6	31.3	29.3
Permeate	3.53	3.24	2.94	2.63	2.32	2.01	1.7
Pressure							
Feed	854	852	850	848	846	844	843
Net Driving	419	385	349	313	276	241	209
Pressure Drop	2.39	2.16	1.96	1.78	1.62	1.49	1.38
Feed Osmotic	368	397	429	463	498	534	570
Other Parameters							
% Recovery	7.68	7.64	7.51	7.27	6.91	6.41	5.82
B Conc Pol	1.1	1.1	1.09	1.09	1.08	1.07	1.06
A Value	2.32E-09	2.33E-09	2.34E-09	2.34E-09	2.34E-09	2.32E-09	2.29E-09
B Value	2.12E-08	2.12E-08	2.11E-08	2.10E-08	2.15E-08	2.18E-08	2.22E-08
Flux	13.8	12.6	11.5	10.3	9.06	7.82	6.64

Errors & Warnings

Warning - High LSI. LSI > zero. Concentrate CaCO3 greater than saturation. Scale inhibitor required.
The feed water analysis was balanced with added Na or Cl.

Database version used for design : 2.028

TORAY

Toray Industries, Inc. Membrane Products Dept.
8-1, Mihama 1-chome, Urayasu, Chiba 279-8555, Japan
TEL: (+81) 47-350-6030
Fax: (+81) 47-350-6066

TORAY Membrane America, Inc.
USA, South America, Canada
12520 High Bluff Drive, Suite 120
San Diego, CA 92130, USA
Tel: +1 (858) 523 0476
Fax: +1 (858) 523 0861

ROPUR AG
Europe, Middle East and Africa
Grabenackerstrasse 8
CH-4142 Munchenstein 1, Switzerland
Tel: +41 (61) 415 87 10
Fax: +41 (61) 415 87 20

ROMEMBRA
TORAY REVERSE OSMOSIS ELEMENTS

Project: Starting Configuration BW 5000ppm TDS
Comments: Feasible Configuration for Brackish Water with 5000 ppm TDS

Prepared For:
Location:
Prepared By: Markus Forstmeier
Date Prepared: 31 May 2005

System Results

Flow Rates	Gal/min	Concentrations	mg/l
RO Feed	3900	RO Feed TDS	4807
Permeate	3198	Permeate TDS	132
Concentrate	702	Concentrate TDS	26151
Total Feed	3900	Total Feed TDS	5000
Total Product	3198	Total Product TDS	132

System Details **Single Stage Design**

Temperature: 25.0 Deg C Water Type: Seawater -well
System Recovery: 82.0 %

Pass 1 **Units: Pressure - Psi** **Flow - Gal/min** **TDS - mg/l**

Array 1 Recovery: 82.0% Concentrate TDS: 26151 Concentrate Flow: 702

Bank	Total Vessels	Total Elements	Element Model	Feed Flow	Perm Flow	Feed Press	Delta Press	Perm TDS
1	82	574	TM720-370	3900	2686	268	9.98	74.9
2	39	273	TM720-370	1214	512	258	6.97	433
Total	**121**	**847**		**3900**	**3198**			**132**

Concentration, Saturation and pH Data **mg/l**

Ion	Permeate	Treated Feed	Feed	Concentrate
Ca	0.0	0.0	0.0	0.0
Mg	0.0	0.0	0.0	0.0
Na	36.9	1370	1370	7438
K	0.0	0.0	0.0	0.0
Ba	0.0	0.0	0.0	0.0
Sr	0.0	0.0	0.0	0.0
NH4	0.0	0.0	0.0	0.0
Fe	0.0	0.0	0.0	0.0
HCO3	89.3	3626	3626	14671
Cl	0.0084	0.41	0.41	2.24
SO4	6.12	0.0	0.0	3998
NO3	0.0	0.0	0.0	0.0
F	0.0	0.0	0.0	0.0
B	0.0	0.0	0.0	0.0

Ion	Permeate	Treated Feed	Feed	Concentrate
SiO2	0.0	0.0	0.0	0.0
PO4	0.0	0.0	0.0	0.0
CO3	0.0006	3.61	3.61	41.7
CO2	1141	486	486	1139
TDS	132	4807	5000	26151
pH	5.09	6.5	7.0	7.16
Saturation Data (%)				
CaSO4	0.0	0.0	0.0	0.0
CaPO4	0.0	0.0	0.0	0.0
CaF2	0.0	0.0	0.0	0.0
BaSO4	0.0	0.0	0.0	0.0
SiO2	0.0	0.0	0.0	0.0
SrSO4	0.0	0.0	0.0	0.0
LSI	-6.62	-3.8	-3.17	-2.44
SDSI	0.0	0.0	0.0	0.0

System Summary

System Configuration

System Type:	
Feed Predosing?:	Yes
Feed Afterdosing?:	No
Interpass Dosing?:	No
Product Dosing?:	No
Feed CO2 Stripping?:	No
Interpass CO2 Stripping?:	No
Product CO2 Stripping?:	No
Raw Feed Bypass?:	No
First Pass Recycle?:	No
Interpass Pumping?:	No

Feed Information

Water Type:	Seawater -well
Temperature, Deg C:	25.0
Feed pH:	7.0
Silt Density Index:	5.5

Feed Ion Concentration (mg/l)

Ca	0.0
Mg	0.0
Na	1370
K	0.0
Ba	0.0
Sr	0.0
NH4	0.0
Fe	0.0
HCO3	3626
Cl	0.41
SO4	0.0
NO3	0.0
F	0.0
B	0.0
SiO2	0.0
PO4	0.0
CO3	3.61
CO2	486

System Flux, Flows and Recoveries

Average System Flux:	14.7 Gal/ft2/day
Feed Flow:	3,900.00 Gal/min
Product Flow:	3,198.00 Gal/min
Concentrate Flow:	702.00 Gal/min
First Pass Recovery:	82.0 %
System Recovery:	82.0 %

First Pass Array

Interbank Pressure Drop: 0.0 Psi

Interbank Pressure Boost
Bank 1-2: 0.0 Psi

Bank 1 Back Pressure: 15.0 Psi
Bank 2 Back Pressure: 15.0 Psi

Number of Banks: 2 Total Elements: 847

Bank	# Vessels	# Elements/Vessel	Element Type	Element Age
1	82	7	TM720-370	3
2	39	7	TM720-370	3

Chemical Treatment

Station	Chemical	Target pH
Feed Pre-Treat	Sulfuric Acid	6.5

Process Data

Flow Units: Gal/min
Pressure Units: psi

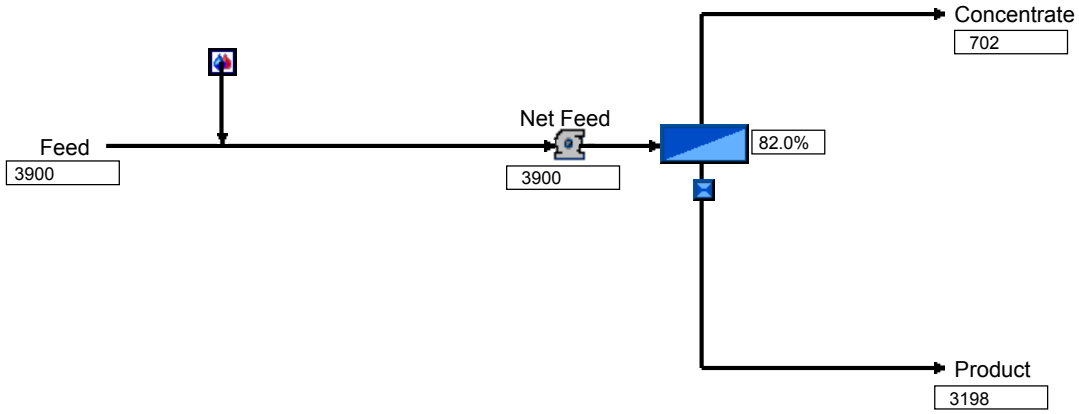

System Recovery 82.0%

Flow Rates	Gal/min	Concentrations	mg/l
RO Feed	3900	RO Feed TDS	4807
Permeate	3198	Permeate TDS	132
Concentrate	702	Concentrate TDS	26151
Total Feed	3900	Total Feed TDS	5000
Total Product	3198	Total Product TDS	132

System Data **Single Stage Design**

Temperature: 25.0 Deg C

	Stage 1	
Fouling Allowance	85.0	%
Salt Passage Increase Per Year	10.0	%
Feed Pressure	268	Psi
Interbank Loss	0.0	Psi
Element Age	3.0	Years

Interbank Boost Pressure	Stage 1	
Banks 1-2	0.0	Psi

Chemical Usage	Chemical	lb/day	kg/day	Target pH
Feed Pre-Treat	Sulfuric Acid	34669	15759	6.5

Stream Data

Units: Pressure - psi Flow - Gal/min TDS - mg/l Saturation - %

Stream --->	System Feed	1st Pass Feed	Total Permeate	System Product	System Concentrate
Ca	0.0	0.0	0.0	0.0	0.0
Mg	0.0	0.0	0.0	0.0	0.0
Na	1370	1370	36.9	36.9	7438
K	0.0	0.0	0.0	0.0	0.0
Ba	0.0	0.0	0.0	0.0	0.0
Sr	0.0	0.0	0.0	0.0	0.0
NH4	0.0	0.0	0.0	0.0	0.0
Fe	0.0	0.0	0.0	0.0	0.0
HCO3	3626	2711	89.3	89.3	14671
Cl	0.41	0.41	0.0084	0.0084	2.24
SO4	0.0	725	6.12	6.12	3998
NO3	0.0	0.0	0.0	0.0	0.0
F	0.0	0.0	0.0	0.0	0.0
B	0.0	0.0	0.0	0.0	0.0
SiO2	0.0	0.0	0.0	0.0	0.0
PO4	0.0	0.0	0.0	0.0	0.0
CO3	3.61	0.85	0.0006	0.0006	41.7
CO2	486	1148	1141	1141	1139
TDS	5000	4807	132	132	26151
pH	7.0	6.5	5.09	5.09	7.16
LSI	-3.17	-3.8	-6.62	-6.62	-2.44
Stiff-Davis	0.0	0.0	0.0	0.0	0.0
BaSO4 Sat	0.0	0.0	0.0	0.0	0.0
CaSO4 Sat	0.0	0.0	0.0	0.0	0.0
CaPO4 Sat	0.0	0.0	0.0	0.0	0.0
CaF2 Sat	0.0	0.0	0.0	0.0	0.0
SrSO4 Sat	0.0	0.0	0.0	0.0	0.0
SiO2 Sat	0.0	0.0	0.0	0.0	0.0
Flow	3900	3900	3198	3198	702
Temp, Deg C	25.0	25.0	25.0	25.0	25.0
Pressure	268	268	0.0	0.0	251
Osm Pressure	41.5	38.5	1.12	1.12	203

Element Data

Pass 1, Bank 1 **Units: Pressure - psi, Flow - Gal/min, TDS - mg/l, Saturation - %, Flux - gal/ft2/day**

Bank Permeate Back Pressure: 15.0

	Elem 1	Elem 2	Elem 3	Elem 4	Elem 5	Elem 6	Elem 7
Permeate Ions							
Ca	0.0	0.0	0.0	0.0	0.0	0.0	0.0
Mg	0.0	0.0	0.0	0.0	0.0	0.0	0.0
Na	9.42	11.5	14.4	18.6	24.8	34.6	50.5
K	0.0	0.0	0.0	0.0	0.0	0.0	0.0
Ba	0.0	0.0	0.0	0.0	0.0	0.0	0.0
Sr	0.0	0.0	0.0	0.0	0.0	0.0	0.0
NH4	0.0	0.0	0.0	0.0	0.0	0.0	0.0
Fe	0.0	0.0	0.0	0.0	0.0	0.0	0.0
HCO3	22.5	27.6	34.6	44.8	60.1	83.9	123
Cl	0.0021	0.0026	0.0032	0.0042	0.0056	0.0079	0.0115
SO4	1.51	1.85	2.33	3.02	4.06	5.69	8.34
NO3	0.0	0.0	0.0	0.0	0.0	0.0	0.0
F	0.0	0.0	0.0	0.0	0.0	0.0	0.0
B	0.0	0.0	0.0	0.0	0.0	0.0	0.0
SiO2	0.0	0.0	0.0	0.0	0.0	0.0	0.0
PO4	0.0	0.0	0.0	0.0	0.0	0.0	0.0
CO3	3.39E-05	5.12E-05	8.14E-05	0.0001	0.0003	0.0005	0.0011
CO2	1141	1141	1141	1141	1141	1141	1141
TDS	33.4	40.9	51.3	66.4	88.9	124	181
pH	4.5	4.59	4.69	4.8	4.92	5.07	5.23
LSI	-7.83	-7.64	-7.44	-7.21	-6.96	-6.67	-6.35
Stiff-Davis	0.0	0.0	0.0	0.0	0.0	0.0	0.0
Conc Saturation							
BaSO4 Sat	0.0	0.0	0.0	0.0	0.0	0.0	0.0
CaSO4 Sat	0.0	0.0	0.0	0.0	0.0	0.0	0.0
CaF2 Sat	0.0	0.0	0.0	0.0	0.0	0.0	0.0
SrSO4 Sat	0.0	0.0	0.0	0.0	0.0	0.0	0.0
SiO2 Sat	0.0	0.0	0.0	0.0	0.0	0.0	0.0
Flow							
Feed	47.6	41.8	36.2	31.0	26.2	21.8	18.0
Permeate	5.8	5.52	5.2	4.82	4.37	3.83	3.2
Pressure							
Feed	268	266	264	262	261	260	259
Net Driving	202	193	181	168	153	134	112
Pressure Drop	2.51	2.06	1.67	1.32	1.03	0.79	0.6
Feed Osmotic	38.6	43.8	50.3	58.6	69.0	82.4	99.3
Other Parameters							
% Recovery	12.2	13.2	14.4	15.5	16.7	17.5	17.8
B Conc Pol	1.22	1.23	1.24	1.24	1.24	1.23	1.22
A Value	7.74E-09	7.75E-09	7.75E-09	7.76E-09	7.76E-09	7.76E-09	7.76E-09
B Value	4.76E-08	4.82E-08	4.90E-08	4.98E-08	5.08E-08	5.20E-08	5.33E-08
Flux	22.6	21.5	20.3	18.8	17.0	14.9	12.5

Pass 1, Bank 2 **Units: Pressure - psi, Flow - Gal/min, TDS - mg/l, Saturation - %, Flux - gal/ft2/day**

Bank Permeate Back Pressure: 15.0
Bank Boost Pressure: 0.0

	Elem 1	Elem 2	Elem 3	Elem 4	Elem 5	Elem 6	Elem 7
Permeate Ions							
Ca	0.0	0.0	0.0	0.0	0.0	0.0	0.0
Mg	0.0	0.0	0.0	0.0	0.0	0.0	0.0
Na	61.1	77.0	98.0	126	162	210	272
K	0.0	0.0	0.0	0.0	0.0	0.0	0.0
Ba	0.0	0.0	0.0	0.0	0.0	0.0	0.0
Sr	0.0	0.0	0.0	0.0	0.0	0.0	0.0
NH4	0.0	0.0	0.0	0.0	0.0	0.0	0.0
Fe	0.0	0.0	0.0	0.0	0.0	0.0	0.0
HCO3	148	187	238	305	394	510	660
Cl	0.014	0.0177	0.0225	0.0289	0.0375	0.0487	0.0633
SO4	10.1	12.8	16.4	21.1	27.4	35.7	46.7
NO3	0.0	0.0	0.0	0.0	0.0	0.0	0.0
F	0.0	0.0	0.0	0.0	0.0	0.0	0.0
B	0.0	0.0	0.0	0.0	0.0	0.0	0.0
SiO2	0.0	0.0	0.0	0.0	0.0	0.0	0.0
PO4	0.0	0.0	0.0	0.0	0.0	0.0	0.0
CO3	0.0016	0.0026	0.0044	0.0074	0.0126	0.0218	0.0379
CO2	1141	1140	1140	1140	1140	1140	1140
TDS	220	277	352	452	583	755	979
pH	5.31	5.41	5.51	5.61	5.72	5.83	5.93
LSI	-6.18	-5.99	-5.78	-5.58	-5.36	-5.15	-4.93
Stiff-Davis	0.0	0.0	0.0	0.0	0.0	0.0	0.0
Conc Saturation							
BaSO4 Sat	0.0	0.0	0.0	0.0	0.0	0.0	0.0
CaSO4 Sat	0.0	0.0	0.0	0.0	0.0	0.0	0.0
CaF2 Sat	0.0	0.0	0.0	0.0	0.0	0.0	0.0
SrSO4 Sat	0.0	0.0	0.0	0.0	0.0	0.0	0.0
SiO2 Sat	0.0	0.0	0.0	0.0	0.0	0.0	0.0
Flow							
Feed	31.1	28.2	25.7	23.5	21.7	20.2	19.0
Permeate	2.91	2.53	2.16	1.82	1.5	1.22	0.99
Pressure							
Feed	258	257	256	255	254	253	252
Net Driving	102	88.7	75.9	63.8	52.8	43.1	34.8
Pressure Drop	1.4	1.22	1.07	0.95	0.85	0.77	0.71
Feed Osmotic	120	132	144	157	170	182	193
Other Parameters							
% Recovery	9.34	8.96	8.42	7.72	6.92	6.06	5.2
B Conc Pol	1.14	1.12	1.11	1.1	1.09	1.07	1.06
A Value	7.77E-09	7.77E-09	7.77E-09	7.77E-09	7.78E-09	7.78E-09	7.78E-09
B Value	5.47E-08	5.53E-08	5.58E-08	5.63E-08	5.67E-08	5.71E-08	5.74E-08
Flux	11.3	9.87	8.43	7.09	5.86	4.77	3.85

Errors & Warnings

The feed water analysis was balanced with added Na or Cl.

Database version used for design : 2.028

TORAY

Toray Industries, Inc. Membrane Products Dept.
8-1, Mihama 1-chome, Urayasu, Chiba 279-8555, Japan
TEL: (+81) 47-350-6030
Fax: (+81) 47-350-6066

TORAY Membrane America, Inc.
USA, South America, Canada
12520 High Bluff Drive, Suite 120
San Diego, CA 92130, USA
Tel: +1 (858) 523 0476
Fax: +1 (858) 523 0861

ROPUR AG
Europe, Middle East and Africa
Grabenackerstrasse 8
CH-4142 Munchenstein 1, Switzerland
Tel: +41 (61) 415 87 10
Fax: +41 (61) 415 87 20

Seawater RO Elements

TM800

Type	Diameter inch	Membrane Area ft^2 (m^2)	Salt Rejection %	Product Flow Rate gpd (m^3/d)
TM820-370	8"	370 (34)	99.75	6,000 (23)
TM820-400	8"	400 (37)	99.75	6,500 (25)

1. Membrane Type		Cross Linked Fully Aromatic Polyamide Composite
2. Test Conditions	Feed Water Pressure Feed Water Temperature Feed Water Concentration Recovery Rate Feed Water pH	800 psi (5.52 MPa) 77 °F (25 °C) 32,000 mg/l NaCl 8 % 7
3. Minimum Salt Rejection		99.5 %
4. Minimum Product Flow Rate		4,800 gpd (18 m^3/d) (TM820-370) 5,200 gpd (20 m^3/d) (TM820-400)

Dimensions

All dimensions shown in inches (millimeter).

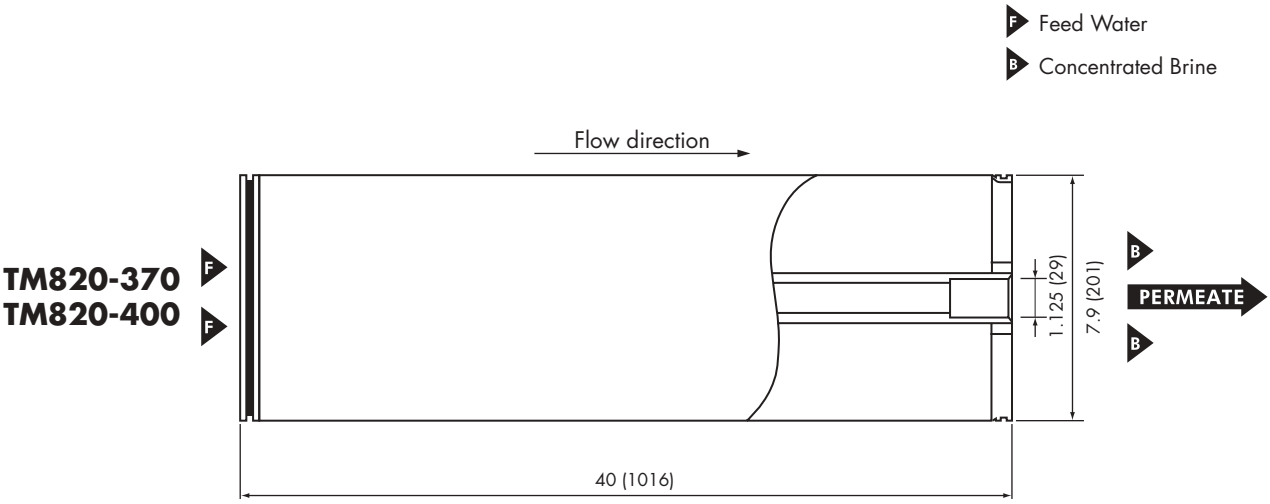

Operating Limits

Maximum Operating Pressure	1000 psi (6.9 MPa)
Maximum Feed Water Temperature	113 °F (45 °C)
Maximum Feed Water SDI_{15}	5
Feed Water Chlorine Concentration	Not Detectable
Feed Water pH Range, Continuous Operation	2-11
Feed Water pH Range, Chemical Cleaning	1-12
Maximum Pressure Drop per Element	20 psi (0.14 MPa)
Maximum Pressure Drop per Vessel	60 psi (0.4 MPa)

Operating Information

1. For the recommended design range, please consult the latest Toray technical bulletin, design guidelines, computer design program, and/or call an application specialist. If the operating limits given in this Product Information Bulletin are not strictly followed, the Limited Warranty will be null and void.
2. All elements are wet tested, treated with a 1% by weight percent sodium bisulfite storage solution, and then vacuum packed in oxygen barrier bags. To prevent biological growth during short term storage, shipment, or system shutdown, it is recommended that Toray elements be immersed in a protective solution containing 500 - 1,000 ppm of sodium bisulfite (food grade) dissolved in permeate.
3. Permeate from the first hour of operation shall be discarded.
4. The customer is fully responsible for the effects of chemicals that are incompatible with the elements. Their use will void the element Limited Warranty.

Notice

1. Toray accepts no responsibility for results obtained by the application of this information or the safety or suitability of Toray's products, either alone or in combination with other products. Users are advised to make their own tests to determine the safety and suitability of each product combination for their own purposes.
2. All data may change without prior notice, due to technical modifications or production changes.

Asia and Oceania:
Toray Industries, Inc.
Membrane Products Department

8-1, Mihama 1-chome
Urayasu, Chiba 279-8555, Japan
Tel: +81 47 350 6030
Fax: +81 47 350 6066
http://www.toray-membrane.com

Americas:
Toray Membrane America, Inc.
Sales Office

12520 High Bluff Drive, Suite 120
San Diego, CA 92130, U.S.A.
Tel: +1 858 523 0476
Fax: +1 858 523 0861

Europe, Middle East and Africa:
Toray Membrane Europe AG

Grabenackerstrasse 8
CH-4142 Münchenstein 1, Switzerland
Tel: +41 61 415 87 10
Fax: +41 61 415 87 20

RO Membrane Elements for Brackish Water

TM700

Type	Diameter inch	Membrane Area ft² (m²)	Salt Rejection %	Product Flow Rate gpd (m³/d)
TM710	4"	87 (8)	99.7	2,400 (9.1)
TM720-370	8"	370 (34)	99.7	9,500 (36)
TM720-400	8"	400 (37)	99.7	10,200 (39)
TM720-430	8"	430 (40)	99.7	11,000 (42)

1. Membrane Type		Cross Linked Fully Aromatic Polyamide Composite
2. Test Conditions	Feed Water Pressure Feed Water Temperature Feed Water Concentration Recovery Rate Feed Water pH	225 psi (1.55 MPa) 77 °F (25 °C) 2,000 mg/l NaCl 15 % 7
3. Minimum Salt Rejection		99.0 %
4. Minimum Product Flow Rate		2,000 gpd (7.6 m³/d) (TM710) 7,500 gpd (28 m³/d) (TM720-370) 8,200 gpd (31 m³/d) (TM720-400) 8,800 gpd (33 m³/d) (TM720-430)

Dimensions

All dimensions shown in inches (millimeter).

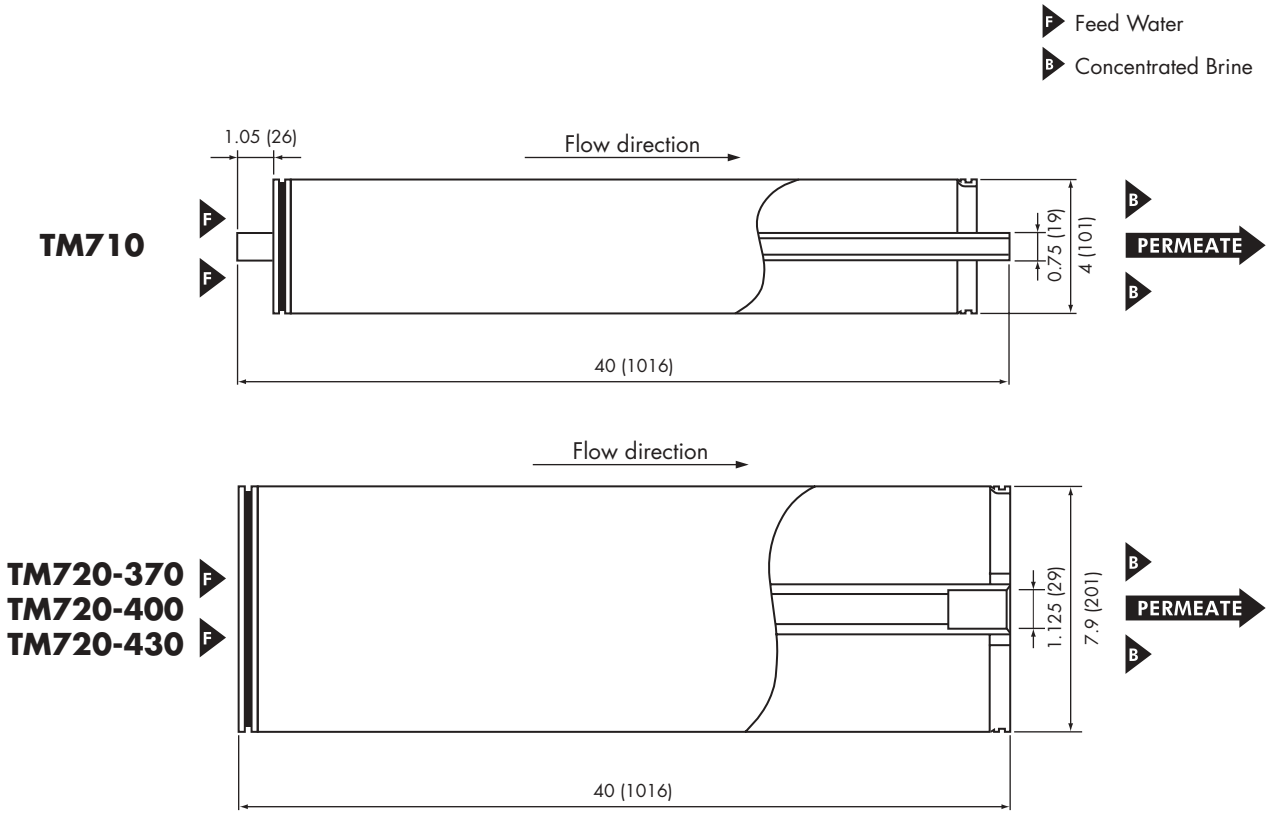

Operating Limits

Maximum Operating Pressure	600 psi (4.1 MPa)
Maximum Feed Water Temperature	113 °F (45 °C)
Maximum Feed Water SDI_{15}	5
Feed Water Chlorine Concentration	Not Detectable
Feed Water pH Range, Continuous Operation	2-11
Feed Water pH Range, Chemical Cleaning	1-12
Maximum Pressure Drop per Element	20 psi (0.14 MPa)
Maximum Pressure Drop per Vessel	60 psi (0.4 MPa)

Operating Information

1. For the recommended design range, please consult the latest Toray technical bulletin, design guidelines, computer design program, and/or call an application specialist. If the operating limits given in this Product Information Bulletin are not strictly followed, the Limited Warranty will be null and void.
2. All elements are wet tested, treated with a 1% by weight percent sodium bisulfite storage solution, and then vacuum packed in oxygen barrier bags. To prevent biological growth during short term storage, shipment, or system shutdown, it is recommended that Toray elements be immersed in a protective solution containing 500 - 1,000 ppm of sodium bisulfite (food grade) dissolved in permeate.
3. Permeate from the first hour of operation shall be discarded.
4. The customer is fully responsible for the effects of chemicals that are incompatible with the elements. Their use will void the element Limited Warranty.

Notice

1. Toray accepts no responsibility for results obtained by the application of this information or the safety or suitability of Toray's products, either alone or in combination with other products. Users are advised to make their own tests to determine the safety and suitability of each product combination for their own purposes.
2. All data may change without prior notice, due to technical modifications or production changes.

Asia and Oceania:
Toray Industries, Inc.
Membrane Products Department

8-1, Mihama 1-chome
Urayasu, Chiba 279-8555, Japan
Tel: +81 47 350 6030
Fax: +81 47 350 6066
http://www.toray-membrane.com

Americas:
Toray Membrane America, Inc.
Sales Office

12520 High Bluff Drive, Suite 120
San Diego, CA 92130, U.S.A.
Tel: +1 858 523 0476
Fax: +1 858 523 0861

Europe, Middle East and Africa:
Toray Membrane Europe AG

Grabenackerstrasse 8
CH-4142 Münchenstein 1, Switzerland
Tel: +41 61 415 87 10
Fax: +41 61 415 87 20

FEB/2004

REPORT DOCUMENTATION PAGE

Form Approved
OMB No. 0704-0188

PLEASE DO NOT RETURN YOUR FORM TO THE ABOVE ORGANIZATION.

1. REPORT DATE *(DD-MM-YYYY)*	2. REPORT TYPE	3. DATES COVERED *(From - To)*
October 2006	Subcontract report	10/11/2004 - 7/29/2005

4. TITLE AND SUBTITLE
Integrated Wind Energy/Desalination System

5a. CONTRACT NUMBER
DE-AC36-99-GO10337

5b. GRANT NUMBER

5c. PROGRAM ELEMENT NUMBER

6. AUTHOR(S)
GE Global Research

5d. PROJECT NUMBER
NREL/SR-500-39485

5e. TASK NUMBER
WER6.7502

5f. WORK UNIT NUMBER

7. PERFORMING ORGANIZATION NAME(S) AND ADDRESS(ES)
GE Gobal Research
Niskayuna, New York

8. PERFORMING ORGANIZATION REPORT NUMBER
YAM-4-33200-09

9. SPONSORING/MONITORING AGENCY NAME(S) AND ADDRESS(ES)
National Renewable Energy Laboratory
1617 Cole Blvd.
Golden, CO 80401-3393

10. SPONSOR/MONITOR'S ACRONYM(S)
NREL

11. SPONSORING/MONITORING AGENCY REPORT NUMBER
NREL/SR-500-39485

12. DISTRIBUTION AVAILABILITY STATEMENT
National Technical Information Service
U.S. Department of Commerce
5285 Port Royal Road
Springfield, VA 22161

13. SUPPLEMENTARY NOTES
NREL Technical Monitor: Scott Schreck

14. ABSTRACT *(Maximum 200 Words)*
This study investigates the feasibility of multiple concepts for integrating wind turbines and reverse osmosis desalination systems for water purification.

15. SUBJECT TERMS
wind energy; water purification; desalination

16. SECURITY CLASSIFICATION OF:			17. LIMITATION OF ABSTRACT	18. NUMBER OF PAGES	19a. NAME OF RESPONSIBLE PERSON
a. REPORT	b. ABSTRACT	c. THIS PAGE			
Unclassified	Unclassified	Unclassified	UL		19b. TELEPHONE NUMBER (*Include area code*)

Standard Form 298 (Rev. 8/98)
Prescribed by ANSI Std. Z39.18